

UNIVERSITY OF NOTTINGHAM



SCHOOL OF MATHEMATICAL SCIENCES

# Performance characterization for noisy quantum technologies

Pietro Liuzzo Scorpo

A thesis submitted to the University of Nottingham for the degree of  
DOCTOR OF PHILOSOPHY

APRIL 2018



## ABSTRACT

The fast development of quantum technologies requires a new theoretical effort to characterize their performance in practical scenarios. By studying both discrete and continuous variable systems, we will explore several research lines, such as control theory, quantum metrology and non-Markovianity. The thread connecting these different fields will be an approach that attempts to determine the limits and the potentiality of quantum performance in the presence of noise and scarcity of resources. Indeed, the goal of this thesis is to investigate whether quantum features can enhance the performance of particular instances of quantum protocols, and, if this is the case, how this enhancement is affected when some restrictions on the practical implementation of these protocols are in place.



## ACKNOWLEDGEMENTS

This is the only part of the thesis where I use the first person singular. In the rest, I felt like the first person plural was more appropriate. Simply because, during my PhD, I've never been alone. In this unique part of the thesis, I, Pietro, want to thank all of you, who have been there for me.

Gerardo, you have been a great supervisor. Thank you for your support. I had some difficult and discouraged moments in these years, but I've always known that I could count on you, for a good word of motivation or advice, without the fear of being judged. Thank you for your patience, for always finding time to discuss with me when I appeared in your office unannounced. Thank you for the knowledge you shared with me.

Many thanks to all the people who are, or have been, part of the Quantum Correlations Group in these years. It has been a pleasure to work in such a great environment. I learned something from each of you. Thanks Sammy, Tom, Marco, Rebecca, Ioannis, Sara, Isabela, Matteo, Onam, Yu, Leonardo, Gökan, Benjamin, Giorgio, Carmine, Buqing, Bartosz, Rosanna, Ludovico, Paul, Tommaso and Luis. I also want to thank all the other people I collaborated with: Himadri Shekhar Dhar, Manabendra Nath Bera, Wojciech Roga, Nadja Bernardes, Andrea Mari, Vittorio Giovannetti, Felix Pollock, Agnieszka Górecka and Kavan Modi.

I also would like to thank Paola Verrucchi and Alessandro Cuccoli for their guidance and advice when I was applying for PhD positions and for encouraging me to go to Nottingham.

Stepping out of academic life, I want to thank in particular the Postgraduate New Theatre group. I am so glad for the good time spent with you lot, at Highfield House or at the Performing Art Studio rehearsing, on stage and backstage at the New Theatre, and at all the parties. It wouldn't have been the same without you.

Thanks to my housemates, Peter and Eliana, and my friends, Lia, Giulia, Mariele, Adele, Carmine, James, Martien, Paul and Ben. Thanks for all the dinners, the chats, the coffees, the nights spent watching tv series and films, the Sunday meals and, last but not least, for all the dinners (did I say that

already?). You are wonderful people and I am so glad you are part of my life.

A special mention for Marco. You made me grow as a person and taught me so many things. *You helped me emancipating from the tediousness of the Italian province.* And for this I will always be grateful.

Last but not least, I dedicate this thesis to the following people: To my parents, for your constant support and for teaching me the value of education. And to Isha, my partner and accomplice, thanks from the bottom of my heart for all the memories, the runaways, the time, the words, the silences, the videocalls, the caresses, the dances, the videogames, the projects for the future. Thanks for all the love.

---

# CONTENTS

---

ABSTRACT	i
ACKNOWLEDGEMENTS	iii
LIST OF PUBLICATIONS	ix
INTRODUCTION	1
<b>I Preliminaries</b>	<b>5</b>
1 QUANTUM INFORMATION IN A (TINY) NUTSHELL	7
1.1 Quantum systems . . . . .	7
1.1.1 Pure states and selective measurements . . . . .	7
1.1.2 Beyond pure states: density matrix formalism . . . . .	10
1.1.3 Correlations . . . . .	16
1.2 Quantum Dynamics . . . . .	23
1.2.1 Stinespring dilation . . . . .	24
1.2.2 Master equations for Markovian dynamics . . . . .	25
1.2.3 Master equations for Non-Markovian dynamics . . . . .	28
2 GAUSSIAN STATES AND GAUSSIAN CHANNELS	33
2.1 Introduction to Continuous Variable systems . . . . .	34
2.2 Gaussian states . . . . .	40
2.2.1 Mean excitation number . . . . .	41
2.2.2 Gaussian Unitaries . . . . .	42
2.2.3 Bipartite Gaussian states and local operations . . . . .	48
2.3 Gaussian channels . . . . .	51
2.3.1 Open Gaussian dynamics . . . . .	52
2.3.2 Single-mode Gaussian channels . . . . .	53
3 QUANTUM METROLOGY ESSENTIALS	57
3.1 Background . . . . .	57

Contents

3.2	The quantum case . . . . .	58
3.2.1	Single-parameter estimation . . . . .	59
3.2.2	Multi-parameter estimation . . . . .	63
<b>II</b>	<b>Original results</b>	<b>65</b>
4	THERMODYNAMIC EFFICIENCY OF COHERENT FEEDBACK	
	COOLING	67
4.1	Feedback cooling algorithm . . . . .	68
4.1.1	Initialization . . . . .	70
4.1.2	(Pre-)measurement . . . . .	71
4.1.3	Feedback . . . . .	71
4.1.4	Reset of the ancillas . . . . .	72
4.2	Thermodynamical analysis . . . . .	72
4.2.1	Energy book-keeping . . . . .	72
4.2.2	Performance of algorithmic cooling . . . . .	74
4.3	Information-theoretical analysis . . . . .	76
4.4	Remarks . . . . .	80
5	ENERGY-EFFICIENT QUANTUM FREQUENCY ESTIMATION	81
5.1	Phase covariant noise: a phenomenological model . . . . .	82
5.1.1	Phenomenological master equation . . . . .	82
5.1.2	Dissipative dynamics as phase-covariant channel . . . . .	83
5.2	The protocol . . . . .	85
5.2.1	Probe initialisation . . . . .	85
5.2.2	Parameter encoding transformation: free evolution . . . . .	87
5.2.3	Preparation for the measurement . . . . .	88
5.3	'Error bars' of the estimate . . . . .	90
5.3.1	(Classical) Fisher information . . . . .	90
5.3.2	Quantum Fisher Information . . . . .	91
5.4	Metrological efficiencies of the protocol . . . . .	93
5.5	Remarks . . . . .	94
6	GAUSSIAN QUANTUM METROLOGY	97
6.1	Gaussian Symmetric Logarithmic Derivative . . . . .	98
6.2	QFI and 'compatibility' matrices for Gaussian states . . . . .	99

6.3	Noisy optical interferometry . . . . .	100
6.4	Remarks . . . . .	103
7	GAUSSIAN NON-MARKOVIANITY	105
7.1	A new witness for Gaussian non-Markovianity . . . . .	107
7.1.1	Gaussian interferometric power . . . . .	108
7.1.2	GIP as Gaussian non-Markovianity witness . . . . .	110
7.2	non-Markovianity hierarchy of Gaussian evolutions . . . . .	110
7.2.1	$k$ -mode positivity of Gaussian maps . . . . .	111
7.2.2	Hierarchy of Gaussian non-Markovianity . . . . .	112
7.2.3	Complete classification of one-mode Gaussian maps . . . . .	113
7.2.4	Phase-insensitive maps: allowed trajectories . . . . .	118
7.2.5	Operational significance of Gaussian non-Markovianity degree . . . . .	120
7.3	Remarks . . . . .	122
8	GAUSSIAN QUANTUM TELEPORTATION WITH LIMITED RESOURCES	123
8.1	Quantum teleportation . . . . .	123
8.1.1	Gaussian teleportation protocol . . . . .	125
8.1.2	Figure of merit for certified teleportation . . . . .	127
8.2	Optimal certified quantum teleportation . . . . .	130
8.2.1	Phase-insensitive channels implementable with finite entanglement . . . . .	130
8.2.2	Optimal teleportation fidelity . . . . .	131
8.3	Optimal certified secure quantum teleportation . . . . .	134
8.3.1	Phase-insensitive channels implementable with finite steerability . . . . .	135
8.3.2	Optimal fidelity . . . . .	137
8.4	Remarks . . . . .	141
	CONCLUSIONS	143
	<b>III Appendices</b>	<b>147</b>
A	GAUSSIAN CHANNELS	149
A.1	Proof of Proposition 2.2 . . . . .	149

## Contents

A.2 Proof of Proposition 2.3 . . . . .	150
B DAMPED JAYNES-CUMMINGS MODEL	155
C MEASUREMENT COMPATIBILITY MATRIX	157
D $k$ -MODE POSITIVITY OF GAUSSIAN MAPS	165
E TELEPORTATION OUTPUT	171
BIBLIOGRAPHY	176

---

## LIST OF PUBLICATIONS

---

This thesis contains work from the following papers

- [A] L. A. M. Souza, H. Shekhar Dhar, M. Nath Bera, P. Liuzzo-Scorpo, G. Adesso, "Gaussian interferometric power as a measure of continuous variable non-Markovianity," *Phys. Rev. A*, vol. 92, p. 052122, Nov 2015
- [B] P. Liuzzo-Scorpo, L. A. Correa, R. Schmidt, G. Adesso, "Thermodynamics of Quantum Feedback Cooling," *Entropy*, vol. 18, no. 48, Feb 2016
- [C] P. Liuzzo-Scorpo, W. Roga, L. A. M. Souza, N. K. Bernardes, G. Adesso, "Non-Markovianity Hierarchy of Gaussian Processes and Quantum Amplification," *Phys. Rev. Lett.*, vol. 118, p. 050401, Jan 2017.
- [D] P. Liuzzo-Scorpo, A. Mari, V. Giovannetti, G. Adesso, "Optimal continuous variable quantum teleportation with limited resources," *Phys. Rev. Lett.*, vol. 119, p. 120503, Sep 2017.
- [E] P. Liuzzo-Scorpo, G. Adesso, "Optimal secure quantum teleportation of coherent states of light," *Proceedings of SPIE - Quantum Photonic Devices*, vol. 10358, p. 103580, Jun 2017.
- [F] R. Nichols, P. Liuzzo-Scorpo, P. A. Knott, Gerardo Adesso, "Multiparameter Gaussian Quantum Metrology," *arXiv:1711.09132*, Nov 2017, (Submitted to *Phys. Rev. Lett.*).
- [G] P. Liuzzo-Scorpo, L. A. Correa, F. A. Pollock, A. Górecka, K. Modi, G. Adesso, "Energy-efficient quantum frequency estimation," *arXiv: 1712.08143*, Dec 2017, (Submitted to *New Journal of Physics*).

Other papers co-authored by the candidate, which are not included in this thesis, are

- [H] P. Liuzzo-Scorpo, A. Cuccoli, P. Verrucchi, "Getting Information via a Quantum Measurement: The Role of Decoherence," *International Journal of Theoretical Physics*, vol. 54, pp 4356–4366, Dec 2015.
- [I] P. Liuzzo-Scorpo, A. Cuccoli, P. Verrucchi, "Parametric description of the quantum measurement process," *Europhysics Letters*, Volume 111, p. 400008, Sep 2015.
- [J] A. Górecka, F. A. Pollock, P. Liuzzo-Scorpo, R. Nichols, G. Adesso, K. Modi, "Noisy frequency estimation with noisy probes," *arXiv: 1712.08142*, Dec 2017, (Submitted to *Quantum Science and Technology*).



---

## INTRODUCTION

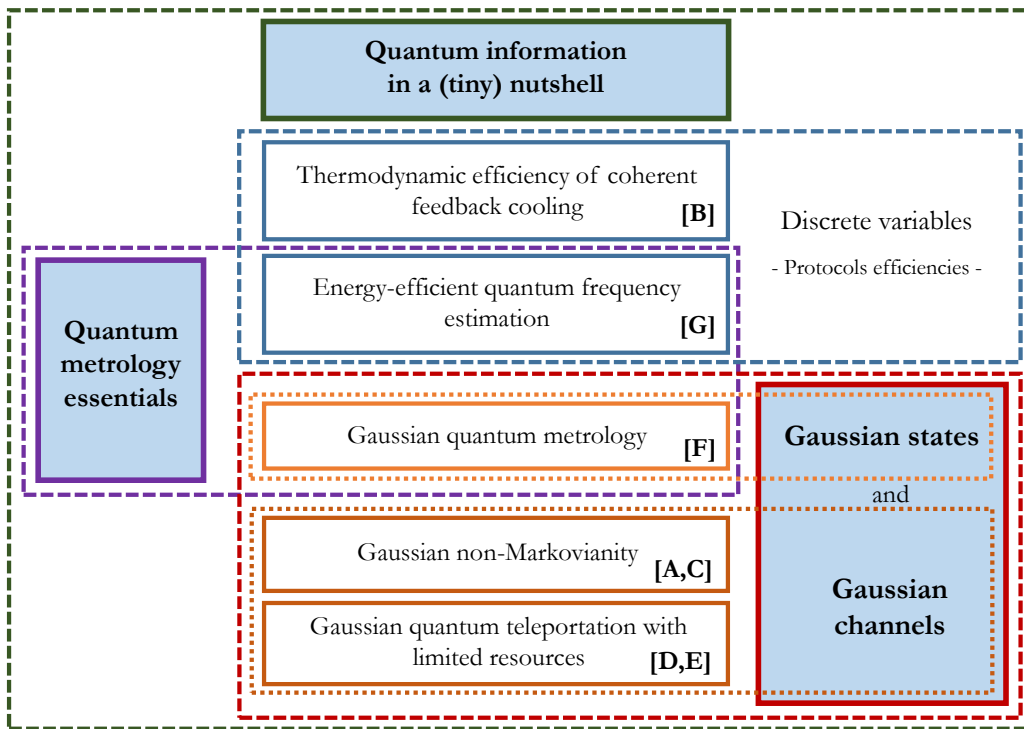
---

In the last few years we have witnessed a flourish of long-awaited scientific and technological achievements: from the detection of gravitational waves, to the first prototypes of quantum computers, encompassing the teleportation of photons into orbit. We live in an exciting era where we feel on the edge of a new technological revolution, however, the road ahead is still long: the building blocks of these novel technologies are quantum systems and *quantum* is fragile. Indeed, interactions between any quantum system and an environment, over which the experimentalists have no control, can often cause the system to lose its quantum properties [1, 2], and therefore any desirable advantage they could give.

Quantum features, such as entanglement [3] or coherence [4], are fundamental resources for the implementation of protocols, such as teleportation [5], which would be impossible to realize when using classical physical systems. The performance of other tasks can be enhanced by the exploitation of quantum resources, for example, estimating a parameter using quantum probes (as is the case for gravitational waves detection [6]) can give smaller error bars than their classical counterparts [7].

Unfortunately, as we said above, unavoidable disturbances can make it hard to create, preserve and control these quantum resources. Even with the best efforts to reduce these disturbances, in realistic scenarios, their complete elimination is impossible. Perfect ideal situations where quantum systems exist in a bubble, shielded from the scary, noisy world outside, are important to be studied for their foundational impact, for their capability to fuel novel lines of research and to raise interesting new questions, however, they appear to be only remote dreams when stepping into a lab.

The work contained in this thesis is placed in between the (comfortable) ideal world, and a realistic experimental scenario (keeping, however, a safe distance from both). The goal of this thesis is that of characterizing the performance of some quantum information protocols in which the quantum constituents, or their manipulation, are not free from imperfections, or in



Schematic representation of the structure of the thesis. The capital letters in square brackets are the references to the papers the Chapters are based on, see LIST OF PUBLICATIONS.

which the resources one is provided with are limited. In other words, we ask ourselves: given some specific quantum information task, which could be optimally accomplished in a perfect noiseless world, how well can we do if we relax some of the most stringent assumptions responsible for putting distance between idealized theory and actual experimental implementation? And also: under which circumstances, can one, in principle, gain some advantage from unavoidable disturbances?

To be more specific, this thesis is divided into two main parts: in the first part (composed of three Chapters) we will introduce the formalism and the mathematical tools of quantum information, which are necessary to understand the original results presented in the second part. In the Figure above a schematic representation of the structure of this thesis is presented: the light blue filled rectangles correspond to the introductory Chapters, the dashed and dotted lines group together the original results Chapters by themes and link them to the relevant introductory Chapters.

In Chapter 1 we will review some basic concepts of quantum information such as: quantum systems and their description, quantum correlations and open quantum systems dynamics. In Chapter 2 we will focus on continuous variable quantum systems, in particular on Gaussian states, introducing the appropriate formalism to describe them. We will also discuss Gaussian channels, i.e. quantum operations that transform Gaussian states into Gaussian states. In the last Chapter of this introductory part, Chapter 3, we will revise the fundamental concepts of quantum parameter estimation.

In Chapter 4 we tackle the problem of reducing the entropy and the average energy of an ensemble of thermal qubits in the framework of coherent feedback control. We will investigate what role quantum correlations between target system and controller play in a simple feedback cooling protocol. In order to do this we will look for a connection between these correlations and some figures of merit assessing the efficiency of such a protocol which takes into account the work cost of implementing it.

In Chapter 5 we will study a frequency estimation protocol in the case in which the parameter-imprinting channel is affected by non-Markovian noise and the probes used for sensing are initially in a thermal state. We will investigate whether one can obtain some quantum advantage when putting a cap on the energy available for the estimation, as it happens when, instead of energy, one considers time as the limited resource.

In Chapter 6 we move to the realm of continuous variable Gaussian systems. We will give simple analytical formulae that allow to determine when it is possible to achieve the ultimate precision in a multiparameter estimation problem. As an application of our results, we will study a simple example in which one wants to estimate the relative phase between two arms of an interferometer and at the same time two parameters characterizing the noise affecting them.

In Chapter 7 we will introduce a non-Markovianity witness for Gaussian channels based on the breakdown of monotonicity of a measure of quantum discord of bipartite Gaussian systems. Moreover, we will characterize continuous time Gaussian channels according to their divisibility properties. We will classify these channels according to their non-Markovianity degree: a time-continuous Gaussian channel could be Markovian, weak or strongly

## INTRODUCTION

non-Markovian. Eventually, we will look for an operational interpretation of this non-Markovianity degree.

In Chapter 8 we will study the connection between phase-covariant Gaussian channels and teleportation protocols which exploit resources with finite entanglement and steerability. We will therefore tackle the problem of determining the best resource state for certified and certified secure teleportation of an ensemble of coherent states of light.

Finally, in the last Chapter, we will draw the conclusions.

Part I.  
Preliminaries



---

## QUANTUM INFORMATION IN A (TINY) NUTSHELL

---

In this Chapter we will summarise the basic notions of quantum mechanics and quantum information necessary to read this thesis. We will first introduce the tools to describe quantum systems and we will define some crucial quantities and properties of these systems. We refer the reader who wishes to delve deeper into these concepts, to the textbook [8]. In the last part of this first section we will give a brief zoology of the possible correlations present in bipartite quantum systems. In the second and last section we will provide a bird's-eye-view introduction about the dynamics of open quantum systems. This section is based on the exhaustive textbooks [2, 9].

### 1.1 QUANTUM SYSTEMS

#### 1.1.1 *Pure states and selective measurements*

A quantum system is a physical system whose relevant degrees of freedom (what we wish to measure at some point) are associated to hermitian operators acting on a Hilbert space  $\mathcal{H}$  of some dimension  $d^1$ . Depending on the degrees of freedom we are interested in, the Hilbert space we focus on to describe the system may vary considerably. As an example consider the case of our system of interest being an electron, before deciding *how* to describe the state of such a system, we should first ask ourselves *what* we want to describe: its angular momentum with respect to another system? Its position and momentum? Or is it sufficient, for our purposes, to focus our attention on its spin? The answer to the *what*-question

---

<sup>1</sup> A Hilbert space is a vector space with an inner product  $\langle \cdot | \cdot \rangle$ , such that the metric induced by this inner product turns  $\mathcal{H}$  into a complete metric space.

gives us a set of *observables*  $\{\hat{O}_k\}$ , i.e. Hermitian operators acting on a Hilbert space  $\mathcal{H} = \text{Span}\{|\phi_i\rangle, i = 1 \dots d \text{ s.t. } \langle\phi_i|\phi_j\rangle = \delta_{ij}\}$ . Every observable admits a spectral decomposition :  $\hat{O} = \sum_i^d \omega_i |\phi_i\rangle\langle\phi_i|$ , where  $|\phi_i\rangle$  is some orthonormal basis of  $\mathcal{H}$  (and therefore  $\sum_i^d |\phi_i\rangle\langle\phi_i| = \mathbb{1}_d$ ) and  $\omega_i \in \mathbb{R}$  are the possible outcomes of a measurement of  $\hat{O}$ . A unit vector of the Hilbert space,  $|\psi\rangle = \sum_i^d c_i |\phi_i\rangle \in \mathcal{H}$ , such that  $\langle\psi|\psi\rangle = \sum_i |c_i|^2 = 1$ , is a *pure state*, and it describes a *closed system*, i.e. one that has never interacted with any other quantum system but only with classical fields. Two unit vectors differing only by a phase, e.g.  $|\psi\rangle$  and  $e^{i\theta}|\psi\rangle$ , describe the same physical state. A measurement of the observable  $\hat{O}$  on the system described by  $|\psi\rangle$  gives a random outcome  $\omega_i$  with probability  $p_i = |\langle\phi_i|\psi\rangle|^2$ , and, if the outcome of the measurement is recorded, in which case we say that the measurement is *selective*, the state of the system after the measurement,  $|\psi'\rangle$ , becomes the corresponding eigenvector  $|\psi'\rangle = |\phi_i\rangle$ . This kind of measurement operation is known in the literature as *projective measurement* and, as the name suggests, it is described by a set of projectors  $\{\hat{\Pi}_i = |\phi_i\rangle\langle\phi_i|\}$ . The post-measurement state can be rewritten as  $|\psi'\rangle = \hat{\Pi}_i |\psi\rangle / \sqrt{p_i}$ , with  $p_i = |\hat{\Pi}_i |\psi\rangle|^2$ . Projective measurements are very invasive since they cause an abrupt change of the state of the system and no other information about the degree of freedom, described by  $\hat{O}$ , of the system  $|\psi\rangle$  can be inferred from the state after the measurement. Indeed, if we measure again the observable  $\hat{O}$  on the state  $|\psi'\rangle$ , we would obtain the same outcome  $\omega_i$  with probability 1, independently on the state  $|\psi\rangle$  prior to the first measurement, and, given that the projectors  $\hat{\Pi}_i$  are idempotent  $\hat{\Pi}_i^2 = \hat{\Pi}_i$ , the new state would be  $|\psi''\rangle = \hat{\Pi}_i |\psi'\rangle / |\hat{\Pi}_i |\psi'\rangle| = |\psi'\rangle$ . In order to gain new information, one has to re-prepare the system in its initial state  $|\psi\rangle$  and perform another measurement. The expectation value of the measurement of an observable on a system is the weighted sum of the possible outcomes of such a measurement, i.e.

$$\langle\hat{O}\rangle = \langle\psi|\hat{O}|\psi\rangle = \sum_i \omega_i \langle\psi|\phi_i\rangle\langle\phi_i|\psi\rangle = \sum_i p_i \omega_i . \quad (1.1)$$

One can extend the notion of measurement we just presented to more general *non-projective* measurements, known as Positive Operator-Valued Measurements (POVMs). This is necessary whenever one wants to consider measurements that do not leave the state invariant when repeated, as

often observed in experiments. A POVM is described by a set of hermitian operators  $\{\hat{M}_k\}$ , each associated with a measurement outcome  $m_k$ , such that

$$\sum_k \hat{M}_k^\dagger \hat{M}_k = \mathbb{1}, \quad \text{and} \quad \hat{M}_k^\dagger \hat{M}_k \geq 0. \quad (1.2)$$

The probability of obtaining the outcome  $m_k$  when measuring the pure state  $|\psi\rangle$  is given by  $p_k = \langle \psi | \hat{M}_k^\dagger \hat{M}_k | \psi \rangle$ . Eq.1.2 is necessary to ensure that these probabilities sum up to unity  $\sum_k p_k = 1$ . If the outcome of the measurement is registered to be  $m_k$ , the state of the system transforms as  $|\psi'\rangle = \hat{M}_k |\psi\rangle / \sqrt{p_k}$ . It is clear that if these operators are orthogonal projectors, i.e.  $\hat{M}_k = |\phi_k\rangle\langle\phi_k|$ , we recover the projective measurement discussed above. However, in general, since  $\hat{M}_k^2 \neq \hat{M}_k$ , on the contrary to the projective measurement case,  $M_k |\psi'\rangle = M_k^2 |\psi\rangle / \sqrt{p_k} \neq |\psi'\rangle$ .

We consider now the pure state of a system  $S$  which can be decomposed into two subsystems,  $A$  and  $B$ . This bipartite pure state is described by a vector in the Hilbert space  $\mathcal{H} = \mathcal{H}_A \otimes \mathcal{H}_B$ . If the two subsystems have never interacted with each other, nor with any other system, then each of them is described by a vector in the respective Hilbert spaces and the state of the composite system  $S$  is simply  $|\psi\rangle_S = |\zeta\rangle_A \otimes |\xi\rangle_B$ , with  $|\zeta\rangle_A \in \mathcal{H}_A$  and  $|\xi\rangle_B \in \mathcal{H}_B$ . This state is a pure *separable* state, or *product state*. When a pure state is not separable, i.e.  $|\psi\rangle_S \neq |\zeta\rangle_A \otimes |\xi\rangle_B$ , then it is said to be *entangled*, in which case the two subsystems are not pure states. A pure entangled state can be prepared by applying, to a pure product state, a unitary  $e^{-i\hat{O}_A \otimes \hat{O}_B}$ , with  $\hat{O}_{A(B)} = \hat{O}_{A(B)}^\dagger$ , acting on the Hilbert space of the composite system  $\mathcal{H}_S$ . In general, if  $\{|\phi_i\rangle_A\}_{i=1}^{d_A}$  and  $\{|\varphi_j\rangle_B\}_{j=1}^{d_B}$  are two orthonormal basis for  $\mathcal{H}_A$  and  $\mathcal{H}_B$  respectively, a pure state of the composite system  $S$  is described by a unit vector in  $\mathcal{H}_S$ :

$$|\psi\rangle_S = \sum_{i=1}^{d_A} \sum_{j=1}^{d_B} c_{ij} |\phi_i\rangle_A \otimes |\varphi_j\rangle_B, \quad (1.3)$$

with  $\sum_{i=1}^{d_A} \sum_{j=1}^{d_B} |c_{ij}|^2 = 1$ . Thanks to the Schmidt decomposition theorem we know that for any state  $|\psi\rangle_S$  there exists an orthonormal basis  $\{|\tilde{\phi}_k\rangle_A\}$  for  $\mathcal{H}_A$ , and  $\{|\tilde{\varphi}_k\rangle_B\}$  for  $\mathcal{H}_B$ , such that

$$|\psi\rangle_S = \sum_{k=1}^d \lambda_k |\tilde{\phi}_k\rangle_A \otimes |\tilde{\varphi}_k\rangle_B, \quad (1.4)$$

with  $d = \min\{d_A, d_B\}$  and  $\sum_k |\lambda_k|^2 = 1$ . The coefficients  $\lambda_k$  are called Schmidt coefficients. It is obvious that a product state has only one Schmidt coefficient different from zero:  $\lambda_i = 1$  and  $\lambda_j = 0$  for  $j \neq i$ .

We conclude this section by stating a crucial property of pure states, with important consequences for quantum communication and quantum cryptography: a pure quantum state cannot be cloned [10, 11]. This property is captured by the so-called no-cloning theorem, which states that, given a separable pure state  $|\psi\rangle \otimes |\Sigma\rangle$  where  $|\psi\rangle$  has been secretly prepared, it does not exist a unitary  $\hat{U}$  through which one can “duplicate”  $|\psi\rangle$  onto  $|\Sigma\rangle$  [10, 11]:

**Theorem 1.1. (No-cloning)** *Given  $|\psi_s\rangle \otimes |\Sigma\rangle \in \mathcal{H} \otimes \mathcal{H}$ , with  $|\psi_s\rangle \in \mathcal{S}$ , where  $\mathcal{S}$  is a set of non-orthogonal states,*

$$\nexists \hat{U} \text{ such that } \hat{U}|\psi_s\rangle \otimes |\Sigma\rangle = e^{i\theta} |\psi_s\rangle \otimes |\psi_s\rangle. \quad (1.5)$$

Notice that if,  $\mathcal{S}$  is a set of orthogonal states,  $\mathcal{S} = \{|\psi_0\rangle, |\psi_1\rangle\}$  with  $\langle \psi_1 | \psi_0 \rangle = 0$ , then it is possible to find a physical process which copies  $|\psi_s\rangle$  into the ancillary system. This was already noticed in [10] where the two authors pointed out that it is possible to clone the polarization degree of freedom of a photon if this is either horizontal or vertical,  $\mathcal{S} = \{|\leftrightarrow\rangle, |\updownarrow\rangle\}$  with  $\langle \leftrightarrow | \updownarrow \rangle = 0$ . However, they proved that the cloning task is impossible when the polarization is an arbitrary linear combination of the two,  $\mathcal{S} = \text{Span}\{|\leftrightarrow\rangle, |\updownarrow\rangle\}$ .

### 1.1.2 Beyond pure states: density matrix formalism

When the system under study cannot be assumed to be a pure state, meaning that at some point in the past it has interacted with some other system, the description with a unit vector  $|\psi\rangle$  is not sufficient anymore. In the most general case, one can describe a quantum system by an operator  $\hat{\rho}$  acting on the Hilbert space  $\mathcal{H}$ , which satisfies the following properties: (i) it is hermitian,  $\hat{\rho} = \hat{\rho}^\dagger$ ; (ii) it is positive-semidefinite,  $\hat{\rho} \geq 0$ ; (iii) it has unit trace,  $\text{Tr}\hat{\rho} = 1$ . We call any operator which satisfies (i)-(iii) *density matrix*, and with  $\mathcal{B}(\mathcal{H})$  we indicate the set of density matrices on a Hilbert space  $\mathcal{H}$ . Because of property (i), we know that there exists a unitary transformation  $\hat{U}$  which brings  $\hat{\rho}$  in diagonal form, moreover, not only its eigenvalues  $p_i$

are real but, because of properties (ii) and (iii), they are non-negative and sum up to unity. Mathematically, given a density operator  $\hat{\rho}$ , there exists an orthonormal basis  $\{|\psi_i\rangle\}_{i=1}^d$  such that

$$\hat{\rho} = \sum_{i=1}^d p_i |\psi_i\rangle \langle \psi_i|, \quad (1.6)$$

with  $0 \leq p_i \in \mathbb{R}$  such that  $\sum_{i=1}^d p_i = 1$ . When  $p_k = 1$ ,  $p_i = 0 \ \forall i \neq k$ ,  $\hat{\rho}$  describes the pure state  $|\psi_k\rangle$ ; in other words, the density matrix of a pure state corresponds to a projector  $\hat{\rho}_{\text{pure}} = |\psi_k\rangle \langle \psi_k|$ , hence  $\hat{\rho}_{\text{pure}}^2 = \hat{\rho}_{\text{pure}}$ . We can therefore define the purity of a state  $\hat{\rho}$  as

$$\mu = \text{Tr} \hat{\rho}^2 \leq 1, \quad (1.7)$$

and the inequality is saturated if and only if  $\hat{\rho}$  is a pure state. If a state is not pure, then it is said to be *mixed*; if  $p_i = 1/d \ \forall i = 1 \dots d$ , i.e.  $\hat{\rho} = \mathbb{1}/d$ , the state is said to be maximally mixed and the purity assumes the minimum possible value  $\mu = 1/d$ . Mixed states can be viewed as statistical mixtures of pure states  $\hat{\rho}_{\text{pure}}^{(i)} = |\psi_i\rangle \langle \psi_i|$ . It seems then natural to define the expectation value of an observable  $\hat{O}$  on a mixed state, as the weighted sum of its expectation values on every pure state of the statistical mixture:

$$\langle \hat{O} \rangle = \sum_i p_i \langle \psi_i | \hat{O} | \psi_i \rangle = \sum_i p_i \text{Tr} (\hat{O} |\psi_i\rangle \langle \psi_i|) = \text{Tr} (\hat{O} \hat{\rho}). \quad (1.8)$$

It is clear that the above coincides with Eq.1.1 when  $\hat{\rho}$  is a projector, i.e. a pure state.

We introduced above the concept of selective measurement, both projective and POVMs. Thanks to the density matrix formalism we can take now a step forward and consider the case in which the measurement outcome is not registered, or the case for which the measurement is performed on multiple copies of the state and the post-measurement states are then mixed. In these cases we talk of *non-selective* quantum measurements. For a general POVM  $\{M_i\}$ , the non-selective post-measurement state reads

$$\hat{\rho}' = \sum_i M_i \hat{\rho} M_i^\dagger = \sum_i p_i \hat{\rho}_i \quad \text{with} \quad \hat{\rho}_i = \frac{\hat{M}_i \hat{\rho} \hat{M}_i^\dagger}{p_i}, \quad (1.9)$$

where  $p_i = \text{Tr}(\hat{\rho} \hat{M}_i^\dagger \hat{M}_i)$  is the probability of obtaining a particular outcome  $m_i$ .

It is also worth mentioning that from Naimark's theorem, every POVM  $\{\hat{M}_i\}$  is equivalent to a projective measurement on a larger system, i.e. for every system  $\hat{\rho} \in \mathcal{B}(\mathcal{H})$  there exists a state  $\hat{\sigma} \in \mathcal{B}(\mathcal{H}_A)$  of an auxiliary system and a set of projectors  $\{\hat{\Pi}_i\}$  on  $\mathcal{H} \otimes \mathcal{H}_A$ , such that

$$\text{Tr} \left( \hat{\rho} \hat{M}_i^\dagger \hat{M}_i \right) = \text{Tr} \left( (\hat{\rho} \otimes \hat{\sigma}) \hat{\Pi}_i \right) . \quad (1.10)$$

### Quantum operations

We define *quantum operation* a mapping  $\Phi : \mathcal{B}(\mathcal{H}) \rightarrow \mathcal{B}(\mathcal{H})$  which is completely positive and trace preserving (CPTP), i.e.  $\text{Tr}(\hat{\rho}) = \text{Tr}(\Phi(\hat{\rho})) = 1$   $\forall \hat{\rho} \in \mathcal{B}(\mathcal{H})$  and such that  $\forall \hat{\rho} \in \mathcal{B}(\mathcal{H} \otimes \mathcal{H}_k)$ , with  $\mathcal{H}_k$  being a Hilbert space of arbitrary dimension  $\dim(\mathcal{H}_k) = k$ , the following holds:

$$\Phi \otimes \mathbb{1}_k(\hat{\rho}) \geq 0, \quad \forall k \in \mathbb{N}. \quad (1.11)$$

This latter condition reflects the expectation that any quantum state  $\hat{\rho}$  living in an extended Hilbert space is still a physical state (i.e. satisfies the properties (i)-(iii) for a physical density matrix) after the application of the map  $\Phi \otimes \mathbb{1}_A$ . A map  $\Phi : \mathcal{B}(\mathcal{H}) \rightarrow \mathcal{B}(\mathcal{H})$  such that  $\Phi \otimes \mathbb{1}_k(\hat{\rho}) \geq 0$ ,  $\forall \hat{\rho} \in \mathcal{B}(\mathcal{H} \otimes \mathcal{H}_k)$ , for  $k < d = \dim(\mathcal{H})$ , is said to be  $k$ -positive. One can show that a map is completely positive if and only if it is  $d$ -positive, i.e.  $\Phi \otimes \mathbb{1}_d(\hat{\rho}) \geq 0$ ,  $\forall \hat{\rho} \in \mathcal{B}(\mathcal{H} \otimes \mathcal{H})$ . It is obvious that  $k$ -positivity implies  $(k-1)$ -positivity, but a  $k$ -positive map is not necessarily  $(k+1)$ -positive.

Any quantum operation  $\Phi$  can be described by a set of operators  $\{\hat{K}_i\}$ , called Kraus operators, such that  $\sum_i \hat{K}_i^\dagger \hat{K}_i = \mathbb{1}$  and

$$\Phi(\hat{\rho}) = \sum_i \hat{K}_i \hat{\rho} \hat{K}_i^\dagger . \quad (1.12)$$

In general, the Kraus representation of a quantum map is not unique.

Thanks to the Choi-Jamilkowski isomorphism one can create a biunivocal correspondence between quantum operations and quantum states. One defines the Choi-Jamilkowski state (or simply Choi state) associated to the quantum operation  $\Phi$  as

$$\hat{\rho}_{\text{Choi}}^\Phi = \Phi \otimes \mathbb{1}(|\mathbb{E}\rangle\langle\mathbb{E}|) \in \mathcal{B}(\mathcal{H} \otimes \mathcal{H}), \quad (1.13)$$

where the state  $|\mathbb{E}\rangle \in \mathcal{B}(\mathcal{H} \otimes \mathcal{H})$  is

$$|\mathbb{E}\rangle = \frac{1}{\sqrt{d}} \sum_{i=1}^d |\phi_i\rangle \otimes |\phi_i\rangle, \quad (1.14)$$

for an orthonormal basis  $\{|\phi_i\rangle\}$  of  $\mathcal{H}$ .

### Fidelity

An important quantity in quantum information is the fidelity between two states:

$$F(\hat{\rho}_1, \hat{\rho}_2) = \text{Tr} \left( \sqrt{\sqrt{\hat{\rho}_1} \hat{\rho}_2 \sqrt{\hat{\rho}_1}} \right)^2, \quad (1.15)$$

The fidelity quantifies the distinguishability of the two quantum states  $\hat{\rho}_1$  and  $\hat{\rho}_2$ . Indeed, it is equal to 1 if and only if  $\hat{\rho}_1 = \hat{\rho}_2$ , and vanishes if and only if the two states are orthogonal,  $\hat{\rho}_1 \hat{\rho}_2 = 0$ , and hence can be distinguished with certainty by some quantum measurement. Moreover, given a POVM  $\{\hat{M}_i\}$ , the similarity between the associated measurement outcome probability distributions over the two states,  $P_{1(2)}^{(i)} = \text{Tr}(\hat{\rho}_{1(2)} \hat{M}_i^\dagger \hat{M}_i)$ , quantified by their overlap

$$\Theta_{1-2}(\{\hat{M}_i\}) = \sum_i \sqrt{P_1^{(i)} P_2^{(i)}}, \quad (1.16)$$

is lower bounded by the fidelity [12]

$$\Theta_{1-2}(\{\hat{M}_i\}) \geq F(\hat{\rho}_1, \hat{\rho}_2). \quad (1.17)$$

The minimization of  $\Theta_{1-2}(\{\hat{M}_i\})$  over all possible POVMs allows to saturate the above inequality. This is telling us that the fidelity quantifies how reproducible are the measurement statistics of any POVM on  $\hat{\rho}_1$  by measuring  $\hat{\rho}_2$ .

Thanks to the fidelity, one can define a distance function on the space of quantum states  $\mathcal{B}(\mathcal{H})$ :

$$D_B(\hat{\rho}_1, \hat{\rho}_2) = \sqrt{2 \left( 1 - \sqrt{F(\hat{\rho}_1, \hat{\rho}_2)} \right)}, \quad (1.18)$$

this is known as the Bures distance. An important property of  $D_B$  is that it is contractive under quantum operations, i.e. the following holds

$$D_B(\hat{\rho}_1, \hat{\rho}_2) \geq D_B(\Phi(\hat{\rho}_1), \Phi(\hat{\rho}_2)), \quad (1.19)$$

for any  $\hat{\rho}_1, \hat{\rho}_2 \in \mathcal{B}(\mathcal{H})$  and for any quantum operation  $\Phi$ .

### Partial tracing

We will consider now a bipartite system described by a density matrix  $\hat{\rho}_{AB}$ . We ask ourselves: how can we describe the state of one of the two subsystems? This is a crucial question if, for example, an observer has access to

only one subsystem, say  $A$ , meaning that they cannot perform measurements on  $B$ . The description of the state for such a subsystem must contain all the information that can be extracted, by means of local measurements, i.e. measurements of observables of the kind  $\hat{O}_A \otimes \mathbb{1}_B$ , by the observer. We hence define the *reduced density matrix* for subsystem  $A$  as

$$\hat{\rho}_A \equiv \text{Tr}_B \hat{\rho}_{AB} = \sum_{j=1}^{d_B} \langle \phi | \hat{\rho}_{AB} | \phi \rangle_B, \quad (1.20)$$

where  $\text{Tr}_B$  indicates the so-called *partial trace* and is defined by the second equality with  $\{|\phi\rangle_B\}$  being an orthonormal basis for  $\mathcal{H}_B$ . This operation corresponds to averaging over the degrees of freedom of subsystem  $B$ . The measurement statistics of any observable pertaining only to subsystem  $A$  is contained in  $\hat{\rho}_A$  defined by Eq.1.20.

If the composite system is a pure state  $|\psi\rangle_S$ , thanks to the Schmidt decomposition Eq.1.4, it is easy to verify that the reduced states for the two subsystems read

$$\hat{\rho}_A = \sum_{k=1}^d \lambda_k |\tilde{\phi}\rangle_A \langle \tilde{\phi}|, \quad \hat{\rho}_B = \sum_{k=1}^d \lambda_k |\tilde{\phi}\rangle_B \langle \tilde{\phi}|. \quad (1.21)$$

### *No-broadcasting theorem*

We have previously seen that, as a consequence of the no-cloning Theorem, Theorem 1.1, pure states cannot be copied. This result has been extended to mixed states [13] and goes by the name of no-broadcasting theorem. Let us suppose that a system  $S$  is secretly prepared in one of either states  $\hat{\rho}_s \in \mathcal{S} = \{\hat{\rho}_0, \hat{\rho}_1\} \subset \mathcal{H}_S$ , and that one wants to copy such a state on an ancillary system  $\hat{\sigma} \in \mathcal{H}_A$ , with  $\dim(\mathcal{H}_S) = \dim(\mathcal{H}_A)$ . We consider these two systems initially in a product state  $\hat{\rho}_s \otimes \hat{\sigma}$ . It can be shown that a quantum operation  $\Phi : \mathcal{B}(\mathcal{H}_S \otimes \mathcal{H}_A) \rightarrow \mathcal{B}(\mathcal{H}_S \otimes \mathcal{H}_A)$  such that

$$\text{Tr}_A (\Phi(\hat{\rho}_s \otimes \hat{\sigma})) = \hat{\rho}_s, \quad \text{and} \quad \text{Tr}_S (\Phi(\hat{\rho}_s \otimes \hat{\sigma})) = \hat{\rho}_s, \quad (1.22)$$

for both  $s = 0, 1$ , does not exist, unless the two states are identical  $\hat{\rho}_0 = \hat{\rho}_1$  or orthogonal  $\hat{\rho}_1 \hat{\rho}_0 = 0$ .

### *Information content of a quantum state*

In classical information theory, given a discrete random variable  $X$  with possible outcomes  $x = \{x_1, \dots, x_d\}$ , and associated probability distribution

$p(X) = \{p(x_1), \dots, p(x_d)\}$ , one can define the Shannon entropy  $H(X) = -\sum_{i=1}^d p(x_i) \log p(x_i)$ , which is an indicator of the “unpredictability” of the random variable  $X$ . Indeed,  $S(X)$  is maximal for equiprobable events, i.e.  $p(x_i) = 1/d$ ,  $\forall i$ , and vanishes when the outcome is certain, i.e.  $p(x_j) = 1$  and  $p(x_i) = 0$ ,  $\forall i \neq j$ . The Shannon entropy can also be regarded as the information content of a string composed by characters  $x_i$  in the alphabet  $x$ , each appearing with probabilities  $p(x_i)$ , i.e. the average number of bits per letter in the string that have to be transmitted in order to reconstruct the string.

Analogously, it is possible to define the Von Neumann entropy for a quantum state  $\hat{\rho} \in \mathcal{B}(\mathcal{H})$  with  $\dim \mathcal{H} = d$ , which tells us the information content of a quantum state:

$$S(\hat{\rho}) = \text{Tr}(\hat{\rho} \log \hat{\rho}) . \quad (1.23)$$

We can identify with  $x$  the set of outcomes of a measurement of a non-degenerate observable  $\hat{O}$  such that  $[\hat{O}, \hat{\rho}] = 0$ , the probabilities  $p(x_i)$  correspond to the eigenvalues  $p_i$  of the density matrix. In some orthonormal basis  $\{|\psi_i\rangle\}$  we have  $\hat{\rho} = \sum_i p_i |\psi_i\rangle\langle\psi_i|$ , then Eq.1.23 can be rewritten as

$$S(\hat{\rho}) = \sum_{i=1}^d p_i \log p_i . \quad (1.24)$$

It is easy to see that  $0 \leq S(\hat{\rho}) \leq \log d$ . The lower bound is saturated when the state considered is a pure state, described by a projector on  $\mathcal{H}$ . The upper bound is saturated for maximally mixed states. It can be shown that the Von Neumann entropy, Eq.1.23, has several properties: it is concave,  $S(\sum_k \lambda_k \hat{\rho}_k) \geq \sum_k \lambda_k S(\hat{\rho}_k)$  for  $\sum_k \lambda_k = 1$ , i.e. the entropy grows under mixing, it is invariant under unitary transformation  $S(\hat{\rho}) = S(\hat{U} \hat{\rho} \hat{U}^\dagger)$ , it is additive for product states,  $S(\hat{\rho}_A \otimes \hat{\rho}_B) = S(\hat{\rho}_A) + S(\hat{\rho}_B)$ , it is strongly subadditive, given any  $\hat{\rho}_{ABC} \in \mathcal{B}(\mathcal{H}_A \otimes \mathcal{H}_B \otimes \mathcal{H}_C)$  one has  $S(\hat{\rho}_{ABC}) + S(\hat{\rho}_C) \leq S(\hat{\rho}_{BC}) + S(\hat{\rho}_{AC})$  and, by taking  $\hat{\rho}_{ABC} = \hat{\rho}_{AC} \otimes |\psi\rangle_C \langle\psi|$  one immediately gets the subadditive property

$$S(\hat{\rho}_{AB}) \leq S(\hat{\rho}_A) + S(\hat{\rho}_B) . \quad (1.25)$$

## 1.1.3 Correlations

Eq.1.25 tells us that the information content of a composite bipartite system cannot be greater than the information content of both the subsystems, i.e. when considering  $\hat{\rho}_A$  and  $\hat{\rho}_B$  as separate systems, there could be some redundant information. This redundant information, when present, is due to the correlations between the subsystems.

*Mutual information and classical correlations*

The redundant information contained in the subsystems  $\hat{\rho}_A$  and  $\hat{\rho}_B$  is the *mutual information*

$$\mathcal{I}(\hat{\rho}_{AB}) = S(\hat{\rho}_A) + S(\hat{\rho}_B) - S(\hat{\rho}_{AB}) . \quad (1.26)$$

This quantity is invariant under local unitaries, and it is non-increasing under local quantum operations.

In classical information theory, given two random variables  $X$  and  $Y$  with possible set of outcomes  $(x, y)$  and associated joint probability distribution  $p_{xy}$  one can define the mutual information in three equivalent ways:

$$\mathcal{M}(X : Y) = H(X) - H(X|Y) = H(Y) - H(Y|X) , \quad (1.27)$$

$$\mathcal{I}(X : Y) = H(X) + H(Y) - H(X, Y) , \quad (1.28)$$

where  $H(X|Y)$  is the conditional entropy of  $X$  given  $Y$

$$H(X|Y) = \sum_y p_y H(X|Y = y) , \quad (1.29)$$

with  $p_y = \sum_x p_{xy}$  (and analogously  $H(Y|X) = \sum_x p_x H(Y|X = x)$ , with  $p_x = \sum_y p_{xy}$ ). The equivalence between the above equations follows from Bayes rule  $p_{x|y} = p_{xy}/p_y$ , which gives  $H(X|Y) = H(X, Y) - H(Y)$ . This latter equation tells us that  $H(X, Y) \geq H(X)$ , and analogously one finds  $H(X, Y) \geq H(Y)$ . One immediately sees that this is not true in the quantum case:  $S(\hat{\rho}_{AB}) \not\geq S(\hat{\rho}_A), S(\hat{\rho}_B)$ . To see this it is sufficient to consider  $\hat{\rho}_{AB} = |\psi\rangle_{AB} \langle\psi|$  with  $|\psi\rangle_{AB} \neq |\phi\rangle_A \otimes |\varphi\rangle_B$ , for which  $S(\hat{\rho}_{AB}) = 0$  but  $S(\hat{\rho}_A), S(\hat{\rho}_B) > 0$ .

This difference between the classical and the quantum cases is reflected in the non-equivalence of Eq.1.27 and Eq.1.28 in the quantum case [14, 15].

Indeed, the quantum equivalent of  $H(X|Y)$  requires to specify the state of subsystem  $A$  given the state of  $B$ , which is an ambiguous concept. However, one can construct an analogous quantity for the quantum case by selecting a POVM  $\{\hat{M}_i^B\}$ . Indeed, one can specify the state of  $A$  given that a measurement on  $B$  produced an outcome  $m_i^B$ . One hence defines

$$\mathcal{M}(\hat{\rho}_{AB}, A : B)_{\{\hat{M}_i^B\}} = S(\hat{\rho}_A) - S(\hat{\rho}_A | \{\hat{M}_i^B\}), \quad (1.30)$$

where

$$S(\hat{\rho}_A | \{\hat{M}_i^B\}) = \sum_i p_i S\left(\frac{\text{Tr}_B(\mathbb{1} \otimes \hat{M}_i^B \hat{\rho}_{AB} \mathbb{1} \otimes \hat{M}_i^{B\dagger})}{p_i}\right), \quad (1.31)$$

with  $p_i = \text{Tr}(\mathbb{1} \otimes \hat{M}_i^B \hat{\rho}_{AB} \mathbb{1} \otimes \hat{M}_i^{B\dagger})$ . The quantity  $\mathcal{M}(\hat{\rho}_{AB}, A : B)_{\{\hat{M}_i^B\}}$  represents the information about the system  $A$ , gained by measuring the POVM  $\{\hat{M}_i^B\}$  on the system  $B$ . Maximizing this quantity above all possible POVMs on  $B$  one finds the classical correlations of the composite system with respect to the bipartition  $A : B$

$$\mathcal{C}(\hat{\rho}_{AB}, A : B) = \max_{\{\hat{M}_i^B\}} \mathcal{M}(\hat{\rho}_{AB}, A : B)_{\{\hat{M}_i^B\}}. \quad (1.32)$$

Notice that this definition is in general asymmetric:  $\mathcal{C}(\hat{\rho}_{AB}, A : B) \neq \mathcal{C}(\hat{\rho}_{AB}, B : A)$ .

### Quantum Discord

We can hence split the mutual information of the system  $\hat{\rho}_{AB}$  into two contributions: a classical contribution and a quantum one. The first is given by Eq.1.32 and the second, which is called *quantum discord* (or simply *discord*), by [14, 15]

$$\mathcal{D}(\hat{\rho}_{AB}, A : B) = \mathcal{I}(\hat{\rho}_{AB}) - \mathcal{C}(\hat{\rho}_{AB}, A : B). \quad (1.33)$$

As for the classical correlations, also the quantum discord is, in general, asymmetric:  $\mathcal{D}(\hat{\rho}_{AB}, A : B) \neq \mathcal{D}(\hat{\rho}_{AB}, B : A)$ . The reason of this asymmetry is that both classical correlations and quantum discord, by definition, depend on measurements performed on either of the two subsystems. A particular case to consider is that of the so-called *quantum-classical* states:

$$\hat{\rho}_{AB}^{\text{qc}} = \sum_i p_i \hat{\rho}_A^{(i)} \otimes |\varphi_i\rangle_B \langle \varphi_i|, \quad (1.34)$$

for some orthonormal basis  $\{|\varphi_i\rangle_B\}$  of  $\mathcal{H}_B$  and quantum states  $\hat{\rho}_A^{(i)} \in \mathcal{B}(\mathcal{H}_A)$ . For this kind of states one has  $\mathcal{D}(\hat{\rho}_{AB}^{\text{qc}}, A : B) = 0$ , however, in general  $\mathcal{D}(\hat{\rho}_{AB}^{\text{qc}}, B : A) \neq 0$ . Swapping the roles of  $A$  and  $B$  one gets the *classical-quantum* states. States with zero discord for measurements on either one of the two subsystems,  $\mathcal{D}(\hat{\rho}_{AB}, A : B) = \mathcal{D}(\hat{\rho}_{AB}, B : A) = 0$ , are only classically correlated and they take the form

$$\hat{\rho}_{AB}^{\text{cl}} = \sum_{ij} p_{ij} |\phi_i\rangle_A \langle\phi_i| \otimes |\varphi_j\rangle_B \langle\varphi_j| , \quad (1.35)$$

where  $p_{ij}$  is a joint probability distribution and  $\{|\phi_i\rangle_A\}$  and  $\{|\varphi_j\rangle_B\}$  are orthonormal bases for  $\mathcal{H}_A$  and  $\mathcal{H}_B$ , respectively. The reduced states for subsystems  $A$  and  $B$  are

$$\hat{\rho}_A = \sum_i p_i^A |\phi_i\rangle_A \langle\phi_i| , \quad \hat{\rho}_B = \sum_j p_j^B |\varphi_j\rangle_B \langle\varphi_j| , \quad (1.36)$$

where  $p_i^A = \sum_j p_{ij}$  and  $p_j^B = \sum_i p_{ij}$ .

Two important properties of quantum discord are that it is invariant under local unitaries, i.e.

$$\mathcal{D}(\hat{\rho}_{AB}, A : B) = \mathcal{D}(\hat{U}_A \otimes \hat{U}_B \hat{\rho}_{AB} \hat{U}_A^\dagger \otimes \hat{U}_B^\dagger, A : B) , \quad (1.37)$$

for any state  $\hat{\rho}_{AB}$  and any local unitary operation  $\hat{U}_A$  and  $\hat{U}_B$  acting on subsystems  $A$  and  $B$ , respectively. Moreover it is monotonically non-increasing under local quantum operations on the subsystem which is not being measured:

$$\mathcal{D}(\hat{\rho}_{AB}, A : B) \geq \mathcal{D}(\Phi \otimes \mathbb{1}_B(\hat{\rho}_{AB}), A : B) . \quad (1.38)$$

For a comprehensive review on various approaches to define and quantify general quantum correlations, we refer the reader to [16].

### Entanglement

We can now extend the concept of separable states, already introduced for pure states, to the mixed case. We define a separable mixed state as a convex combination of product pure state projectors:

$$\hat{\rho}_{AB}^{\text{sep}} = \sum_i p_i |\phi_i\rangle_A \langle\phi_i| \otimes |\varphi_i\rangle_B \langle\varphi_i| , \quad (1.39)$$

where  $\{|\phi\rangle_A\}$  and  $\{|\varphi\rangle_B\}$  are arbitrary pure states of  $\mathcal{H}_A$  and  $\mathcal{H}_B$ , in general non-orthogonal. We can therefore define all states  $\hat{\rho}_{AB} \in \mathcal{B}(\mathcal{H})$  which are not separable as *entangled*. Notice that there exist separable states which possess quantum correlations of discord-type. This implies that entanglement is a type of correlation stronger than quantum discord.

Introducing the partial transpose of the density matrix  $\hat{\rho}_{AB}$  defined as the matrix  $\hat{\rho}_{AB}^\Gamma$  such that

$${}_B\langle\varphi_l| {}_A\langle\phi_i|\hat{\rho}_{AB}^\Gamma|\phi_j\rangle_A|\varphi_k\rangle_B \equiv {}_B\langle\varphi_k| {}_A\langle\phi_i|\hat{\rho}_{AB}|\phi_j\rangle_A|\varphi_l\rangle_B , \quad (1.40)$$

(where  $|\phi\rangle_A|\varphi\rangle_B \equiv |\phi\rangle_A \otimes |\varphi\rangle_B$ ) we enunciate the Positivity of Partial Transpose (PPT) criterion (or Peres-Horodecki criterion)

**Theorem 1.2. (PPT criterion)** *If  $\hat{\rho}_{AB} \in \mathcal{B}(\mathcal{H} \otimes \mathcal{H})$  is a separable state, Eq.1.39, then*

$$\hat{\rho}_{AB}^\Gamma \geq 0 , \quad (1.41)$$

with  $\hat{\rho}_{AB}^\Gamma$  defined in Eq.1.40

The Positivity of the Partial Transpose (PPT), Eq.1.41, is, in general, a necessary but not sufficient condition for  $\hat{\rho}_{AB}$  being a separable state, hence, if a quantum state satisfies Eq.1.41 it is not possible to conclude that it is separable. On the other hand, any state which violates it is entangled. One can hence define the *logarithmic-negativity* [17]

$$\mathcal{N}_{\log}(\hat{\rho}_{AB}) = \log_2 \|\hat{\rho}_{AB}^\Gamma\|_1 , \quad (1.42)$$

where  $\|\cdot\|_1$  indicates the trace norm<sup>2</sup>. Obviously, because of Theorem 1.2, the above measure vanishes on all separable state, however it vanishes also on some entangled state, the so-called *bound entangled* states. For this reason  $\mathcal{N}_{\log}$  is said to be *non-faithful*. The logarithmic negativity is non-increasing under Local Operations and Classical Communication (LOCC):

$$\mathcal{N}_{\log}(\hat{\rho}_{AB}) \geq \mathcal{N}_{\log}(\Lambda(\hat{\rho}_{AB})) , \quad (1.43)$$

where  $\Lambda$  is a LOCC which consists of local quantum operations on subsystems  $A$  and  $B$ , combined with classical communication between  $A$  and  $B$ .  $\mathcal{N}_{\log}$  is additive on product states.

<sup>2</sup> For any operator  $X$ , its trace norm is defined as  $\|X\|_1 = \text{Tr}\sqrt{X^\dagger X}$ .

A lot of effort has been devoted to define quantitative measures of entanglement [3], the logarithmic-negativity defined above is only one of the many and we introduced it because of its relevance and ease of computability in the case of Gaussian states (see Chapter 2). We will introduce now just another entanglement measure, which we are going to use in Chapter 4 in the particular case of two-qubits<sup>3</sup> systems, namely the *entanglement of formation* (EoF) [18]: given a bipartite quantum system  $\hat{\rho}_{AB}$ , we consider all its pure-state decompositions, i.e. all  $\{p_i, |\psi_i\rangle\}$  such that

$$\hat{\rho}_{AB} = \sum_i p_i |\psi_i\rangle_{AB} \langle \psi_i|_{AB} . \quad (1.44)$$

For each pure state one can define the *entropy of entanglement* as

$$\mathcal{E}_S(|\psi\rangle_{AB}) = S(\hat{\rho}_A) = S(\hat{\rho}_B) , \quad (1.45)$$

with  $\hat{\rho}_{A(B)} = \text{Tr}_{B(A)}(|\psi\rangle_{AB} \langle \psi|_{AB})$ , and  $S(\cdot)$  as in Eq.1.23 (obviously  $\mathcal{E}_S(|\psi\rangle_{AB}) = 0$  iff  $|\psi\rangle_{AB}$  is separable). The EoF for the state  $\hat{\rho}_{BC}$  is defined as the average entropy of entanglement of the pure states of the decomposition, minimized over all decompositions:

$$\mathcal{E}_F(\hat{\rho}_{AB}) = \min_{\{p_i, |\psi_i\rangle\}} \sum_i p_i \mathcal{E}(|\psi_i\rangle) . \quad (1.46)$$

The operational meaning of this quantity is the following: if two parties  $A$  and  $B$ , usually referred to as Alice and Bob, wish to create the state  $\hat{\rho}_{AB}$ , with  $\mathcal{E}_F(\hat{\rho}_{AB})$ , without any transfer of quantum states between them, then they must already share the equivalent of  $\mathcal{E}_F(\hat{\rho}_{AB})$  pure singlet states  $|\Psi_-\rangle = (|01\rangle - |10\rangle)/\sqrt{2}$ . It was shown in [19] that for a pair of qubits, the EoF is

$$\mathcal{E}_F(\hat{\rho}_{AB}) \equiv h \left( \frac{1 + \sqrt{1 - C(\hat{\rho}_{AB})^2}}{2} \right) , \quad (1.47)$$

with  $h(x) \equiv -x \log x - (1-x) \log (1-x)$ . The quantity  $C(\hat{\rho}_{AB})$ , also known as *concurrence*, can be computed as

$$C(\hat{\rho}_{AB}) = \max \{0, 2\lambda_{\max} - \text{Tr} \hat{R}(\hat{\rho}_{AB})\} , \quad (1.48)$$

where  $\lambda_{\max}$  is the largest eigenvalue of the operator  $\hat{R}(\hat{\rho}_{AB})$ , defined as

$$\hat{R}(\hat{\rho}_{AB}) = \sqrt{\sqrt{\hat{\rho}_{AB}} (\hat{\sigma}_y^{(A)} \otimes \hat{\sigma}_y^{(B)}) \hat{\rho}_{AB}^* (\hat{\sigma}_y^{(A)} \otimes \hat{\sigma}_y^{(B)}) \sqrt{\hat{\rho}_{AB}}} . \quad (1.49)$$

<sup>3</sup> A qubit is a physical system  $\hat{\rho} \in \mathcal{B}(\mathcal{H})$  with  $\dim(\mathcal{H}) = 2$ . In other words, a qubit is a two-level system.

### Quantum steering and Bell non-locality

Let us consider now the scenario in which there are two spatially separated parties, Alice and Bob. Alice sends to Bob a quantum state that, she claims, is part ( $B$ ) of an entangled state whose other part ( $A$ ) is in her possession. Bob however, does not trust Alice (or her measurement device), i.e. he does not make any assumption about her Hilbert space  $\mathcal{H}_A$ , so, in order to verify that she is telling the truth, he asks her to perform some measurement  $x = 1, \dots, n$  on her part and to communicate him the outcome  $a \in \lambda(x)$  of such a measurement, where  $\lambda(x)$  represents the set of outcomes corresponding to the measurement  $x$ . He will then measure the state in his possession and, by studying the correlations between his and Alice's measurement outcomes, he wishes to be able to tell whether they truly shared an entangled state [20,21]. Now, Bob will not be convinced by Alice's claim if, after Alice announces the pair  $(a, x)$ , Bob finds, after performing his set of measurements, that he is in possession of a conditional (unnormalized) state in the form

$$\hat{\sigma}_{a|x}^B = \sum_{\lambda} q_{\lambda} p(a|x, \lambda) \hat{\rho}_B^{(\lambda)}, \quad (1.50)$$

called *assemblage*, where  $p(a|x, \lambda)$  is the probability of obtaining the outcome  $a$  when the measurement  $x$  is performed by Alice and  $\lambda$  indicates some (hidden) classical variable he does not know about distributed according to  $q_{\lambda}$ . His skepticism is due to the following reasoning: Alice gave him some quantum state  $\hat{\rho}_{\lambda}^B$  drawn from some distribution  $q_{\lambda}$ , therefore, given a particular  $\lambda$  and announced pair  $(a, x)$ , Bob's conditional unnormalized state would be  $\hat{\sigma}_{a|x, \lambda} = q_{\lambda} p(a|x, \lambda) \hat{\rho}_{\lambda}^B$ , but since he has no access to the variable  $\lambda$ , he would observe the assemblage Eq.1.50, and this can indeed be reproduced by Alice performing projective measurements, described by mutually commuting observables, on her part of some separable state. Such an assemblage is called *unsteerable*. Hence, a bipartite quantum state  $\hat{\rho}_{AB}$  such that, given any set of measurements  $\{\hat{M}_{a|x}\}_x$  on Alice's part, Bob's assemblage

$$\hat{\sigma}_{a|x} = \text{Tr}_A \left( (\hat{M}_{a|x} \otimes \mathbb{1}_B) \hat{\rho}_{AB} (\hat{M}_{a|x}^{\dagger} \otimes \mathbb{1}_B) \right), \quad (1.51)$$

is equivalent to an assemblage in the form Eq.1.50, is said to be  $A \rightarrow B$  unsteerable and Bob, not trusting Alice, cannot certify that  $\hat{\rho}_{AB}$  is entangled.

On the other hand, if  $\hat{\rho}_{AB}$  is such that Eq.1.51 is not equivalent to Eq.1.50, then it is said to be  $A \rightarrow B$  steerable.

Let us assume now that Alice and Bob share a separable state in the form Eq.1.39. Given a set of measurement  $\{\hat{M}_{a|x}\}_x$  on Alice's side, the corresponding conditional assemblage on Bob's side reads

$$\hat{\sigma}_{a|x}^B = \sum_i p_i p(a|x; \hat{\rho}_A^{(i)}) \hat{\rho}_B^{(i)}. \quad (1.52)$$

Comparing the above with Eq.1.50, we notice that the latter is a generalization of the former, where the conditional probability of obtaining the outcome  $a$  when measuring  $x$  on Alice's state  $\hat{\rho}_A^{(i)}$ ,  $p(a|x; \hat{\rho}_A^{(i)})$ , becomes  $p(a|x, \lambda)$ . The conditional probability  $p(a|x; \hat{\rho}_A^{(i)})$  is constrained by Alice's Hilbert space  $\mathcal{H}_A$  and possibly by uncertainty relations between the measurements  $\{\hat{M}_{a|x}\}_x$ . On the other hand,  $p(a|x, \lambda)$ , is an unconstrained probability distribution, meaning that it does not depend on  $\mathcal{H}_A$  nor on any other quantum mechanical restriction. This implies that one can have a bipartite state which is not separable but it is unsteerable, i.e. steering is an asymmetric type of correlation (analogous reasoning to the above can be done in the case in which Bob is the untrusted party) stronger than entanglement.

Steering can be detected [22] by studying the correlations between measurements  $x$  of unknown observables  $\hat{A}_x = \sum_a a \hat{\Gamma}_{a|x}$  on Alice's side and measurements  $y$  of known observables  $\hat{B}_y \in \mathcal{B}(\mathcal{H}_B)$ :

$$\langle \hat{A}_x^l \otimes \hat{B}_y^j \rangle = \sum_a a^l \text{Tr} \left( \hat{\sigma}_{a|x}^B \hat{B}_y^j \right), \quad (1.53)$$

where  $l$  and  $j$  are integer powers. One can indeed define a moment matrix  $\Gamma_{ik} \equiv \langle \hat{S}_i^\dagger \hat{S}_k \rangle$ , where each operator  $\hat{S}_i$  is some product of operators for Alice and Bob. It is easy to check that, when constructed from physical observables on quantum states,  $\Gamma \geq 0$ . The algebraic properties satisfied by Bob's operators give rise to some linear constraints between the matrix elements of  $\Gamma$ , however, matrix elements which involve products of Alice's unknown operators alone, are treated as a set  $\mathcal{R}$  of arbitrary free parameters. Moreover, assuming commutativity of the observables  $\hat{A}_x$  (this is justified because, as we previously said, an unsteerable assemblage, Eq.1.50, can be reproduced by Alice measuring commuting observables on her part of a separable state) gives additional linear constraints.  $A \rightarrow B$  steering is therefore detected from  $\Gamma_{\mathcal{R}}$  when for any possible assignment  $\mathcal{R}$  of the free

parameters, one gets  $\Gamma_{\mathcal{R}} < 0$ . From this approach it is quite clear how quantum mechanical restrictions on Alice's measurements, have a crucial role in the steerability detection.

In the case in which both parties (or their measurement devices) are untrusted, i.e. without assuming anything about Alice's and Bob's Hilbert spaces, they can certify that a bipartite state  $\hat{\rho}_{AB}$  is entangled if it is *Bell-nonlocal* [23], i.e. if the correlations between the outcomes  $a$  and  $b$  of measurements  $x$  and  $y$  on Alice and Bob sides cannot be explained by a separable model of the form:

$$p(a, b|x, y) = \sum_{\lambda} q_{\lambda} p(a|x, \lambda) p(b|y, \lambda), \quad \forall x, y, a, b, \quad (1.54)$$

where, again,  $\lambda$  plays the role of some (hidden) classical variable. Both probability distributions,  $p(a|x, \lambda)$  and  $p(b|y, \lambda)$  are arbitrary and they are not subject to any quantum mechanical constraint. Bell-nonlocality is hence a symmetric kind of correlation stronger than steerability (and therefore stronger than entanglement). Detection of Bell-nonlocal correlation in a bipartite quantum state enable entanglement detection between the two parties in a device independent manner, i.e. it is possible to certify entanglement even without making any assumption on  $\mathcal{H}_A$  nor  $\mathcal{H}_B$ .<sup>4</sup>

## 1.2 QUANTUM DYNAMICS

A closed quantum system in a pure state evolves according to the Schrödinger equation (in natural units  $\hbar = 1$ )

$$i \frac{d}{dt} |\psi(t)\rangle = \hat{H}(t) |\psi(t)\rangle, \quad (1.55)$$

where  $\hat{H}(t)$  is the Hamiltonian of the system. The time dependence of the Hamiltonian is in principle due to some classical field interacting with the system. If the Hamiltonian does not depend explicitly on time, then the system is said to be *isolated*. The solution to the above is given by

$$|\psi(t)\rangle = \hat{U}(t, t_0) |\psi(t_0)\rangle, \quad (1.56)$$

<sup>4</sup> The curious reader who approaches these topics for the first time, is encouraged to read the enlightening fictional dialogue between Alice, Bob and Bell in Chapter 4 (updated version) of [24].

where  $\hat{U}(t, t_0)$  is a unitary operator defined as

$$\hat{U}(t, t_0) = \mathcal{T} \exp \left\{ -i \int_{t_0}^t ds \hat{H}(s) \right\} , \quad (1.57)$$

with  $\mathcal{T}$  indicating the time ordering operator. If the system is isolated, one simply gets  $\hat{U}(t, t_0) = \exp \{ -i\hat{H}(t - t_0) \}$ .

If the system is initially in a mixed state  $\hat{\rho}(t_0)$ , its evolution is described by the Liouville-Von Neumann equation

$$i \frac{d}{dt} \hat{\rho}(t) = -i [\hat{H}(t), \hat{\rho}(t)] , \quad (1.58)$$

with solution given by

$$\hat{\rho} = \hat{U}(t, t_0) \hat{\rho}(t_0) \hat{U}(t, t_0)^\dagger , \quad (1.59)$$

with  $\hat{U}(t, t_0)$  defined as in Eq.1.57. From now on, we will assume  $t_0 = 0$ , unless otherwise stated.

### 1.2.1 Stinespring dilation

We already anticipated that a quantum operation is a CPTP map. We can hence define a *quantum evolution*, usually called *dynamical map*, a one-parameter family of CPTP maps  $\Phi_t : \mathcal{B}(\mathcal{H}) \rightarrow \mathcal{B}(\mathcal{H})$  such that  $\Phi_0 = \mathbb{1}$ , where the parameter  $t$  plays the role of time. It can be shown that any quantum evolution  $\Phi_t$  is equivalent to the reduced unitary evolution of the system  $\hat{\rho} \in \mathcal{B}(\mathcal{H})$  with an initially uncorrelated ancillary system  $\hat{\sigma}$ . This important result is summarized in the following

**Theorem 1.3. (Stinespring)**  $\Phi_t : \mathcal{B}(\mathcal{H}_S) \rightarrow \mathcal{B}(\mathcal{H}_S)$  is a quantum evolution if and only if there exists an ancillary system  $\hat{\sigma} \in \mathcal{B}(\mathcal{H}_A)$  and a unitary  $\hat{U}(t) : \mathcal{B}(\mathcal{H}_S \otimes \mathcal{H}_A) \rightarrow \mathcal{B}(\mathcal{H}_S \otimes \mathcal{H}_A)$  such that

$$\Phi_t(\hat{\rho}) = \text{Tr}_A \left( \hat{U}(t) \hat{\rho} \otimes \hat{\sigma} \hat{U}(t)^\dagger \right) , \quad \forall \hat{\rho} \in \mathcal{B}(\mathcal{H}_S) . \quad (1.60)$$

Any quantum evolution, being a family of quantum operations, has a Kraus representation  $\{\hat{K}_i(t)\}$ .

A quantum evolution can hence describe the open dynamics of a quantum system  $S$ , or in other words, it describes the dynamics of an open quantum system (OQS). In general, an OQS is a quantum system  $S$  which

is coupled to another quantum system  $E$ , which we will refer to as the environment. By opportunely choosing  $E$ , the overall  $S + E$  quantum system can be considered closed, and its evolution is generated by the Hamiltonian

$$\hat{H}_{SE} = \hat{H}_S \otimes \mathbb{1}_E + \mathbb{1}_S \otimes \hat{H}_E + \hat{H}_I , \quad (1.61)$$

where the terms  $\hat{H}_S$  and  $\hat{H}_E$  are the self-Hamiltonians of the system and the environment, respectively, while  $\hat{H}_I$  describes the interaction between them.

### 1.2.2 Master equations for Markovian dynamics

Let us consider to have a quantum system  $S$  interacting with an environment  $E$ , the overall system evolves unitarily according to the Hamiltonian Eq.1.61 with

$$\hat{H}_I = \sum_{\alpha} \hat{S}_{\alpha} \otimes \hat{E}_{\alpha} , \quad (1.62)$$

with  $\hat{S}_{\alpha} \in \mathcal{B}(\mathcal{H}_S)$  and  $\hat{E}_{\alpha} \in \mathcal{B}(\mathcal{H}_E)$  Hermitian operators. In the interaction picture<sup>5</sup> the Liouville-Von Neumann equation, Eq.1.58, for  $\hat{\rho} \in \mathcal{B}(\mathcal{H}_S \otimes \mathcal{H}_E)$  becomes (we will use the calligraphic  $\hat{\rho}$  to indicate the density operator of the composite system and  $\hat{\rho}$  for the density operator of the system  $S$ )

$$\frac{d}{dt} \hat{\rho}^{(I)}(t) = -i \left[ \hat{H}_I(t), \hat{\rho}^{(I)}(t) \right] . \quad (1.63)$$

Assuming that

$$\text{Tr}_E[\hat{H}_I(t), \hat{\rho}(0)] = 0 , \quad (1.64)$$

(this can always be ensured by subtracting the term  $\text{Tr}_E[\hat{H}_I(t), \hat{\rho}(0)]$  from  $\hat{H}_I$  and including it instead in  $\hat{H}_S$ ) and tracing out the degrees of freedom of the environment, we can rewrite Eq.1.63 as

$$\frac{d}{dt} \hat{\rho}^{(I)}(t) = - \int_0^t ds \text{Tr}_E \left[ \hat{H}_I(t), \left[ \hat{H}_I(s), \hat{\rho}^{(I)}(s) \right] \right] , \quad (1.65)$$

<sup>5</sup> Given the general Hamiltonian  $\hat{H}(t) = \hat{H}_0 + \hat{H}_I(t)$ , in the interaction picture, one defines the unitaries  $\hat{U}_0(t) = \exp\{-i\hat{H}_0 t\}$  and  $\hat{U}_I(t) = \hat{U}_0^\dagger(t) \hat{U}(t)$ , with  $\hat{U}(t)$  defined as in Eq.1.57. Then an operator  $\hat{O}$  evolves as  $\hat{O}^{(I)}(t) = \hat{U}_0^\dagger(t) \hat{O} \hat{U}_0(t)$  and the density operator evolves as  $\hat{\rho}^{(I)}(t) = \hat{U}_I(t) \hat{\rho}(0) \hat{U}_I^\dagger(t)$  such that  $\langle \hat{O} \rangle(t) = \text{Tr}\{\hat{O}^{(I)}(t) \hat{\rho}^{(I)}(t)\}$ . In the case we are considering  $\hat{H}_0 = \hat{H}_S \otimes \mathbb{1}_E + \mathbb{1}_S \otimes \hat{H}_E$ .

for the density matrix  $\hat{\rho} \in \mathcal{B}(\mathcal{H}_S)$  of the system. Notice that this equation is exact, however, for most physical systems, it is intractable. Indeed, the right-hand side depends on the density matrix,  $\hat{\rho}^{(I)}$ , of the composite system evaluated at all times  $s \in [0, t]$ . Yet, it is possible to simplify it by making some approximations and further assumptions.

The first assumption is considering system and environment initially uncorrelated:

$$\hat{\rho}(0) = \hat{\rho}(0) \otimes \hat{\sigma}(0) . \quad (1.66)$$

Moreover, we assume the environment being in a stationary state of its self-Hamiltonian, i.e.  $[\hat{H}_E, \sigma(0)] = 0$ .

The first approximation we make is the Born approximation: we consider the interaction between the system and the environment sufficiently weak and the environment large in comparison with the size of the system (i.e.  $\dim \mathcal{H}_E \gg \dim \mathcal{H}_S$ ) such that (i) the influence of the system on the reservoir is small, meaning that the state of the environment is not affected by the interaction with the system, and that (ii) the system and the environment remain uncorrelated during the evolution:

$$\hat{\rho}(t) \approx \hat{\rho}(t) \otimes \sigma \quad \forall t \geq 0 . \quad (1.67)$$

This assumption together with the assumption of having the environment in a stationary state, results in having time-homogeneous environmental self-correlation functions:

$$\mathcal{C}_{\alpha\beta}(t, s) \equiv \text{Tr} \left( \hat{E}_\alpha^{(I)}(t) \hat{E}_\beta^{(I)}(s) \hat{\sigma} \right) = \mathcal{C}_{\alpha\beta}(t - s) . \quad (1.68)$$

The second approximation we make is the Markov approximation: we consider the environmental self-correlation functions, Eq.1.68, sharply peaked at  $t - s = 0$  and rapidly decaying, i.e. the timescale  $\tau_c$  such that for  $\tau \geq \tau_c$  one has  $\mathcal{C}_{\alpha\beta}(\tau) \approx 0$  is much smaller than the characteristic timescale  $\tau_S$  over which  $\hat{\rho}^{(I)}(t)$  changes noticeably. This approximation is equivalent to assume a ‘short-memory’ environment, i.e. the environment very quickly loses any self-correlation such that the outcome of a measurement of  $\hat{E}_\alpha$  at time  $t$  does not depend on the outcome of a measurement of  $\hat{E}_\beta$  at time  $s \lesssim t$ .

It is possible to show that with these approximations one can considerably simplify Eq.1.65, and, transforming the equation back to the Schrödinger picture<sup>6</sup>, one obtains the Born-Markov master equation

$$\frac{d}{dt}\hat{\rho}(t) = -i [\hat{H}_S, \hat{\rho}(t)] - \sum_{\alpha} ([\hat{S}_{\alpha}, \hat{B}_{\alpha}\hat{\rho}(t)] + [\hat{\rho}(t)\hat{C}_{\alpha}, \hat{S}_{\alpha}]) , \quad (1.69)$$

with

$$\hat{B}_{\alpha} \equiv \int_0^{\infty} d\tau \sum_{\beta} \mathcal{C}_{\alpha\beta}(\tau) \hat{S}_{\beta}^{(I)}(-\tau) , \quad (1.70)$$

$$\hat{C}_{\alpha} \equiv \int_0^{\infty} d\tau \sum_{\beta} \mathcal{C}_{\beta\alpha}(-\tau) \hat{S}_{\beta}^{(I)}(-\tau) . \quad (1.71)$$

This is a time-local master equation, i.e. the change of the reduced density matrix for the system at time  $t$  does not depend on the previous history of the evolution but only on the reduced density matrix itself at that precise time. Moreover we see that this change is due to a unitary part, given by the commutator between the density matrix of the system and its self-Hamiltonian, and a non-unitary part, representing decoherence and dissipation.

#### *Lindblad equation*

We will consider now the most general master equation for a Markov quantum process. Instead of starting from a microscopic model as we did in the previous paragraph, we require that the quantum evolution  $\Phi_t : \mathcal{B}(\mathcal{H}) \rightarrow \mathcal{B}(\mathcal{H})$ , i.e. a family of CPTP map such that  $\Phi_0 = \mathbb{1}$ , satisfies the semigroup property

$$\Phi_{t_2}\Phi_{t_1} = \Phi_{t_2+t_1} , \quad (1.72)$$

in analogy with the classical theory of Markovian processes. Given a quantum evolution satisfying the above property, there exists a linear map  $\mathcal{L}$  such that

$$\Phi_t = e^{\mathcal{L}t} , \quad (1.73)$$

where the super-operator  $\mathcal{L}$  is the generator of the semigroup. With this representation one easily gets the Markovian master equation

$$\frac{d}{dt}\hat{\rho}(t) = \mathcal{L}\hat{\rho}(t) . \quad (1.74)$$

<sup>6</sup>  $\frac{d}{dt}\hat{\rho}^{(S)}(t) = -i[\hat{H}_S, \hat{\rho}(t)] + e^{-i\hat{H}_S t} \frac{d}{dt}\hat{\rho}^{(I)}(t) e^{i\hat{H}_S t}$ .

It can be shown that the most general form for the generator  $\mathcal{L}$  is given by the so-called Lindblad equation [2]

$$\mathcal{L}\hat{\rho}(t) = -i[\hat{H}, \hat{\rho}(t)] + \sum_{k=1}^{N^2-1} \gamma_k \left( \hat{A}_k \hat{\rho}(t) \hat{A}_k^\dagger - \frac{1}{2} \left\{ \hat{A}_k^\dagger \hat{A}_k, \hat{\rho}(t) \right\}_+ \right), \quad (1.75)$$

where  $\{\cdot, \cdot\}_+$  denotes the anticommutator,  $N = \dim \mathcal{H}_S$ ,  $\gamma_k \geq 0$  are constants related to the Kraus operators of the evolution. The operators  $\hat{A}_k$ , called Lindblad operators, correspond to a unitary transformation of a vector of operators forming an orthonormal basis for the Liouville space associated with  $\mathcal{H}_S$  (i.e. the space of operators  $X$  on  $\mathcal{H}$ , such that  $\text{Tr} X^\dagger X$  is finite, equipped with the scalar product  $(X, Y) \equiv \text{Tr}(X^\dagger Y)$ ). The Hamiltonian  $\hat{H}$  appearing in the commutator cannot be identified with  $\hat{H}_S$ : it may indeed contain some corrections due to the perturbation of the free Hamiltonian of the open system by the environment, leading to a rescaling of its energy levels. This effect is known as the Lamb-shift effect.

The Lindblad master equation is local in time and Markovian and can be derived from phenomenological models. We want to remark that it is possible to reduce Eq.1.69 into Lindblad form, Eq.1.75, by making a further approximation, namely the secular (or rotating wave) approximation. This is valid when the relaxation time of the system is large compared to the typical time scale of the evolution generated by the system's Hamiltonian.

### 1.2.3 Master equations for Non-Markovian dynamics

In the previous paragraphs we summarized the approximation introduced to obtain the Born-Markov equation: weak-coupling and large environment (Born), and negligible environmental memory effects (Markov). In many physical situations however, these approximations do not hold. If one drops the Markov approximation, then the environmental memory effects can cause the evolution to depend on the state of the total system  $S + E$  at previous times, making it impossible to obtain a time-local differential equation describing the dynamics.

*Nakajima-Zwanzig master equation*

This is obtained through the projection operator technique, which consists in defining the super-operators  $\mathcal{P}$  and  $\mathcal{Q} = \mathbb{1} - \mathcal{P}$ , acting on  $\mathcal{B}(\mathcal{H}_S \otimes \mathcal{H}_E)$ , as

$$\mathcal{P}\hat{\rho} \equiv \text{Tr}_E(\hat{\rho}) \otimes \sigma, \quad (1.76)$$

$$\mathcal{Q}\hat{\rho} \equiv \hat{\rho} - \mathcal{P}\hat{\rho} \quad (1.77)$$

where  $\sigma$ , called reference state, is chosen according to the specific model one wishes to study, and it is usually chosen to be the stationary Gibbs state of the environment  $\sigma = e^{-\beta\hat{H}_E}/Z$ , where  $\beta$  is the inverse temperature ( $k_B = 1$ ) and  $Z = \text{Tr}e^{-\beta\hat{H}_E}$  is the partition function.  $\mathcal{P}\hat{\rho}$  still contains the complete information required to reconstruct the open system's density matrix  $\hat{\rho}$ , i.e.  $\mathcal{P}$  represents a projection on the part of  $\hat{\rho}$  relevant to the system's dynamics. By construction  $\mathcal{P}$  and  $\mathcal{Q}$  are idempotent, commute and sum up to the identity.

Considering the Hamiltonian of the composite system  $S + E$  to be

$$\hat{H} = \hat{H}_0 + \alpha\hat{H}_I, \quad \text{with} \quad \hat{H}_0 = \hat{H}_S \otimes \mathbb{1}_E + \mathbb{1}_S \otimes \hat{H}_E, \quad (1.78)$$

where  $\alpha$  is a dimensionless parameter carrying the order of magnitude of the system-bath interaction, we implicitly define the super-operator  $\mathcal{L}$  as

$$\frac{d}{dt}\hat{\rho}^{(I)}(t) = -i\alpha \left[ \hat{H}_I(t), \hat{\rho}^{(I)}(t) \right] \equiv \alpha\mathcal{L}(t)\hat{\rho}^{(I)}(t). \quad (1.79)$$

Assuming that<sup>7</sup>

$$\text{Tr}_E(\hat{H}_I(t_1) \dots \hat{H}_I(t_{2j+1})\sigma) = 0, \quad (1.80)$$

the master equation for the relevant part  $\mathcal{P}\hat{\rho}$  reads

$$\frac{d}{dt}\mathcal{P}\hat{\rho}^{(I)}(t) = \int_0^t ds \mathcal{K}(t,s)\mathcal{P}\hat{\rho}^{(I)}(s) + \alpha\mathcal{P}\mathcal{L}(t)\mathcal{G}(t,0)\mathcal{Q}\hat{\rho}(0), \quad (1.81)$$

where

$$\mathcal{G}(t,s) = \mathcal{T} \exp \left\{ \alpha \int_s^t du \mathcal{Q}\mathcal{L}(u) \right\}, \quad (1.82)$$

<sup>7</sup> Even though this assumption is not required for the derivation of the equation of motion, it allows to simplify considerably the calculations when performing the expansion in  $\alpha$ . However, it is worth noticing that Eq.1.80 is satisfied in the relevant case of the environment being a collection of harmonic oscillators in thermal equilibrium linearly coupled to the system.

and

$$\mathcal{K}(t, s) = \alpha^2 \mathcal{P} \mathcal{G}(t, s) \mathcal{Q} \mathcal{L}(s) \mathcal{P} , \quad (1.83)$$

is the memory-kernel. The integro-differential equation Eq.1.81 is the Nakajima-Zwanzig equation. It is exact and, it is worth noticing, holds for arbitrary initial conditions. However, assuming an initial state in the form Eq.1.66 (and hence  $\mathcal{P} \hat{\rho}(0) = \hat{\rho}(0)$  and  $\mathcal{Q} \hat{\rho}(0) = 0$ ) allows us to simplify Eq.1.81 further:

$$\frac{d}{dt} \mathcal{P} \hat{\rho}^{(I)}(t) = \int_0^t ds \mathcal{K}(t, s) \mathcal{P} \hat{\rho}^{(I)}(s) , \quad (1.84)$$

and tracing out the environmental degrees of freedom

$$\frac{d}{dt} \hat{\rho}^{(I)}(t) = \int_0^t ds \mathcal{K}_S(t, s) \hat{\rho}^{(I)}(s) , \quad (1.85)$$

where

$$\mathcal{K}_S(t, s) \hat{\rho}^{(I)}(t) \equiv \text{Tr}_E \left( \mathcal{K}(t, s) \hat{\rho}^{(I)}(s) \otimes \sigma \right) . \quad (1.86)$$

If the memory kernel  $\mathcal{K}_S(t, s)$  is time-homogeneous, i.e.  $\mathcal{K}_S(t, s) = \mathcal{K}_S(t - s)$ , Eq.1.86 can be rewritten as

$$\frac{d}{dt} \hat{\rho}^{(I)}(t) = \int_0^t ds \mathcal{K}_S(t - s) \hat{\rho}^{(I)}(s) = \left( \mathcal{K}_S * \hat{\rho}^{(I)} \right) (t) , \quad (1.87)$$

where  $*$  indicates the convolution product over the finite range  $[0, t]$ .

Notice also that if, in Eq.1.85, one also expands the memory kernel up to second order in the parameter  $\alpha$  one recovers Eq.1.65 after making the Born approximation:

$$\frac{d}{dt} \hat{\rho}^{(I)}(t) = - \alpha^2 \int_0^t ds \text{Tr}_E \left[ \hat{H}_I(t), \left[ \hat{H}_I(s), \hat{\rho}^{(I)}(s) \otimes \hat{\rho}_E \right] \right] . \quad (1.88)$$

#### *Time-convolutionless form of the master equation*

Sometimes, for sufficiently small coupling and assuming factorized initial conditions Eq.1.66, with techniques similar to the ones used in the previous paragraph, Eq.1.79 can be brought into convolutionless form

$$\frac{d}{dt} \hat{\rho}^{(I)}(t) = \mathcal{V}_S(t) \hat{\rho}^{(I)}(t) , \quad (1.89)$$

with  $\mathcal{Y}_S(t)\hat{\rho}^{(I)}(t) \equiv \text{Tr}_E \left( \mathcal{Y}(t)\hat{\rho}^{(I)}(t) \right)$  where  $\mathcal{Y}(t)$  indicates the time convolutionless generator

$$\mathcal{Y}(t) = \alpha \mathcal{P} \mathcal{L}(t) [1 - \Sigma(t)]^{-1} \mathcal{P} , \quad (1.90)$$

where

$$\Sigma(t) = \alpha \int_{t_0}^t ds \mathcal{G}(t,s) \mathcal{Q} \mathcal{L}(s) \mathcal{P} \mathcal{G}^{-1}(t,s) (\mathcal{P} + \mathcal{Q}) \hat{\rho}(t) , \quad (1.91)$$

with  $\mathcal{G}(t,s)$  and  $\mathcal{L}(t)$  defined in Eq.1.82 and Eq.1.79, respectively. This can also be expanded up to second order in  $\alpha$  obtaining

$$\frac{d}{dt} \hat{\rho}^{(I)}(t) = -\alpha^2 \int_0^t ds \text{Tr}_E \left[ \hat{H}_I(t), \left[ \hat{H}_I(s), \hat{\rho}^{(I)}(t) \otimes \hat{\rho}_E \right] \right] , \quad (1.92)$$

which is a time-local master equation. Notice that this equation is not Markovian since it still depends upon an explicit choice of the initial condition.

#### *Non-divisible quantum evolutions*

Let us consider now a quantum evolution  $\Phi_t$ . If we suppose that its inverse map  $\Phi_t^{-1}$  exists for all times  $t > 0$ , we can define the *intermediate evolution* as a two-parameter family of maps

$$\Phi_{t,s} = \Phi_t \Phi_s^{-1} , \quad \text{with } t \geq s \geq 0 . \quad (1.93)$$

We have seen in Paragraph 1.2.2 that if the maps  $\Phi_t$  form a semigroup, then  $\Phi_{t,s} = \Phi_{t-s}$  is completely positive. In general, however, this is not the case and  $\Phi_{t,s}$  is not necessarily completely positive. We say that the quantum evolution  $\Phi_t$  is CP-divisible if  $\Phi_{t,s}$  is completely positive, and  $k$ -divisible if  $\Phi_{t,s}$  is  $k$ -positive.

Quantum evolutions for which  $\Phi_t^{-1}$  exists give rise to time-local convolutionless quantum master equations, Eq.1.89, with similar form to a Lindblad master equation, which in Schrödinger picture read [25]

$$\begin{aligned} \frac{d}{dt} \hat{\rho}(t) = & -i [\hat{H}(t), \hat{\rho}(t)] + \\ & + \sum_k \gamma_k(t) \left( \hat{A}_k(t) \hat{\rho}(t) \hat{A}_k^\dagger(t) - \frac{1}{2} \left\{ \hat{A}_k^\dagger(t) \hat{A}_k(t), \hat{\rho}(t) \right\}_+ \right) , \end{aligned} \quad (1.94)$$

where now the Hamiltonian contribution  $\hat{H}(t)$ , the operators  $\hat{A}_k(t)$  and the parameters  $\gamma_k(t)$  may, in general, depend on time since the quantum evolution does not have the semigroup property.

The parameters  $\gamma_k(t)$  for a semigroup dynamics are constant and non-negative. However, for a master equation with time-dependent generator as in Eq.1.89, these parameters could assume negative values for some times, without violating the complete positivity of the quantum evolution. On the other hand, one can show that Eq.1.94 corresponds to a CP-divisible quantum evolution if and only if  $\gamma_k(t) \geq 0 \quad \forall k$ , at all times  $t \geq 0$ .

As a last remark, we point out that, unfortunately, a general formulation of necessary and sufficient conditions for which Eq.1.69 and Eq.1.94 describe a completely positive evolution has not been found yet. However, when these equations are carefully derived from microscopical or phenomenological models, they can describe a legitimate dynamics, even when the dynamical map is not CP, if the parameters involved (e.g. temperature and coupling constants) are chosen consistently with the introduced approximations.

---

## GAUSSIAN STATES AND GAUSSIAN CHANNELS

---

In this Chapter we are going to introduce the basic concepts and mathematical tools to study Gaussian states and Gaussian channels. Gaussian states have a crucial role in many fields of physics since they occur as the ground or thermal equilibrium states of any bosonic Hamiltonian in the small oscillation regime. In the same limit, the unitary free evolution generated by such Hamiltonian maps Gaussian states into Gaussian states, i.e. it preserves their Gaussianity; moreover, since any subsystem of a Gaussian state is Gaussian, also the non-unitary evolution of its subsystems preserves their Gaussianity. These kind of (unitary and non-unitary) evolutions give rise to Gaussian channels.

This Chapter is organized as follows: first, we will introduce the concept of continuous variable systems, thanks to the construction of coherent states for such systems we will see how the notion of a classical-like phase space arises. We will hence establish the connection between quantum states and square-integrable functions on this phase space: to every quantum state it is possible to associate a characteristic function. In the second section we will focus on the states whose characteristic function is a Gaussian, namely Gaussian states. We will characterize these states in terms of the first and second statistical moments of the operators associated with their relevant degrees of freedom, the quadrature operators. Then we will discuss unitary transformation of Gaussian states generated by a Hamiltonian quadratic in the quadrature generators. After a brief excursus on bipartite Gaussian states, in the third section we will show how to describe an open Gaussian dynamics.

The main references used in the writing of this chapter are some comprehensive textbooks and reviews [26–29].

## 2.1 INTRODUCTION TO CONTINUOUS VARIABLE SYSTEMS

Quantum continuous variable (CV) systems are systems with  $m$  dynamical degrees of freedom, called *modes*, associated with pairs of operators with a continuous spectrum  $\hat{\mathbf{R}} = \{\hat{q}_1, \hat{p}_1, \dots, \hat{q}_m, \hat{p}_m\}^\top$ , usually referred to as quadratures. These quadrature operators satisfy the canonical commutation relation  $[\hat{R}_j, \hat{R}_k] = i\Omega_{jk}$  (here and in the rest of this thesis we assume to work in natural units, i.e.  $\hbar = 1$ ), where

$$\Omega = \bigoplus_{i=1}^m \Omega_i, \quad \text{with} \quad \Omega_i = \begin{pmatrix} 0 & 1 \\ -1 & 0 \end{pmatrix} \equiv \Omega_1, \quad (2.1)$$

is called symplectic form for reasons that are going to be clear later. By unitarily rotating the quadrature vector  $\hat{\mathbf{R}}$ , one can also define the vector  $\hat{\mathbf{a}} = \{\hat{a}_1, \hat{a}_1^\dagger, \dots, \hat{a}_m, \hat{a}_m^\dagger\}^\top$  of annihilation and creation operators:

$$\hat{a}_k \equiv \frac{\hat{q}_k + i\hat{p}_k}{\sqrt{2}}, \quad \hat{a}_k^\dagger \equiv \frac{\hat{q}_k - i\hat{p}_k}{\sqrt{2}}, \quad (2.2)$$

satisfying the commutation relation  $[\hat{a}_j, \hat{a}_k^\dagger] = \delta_{jk}$ . These operators allow one to construct an orthonormal basis for the infinite-dimensional Hilbert space of the system  $\mathcal{H} = \bigotimes_i^m \mathcal{H}_i = \text{Span}\{|n_1, \dots, n_m\rangle\}_{n_1, \dots, n_m \in \mathbb{N}}$  where the vectors  $|n_1, \dots, n_m\rangle = \frac{(\hat{a}_1^\dagger)^{n_1}}{\sqrt{n_1!}} \dots \frac{(\hat{a}_m^\dagger)^{n_m}}{\sqrt{n_m!}} |0\rangle$  (with  $|0\rangle$  defined as the vector in  $\mathcal{H}$  such that  $\hat{a}_k |0\rangle = 0 \forall k = 1, \dots, m$ ) are eigenstates of the number operators  $\hat{a}_k^\dagger \hat{a}_k \equiv \hat{n}_k$

$$\hat{a}_k^\dagger \hat{a}_k |n_1, \dots, n_k, \dots, n_m\rangle = n_k |n_1, \dots, n_k, \dots, n_m\rangle, \quad (2.3)$$

whose respective eigenvalues,  $n_1, \dots, n_m \in \mathbb{N}$ , represent the number of bosons in each mode. The state  $|0\rangle$  is hence called the vacuum. The states  $|n_1, \dots, n_m\rangle$  are also known as Fock states, hence the basis they form is known as the Fock-basis.

In general, however, it is not convenient to represent a CV system state with its infinite-dimensional density matrix. Indeed, it is common to exploit the correspondence between quantum states and the space of square-integrable functions  $L^2(\mathbb{R}^m)$  established by the Fourier-Weyl relation. This relation associates a quasi-probability distribution function on a classical-like phase space to each CV quantum state. In order to enunciate this rela-

tion we have to introduce first the Weyl displacement operator  $\hat{D}_k(\alpha_k)$  acting on the  $k$ -th mode:

$$\hat{D}_k(\alpha_k) = e^{\alpha_k \hat{a}_k^\dagger - \alpha_k^* \hat{a}_k}, \quad \alpha_k \in \mathbb{C} \quad (2.4)$$

which, by setting  $\alpha_k = \frac{q_k + ip_k}{\sqrt{2}}$ , could be easily recast in terms of the two real variables  $\mathbf{r}_k = \{q_k, p_k\}$  and the quadrature vector  $\hat{\mathbf{R}}_k = \{\hat{q}_k, \hat{p}_k\}$

$$\hat{D}_k(-\mathbf{r}_k) = e^{-i(p_k \hat{q}_k - q_k \hat{p}_k)} = e^{-ir_k \Omega \hat{\mathbf{R}}_k}. \quad (2.5)$$

The displacement operator for an  $m$ -mode CV system reads

$$\hat{D}_\alpha = e^{\alpha^\top \Omega \hat{\mathbf{a}}} = \bigotimes_k^m \hat{D}_k(\alpha_k) = \bigotimes_k^m \hat{D}_k(-\mathbf{r}_k) = e^{-ir^\top \Omega \hat{\mathbf{R}}} = \hat{D}_{-\mathbf{r}}, \quad (2.6)$$

with  $\alpha = \{\alpha_1, \alpha_1^*, \dots, \alpha_m, \alpha_m^*\}$  and  $\mathbf{r} = \{q_1, p_1, \dots, q_m, p_m\} = \mathbf{u}\alpha = (\bigoplus_{i=1}^m u) \alpha \in \mathbb{R}^{2m}$ , where  $u = \frac{1}{\sqrt{2}} \begin{pmatrix} 1 & 1 \\ -i & i \end{pmatrix}$  is the same unitary transformation which brings creation and annihilation operators into quadrature operators  $\hat{\mathbf{R}} = \mathbf{u}\hat{\mathbf{a}}$ . Moreover, since for any  $\hat{A}, \hat{B}$  such that  $[\hat{A}, \hat{B}] \in \mathbb{C}$  one has

$$e^{\hat{A}} e^{\hat{B}} = e^{\frac{1}{2}[\hat{A}, \hat{B}]} e^{\hat{A} + \hat{B}}, \quad (2.7)$$

(a particular instance of the Baker-Campbell-Hausdorff (BCH) formula), and since  $\hat{D}_\alpha^\dagger = \hat{D}_{-\alpha}$  (and analogously  $\hat{D}_{-\mathbf{r}}^\dagger = \hat{D}_{\mathbf{r}}$ ), as one immediately sees from Eq.2.4 (and Eq.2.5), it is clear that the Weyl displacement operator is a unitary operator:  $\hat{D}_\alpha^\dagger \hat{D}_\alpha = \hat{D}_{-\alpha} \hat{D}_\alpha = \mathbb{1}$ . These operators allow one to construct the coherent states of the system [30]:

$$|\alpha\rangle = \hat{D}_\alpha |0\rangle. \quad (2.8)$$

Let us now have a brief digression before moving forward: it is worth noticing that there exists a general group theoretical construction of coherent states [30] whose starting point is a closed algebra of operators  $\mathfrak{g}$ , generators of the group  $G$ . Usually these are the operators in terms of which one can express the Hamiltonian and they are therefore associated with the dynamical degrees of freedom of the system. Once a reference state  $|\Phi_0\rangle$  in the Hilbert space of the system is chosen, one can determine the maximum stability subgroup  $F$ , i.e. the set of operators belonging to the group  $G$  which leave the reference state invariant up to a phase factor. Coherent states are

constructed by acting with an element  $\mathcal{D}_\omega$  of the coset space  $G/F$ , which is a differentiable manifold, on the reference state:  $|\omega\rangle \equiv \mathcal{D}_\omega|\Phi_0\rangle$ . This definition guarantees a one-to-one correspondence between coherent states and points on the differentiable manifold  $G/F$ , i.e.  $|\omega\rangle$  and  $G/F$  are topologically equivalent. The differentiable manifold is provided with a metric and a measure  $d\mu(\omega)$ , and, when the reference state is chosen appropriately, with a natural symplectic structure, i.e. with Poisson bracket. For these reasons, the coset space  $G/F$  can be regarded as a classical-like phase-space.

In the case we are considering, where the dynamical degrees of freedom are associated with position and momentum operators, for a single mode, the algebra  $\mathfrak{g}$  is the Heisenberg-Weyl algebra  $\mathfrak{h} = \{\hat{a}, \hat{a}^\dagger, \hat{a}^\dagger\hat{a}, \mathbb{1}\}$ , the maximum-stability subgroup is  $U(1)$  generated by  $\hat{a}^\dagger\hat{a}$  and  $\mathbb{1}$ , and, when the reference state is chosen to be the vacuum  $|0\rangle$ , the elements of the coset space are the displacement operators  $\hat{D}_\alpha$  defined in Eq.2.4. The phase-space is therefore the complex plane  $\mathbb{C}$ , isomorphic to  $\mathbb{R}^2$ . Moreover, the coherent states constructed from this group, known as *field* (or *Glauber's*) coherent states, have another important property, which is that they are minimum-uncertainty states, i.e. they saturate the Heisenberg uncertainty relation  $\Delta\hat{q}\Delta\hat{p} = 1/2$ , where  $\Delta\hat{x}^2 = \langle\hat{x}^2\rangle - \langle\hat{x}\rangle^2$ .

Last but not least, the evolution of a coherent state  $|\omega\rangle$ , constructed from the dynamical group of the Hamiltonian, is still a coherent state, i.e. “once a coherent state, always a coherent state”, and the dynamics of the variable  $\omega$  on the differentiable manifold is described by classical-like equation of motion. Moreover, if the bosonic system is closed, one has  $\Delta\hat{q} = \Delta\hat{p} = \text{const}$ , i.e. a coherent state, as a classical particle, does not spread [30]. These features, resembling classical systems, are the reasons why Schrödinger proposed such states.

Moving on, by using the BCH formula, Eq.2.10, it is easy to show that

$$\hat{D}_\alpha|\beta\rangle = \hat{D}_\alpha\hat{D}_\beta|0\rangle = e^{\frac{1}{2}\alpha^\top\Omega\beta}\hat{D}_{\alpha+\beta}|0\rangle = e^{\frac{1}{2}\alpha^\top\Omega\beta}|\alpha + \beta\rangle, \quad (2.9)$$

As previously anticipated, coherent states  $|\beta\rangle$  are in one-to-one correspondence with points  $\beta$  in the complex hyperplane  $\mathbb{C}^m \sim \mathbb{R}^{2m}$ , our classical-like phase-space, and the action of  $\hat{D}_\alpha$  corresponds to a translation on the complex hyperplane  $\beta \rightarrow \beta + \alpha$ , from which the name ‘displacement operator’.

Thanks to the BCH formula, we can also factorize the displacement as

$$\hat{D}_\alpha = e^{\frac{1}{2}\sum_k \alpha_k^* \alpha_k} e^{-\sum_k \alpha_k^* \hat{a}_k} e^{\sum_k \alpha_k \hat{a}_k^\dagger} = e^{-\frac{1}{2}\sum_k \alpha_k^* \alpha_k} e^{\sum_k \alpha_k \hat{a}_k^\dagger} e^{-\sum_k \alpha_k^* \hat{a}_k}, \quad (2.10)$$

where the sum over  $k$  runs from 0 to  $m$ . Using the above we find

$$\begin{aligned} [\hat{a}_l, \hat{D}_\alpha] &= e^{-\frac{1}{2}\sum_k \alpha_k^* \alpha_k} \left[ \hat{a}_l, e^{\sum_k \alpha_k \hat{a}_k^\dagger} \right] e^{\sum_k \alpha_k \hat{a}_k^\dagger} e^{-\sum_k \alpha_k^* \hat{a}_k} = \\ &= e^{-\frac{1}{2}\sum_k \alpha_k^* \alpha_k} \left( \sum_{j=0}^{\infty} \frac{\alpha_l^j}{j!} [\hat{a}_l, (\hat{a}_l^\dagger)^j] \right) e^{\sum_k \alpha_k \hat{a}_k^\dagger} e^{-\sum_k \alpha_k^* \hat{a}_k} = \\ &= e^{-\frac{1}{2}\sum_k \alpha_k^* \alpha_k} \alpha_l \left( \sum_{j=1}^{\infty} \frac{\alpha_l^{j-1}}{(j-1)!} (\hat{a}_l^\dagger)^{j-1} \right) e^{\sum_k \alpha_k \hat{a}_k^\dagger} e^{-\sum_k \alpha_k^* \hat{a}_k} = \\ &= \alpha_l e^{-\frac{1}{2}\sum_k \alpha_k^* \alpha_k} e^{\sum_k \alpha_k \hat{a}_k^\dagger} e^{-\sum_k \alpha_k^* \hat{a}_k} = \alpha_l \hat{D}_\alpha, \end{aligned} \quad (2.11)$$

where, in the third equality we used the identity  $[\hat{a}_l, (\hat{a}_l^\dagger)^j] = j(\hat{a}_l^\dagger)^{j-1}$ . From this, it follows straightforwardly that coherent states, Eq.2.8, are eigenstates of the annihilation operators:

$$\hat{a}_l |\alpha\rangle = \hat{a}_l \hat{D}_\alpha |0\rangle = \alpha_l \hat{D}_\alpha |0\rangle + \hat{D}_\alpha \hat{a}_l |0\rangle = \alpha_l \hat{D}_\alpha |0\rangle = \alpha_l |\alpha\rangle. \quad (2.12)$$

One can also show that coherent states have the following expansion in the Fock-basis

$$|\alpha\rangle = e^{-\frac{1}{2}\sum_k \alpha_k^* \alpha_k} \bigotimes_{k=0}^m \sum_{j=0}^{\infty} \frac{\alpha_k^j}{\sqrt{j!}} |j\rangle, \quad (2.13)$$

and one immediately sees that they are not orthogonal:

$$\langle \alpha | \beta \rangle = \langle 0 | \beta - \alpha \rangle e^{-\frac{1}{2}\alpha^\top \Omega \beta} = e^{-\frac{1}{2}\alpha^\top \Omega \beta} e^{-\frac{1}{2}\sum_k |\alpha_k - \beta_k|^2}. \quad (2.14)$$

They provide, however, a continuous resolution of the identity operator:

$$\mathbb{1} = \int \frac{d\alpha}{\pi^m} |\alpha\rangle \langle \alpha|, \quad (2.15)$$

where  $d\alpha = d\text{Re}(\alpha) d\text{Im}\alpha = dr/2^m = dqdp/2^m$  is the measure of the (flat) phase-space.

Thanks to this resolution of the identity one has that, given an operator  $\hat{O}$ ,

$$\begin{aligned} \text{Tr} [\hat{O}] &= \sum_k \langle k | \hat{O} | k \rangle = \sum_k \int \frac{d\alpha}{\pi^m} \langle k | \alpha \rangle \langle \alpha | \hat{O} | k \rangle = \\ &= \int \frac{d\alpha}{\pi^m} \langle \alpha | \hat{O} \sum_k | k \rangle \langle k | \alpha \rangle = \int \frac{d\alpha}{\pi^m} \langle \alpha | \hat{O} | \alpha \rangle, \end{aligned} \quad (2.16)$$

It is possible to prove [29] that the operator  $|\alpha\rangle\langle\beta|$  can be expanded in terms of the displacement operator:

$$|\alpha\rangle\langle\beta| = \int \frac{d\gamma}{\pi^m} \text{Tr} [|\alpha\rangle\langle\beta|\hat{D}_\gamma] \hat{D}_\gamma^\dagger. \quad (2.17)$$

Hence, given any bounded operator  $\hat{O}$  on  $\mathcal{H}$ , using Eqs.2.15,2.16 we get

$$\begin{aligned} \hat{O} &= \int \frac{d\alpha d\beta}{\pi^{2m}} \langle\alpha|\hat{O}|\beta\rangle |\alpha\rangle\langle\beta| = \int \frac{d\alpha d\beta d\gamma}{\pi^{3m}} \langle\alpha|\hat{O}|\beta\rangle \text{Tr} [|\alpha\rangle\langle\beta|\hat{D}_\gamma] \hat{D}_\gamma^\dagger = \\ &= \int \frac{d\alpha d\beta d\gamma d\sigma}{\pi^{4m}} \langle\sigma|\alpha\rangle \langle\alpha|\hat{O}|\beta\rangle \langle\beta|\hat{D}_\gamma|\sigma\rangle \hat{D}_\gamma^\dagger = \\ &= \int \frac{d\gamma}{\pi^m} \text{Tr} [\hat{D}_\gamma \hat{O}] \hat{D}_{-\gamma} = \frac{1}{(2\pi)^m} \int_{\mathbb{R}^{2m}} dr \text{Tr} [\hat{D}_{-r} \hat{O}] \hat{D}_r. \end{aligned} \quad (2.18)$$

This is the Fourier-Weyl relation, which establishes the connection between any bounded operator  $\hat{O}$  on  $\mathcal{H}$  and a square-integrable function

$$\chi_{\hat{O}}(\mathbf{r}) \equiv \text{Tr} [\hat{D}_{-r} \hat{O}]. \quad (2.19)$$

Therefore, given a CV quantum system state  $\hat{\rho}$ , this can be completely described by its *symmetrically ordered characteristic function*

$$\chi_{\hat{\rho}}(\alpha) = \text{Tr} [\hat{D}_\alpha \hat{\rho}], \quad \chi_{\hat{\rho}}(\mathbf{r}) = \text{Tr} [\hat{D}_{-r} \hat{\rho}]. \quad (2.20)$$

By construction, the value of the symmetrically ordered characteristic function of a quantum state, when evaluated in 0 is 1:  $\chi_{\hat{\rho}}(0) = \text{Tr}[\hat{\rho}] = 1$ .

It is worth noticing that, defining  $\tilde{\mathbf{r}} = \{\tilde{r}_1^{(1)}, \tilde{r}_1^{(2)}, \dots, \tilde{r}_m^{(1)}, \tilde{r}_m^{(2)}\} = \mathbf{\Omega} \mathbf{r}$  and making use again of the BCH formula (summation over repeated indices is assumed for  $l = 1, \dots, m$ )

$$\hat{D}_{-r} = e^{i\tilde{r}_l \hat{R}_l} = e^{\frac{i}{2}\tilde{r}_l^{(1)}\tilde{r}_l^{(2)}} e^{i\tilde{r}_l^{(1)}\hat{q}_l} e^{i\tilde{r}_l^{(2)}\hat{p}_l} = e^{-\frac{i}{2}\tilde{r}_l^{(1)}\tilde{r}_l^{(2)}} e^{i\tilde{r}_l^{(2)}\hat{p}_l} e^{i\tilde{r}_l^{(1)}\hat{q}_l}, \quad (2.21)$$

one has

$$\begin{aligned} \partial_{\tilde{r}_l^{(1)}} \hat{D}_{-r} &= \left( \frac{i}{2}\tilde{r}_l^{(2)} + i\hat{q}_l \right) \hat{D}_{-r} = \hat{D}_{-r} \left( -\frac{i}{2}\tilde{r}_l^{(2)} + i\hat{q}_l \right), \\ \partial_{\tilde{r}_l^{(2)}} \hat{D}_{-r} &= \left( -\frac{i}{2}\tilde{r}_l^{(1)} + i\hat{p}_l \right) \hat{D}_{-r} = \hat{D}_{-r} \left( \frac{i}{2}\tilde{r}_l^{(1)} + i\hat{p}_l \right), \end{aligned}$$

From the two equations above one gets

$$\partial_{\tilde{r}_l^{(1)}} \chi_{\hat{O}}(\mathbf{r}) = i\chi_{\hat{O}\hat{q}_l}(\mathbf{r}) + \frac{i}{2}\tilde{r}_l^{(2)} \chi_{\hat{O}}(\mathbf{r}) = i\chi_{\hat{q}_l\hat{O}}(\mathbf{r}) - \frac{i}{2}\tilde{r}_l^{(2)} \chi_{\hat{O}}(\mathbf{r}), \quad (2.22)$$

$$\partial_{\tilde{r}_l^{(2)}} \chi_{\hat{O}}(\mathbf{r}) = i\chi_{\hat{O}\hat{p}_l}(\mathbf{r}) - \frac{i}{2}\tilde{r}_l^{(1)} \chi_{\hat{O}}(\mathbf{r}) = i\chi_{\hat{p}_l\hat{O}}(\mathbf{r}) + \frac{i}{2}\tilde{r}_l^{(1)} \chi_{\hat{O}}(\mathbf{r}), \quad (2.23)$$

which, after some simple manipulations, relabelling  $\tilde{\mathbf{r}} = \{\tilde{r}_1, \dots, \tilde{r}_{2m}\}$ , and recalling that  $\hat{\mathbf{R}} \equiv \{\hat{q}_1, \hat{p}_1, \dots, \hat{q}_m, \hat{p}_m\}$ , become

$$\chi_{\hat{O}\hat{R}_j}(\mathbf{r}) = \left( -i\partial_{\tilde{r}_j} - \frac{1}{2}\Omega_{jj'}\tilde{r}'_j \right) \chi_{\hat{O}}(\mathbf{r}), \quad (2.24)$$

$$\chi_{\hat{R}_j\hat{O}}(\mathbf{r}) = \left( -i\partial_{\tilde{r}_j} + \frac{1}{2}\Omega_{jj'}\tilde{r}'_j \right) \chi_{\hat{O}}(\mathbf{r}), \quad (2.25)$$

for  $j = 1, \dots, 2m$ , from which it follows

$$\chi_{\hat{R}_j\hat{O}+\hat{O}\hat{R}_j}(\mathbf{r}) = -2i\partial_{\tilde{r}_j}\chi_{\hat{O}}(\mathbf{r}). \quad (2.26)$$

$$\chi_{\hat{R}_j\hat{O}-\hat{O}\hat{R}_j}(\mathbf{r}) = \Omega_{jj'}\tilde{r}'_j\chi_{\hat{O}}(\mathbf{r}). \quad (2.27)$$

We will briefly mention here that the characteristic function belongs to a family of  $s$ -ordered characteristic functions [31]

$$\chi_{\hat{\rho}}^{(s)}(\boldsymbol{\alpha}) = \text{Tr} [\hat{\mathbf{D}}_{\boldsymbol{\alpha}}\hat{\rho}] e^{\frac{s}{2}\sum_k |\alpha_k|^2}, \quad s \in [-1, 1]. \quad (2.28)$$

These functions are useful when one wishes to evaluate the expectation value of ordered products of annihilation and creation operators acting on a single mode: normal ordered  $\text{Tr}[(\hat{a}^\dagger)^j \hat{a}^k \hat{\rho}] = \left[ \partial_{\alpha}^j (-\partial_{\alpha^*}^k) \chi_{\hat{\rho}}^{(1)}(\alpha) \right]_{\alpha=0}$ , anti-normal ordered  $\text{Tr}[\hat{a}^k (\hat{a}^\dagger)^j \hat{\rho}] = \left[ \partial_{\alpha}^j (-\partial_{\alpha^*}^k) \chi_{\hat{\rho}}^{(-1)}(\alpha) \right]_{\alpha=0}$ , and symmetrically ordered (i.e. the normalised sum of any permutation  $\mathfrak{p}$  of  $j$  creation operators and  $k$  annihilation operators)  $\text{Tr}[\mathfrak{p}\{\hat{a}^k, (\hat{a}^\dagger)^j\} \hat{\rho}] = \left[ \partial_{\alpha}^j (-\partial_{\alpha^*})^k \chi_{\hat{\rho}}^{(0)}(\alpha) \right]_{\alpha=0}$ .

The complex Fourier transform of  $\chi_{\hat{\rho}}^{(s)}(\boldsymbol{\alpha})$  reads

$$W_{\hat{\rho}}^{(s)}(\boldsymbol{\gamma}) = \int \frac{d\boldsymbol{\alpha}}{\pi^m} \chi_{\hat{\rho}}^{(s)}(\boldsymbol{\alpha}) e^{\boldsymbol{\gamma}\boldsymbol{\Omega}\boldsymbol{\alpha}}, \quad \boldsymbol{\gamma} \in \mathbb{C}^m. \quad (2.29)$$

$W_{\hat{\rho}}^{(0)}(\boldsymbol{\gamma})$  is known as Wigner function,  $W_{\hat{\rho}}^{(1)}(\boldsymbol{\gamma})$  is the so-called  $P$ -representation of the state which allows to rewrite the state in diagonal form in the coherent states basis  $\hat{\rho} = \int d\boldsymbol{\alpha} / \pi^m W_{\hat{\rho}}^{(1)}(\boldsymbol{\alpha}) |\boldsymbol{\alpha}\rangle \langle \boldsymbol{\alpha}|$ , while  $W_{\hat{\rho}}^{(-1)}(\boldsymbol{\gamma})$  is also known as the Husimi function, or the  $Q$ -representation, of the state  $W_{\hat{\rho}}^{(-1)}(\boldsymbol{\gamma}) = 1/\pi^m \langle \boldsymbol{\gamma} | \hat{\rho} | \boldsymbol{\gamma} \rangle$ .

The  $s$ -ordered functions defined in Eq.2.29 are quasiprobability distributions since, even though they can assume negative values, they are normalized and allow to recover the statistics of a measurement of any observable  $\hat{O}$  on the state  $\hat{\rho}$ :

$$\text{Tr} [\hat{O}\hat{\rho}] = \int \frac{d\boldsymbol{\gamma}}{\pi^m} W_{\hat{\rho}}^{(s)}(\boldsymbol{\gamma}) W_{\hat{O}}^{(s)}(\boldsymbol{\gamma}). \quad (2.30)$$

From now on we will refer to the symmetrically ordered characteristic function simply as the characteristic function if not otherwise stated.

## 2.2 GAUSSIAN STATES

A quantum CV system with a Gaussian characteristic function

$$\chi_{\hat{\rho}_G}(\mathbf{r}) = e^{-\frac{1}{4}\mathbf{r}^\top \Omega V \Omega \mathbf{r} - i(\Omega \mathbf{d})^\top \mathbf{r}} = e^{-\frac{1}{4}\tilde{\mathbf{r}}^\top V \tilde{\mathbf{r}} + i(\mathbf{d})^\top \tilde{\mathbf{r}}} \quad , \quad (2.31)$$

is a *Gaussian state*.

A Gaussian state is fully characterized by its first and second statistical moments:

$$\mathbf{d} = \langle \hat{\mathbf{R}} \rangle \quad , \quad (2.32)$$

$$V_{ij} = \langle \{ \hat{R}_i - d_i, \hat{R}_j - d_j \}_+ \rangle \quad , \quad (2.33)$$

where  $\{\cdot, \cdot\}_+$  is the anticommutator.  $\mathbf{d}$  and  $V$  are called displacement vector and covariance matrix respectively. Notice that the diagonal elements of the covariance matrix  $V_{ii}$  are proportional to the variance of the quadratures  $\hat{R}_i$ , in particular  $V_{ii} = 2(\Delta \hat{R}_i)^2$ .

The covariance matrix is symmetric by definition. However, not all symmetric matrices describe a quantum state. Indeed, there is an additional constraint on the covariance matrix equivalent to the requirement that the density matrix is a positive semidefinite operator. This is known as the Robertson-Schrödinger uncertainty relation, or *bona fide* condition:

$$V + i\Omega \geq 0 \quad . \quad (2.34)$$

This is a necessary and sufficient condition on the covariance matrix  $V$  for it to describe any CV physical quantum state. As its name suggests, this condition embodies the Heisenberg uncertainty principle between quadrature observables  $\Delta \hat{q} \Delta \hat{p} \geq 1/2$ . For single-mode systems Eq.2.34 reduces to  $\det V \geq 1$ .

It is easy to check that the characteristic function of any pure coherent state  $|\beta\rangle$  is Gaussian and its covariance matrix is the identity matrix:

$$\begin{aligned} \chi_{|\beta\rangle\langle\beta|}(\boldsymbol{\alpha}) &= \text{Tr}(\hat{\mathbf{D}}_\alpha |\beta\rangle\langle\beta|) = \text{Tr}(\hat{\mathbf{D}}_\beta^\dagger \hat{\mathbf{D}}_\alpha \hat{\mathbf{D}}_\beta |0\rangle\langle 0|) = \\ &= \text{Tr}(\hat{\mathbf{D}}_\alpha |0\rangle\langle 0|) e^{\boldsymbol{\alpha}^\top \Omega \beta} = \langle 0 | \hat{\mathbf{D}}_\alpha | 0 \rangle e^{\boldsymbol{\alpha}^\top \Omega \beta} = \\ &= e^{\frac{1}{4}\boldsymbol{\alpha}^\dagger \boldsymbol{\alpha} + \boldsymbol{\alpha}^\top \Omega \beta} = e^{-\frac{1}{4}\mathbf{r}^\top \Omega \mathbb{1} \Omega \mathbf{r} - i(\Omega \mathbf{d}_\beta)^\top \mathbf{r}} = \chi_{|\beta\rangle\langle\beta|}(\mathbf{r}) \quad , \end{aligned} \quad (2.35)$$

with  $\mathbf{r} = \mathbf{u}\boldsymbol{\alpha}$ . This is equivalent to Eq.2.31 with  $V = \mathbb{1}$  and  $\mathbf{d}_\beta = \mathbf{u}\beta$ . The vacuum state  $|0\rangle\langle 0|$ , being a coherent state, is described by  $V_{|0\rangle\langle 0|} = \mathbb{1}$  and  $\mathbf{d}_{|0\rangle\langle 0|} = 0$ .

## 2.2.1 Mean excitation number

A very important quantity when dealing with continuous variable systems is the mean number of excitation in the system  $\langle \hat{n} \rangle$ . This quantity is indeed related to the energy of the system: for non-interacting bosons with the same frequency (in this thesis we will consider only this particular case) the Hamiltonian is proportional to the number operator

$$\hat{H}_{\text{non-int}} = \frac{1}{2} \sum_{i=1}^m \hat{R}_i \hat{R}_i = \sum_{i=1}^m \left( \hat{a}_i^\dagger \hat{a}_i + \frac{1}{2} \right) = \hat{n} + \frac{m}{2}, \quad (2.36)$$

where  $\hat{n} = \hat{a}^\dagger \hat{a}$ . In general, the mean excitation number appears whenever one wants to put a relevant physical constraint on the system of interest. Exploiting the properties of the characteristic function, it is possible to find a compact expression for it, in terms of the covariance matrix of the system  $V$  and its displacement vector  $\mathbf{d}$ . We first notice that for an  $m$ -mode system (assuming sum over repeated indexes)

$$\langle \hat{a}^\dagger \hat{a} \rangle = \text{Tr} \left( \frac{1}{2} (\hat{R}_i \hat{R}_i - m) \hat{\rho}_G \right) = \frac{1}{2} \text{Tr} (\hat{R}_i \hat{R}_i \hat{\rho}_G) - \frac{m}{2}. \quad (2.37)$$

Recalling that the trace of an operator can be calculated by evaluating its characteristic function in  $\mathbf{r} = 0$ , i.e.  $\text{Tr} (\hat{R}_i \hat{R}_i \hat{\rho}_G) = \chi_{\hat{\rho}_G \hat{R}_i \hat{R}_i} \Big|_{\mathbf{r}=0}$ , and using the property Eq.2.24, one gets

$$\text{Tr} (\hat{R}_i \hat{R}_i \hat{\rho}_G) = \left( -i \partial_{\tilde{r}_i} - \frac{1}{2} \Omega_{ij} \tilde{r}_j \right) \left( -i \partial_{\tilde{r}_i} - \frac{1}{2} \Omega_{ik} \tilde{r}_k \right) \chi_{\hat{\rho}_G} \Big|_{\mathbf{r}=0}. \quad (2.38)$$

From the definition of the characteristic function of a Gaussian state Eq.2.31 it is easy to show that

$$\partial_{\tilde{r}_m} \chi_{\hat{\rho}_G} = \partial_{\tilde{r}_m} e^{-\frac{1}{4} \tilde{r}_k V_{kj} \tilde{r}_j + i d_l \tilde{r}_l} = \left( i d_m - \frac{1}{2} V_{mj} \tilde{r}_j \right) \chi_{\hat{\rho}_G}, \quad (2.39)$$

therefore

$$\begin{aligned} \text{Tr} (\hat{R}_i \hat{R}_i \hat{\rho}_G) &= (-i \partial_{\tilde{r}_i}) \left( -i \partial_{\tilde{r}_i} - \frac{1}{2} \Omega_{ik} \tilde{r}_k \right) \chi_{\hat{\rho}_G} \Big|_{\mathbf{r}=0} = \\ &= -\partial_{\tilde{r}_i} \partial_{\tilde{r}_i} \chi_{\hat{\rho}_G} + \frac{i}{2} \Omega_{ik} \partial_{\tilde{r}_i} (\tilde{r}_k \chi_{\hat{\rho}_G}) + \frac{i}{2} \Omega_{ij} \tilde{r}_j \partial_{\tilde{r}_i} \chi_{\hat{\rho}_G} \Big|_{\mathbf{r}=0} = \\ &= - \left[ \left( i d_i - \frac{1}{2} V_{ij} \tilde{r}_j \right) \left( i d_i - \frac{1}{2} V_{ik} \tilde{r}_k \right) - \frac{1}{2} V_{ii} \right] \chi_{\hat{\rho}_G} + \\ &\quad + \frac{i}{2} \Omega_{ii} \chi_{\hat{\rho}_G} + \frac{i}{2} \Omega_{ik} \tilde{r}_k \partial_{\tilde{r}_i} \chi_{\hat{\rho}_G} \Big|_{\mathbf{r}=0} = d_i d_i + \frac{1}{2} V_{ii}. \end{aligned} \quad (2.40)$$

The mean excitation number of a Gaussian state with covariance matrix  $V$  and displacement vector  $\mathbf{d}$  is

$$\langle \mathbf{a}^\dagger \mathbf{a} \rangle = \frac{1}{4} (\text{Tr}V - 2m) + \frac{|\mathbf{d}|^2}{2}. \quad (2.41)$$

### 2.2.2 Gaussian Unitaries

Let us suppose now that we want to transform unitarily our Gaussian state into another Gaussian state. This could be done by evolving the state through a quadratic Hamiltonian

$$\hat{H} = \frac{1}{2} (\hat{\mathbf{R}} - \bar{\mathbf{r}})^\top H (\hat{\mathbf{R}} - \bar{\mathbf{r}}) = \frac{1}{2} \hat{\mathbf{D}}_{-\bar{\mathbf{r}}} \hat{\mathbf{R}}^\top H \hat{\mathbf{R}} \hat{\mathbf{D}}_{\bar{\mathbf{r}}}, \quad (2.42)$$

where  $\bar{\mathbf{r}}$  is a  $2m$ -dimensional vector of real coordinates,  $H$  is a symmetric positive-definite real matrix and where we used the identity  $\hat{\mathbf{D}}_{-\bar{\mathbf{r}}} \hat{\mathbf{R}} \hat{\mathbf{D}}_{\bar{\mathbf{r}}} = \hat{\mathbf{R}} - \bar{\mathbf{r}}$  (this latter follows from the equivalent equation  $\hat{\mathbf{D}}_{-\alpha} \hat{\mathbf{a}} \hat{\mathbf{D}}_{\alpha} = \hat{\mathbf{a}} + \alpha$  which can be easily derived from Eq.2.11). Without losing generality we set  $\bar{\mathbf{r}} = 0$  and we can calculate the Heisenberg evolution of the quadrature vector  $\hat{\mathbf{R}}^\dagger$ :

$$\begin{aligned} \dot{\hat{R}}_j &= \frac{i}{2} [\hat{H}, \hat{R}_j] = \frac{i}{2} \sum_{l,m} H_{lm} ([\hat{R}_l, \hat{R}_j] \hat{R}_m + \hat{R}_l [\hat{R}_m, \hat{R}_j]) = \\ &= \frac{1}{2} \sum_{l,m} H_{lm} (\Omega_{jl} \hat{R}_m + \hat{R}_l \Omega_{jm}) = \sum_{l,m} \Omega_{jm} H_{ml} \hat{R}_l, \end{aligned} \quad (2.43)$$

which in vector form reads

$$\dot{\hat{\mathbf{R}}} = \mathbf{\Omega} H \hat{\mathbf{R}}. \quad (2.44)$$

This equation could be integrated giving the solution

$$\hat{\mathbf{R}}(t) = e^{\mathbf{\Omega} H t} \hat{\mathbf{R}}(0). \quad (2.45)$$

Notice that, since  $\mathbf{\Omega} \mathbf{\Omega} = -\mathbb{1}$ , the generator  $\mathbf{\Omega} H$  of the transformation  $e^{\mathbf{\Omega} H t}$  belongs to the Lie algebra  $\mathfrak{sp}(2m, \mathbb{R}) = \{g \in GL(2m) \mid g^\top \mathbf{\Omega} + \mathbf{\Omega} g = 0\}$  of the symplectic group, i.e. the set of transformations  $S$  that, acting by

<sup>1</sup> Setting  $\bar{\mathbf{r}} = 0$  is equivalent to studying the evolution of the shifted operator  $\hat{\mathbf{R}}_{\bar{\mathbf{r}}} = \hat{\mathbf{R}} - \bar{\mathbf{r}} = \hat{\mathbf{D}}_{-\bar{\mathbf{r}}} \hat{\mathbf{R}} \hat{\mathbf{D}}_{\bar{\mathbf{r}}}$ . The solution of the equations of motion for  $\hat{\mathbf{R}}_{\bar{\mathbf{r}}}$  can be found straightforwardly as  $\hat{\mathbf{R}}_{\bar{\mathbf{r}}}(t) = \hat{\mathbf{D}}_{-\bar{\mathbf{r}}} \hat{\mathbf{R}}(t) \hat{\mathbf{D}}_{\bar{\mathbf{r}}}$ .

congruence on the symplectic form, leave it invariant, i.e.  $Sp(2m, \mathbb{R}) = \{S \mid S\Omega S^\top = \Omega\}$ . Hence, the transformation  $e^{\Omega Ht}$  satisfies the relation

$$e^{\Omega Ht} \Omega \left( e^{\Omega Ht} \right)^\top = \Omega. \quad (2.46)$$

This ensures that the canonical commutation relations are valid at every time of the evolution  $[\hat{\mathbf{R}}(t), \hat{\mathbf{R}}(t)^\top] = e^{\Omega Ht} [\hat{\mathbf{R}}(0), \hat{\mathbf{R}}(0)^\top] (e^{\Omega Ht})^\top = i\Omega$ .

We can then state the following

**Proposition 2.1.** *A Gaussian unitary transformation  $\hat{s}$  of a Gaussian state  $\hat{\rho}_G$  is equivalent to a symplectic transformation  $S \in Sp(2m, \mathbb{R})$  at the level of the quadrature vector  $\hat{\mathbf{R}}$ :*

$$\hat{s} \hat{\mathbf{R}} \hat{s}^\dagger = S \hat{\mathbf{R}}, \quad \hat{s} = e^{i \frac{1}{2} \hat{\mathbf{R}}^\top h \hat{\mathbf{R}}}, \quad S = e^{\Omega h}, \quad (2.47)$$

with  $h = h^\top$ .

*Displacement vector and covariance matrix transform accordingly:*

$$\hat{\rho}_G \rightarrow \hat{s} \hat{\rho}_G \hat{s}^\dagger \Leftrightarrow \{\mathbf{d}, V\} \rightarrow \{S\mathbf{d}, SVS^\top\}. \quad (2.48)$$

The first equation in the above proposition can be understood considering that Eq.2.45 describes the Heisenberg evolution of the quadrature canonical operators, its solution corresponds then to a unitary transformation of such operators.

An important property of CV quantum states' covariance matrices is given by the following

**Theorem 2.1. (Williamson's)** *Given a  $2m \times 2m$  real symmetric matrix  $V$  such that  $V + i\Omega \geq 0$ , there exists a symplectic matrix  $S_v \in Sp(2m, \mathbb{R})$  such that*

$$S_v V S_v^\top = \bigoplus_{k=1}^m \begin{pmatrix} v_k & 0 \\ 0 & v_k \end{pmatrix} = \mathbf{v}, \quad (2.49)$$

where  $v_k \geq 1$  are the so-called symplectic eigenvalues.

The set of symplectic eigenvalues can be conveniently found by determining the positive spectrum of the matrix  $i\Omega V$ :  $\text{Eig}_+(i\Omega V) = \{v_k\}_{k=1\dots m}$ . This can be seen by noticing that  $\text{Eig}(i\Omega \mathbf{v}) = \text{Eig}(\bigoplus_k i v_k \Omega) = \{\pm v_k\}_{k=1\dots m}$  and that  $i\Omega \mathbf{v}$  and  $i\Omega V$  are related by a similarity transformation, i.e.  $i\Omega \mathbf{v} = i\Omega S V S^\top = S^{-\top} (i\Omega V) S^\top$ , hence they have the same spectrum.

The condition that the symplectic eigenvalues are greater or equal than 1 comes from the *bona fide* condition Eq.2.34. To show this we just have to remember that a congruence transformation preserves the sign of the eigenvalues of a matrix, hence

$$V + i\Omega \geq 0 \quad \Leftrightarrow \quad \mathbf{S}_v (V + i\Omega) \mathbf{S}_v^\top = \bigoplus_{i=1}^m (v_k \mathbb{1}_2 + i\Omega) \geq 0, \quad (2.50)$$

and this is satisfied *iff*

$$v_k \mathbb{1}_2 + i\Omega \geq 0 \quad \forall k \quad \Leftrightarrow \quad v_k \geq 1. \quad (2.51)$$

The relevance of Williamson's theorem is clear when considering Gaussian states. Indeed, if the covariance matrix  $V$  and the displacement vector  $d$  describe a Gaussian state, the Williamson's diagonalization corresponds to unitarily rotate the quantum state, or, in other words, to a change of basis. Moreover, since any Gaussian state  $\hat{\rho}_G$  can be defined as a Gibbs state

$$\hat{\rho}_G = \frac{e^{-\beta \hat{H}}}{\text{Tr}[e^{-\beta \hat{H}}]}, \quad \beta \in [0, +\infty], \quad (2.52)$$

or as the ground state of a quadratic Hamiltonian Eq.2.42, the above symplectic diagonalization amounts to the normal mode decomposition:

$$\hat{H}_\omega = \hat{s}_v \hat{H} \hat{s}_v^\dagger = \sum_{j=1}^m \frac{\omega_j}{2} (\hat{q}_j^2 + \hat{p}_j^2) = \sum_{i=1}^m \hat{H}_{\omega_i}. \quad (2.53)$$

The diagonal covariance matrix  $v$  corresponds to a factorized thermal state

$$\hat{\rho}_{\text{th}} = \bigotimes_{i=1}^m \frac{e^{-\beta \hat{H}_{\omega_i}}}{\text{Tr}[e^{-\beta \hat{H}_{\omega_i}}]}, \quad (2.54)$$

and the symplectic eigenvalues  $v_i$  are related to the normal mode frequencies  $\omega_i$  by

$$v_i = \frac{1 + e^{-\beta \omega_i}}{1 - e^{-\beta \omega_i}}. \quad (2.55)$$

Pure states are recovered in the limit  $\beta \rightarrow \infty$ , i.e. in the limit of 0 temperature, and are therefore characterized by unit symplectic eigenvalues, i.e. the Williamson's form of the covariance matrix of any pure Gaussian state is the identity matrix. Equivalently, the covariance matrix of any  $m$ -mode pure

Gaussian state  $|\psi_G\rangle\langle\psi_G|$  can be decomposed as the product of a symplectic matrix with its transpose:

$$V_{|\psi_G\rangle\langle\psi_G|} = S^\top S, \quad S \in Sp(2m, \mathbb{R}). \quad (2.56)$$

We will conclude this paragraph summarizing the most common one and two-mode Gaussian unitaries.

### *Phase-shift*

The single-mode phase-shift unitary is of the form

$$\hat{U}_\varphi = e^{i\hat{n}\varphi} = e^{i\hat{a}^\dagger\hat{a}\varphi} = e^{i\hat{a}^\dagger\mathbb{1}\hat{a}} = e^{i\hat{\mathbf{R}}^\top\mathbb{1}\hat{\mathbf{R}}\frac{\varphi}{2}}. \quad (2.57)$$

It is easy to identify the  $h$  matrix appearing in Eq.2.47:  $h_\varphi = \varphi\mathbb{1}$ . The corresponding symplectic transformation acting at the level of the quadrature vector is hence given by

$$S_\varphi = e^{\Omega\varphi} = e^{i\sigma_y\varphi} = \cos\varphi\mathbb{1} + \sin\varphi\Omega, \quad (2.58)$$

where we used the well-known identity  $e^{i\theta\vec{v}\cdot\vec{\sigma}} = \cos\theta\mathbb{1} + i\sin\theta\vec{v}\cdot\vec{\sigma}$ , with  $\vec{v}$  a unit three-dimensional vector and  $\vec{\sigma} = \{\sigma_x, \sigma_y, \sigma_z\}$ . It is clear that since the unitary transformation generated by the number operator  $\hat{n}$ , corresponds to a rotation  $S_\varphi \in O(2)$  of the quadrature vector in phase-space, the mean excitation number Eq.2.41 is conserved.

### *Single-mode squeezing*

The single-mode squeezing unitary is of the form

$$\begin{aligned} \hat{U}_{\text{sq}}(\zeta) &= e^{\frac{1}{2}(\zeta\hat{a}^{\dagger 2} - \zeta^*\hat{a}^2)} = \exp\left\{\frac{1}{2}\hat{a}^\dagger\begin{pmatrix} 0 & \zeta \\ -\zeta^* & 0 \end{pmatrix}\hat{a}\right\} = \\ &= \exp\left\{i\frac{1}{2}\hat{\mathbf{R}}^\top\begin{pmatrix} s\sin\theta & -s\cos\theta \\ -s\cos\theta & -s\sin\theta \end{pmatrix}\hat{\mathbf{R}}\right\} = e^{i\frac{1}{2}\hat{\mathbf{R}}^\top h_{\text{sq}}\hat{\mathbf{R}}}, \end{aligned} \quad (2.59)$$

with  $\zeta = se^{i\theta}$ . The corresponding symplectic transformation reads

$$\begin{aligned} S_{\text{sq}} &= e^{\Omega h_{\text{sq}}} = \exp\{i(is)(\sin\theta\sigma_x + \cos\theta\sigma_z)\} = \\ &= \cosh s\mathbb{1} - \sinh s(\sin\theta\sigma_x + \cos\theta\sigma_z). \end{aligned} \quad (2.60)$$

This operation, when applied to the vacuum state and followed by a displacement, allows for the construction of a class of states that, as the field coherent states (which, we recall, have  $V_{|\alpha\rangle\langle\alpha|} = \mathbb{1}$ , i.e.  $\Delta\hat{q} = \Delta\hat{p} = 1/\sqrt{2}$ ), saturate the Heisenberg uncertainty principle but with unbalanced variances of the two canonical quadratures:

$$|\psi_{\zeta,\alpha}\rangle = \hat{D}_\alpha \hat{U}_{\text{sq}}(\zeta)|0\rangle = \hat{D}_\alpha \hat{U}_{\text{sq}}(s, \theta)|0\rangle, \quad (2.61)$$

where the parameter  $s$  is the squeezing degree,  $\theta$  is the squeezing phase. These states are called *squeezed coherent states*, and they are characterized by a covariance matrix which, for  $\theta = 0$ , is diagonal  $V_{|\psi_{s,0,\alpha}\rangle\langle\psi_{s,0,\alpha}|} = S_{\text{sq}}^\top \mathbb{1} S_{\text{sq}} = \text{diag}\{e^{-2s}, e^{2s}\}$ , and displacement vector  $\mathbf{d} = u\boldsymbol{\alpha} = \sqrt{2}\{\text{Re}\alpha, \text{Im}\alpha\}$ . It is clear that  $(\Delta\hat{q})^2(\Delta\hat{p})^2 = 1/4$ : while the variance of the position quadrature is reduced by a factor  $e^{-s}$ , the variance of the momentum quadrature is increased by a factor  $e^s$ . The phase  $\theta$  allows one to choose which quadrature has the minimum variance, e.g. for  $\theta = \pi$  one has  $\Delta\hat{p} = e^{-s}/\sqrt{2}$  and  $\Delta\hat{q} = e^s/\sqrt{2}$ , for other values of  $\theta$ , the quadratures  $\hat{\mathbf{R}}_\theta = \{\hat{q}_\theta, \hat{p}_\theta\}$  such that  $(\Delta\hat{q}_\theta)^2(\Delta\hat{p}_\theta)^2 = 1/4$ , are simply given by rotating the quadrature vector  $\hat{\mathbf{R}}$  with the orthogonal transformation which diagonalizes  $V_{|\psi_{s,\theta,\alpha}\rangle\langle\psi_{s,\theta,\alpha}|}$ .

It can be shown that single-mode undisplaced (i.e.  $\alpha = 0$  in Eq.2.61) squeezed states have the following expansion in the Fock-basis:

$$|\psi_\zeta\rangle = \frac{1}{\sqrt{\cosh s}} \sum_{n=0}^{\infty} (-1)^n \frac{\sqrt{(2n)!}}{2^n n!} e^{in\theta} \tanh^n s |2n\rangle. \quad (2.62)$$

### Beam Splitter

This is a two-mode unitary of the form

$$\begin{aligned} \hat{U}_{\text{b-s}} &= \exp \left\{ \frac{1}{2} \phi \left( \hat{a}_1 \hat{a}_2^\dagger - \hat{a}_1^\dagger \hat{a}_2 \right) \right\} = \exp \left\{ -i \frac{1}{2} \phi \hat{\mathbf{a}}^\dagger \sigma_y \otimes \sigma_z \hat{\mathbf{a}} \right\} = \\ &= \exp \left\{ -i \frac{1}{2} \phi \hat{\mathbf{R}}^\top \Omega \otimes \Omega \hat{\mathbf{R}} \right\} = e^{i \frac{1}{2} \hat{\mathbf{R}}^\top h_{\text{b-s}} \hat{\mathbf{R}}}. \end{aligned} \quad (2.63)$$

The corresponding symplectic transformation hence is

$$\hat{S}_{\text{b-s}} = e^{\Omega h_{\text{b-s}}} = e^{i\phi \sigma_y \otimes \mathbb{1}} = \cos \phi \mathbb{1} + i \sin \phi \sigma_y \otimes \mathbb{1}. \quad (2.64)$$

One can define the transmissivity of the beam-splitter as  $\tau = \cos^2 \phi$ . For  $\phi = \pi/4$  one gets a balanced 50:50 beam splitter. The beam splitter transformation acts on quadrature and annihilation operators as follows:

$$\begin{cases} \hat{R}_1^{(i)} \rightarrow \hat{R}_1^{(i)} \cos \phi + \hat{R}_2^{(i)} \sin \phi \\ \hat{R}_2^{(i)} \rightarrow \hat{R}_1^{(i)} \sin \phi - \hat{R}_2^{(i)} \cos \phi \end{cases}, \quad \begin{cases} \hat{a}_1 \rightarrow \hat{a}_1 \cos \phi + \hat{a}_2 \sin \phi \\ \hat{a}_2 \rightarrow \hat{a}_2 \cos \phi - \hat{a}_1 \sin \phi \end{cases}. \quad (2.65)$$

Also in this case, as for the one-mode phase shifter, the symplectic matrix describing the transformation at the level of the quadrature vector is an orthogonal matrix, hence the mean excitation number is conserved.

### Two-mode squeezing

The two mode squeezing unitary is of the form:

$$\begin{aligned} \hat{U}_{2S} &= e^{\frac{1}{2}r(\hat{a}_1^\dagger \hat{a}_2^\dagger - \hat{a}_1 \hat{a}_2)} = \exp \left\{ i \frac{1}{2} r \hat{\mathbf{a}}^\dagger \sigma_x \otimes \sigma_y \hat{\mathbf{a}} \right\} = \\ &= \exp \left\{ -i \frac{1}{2} r \hat{\mathbf{R}}^\top \sigma_x \otimes \sigma_x \hat{\mathbf{R}} \right\} = e^{i \frac{1}{2} \hat{\mathbf{R}}^\top h_{2S} \hat{\mathbf{R}}}, \end{aligned} \quad (2.66)$$

where  $r$  is the so-called squeezing parameter. The corresponding symplectic transformation hence is

$$\hat{S}_{2S} = e^{\Omega h_{2S}} = e^{-i(ir)\sigma_x \otimes \sigma_z} = \cosh r \mathbb{1} - \sinh r \sigma_x \otimes \sigma_z. \quad (2.67)$$

Applying this transformation to the vacuum state, one obtains the so-called two-mode squeezed vacuum state (TMSV):

$$V_{\text{TMSV}} = \begin{pmatrix} \cosh(2r) & 0 & -\sinh(2r) & 0 \\ 0 & \cosh(2r) & 0 & \sinh(2r) \\ -\sinh(2r) & 0 & \cosh(2r) & 0 \\ 0 & \sinh(2r) & 0 & \cosh(2r) \end{pmatrix}. \quad (2.68)$$

The Fock basis expansion of this state is

$$|\text{TMSV}_r\rangle = \frac{1}{\sqrt{\cosh r}} \sum_{n=0}^{\infty} \tanh^n r |nn\rangle. \quad (2.69)$$

In the limit of infinite squeezing this state approaches the maximally entangled state  $|\text{TMSV}_{r \rightarrow \infty}\rangle \propto \sum_n |nn\rangle$ .

It is clear that, in this case, as for the single-mode squeezing transformation, the mean excitation number is not conserved: while for the vacuum  $\langle \hat{n} \rangle_{|0\rangle} = 0$ , for a TMSS it is a monotonically increasing function of the squeezing parameter  $r$

$$\langle \hat{n} \rangle_{\text{TMSV}} = 2 \sinh^2 r . \quad (2.70)$$

Since they preserve the number of excitation of the system, phase-shift and beam splitter are said to be passive transformations, on the other hand, one and two-mode squeezing are called active transformations. One can easily see that such distinction can be made at the level of the generator  $\Omega h$  of the symplectic transformation: passive transformations are characterized by antisymmetric generators, while active transformations by symmetric generators.

### 2.2.3 Bipartite Gaussian states and local operations

In the previous Chapter we highlighted the relevance of bipartite systems in quantum information. In particular, when dealing with bipartite systems, it is important to know how to perform *local* operations, i.e. all operations acting on the degrees of freedom of a single subsystem. As one could expect, these operations, which are well defined at the level of the density matrix but that could be tricky to understand and implement in an infinite dimensional scenario, have simple phase-space counterparts.

#### *Partial Trace*

We have seen in the previous chapter that given a bipartite system described by a density matrix  $\hat{\rho}_{AB}$ , it is possible to describe the state of one of the two subsystems  $A(B)$  by a density matrix obtained tracing out the degrees of freedom of the other subsystem  $B(A)$ :  $\hat{\rho}_{A(B)} = \text{Tr}_{B(A)} \hat{\rho}_{AB}$ . At the level of the covariance matrix the partial trace assumes a very simple form: given an  $m$ -mode Gaussian state, it is possible to recover the covariance matrix of any  $k$ -mode subsystem  $A$  by removing from the covariance matrix and from the displacement vector the rows and columns relative to the modes

we want to trace out, the subsystem  $B$ . In formulae, given displacement and covariance matrix of the bipartite system

$$\mathbf{d}_{AB} = \begin{pmatrix} \mathbf{d}_A \\ \mathbf{d}_B \end{pmatrix}, \quad V_{AB} = \begin{pmatrix} A & C \\ C^\top & B \end{pmatrix}, \quad (2.71)$$

where  $\mathbf{d}_A$  and  $\mathbf{d}_B$  are  $2k$  and  $2m$ -dimensional vectors,  $A$  and  $B$  are  $2k \times 2k$  and  $2m \times 2m$  blocks of  $V_{AB}$  and  $C$  is its off-diagonal  $2k \times (2m - 2k)$  block, the reduced displacement vector and covariance matrix for the  $k$ -mode subsystem  $A$  are  $\mathbf{d}_A$  and  $A$  respectively. Conversely, the tensor product of two Gaussian states  $\hat{\rho}_G^A \otimes \hat{\rho}_G^B$ , with displacement vectors  $\mathbf{d}_A, \mathbf{d}_B$ , and covariance matrix  $A$  and  $B$  respectively, is the Gaussian state with displacement vector  $\mathbf{d}_{AB} = \mathbf{d}_A \oplus \mathbf{d}_B$  and covariance matrix  $V_{AB} = A \oplus B$ .

### Local Unitaries

The same is true for local unitaries: a tensor product of unitaries acting on different Hilbert spaces  $\mathcal{H}_A$  and  $\mathcal{H}_B$  as  $\hat{s}_A \otimes \hat{s}_B \hat{\rho}_{AB} \hat{s}_A^\dagger \otimes \hat{s}_B^\dagger$  translates into a direct sum of symplectic matrices on the phase-spaces  $\mathbb{R}_A^{2k}$  and  $\mathbb{R}_B^{2(m-k)}$ :

$$\{\mathbf{d}_{AB}, V_{AB}\} \rightarrow \{\mathbf{S}_A \oplus \mathbf{S}_B \mathbf{d}_{AB}, \mathbf{S}_A \oplus \mathbf{S}_B V_{AB} \mathbf{S}_A^\top \oplus \mathbf{S}_B^\top\}. \quad (2.72)$$

A consequence of the Williamson's theorem is the CV analogue of the Schmidt decomposition: given an  $m$ -mode pure Gaussian state  $|\psi_G\rangle$ , consider a bipartition  $A|B$  of such a state, where  $A$  and  $B$  are composed of  $k$  and  $l$  modes respectively with  $k < l$ ; by means of local unitaries one can perform the Williamson decomposition on both reduced covariance matrices to find that they have the same  $k$  symplectic eigenvalues, while the remaining  $k - l$  symplectic eigenvalues of the higher dimensional subsystem  $B$  are equal to 1. Therefore, the covariance matrix of the composite system  $V_{|\psi_G\rangle\langle\psi_G|}$  can be

brought by means of local unitaries  $V_{|\psi_G\rangle\langle\psi_G|}^d = S_A \oplus S_B V_{|\psi_G\rangle\langle\psi_G|} S_A^\top \oplus S_B^\top$  in the form

$$V_{|\psi_G\rangle\langle\psi_G|}^d = \left( \begin{array}{ccc|cccc} \mathbf{c}_1 & \diamond & \diamond & \mathbf{s}_1 & \diamond & \diamond & \diamond & \diamond & \diamond \\ \diamond & \ddots & \diamond & \diamond & \ddots & \diamond & \diamond & \diamond & \diamond \\ \diamond & \diamond & \mathbf{c}_k & \diamond & \diamond & \mathbf{s}_k & \diamond & \diamond & \diamond \\ \hline \mathbf{s}_1 & \diamond & \diamond & \mathbf{c}_1 & \diamond & \diamond & \diamond & \diamond & \diamond \\ \diamond & \ddots & \diamond & \diamond & \ddots & \diamond & \diamond & \diamond & \diamond \\ \diamond & \diamond & \mathbf{s}_k & \diamond & \diamond & \mathbf{c}_k & \diamond & \diamond & \diamond \\ \diamond & \diamond & \diamond & \diamond & \diamond & \diamond & \mathbb{1} & \diamond & \diamond \\ \diamond & \ddots & \diamond \\ \diamond & \mathbb{1} \end{array} \right), \quad (2.73)$$

where each element denotes a  $2 \times 2$  submatrix, in particular the diamonds ( $\diamond$ ) correspond to null matrices,  $\mathbb{1}$  to the identity matrix and

$$\mathbf{c}_j = \begin{pmatrix} v_j & 0 \\ 0 & v_j \end{pmatrix}, \quad \mathbf{s}_j = \begin{pmatrix} -\sqrt{v_j^2 - 1} & 0 \\ 0 & \sqrt{v_j^2 - 1} \end{pmatrix}. \quad (2.74)$$

In the relevant case of two-mode states, by means of local unitaries, it is possible to bring the covariance matrix  $V_2$  of any two-mode state, also mixed, to the form (standard form):

$$V_2 = \begin{pmatrix} a & 0 & c_- & 0 \\ 0 & a & 0 & c_+ \\ c_- & 0 & b & 0 \\ 0 & c_+ & 0 & b \end{pmatrix}, \quad (2.75)$$

with  $a, b \geq 1$ ,  $c_+ \geq |c_-|$  and the condition Eq.2.34 becomes

$$(a^2 - 1)(b^2 - 1) - 2c_-c_+ - abc_+^2 + c_-^2(c_+^2 - ab) \geq 0. \quad (2.76)$$

For pure two-mode states one has  $a = b$ ,  $c_+ = -c_- = \sqrt{a^2 - 1}$ , i.e. any pure two-mode Gaussian state  $|\psi_G^{(2)}\rangle\langle\psi_G^{(2)}|$  can be transformed, by means of local unitaries, into a TMSV Eq.2.68, with the squeezing parameter given by  $r = \frac{1}{2} \operatorname{arccosh} a$ .

### *Partial Transposition and Logarithmic Negativity of two-mode states*

Since the density matrix of any quantum system is a Hermitian operator, the transposition operation simply consist in complex conjugation  $\hat{\rho}^\top = \hat{\rho}^*$ .

One can show that, in the continuous variable scenario, complex conjugation corresponds to the inversion of the momentum quadrature operators (and variables) [32]:

$$d \rightarrow \Sigma d, \quad V \rightarrow \Sigma V \Sigma, \quad (2.77)$$

with  $\Sigma = \bigoplus_1^m \sigma_z$ . It is then obvious, given the direct sum structure of phase-space as previously noted, that the partial transposition of a  $k$ -mode subsystem  $B$ , is represented by  $\mathbb{1}_{m-k} \oplus \Sigma_k$ , where  $\Sigma_k = \bigoplus_1^k \sigma_z$ .

Now, as stated in Th.1.2, in general, the positivity of the partially transposed density matrix is not a sufficient condition to discern separable from entangled states. However, it has been shown in [32] that for two-mode Gaussian states the PPT criterion is a necessary and sufficient condition to determine if a state is separable. Therefore, given a bipartite two-mode Gaussian state described by covariance matrix  $V_{AB}$ , we can say that it is separable *iff*  $(\mathbb{1} \oplus \Sigma_B)V(\mathbb{1} \oplus \Sigma_B)$  does not describe a positive semi-definite state, i.e. it does not satisfy the Robertson-Schrödinger relation:

$$(\mathbb{1} \oplus \Sigma_B)V(\mathbb{1} \oplus \Sigma_B) + i\Omega \geq 0. \quad (2.78)$$

Since, as we showed, the relation 2.34 is equivalent to require  $\nu_k \geq 1 \quad \forall k$ , it is possible to estimate the violation of the PPT criterion through the Logarithmic Negativity (see Paragraph 1.1.3), which for two-mode states is defined as

$$\mathcal{N} = \max\{-\log \tilde{\nu}, 0\}, \quad (2.79)$$

with  $\tilde{\nu} = \min \text{Eig}_+ [i\Omega(\mathbb{1} \oplus \Sigma_B)V(\mathbb{1} \oplus \Sigma_B)]$ , which means  $\mathcal{N} > 0$  *iff* the partially transposed covariance matrix does not satisfies the *bona fide* condition. One can immediately see that for a TMSV state  $\mathcal{N}_{\text{TMSV}} = 2r$ .

### 2.3 GAUSSIAN CHANNELS

We have just seen, in the previous section, how unitary transformations are described by symplectic transformation in phase-space. We want to show now how to represent the general (Gaussian) quantum evolution of a Gaussian state, i.e. we want to characterize at the level of the covariance matrix all completely positive, trace and Gaussianity preserving maps. As already

showed in Paragraph 1.2.1, a quantum evolution can be seen as the reduced unitary evolution of a quantum system  $\hat{\rho}$  with an initially uncorrelated environment  $\hat{\sigma}$ . If the joint unitary is Gaussianity preserving, i.e. it is generated by a quadratic Hamiltonian, the corresponding reduced dynamics of  $\hat{\rho}$  is Gaussian.

### 2.3.1 Open Gaussian dynamics

We give the following [29]:

**Proposition 2.2.** *The reduced Gaussian unitary evolution of a  $m$ -mode system in a Gaussian state with an initially uncorrelated environment can always be described by a couple of  $2m \times 2m$  matrices  $(X, Y)$  acting on the covariance matrix  $V$  and displacement vector  $\mathbf{d}$  as*

$$\begin{aligned} \mathbf{d} &\rightarrow X\mathbf{d} \\ V &\rightarrow XVX^\top + Y \end{aligned} \quad (2.80)$$

with  $Y = Y^\top$ , and such that

$$Y + i\Omega - iX\Omega X^\top \geq 0. \quad (2.81)$$

For the proof of this Proposition see Appendix A. Notice that, in general,  $\mathbf{d}$  transforms as  $\mathbf{d} \rightarrow X\mathbf{d} + \mathbf{d}_0$ ; however, one can set  $\mathbf{d}_0 = 0$  without loss of generality (see footnote on page 42).

It is possible to show that also the converse statement is true, i.e. given any pair of  $2m \times 2m$  matrices  $(X, Y)$  fulfilling Eq.2.81 one can construct a unitary evolution of the system and an environment such that the reduced action of this dilation on the  $m$  modes of the system is given by Eq.2.80. It has been proved [33] that one needs at most

$$k = \text{rank}[Y] - \frac{1}{2}\text{rank}[\Omega - X\Omega X^\top], \quad (2.82)$$

number of environmental modes in order to dilate the map given by  $X$  and  $Y$  to a Gaussian unitary evolution. Since in this thesis we will always deal with  $X$  and  $Y$  matrices such that  $\text{rank}[Y] = \text{rank}[\Omega - X\Omega X^\top] = 2m$ , we will enunciate here a Proposition just for this simple case, i.e.  $k = m$ . The proof, which could be found in Appendix A, gives a prescription to construct the symplectic matrix of the Gaussian joint evolution and the environmental covariance matrix.

**Proposition 2.3.** *Given any pair of  $2m \times 2m$  matrices  $(X, Y)$  such that they satisfy Eq.2.81 and such that  $\text{rank}[Y] = \text{rank}[\Omega - X\Omega X^\top] = 2m$ , one can find a symplectic matrix which describes a joint Gaussian unitary evolution of an  $m$ -mode system with a product of  $m$  thermal states, whose reduced dynamics is given by Eq.2.80.*

Notice that in reference [29], the proof of Proposition 2.3 is different from the proof reported in the Appendix A: the author indeed proved that given any  $2m \times 2m$  matrices  $X$  and  $Y$  satisfying Eq.2.81, and such that  $\text{rank}[Y - i(\Omega - X\Omega X^\top)] = 2m$ , there exists a corresponding Gaussian Stinespring dilation where the environment may always be chosen to be a  $2m$ -mode vacuum state. Indeed, in [33] it has also been shown that the minimum number of pure environmental modes to build a Gaussian Stinespring dilation for the channel is

$$k_{\text{pure}} = \text{rank}[Y - i(\Omega - X\Omega X^\top)] = 2m . \quad (2.83)$$

### 2.3.2 Single-mode Gaussian channels

We will now consider the special case of single-mode Gaussian channels. These are maps described by two  $2 \times 2$  matrices satisfying Eq.2.81 which could be recast as

$$\sqrt{\det Y} \geq |1 - \det X| . \quad (2.84)$$

To prove this, it is sufficient to notice that for any  $2 \times 2$  matrix  $X$ , one has  $X\Omega X^\top = \det X \Omega$ , and that since  $Y$  is a positive-definite symmetric matrix, it could be brought, through a symplectic transformation, into its Williamson's form  $\sqrt{\det Y} \mathbb{1}$ . One therefore has  $Y + i\Omega - iX\Omega X \geq 0 \Leftrightarrow \sqrt{\det Y} \mathbb{1} + i\Omega(1 - \det X) \geq 0$ , from which Eq.2.84 follows straightforwardly.

Thanks to Prop.2.3, we know that any single-mode Gaussian channel, described by  $X$  and  $Y$  such that they satisfy Eq.2.84, corresponds to a reduced unitary Gaussian evolution of the system with an environment in a thermal state  $V_E = \nu \mathbb{1}$ . We want now to determine the value of the environmental symplectic eigenvalue in terms of  $X$  and  $Y$ . The covariance matrix of the environmental mode is given by Eq.A.16, and, since symplectic

and orthogonal matrices have unit determinant, its symplectic eigenvalue is  $\nu = \sqrt{\det V_E}$ , therefore

$$\nu^2 = \frac{\det Y}{(\det \Sigma)^2}, \quad (2.85)$$

with  $\Sigma$  defined as in Eq.A.15. To evaluate the determinant of  $\Sigma$  we use the identity A.14, i.e.  $\Sigma\Omega\Sigma = R(\Omega - X\Omega X^\top)R^\top$ :

$$\begin{aligned} (\det \Sigma)^2 &= \det(\Omega - X\Omega X^\top) = \det(\mathbb{1} + \Omega X\Omega X^\top) = \\ &= (1 + \epsilon_1)(1 + \epsilon_2) = 1 + \epsilon_1 + \epsilon_2 + \epsilon_1\epsilon_2, \end{aligned} \quad (2.86)$$

where  $\epsilon_1$  and  $\epsilon_2$  are the eigenvalues of  $\Omega X\Omega X^\top$ . It is easy to check that  $\epsilon_1\epsilon_2 = (\det X)^2$ , while, since for any  $2 \times 2$  matrix one has  $\Omega X\Omega X^\top = -\det X \mathbb{1}$ , then  $\epsilon_1 + \epsilon_2 = \text{Tr}(\Omega X\Omega X^\top) = -2 \det X$ . Therefore

$$(\det \Sigma)^2 = (1 - \det X)^2, \quad (2.87)$$

from which

$$\nu = \frac{y}{|1 - x|}, \quad (2.88)$$

where  $x = \det X$  and  $y = \sqrt{\det Y}$ .

One immediately sees that the channels at the border of the allowed region  $\sqrt{\det Y} = |1 - \det X|$  can be implemented with pure Gaussian states, i.e. thermal states at zero temperature. On the other hand, channels with  $\det X = 1$  are obtained by unitarily evolving the system with an infinite temperature environment.

We will consider now a particular type of single-mode Gaussian channels: phase-covariant channels. These are all single-mode Gaussian channels  $\Phi$ , whose action is completely characterized by  $2 \times 2$  matrices  $X$  and  $Y$ , such that  $\Phi(\hat{U}_{\text{p-s}} \hat{\rho} \hat{U}_{\text{p-s}}^\dagger) = \hat{U}_{\text{p-s}} \Phi(\hat{\rho}) \hat{U}_{\text{p-s}}^\dagger$ , where  $\hat{U}_{\text{p-s}}$  is a single-mode phase shifter unitary Eq.2.57. One immediately notices that these channels are characterized by  $X$  and  $Y$  proportional to the identity matrix. So, any phase-covariant channel is unitarily equivalent to a channel  $X = \sqrt{x} \mathbb{1}$  and  $Y = y \mathbb{1}$  with  $x$  and  $y$  such that

$$y \geq |1 - x|, \quad (2.89)$$

i.e. they satisfy 2.84.

In the next paragraph we classify these channels according to the value of the determinant of  $X$  and their physical implementation.

*Attenuators  $\mathcal{E}_\theta^\eta$* 

Let us consider the class of channels with  $0 < \det X < 1$ :

$$X = \cos \theta \mathbb{1}, \quad Y = \eta \sin^2 \theta \mathbb{1}, \quad (2.90)$$

with  $0 < \theta < 2\pi$  and  $\eta \geq 1$ . Thanks to the above mentioned property of  $2 \times 2$  matrices  $X\Omega X^\top = \det X \Omega$ , one finds  $\Omega - X\Omega X^\top = (1 - \det X)\Omega = \sin^2 \theta \Omega$ , i.e.  $R = \mathbb{1}$  and  $\Sigma = \sin \theta \mathbb{1}$ . The covariance matrix of the environment is then given by

$$V_E = \Sigma^{-1} Y \Sigma^{-1} = \frac{1}{\sin^2 \theta} Y = \eta \mathbb{1}, \quad (2.91)$$

which is already in its Williamson's form, i.e.  $B = \Sigma$ .

The first two blocks of the symplectic matrix describing the Gaussian unitary evolution are

$$(A \ B) = \begin{pmatrix} \cos \theta & 0 & \sin \theta & 0 \\ 0 & \cos \theta & 0 & \sin \theta \end{pmatrix} = \begin{pmatrix} v_1^\top \\ v_2^\top \end{pmatrix}. \quad (2.92)$$

The set  $\{v_1, v_2\}$  can be easily completed to a symplectic basis obtaining  $S = S_{b-s}$  with  $S_{b-s}$  as in Eq.2.64.

Any attenuator channel, as in Eq.2.90, can then be realized by mixing at a beam splitter with transmissivity  $\cos^2 \theta$  the input Gaussian state with a thermal state. This kind of channels are said to be *attenuators* because they reduce the amplitude of the displacement vector  $d$  of a factor  $\cos \theta$ . On the other hand, if one applies this channel to a coherent state with covariance matrix  $V = \mathbb{1}$ , it is easy to see that both variances are increased by a factor  $\cos^2 \theta + \eta \sin^2 \theta \geq 1$ . The attenuators with  $\eta = 1$ , which transform pure coherent states into pure coherent states, are called quantum-limited attenuators.

*Amplifiers  $\mathcal{A}_s^\eta$* 

Phase-covariant channels with  $\det X > 1$  can be parametrized as follows

$$X = \cosh s \mathbb{1}, \quad Y = \eta \sinh^2 s \mathbb{1}, \quad (2.93)$$

with  $s \in \mathbb{R}^+$  and  $\eta \geq 1$ . With analogous steps to the ones above one finds  $R = \sigma_z$ ,  $\Sigma = \sinh s \mathbb{1}$ , therefore  $B = \sinh s \sigma_z$  and  $V_E = \eta \mathbb{1}$ . The set of vectors

given by the rows of  $(A \ B)$ , using Eq.A.21, is completed to form a symplectic basis and, by setting the arbitrary constant  $c = 1/\sqrt{\cosh s}$ , the symplectic matrix obtained is the two-mode squeezing symplectic of Eq.2.67.

As one can guess, these kinds of channels are called amplifiers because they rescale the displacement vector  $d$  by a factor  $\cosh s \geq 1$ . The quantum-limited amplifiers, obtained by setting  $\eta = 1$ , enhance the amplitudes  $d$  of the input state whilst adding minimum noise.

### *Quantum-limited channels*

The quantum-limited channels (both attenuators and amplifiers) have this name because if one supposes to further reduce the added noise by decreasing  $\eta$ , the condition Eq.2.84 would not be satisfied, meaning that the output covariance matrix would not verify the Robertson-Schrödinger relation, violating the Heisenberg uncertainty principle.

It is also worth noticing that any phase covariant channel  $\Phi$  can be decomposed as the action of a quantum limited attenuator followed by the action of a quantum limited amplifier:  $\mathcal{A}_s^1 \circ \mathcal{E}_\theta^1$ . This latter channel is completely characterized by the matrices

$$X_{\mathcal{A}_s \circ \mathcal{E}_\theta} = \cosh s \cos \theta \mathbb{1}, \quad Y_{\mathcal{A}_s \circ \mathcal{E}_\theta} = \left( \sin^2 \theta \cosh^2 s + \sinh^2 s \right) \mathbb{1},$$

which, as one could expect, satisfy the condition Eq.2.84. For any channel  $(X = \sqrt{x} \mathbb{1}, Y = y \mathbb{1})$  such that  $y \geq |1 - x|$ , it is possible to find

$$s_{xy} = \operatorname{arcsinh} \sqrt{\frac{x + y - 1}{2}}, \quad \theta_{xy} = \arccos \sqrt{\frac{2x}{x + y + 1}}, \quad (2.94)$$

such that  $(X = \sqrt{x} \mathbb{1}, Y = y \mathbb{1}) \sim \mathcal{A}_{s_{xy}}^1 \circ \mathcal{E}_{\theta_{xy}}^1$ .

---

 QUANTUM METROLOGY ESSENTIALS
 

---

In this Chapter we will briefly introduce some fundamental concepts for quantum parameter estimation [34, 35].

### 3.1 BACKGROUND

It is very common, in many physical scenarios, that one is interested in measuring quantities which, due to some limitations, are not directly measurable but can, however, be inferred by measuring some observables and processing the obtained measurement outcomes [36, 37]. These quantities to be estimated (the *parameters*) are usually described by a vector  $\boldsymbol{\mu} = (\mu_1, \dots, \mu_N)^\top \in \mathbb{R}^N$ . From the data  $\boldsymbol{x} = (x_1, \dots, x_m)^\top \in \mathbb{R}^m$ , collected after performing the measurements, one can construct an *estimator*  $\tilde{\boldsymbol{\mu}} = (\tilde{\mu}_1(\boldsymbol{x}), \dots, \tilde{\mu}_N(\boldsymbol{x}))^\top$ , i.e. a mapping from the set of measurement outcomes to  $\mathbb{R}^N$ . We will focus on a particular class of estimators, namely *locally unbiased* estimators. Unbiased estimators are those such that their expectation values coincide with the true values of the parameters:

$$\langle \tilde{\boldsymbol{\mu}} \rangle = \int \tilde{\boldsymbol{\mu}}(\boldsymbol{x}) p(\boldsymbol{x}|\boldsymbol{\mu}) d^m \boldsymbol{x} = \boldsymbol{\mu}, \quad (3.1)$$

where  $p(\boldsymbol{x}|\boldsymbol{\mu})$  represents the probability of obtaining the outcomes  $\boldsymbol{x}$  given that the true value of the parameters is  $\boldsymbol{\mu}$ . A *locally unbiased* estimator at  $\boldsymbol{\mu}_0$ , is such that Eq.3.1 holds for  $\boldsymbol{\mu} = \boldsymbol{\mu}_0$  but not necessarily for other values  $\boldsymbol{\mu} \neq \boldsymbol{\mu}_0$ . In this case, the prior probability distribution  $p(\boldsymbol{\mu})$  of finding the values  $\boldsymbol{\mu}$  is very peaked around  $\boldsymbol{\mu}_0$ , i.e.  $p(\boldsymbol{\mu}) \sim \delta(\boldsymbol{\mu} - \boldsymbol{\mu}_0)$ . In general this is not the case, however, one can assume to be in such a situation after performing some rough estimation of  $\boldsymbol{\mu}_0$  through a few trials of an experiment; at that point, given this ‘prior’ knowledge, one can perform the optimal local

strategy, i.e. the strategy which maximizes the precision (sensitivity) of the estimators when considering a fixed value of the parameters. The precision of an estimator is the smallest variation in the value of the parameter which can be discriminated. Maximizing the precision corresponds to minimizing the variance of an estimator. In a multiparameter case one has therefore to study the covariance matrix which, for an unbiased estimator, reads

$$\begin{aligned} \text{Cov}(\tilde{\boldsymbol{\mu}})_{\eta\zeta} &\equiv \langle (\tilde{\mu}_\eta - \langle \tilde{\mu}_\eta \rangle) (\tilde{\mu}_\zeta - \langle \tilde{\mu}_\zeta \rangle) \rangle = \\ &= \int (\tilde{\mu}_\eta - \mu_\eta) (\tilde{\mu}_\zeta - \mu_\zeta) p(\mathbf{x}|\boldsymbol{\mu}) d^m \mathbf{x} . \end{aligned} \quad (3.2)$$

One can evaluate the ultimate bound on estimation accuracy in terms of the Fisher information (FI) matrix

$$\mathcal{F}_{\eta\zeta}(\boldsymbol{\mu}) \equiv \int p(\mathbf{x}|\boldsymbol{\mu}) \frac{\partial \log p(\mathbf{x}|\boldsymbol{\mu})}{\partial \mu_\eta} \frac{\partial \log p(\mathbf{x}|\boldsymbol{\mu})}{\partial \mu_\zeta} d^m \mathbf{x} , \quad (3.3)$$

thanks to the Cramér-Rao inequality [34, 35]:

$$\text{Cov}(\tilde{\boldsymbol{\mu}}) \geq (M \mathcal{F}(\boldsymbol{\mu}))^{-1} , \quad (3.4)$$

where  $M$  is the number of measurement repetitions.

### 3.2 THE QUANTUM CASE

When considering a quantum system as the estimation probe, as for the classical case, the parameters  $\boldsymbol{\mu}$  do not in general correspond to a specific quantum observable, but they have to be inferred by means of an indirect procedure: a (quantum) measurement, described by a POVM  $\{\hat{\Pi}_x\}$ , on the parameter-dependent state  $\hat{\rho}_\mu$ , followed by classical data processing. The probabilities  $p(\boldsymbol{\mu}|\mathbf{x})$  introduced above become the probabilities of obtaining certain outcomes  $\mathbf{x}$  from the quantum measurement, i.e.  $p(\boldsymbol{\mu}|\mathbf{x}) = \text{Tr}(\hat{\rho}_\mu \hat{\Pi}_x)$ . One can hence define the FI matrix for this case as

$$\mathcal{F}_{\eta\zeta}(\hat{\Pi}_x, \boldsymbol{\mu}) = \int \frac{\text{Re} [\text{Tr}(\hat{\rho}_\mu \hat{\Pi}_x \hat{\mathcal{L}}_\eta)] \text{Re} [\text{Tr}(\hat{\rho}_\mu \hat{\Pi}_x \hat{\mathcal{L}}_\zeta)]}{\text{Tr}(\hat{\rho}_\mu \hat{\Pi}_x)} d^m \mathbf{x} , \quad (3.5)$$

where  $\hat{\mathcal{L}}_\eta$  is the Symmetric Logarithmic Derivative (SLD) operator, implicitly defined by the equation

$$\frac{\partial \hat{\rho}_\mu}{\partial \mu_\eta} = \frac{1}{2} (\hat{\rho}_\mu \hat{\mathcal{L}}_\eta + \hat{\mathcal{L}}_\eta \hat{\rho}_\mu) . \quad (3.6)$$

One immediately sees that Eq.3.5 is equivalent to Eq.3.3, by noticing that

$$\frac{\partial p(\mathbf{x}|\boldsymbol{\mu})}{\partial \mu_\eta} = \text{Tr} \left( \frac{\partial \hat{\rho}_\mu}{\partial \mu_\eta} \hat{\Pi}_x \right) = \text{Re} [\text{Tr} (\hat{\rho}_\mu \hat{\Pi}_x \hat{\mathcal{L}}_\eta)] . \quad (3.7)$$

### 3.2.1 Single-parameter estimation

Let us consider now the single parameter case:  $\boldsymbol{\mu} \equiv \{\mu\}$ . In this case, the FI, Eq.3.5, reduces to:

$$\mathcal{F}(\hat{\Pi}_x, \mu) = \int \frac{\text{Re} [\text{Tr} (\hat{\rho}_\mu \hat{\Pi}_x \hat{\mathcal{L}}_\mu)]^2}{\text{Tr} (\hat{\rho}_\mu \hat{\Pi}_x)} d^m \mathbf{x} . \quad (3.8)$$

By making use of the fact that  $(\text{Re } z)^2 \leq |z|^2, \forall z \in \mathbb{C}$ , and of the Schwartz inequality  $|\text{Tr} (\hat{O}^\dagger \hat{P})|^2 \leq \text{Tr} (\hat{O}^\dagger \hat{O}) \text{Tr} (\hat{P}^\dagger \hat{P})$ , one can show that

$$\mathcal{F}(\mu) \leq \mathcal{F}(\mu) , \quad (3.9)$$

where

$$\mathcal{F}(\mu) \equiv \text{Tr} (\hat{\rho}_\mu \hat{\mathcal{L}}_\mu^2) , \quad (3.10)$$

is the quantum Fisher information (QFI). Inequality Eq.3.9 tells us that the FI of any quantum measurement is bounded by the QFI. The inequality can always be saturated [38] when (i)  $\text{Tr}(\hat{\rho}_\mu \hat{\Pi}_x \hat{\mathcal{L}}_\mu) \in \mathbb{R}, \forall \mu$ , and (ii) when the POVM elements  $\{\hat{\Pi}_x\}$  are projectors over the eigenbasis of  $\mathcal{L}_\mu$ . It is worth noticing that the QFI is a convex quantity and additive on product states.

It is then clear that in the quantum scenario, the ultimate bound on the estimation precision of a parameter given the density matrix,  $\hat{\rho}_\mu$ , is given by the so-called quantum Cramér-Rao bound:

$$\Delta\mu^2 \geq \frac{1}{M\mathcal{F}(\mu)} , \quad (3.11)$$

where  $\Delta\mu^2$  is the variance of the estimator. The relation between estimation precision and QFI is better understood by considering that the QFI is proportional to the Fidelity susceptibility

$$\chi_F(\hat{\rho}_\mu) \equiv - \left. \frac{\partial^2 F(\hat{\rho}_\mu, \hat{\rho}_{\mu+\delta\mu})}{\partial (\delta\mu)^2} \right|_{\delta\mu=0} , \quad (3.12)$$

where  $F$  is the fidelity, Eq.1.15. This quantity is informative about how susceptible to an infinitesimal small change of the parameter  $\mu$  a quantum state is: the greatest the susceptibility, the more distinguishable are the states  $\hat{\rho}_\mu$  and  $\hat{\rho}_{\mu+\delta\mu}$ . It was proven in [39] that

$$\mathcal{F}(\mu) = 4 \chi_F(\hat{\rho}_\mu) . \quad (3.13)$$

It is then clear that the more susceptible a quantum state is to a change of the parameter, the better this parameter can be estimated.

For discrete variables systems, given the density matrix

$$\hat{\rho}_\mu = \sum_i p_i |\psi_i\rangle \langle \psi_i| , \quad (3.14)$$

the QFI reads

$$\mathcal{F}(\mu) = 4 \sum_{ij} \frac{p_i}{p_i + p_j} |\langle \psi_i | \partial_\mu \hat{\rho}_\mu | \psi_j \rangle|^2 , \quad (3.15)$$

where  $\partial_\mu \hat{\rho}_\mu = \frac{\partial \hat{\rho}_\mu}{\partial \mu}$ , and the sum is over all terms such that  $p_i + p_j \neq 0$ .

### *The Heisenberg scaling*

The enthusiasm surrounding quantum metrology comes from the promise of a considerable improvement in the performance of estimation protocols which exploit entanglement. To see this, let us consider the simple scenario of linear-unitary quantum metrology, where one wishes to estimate the phase  $\varphi$  imprinted on a quantum state by a unitary operation  $\hat{U} = e^{i\varphi \hat{H}}$ , where  $\hat{H}$  is the generator of the transformation. For the sake of simplicity we consider the case of  $\hat{H}$  acting on two-level systems, and let us call  $|0\rangle$  and  $|1\rangle$  its eigenstates relative to the eigenvalues 0 and 1 respectively. In order to estimate  $\varphi$  one can resort to Ramsey interferometry whose aim is exactly to measure the unknown relative phase between two orthogonal states,  $|0\rangle$  and  $|1\rangle$ , of an atomic system which underwent a unitary rotation. Let us compare now two strategies employing  $n = N\nu$  probing qubits, with  $\nu \gg 1$ , one which does not makes use of entanglement and one which does:

- (i) All qubits are prepared in the superposition  $|+\rangle = (|0\rangle + |1\rangle)/\sqrt{2}$  and each of them undergoes the unitary rotation. Then, for each probe, one evaluates the probability that, after the unitary transformation, the rotated state coincides with the initial state, and from this probability one can infer the unknown phase.

- (ii) The total number of probes is split in  $\nu$  groups of  $N$  qubits; each group of qubits is prepared in the same entangled GHZ state

$$|\Psi_0^{(N)}\rangle = \frac{|0\rangle^{\otimes N} + |1\rangle^{\otimes N}}{\sqrt{2}}. \quad (3.16)$$

Each qubit is then let undergo the unitary rotation, obtaining as output state

$$|\Psi_\varphi^{(N)}\rangle^{\otimes \nu} = \hat{U}^{\otimes \nu} |\Psi_0^{(N)}\rangle = \left( \frac{|0\rangle^{\otimes N} + e^{-iN\varphi} |1\rangle^{\otimes N}}{\sqrt{2}} \right)^{\otimes \nu}. \quad (3.17)$$

At this point, by projecting this state on the initial one,  $|\Psi_0^{(N)}\rangle^{\otimes \nu}$ , one can evaluate the probability  $p(\varphi)$  that they coincide and therefore the phase  $\varphi$ .

One can show that, for the central limit theorem, the error in the estimation of the phase in the first case scales asymptotically as  $1/\sqrt{N\nu}$ . This scaling is the so-called standard quantum limit (SQL). On the other hand, the entangled strategy (ii) enhances the performance of the estimation of a factor  $\sqrt{N}$ , i.e. the error on the estimation of  $\varphi$  asymptotically scales as  $1/(N\sqrt{\nu})$ . This is known as the Heisenberg scaling. It is not uncommon, in the literature, to consider  $\nu = 1$  and  $N \gg 1$ .

It is also worth noticing that the entangled strategy described above is equivalent to a sequential strategy which uses  $\nu$  probe qubits prepared in the  $|+\rangle$  state, and each of them undergoes the unitary  $N$  times. Also with this strategy, the precision in the estimation of the phase shows Heisenberg scaling [40].

### *Noisy evolutions*

In general, the transformation encoding the parameter one wishes to measure onto the probe state, can be non-unitary, but rather subject to noise. Many metrological protocols are extremely fragile to noise, and, for such protocols, the minimal disturbance could frustrate any quantum advantage. A paradigmatic example is the Mach-Zehnder interferometer setup for the estimation of a phase, where a bipartite state is sent through an interferometer with an unknown phase difference between the two paths and the output state is eventually projected onto the input. One can show that when using an entangled NOON probe state,  $|\Psi^{\text{Noon}}\rangle = (|N\rangle \otimes |0\rangle + |0\rangle \otimes |N\rangle)/\sqrt{2}$ ,

where the two degrees of freedom considered are the number of photons in each arm of the interferometer, it is possible to achieve Heisenberg scaling. On the other hand, the loss of a single photon transforms  $|\Psi^{\text{Noon}}\rangle$  into the useless maximally mixed state.

For the purposes of this thesis, we will briefly discuss parameter estimation in the presence of dephasing, in the particular case of frequency estimation. Even though phase  $\varphi$  and frequency  $\omega$  are related by the simple relation  $\varphi = \omega t$ , the quantum advantage one gets when estimating the former is robust also when the probe is subject to Markovian (Lindbladian) dephasing; on the contrary, when estimating a frequency any quantum enhancement is lost. As well summarized in [7], the difference lies in the fact that when estimating a phase one can safely assume that the time between the probe preparation and the measurement is short enough that one can neglect dephasing effects. On the other hand, for frequency estimates, the error on the frequency diverges for a vanishing sampling time,  $\Delta\omega = \Delta\varphi/t$ . Let us consider the case in which the frequency to be measured is encoded onto the quantum state by the unitary  $\hat{U} = e^{i\omega t\hat{\sigma}_z}$  and we have  $N$  qubits. During the unitary evolution, the qubits are also subject to Markovian dephasing with decay rate  $\gamma$ . The non-quantum strategy consists in preparing all the qubits in the state  $|+\rangle$  and let them undergo the unitary evolution. By using Eq.3.15 and considering that the QFI is additive on product states, the total QFI for this (uncorrelated) case reads

$$\mathcal{F}_u(\omega) = Ne^{-2t\gamma}t^2 . \quad (3.18)$$

This is maximized for the sampling time  $t_u^* = 1/\gamma$ , leading to an estimation error (obtained for the optimal measurement) of

$$\Delta\omega_u = \frac{e\gamma}{\sqrt{N}} . \quad (3.19)$$

On the other hand, if the  $N$  qubits are initially prepared in the GHZ state, Eq.3.16, the QFI reads

$$\mathcal{F}_e(\omega) = N^2e^{-2Nt\gamma}t^2 . \quad (3.20)$$

This is maximized for the sampling time  $t_e^* = 1/(\gamma N)$ , i.e. in this case the QFI reaches its peak,  $\mathcal{F}_e^*(\omega) = 1/(e^2\gamma^2) = \mathcal{F}_u^*(\omega)$ ,  $N$  times faster than in

the previous case. For a single run of the protocol, the error on the estimate of  $\omega$  reads

$$\Delta\omega_e(\text{ single run}) = e\gamma . \quad (3.21)$$

However, in the same time required to carry out the optimal estimation in the uncorrelated case, we can repeat the entangled protocol  $N$  times, therefore reducing by a factor  $\sqrt{N}$  the error on  $\omega$ , Eq.3.21, matching the precision of the uncorrelated protocol. In presence of Markovian dephasing the quantum enhancement due to the exploitation of entangled probes ceases to exist and the SQL is the best achievable scaling. However, it has been shown in [41] that it is still possible in frequency estimation to asymptotically beat the SQL, even though by only a constant factor, when using pure probing systems prepared in highly symmetric<sup>1</sup> but only partially entangled states.

Interestingly, it has been shown in [42,43] that the SQL can be surpassed when the noise is Non-Markovian (in particular time-inhomogeneous). Indeed, for such noisy evolutions, with entangled probes one can achieve the so called Zeno scaling, i.e. fixing the total time of the estimation, it is possible to get a scaling such that the error on  $\omega$  decreases with the size of the probe faster than the SQL by a factor  $N^{-1/4}$ .

As we already pointed out, a crucial hypothesis in the treatment of frequency estimation described above, is that one considers the total time of the estimation as the limiting resource. In Chapter 5 we will change perspective: instead of time, we will consider energy as the scarce resource one needs to economise on.

### 3.2.2 Multi-parameter estimation

Let us go back now to the general case in which the parameters to be estimated are more than one. In this scenario the quantum Cramér-Rao bound becomes

$$\text{Cov}(\hat{\boldsymbol{\mu}}) \geq (M\mathcal{F})^{-1} , \quad (3.22)$$

---

<sup>1</sup> The family of states proposed in [41] is completely symmetric under permutations of the  $N$  qubits and under exchange of the excited and the ground state for each qubit.

where  $\mathcal{F}$  is the quantum Fisher information matrix, defined in terms of the SLD operators

$$\mathcal{F}_{\eta\zeta} \equiv \frac{1}{2} \text{Tr} (\hat{\rho} \{ \hat{\mathcal{L}}_\eta, \hat{\mathcal{L}}_\zeta \}_+) = \text{Re} [\text{Tr} (\hat{\rho}_\mu \hat{\mathcal{L}}_\eta \hat{\mathcal{L}}_\zeta)] , \quad (3.23)$$

where  $\{\cdot, \cdot\}_+$  indicates the anticommutator. One immediately sees that, in the single parameter case, Eq.3.22 is equivalent to Eq.3.11. Contrary to the single-parameter case though, this bound is not always tight. It can however be saturated in the asymptotic limit, i.e. for a large number of repetitions of the protocol,  $M \gg 1$ , if an optimal measurement can be performed on the parameter-dependent state. As we already pointed out, an optimal measurement for each parameter is described by a set of projectors diagonal in the SLD basis. This implies that, if  $[\hat{\mathcal{L}}_\eta, \hat{\mathcal{L}}_\zeta] = 0$ , then the existence of a common eigenbasis for the two SLDs is ensured, hence a jointly optimal measurement for extracting information on both parameters  $\mu_\eta$  and  $\mu_\zeta$  can be found. However, this condition is sufficient but not necessary. A weaker condition [37,44] states that the multiparameter Cramér-Rao bound can be asymptotically saturated if and only if all pairs of SLDs commute ‘on average’: (i)  $\mathcal{J}_{\eta\zeta} = 0 \quad \forall \eta, \zeta \in \mu$ , with

$$\mathcal{J}_{\eta\zeta} \equiv \frac{1}{2i} \text{tr} (\hat{\rho}_\mu [\hat{\mathcal{L}}_\eta, \hat{\mathcal{L}}_\zeta]) = \text{Im} [\text{tr} (\hat{\rho}_\mu \hat{\mathcal{L}}_\eta \hat{\mathcal{L}}_\zeta)] . \quad (3.24)$$

Moreover, if one wishes to estimate each parameter as precisely as one would estimate them individually when assuming perfect knowledge of the other parameters, then two more conditions need to be satisfied: (ii) there must exist a single probe state  $\hat{\rho}_0$  that yields the optimal QFI for each of the parameters, and (iii) the parameters must be statistically independent, i.e.,  $\mathcal{F}_{\eta\zeta} = 0 \quad \forall \eta \neq \zeta$ . The latter condition ensures that the uncertainty on one parameter does not affect the estimation precision of the others. When all conditions (i)–(iii) are met, then the parameters are said to be *compatible* [44].

The compatibility condition (i) for continuous variable Gaussian quantum metrology will be the subject of Chapter 6.

## Part II.

### Original results



---

## THERMODYNAMIC EFFICIENCY OF COHERENT FEEDBACK COOLING

---

The possibility to exploit quantum effects in many technological applications relies heavily on the ability to achieve low enough temperatures. In the last decades we witnessed great improvements of the experimental techniques for manipulating quantum systems in this direction [45–51]. This boosted an intense theoretical effort into the investigation of the potentiality and the limitations of quantum thermodynamics: from cooling performance optimization and cycle diagnosis in the search for friction, heat leaks and internal dissipation [52–58], to the study and characterization of nanoscale cooling cycles and proposed models of quantum refrigerators [59–64], encompassing more fundamental studies about the emergence of the thermodynamic laws from quantum theory [65–67] and the role of quantum signatures in thermodynamical processes [68–74].

The work presented in this Chapter lies in the last set, indeed we try to address the question of whether the quantum share of correlations between a quantum system and an ancilla, playing the role of the controller, are a resource for energy-efficient feedback cooling. We consider the algorithmic cooling [75, 76] of spins in nuclear magnetic resonance setups. The goal of algorithmic cooling is to increase the polarization bias of an ensemble of spins, the *register*, by exploiting a second auxiliary ensemble of spins, the *ancillas* with a larger polarization bias and much shorter relaxation time. By applying a suitable joint unitary operation, part of the register’s entropy is transferred to the auxiliary spins. After this operation, the entropy in excess of the ancillas is dumped into the reservoir and they are thus reset to their initial state. During this reset operation, we can assume the register remains essentially unchanged while any correlations between the register

and the auxiliary spins vanish. Moreover, this reinitialization of the ancillas allows for iteration of the cooling algorithm and for a further reduction of the register's entropy.

We work in the framework of coherent feedback cooling [77,78] splitting the joint unitary manipulation of the systems involved into two distinct steps: (i) the *(pre-)measurement*, where correlations between register and auxiliary spins are built, allowing the latter to acquire information about the former, (ii) the *feedback*, which, by exploiting the information acquired during the pre-measurement step, allows for the cooling of the register. This cooling algorithm will be presented with more details in the first section of the Chapter.

The main goal of this work is to understand whether there is a connection between the quantum correlations built during the measurement step and the efficiency of the algorithm. In order to do this, in Section 4.2, we will first carry a thermodynamic analysis of the protocol, identifying the relevant quantities such as work, heat and entropy reduction rate. Thanks to these, we will then introduce appropriate figures of merit to assess *energy efficiency* and *effectiveness* of the algorithm, and hence we will be able to identify thermodynamically optimal working points.

Finally, in the last section, we will investigate the relation between performance optimization and the correlations built up between the register and the controller.

#### 4.1 FEEDBACK COOLING ALGORITHM

In many situations, we are interested in having a system in a particular configuration. However, due to disturbing interactions over which we have no control and/or the inaccessibility of our system, this is not always possible. In order to push the system into a target configuration, control theory (classical or quantum) usually adds to it a second system (auxiliary) which, through an appropriate interaction, drives the system of interest towards the desired setup [79]. The auxiliary together with a work source form the so-called *controller*. While *open-loop* controllers act on the system without acquiring any information about it (the interaction is unidirectional), *closed-loop* controllers act on the system on the basis of some acquired information

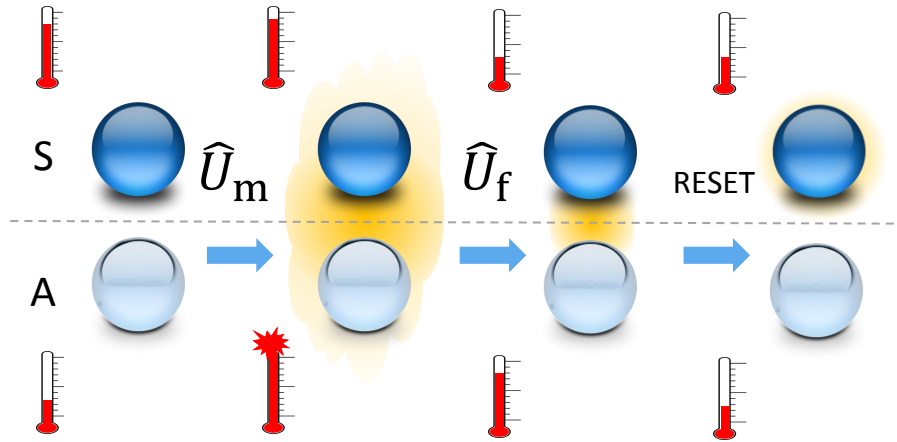


Figure 4.1.: Sketch of the four steps of the spin cooling algorithm. The effective temperatures of the marginals (computed from their populations in the energy eigenbasis) are represented by thermometers, and the correlations and residual coherence are depicted as shaded yellow halos. First,  $S$  and  $A$  are initialized in an uncorrelated state with polarization biases  $\epsilon_S < \epsilon_A$ . The measurement unitary  $\hat{U}_m$  correlates the two parts, yielding marginals with biases  $\epsilon_S \cos \varphi^2$  and  $0$ , respectively (see text for details on notation). After the application of the feedback unitary  $\hat{U}_f$  most correlations are wiped out as  $S$  is mapped to the ‘colder’ target state  $\hat{\rho}_S$ , with polarization bias  $\epsilon_A \sin \varphi$ . The marginal of  $A$  is then dissipatively reset to  $\hat{\rho}_0^{(A)}$ .

about its state. In closed-loop control (also called *feedback control* [80,81]) the controller gains information about the system during an interaction and, on the basis of this acquired information, acts on the system via actuators [77].

In our case, the system of interest is a quantum system, which raises the problem of how the information is actually gained, since any explicit measurement on the system would disturb it and erase the quantum coherence in some pre-selected basis. In such case, we would be performing a classical feedback [77]. Alternatively, we can correlate system and auxiliary (also a quantum system), without making the measurement explicit, and then complete the feedback coherently. This is the situation that we will consider here: a coherent quantum feedback control protocol [77,82].

## 4.1.1 Initialization

In the case we consider, both the quantum register  $S$  and the ancillas  $A$  are qubits. We assume that initially they share no correlations whatsoever and they are in thermal equilibrium with the surroundings, which act as a thermal reservoir at temperature  $T$ :

$$\hat{\rho}_0 = \hat{\rho}_0^{(S)} \otimes \hat{\rho}_0^{(A)}, \quad (4.1)$$

with  $\hat{\rho}_0^{(i)} = (\mathbb{1} - \epsilon_i \hat{\sigma}_z)/2$ . Here,  $\epsilon_i$  represents the polarization bias of the subsystem  $i = S, A$ , i.e. the difference between their ground and excited-state populations. Since we are assuming that register and ancillas are initially in thermal equilibrium with their surroundings at temperature  $T$ , they are described by the reduced Gibbs states,  $\hat{\rho}_0^{(i)} = \text{Tr}_j \left[ e^{-\hat{H}/T} / \text{Tr}(e^{-\hat{H}/T}) \right]$  with  $j \neq i$  (here and in the following we set  $\hbar = k_B = 1$ ), of the global Hamiltonian

$$\hat{H} = \frac{\omega_S}{2} \hat{\sigma}_z \otimes \mathbb{1}_A + \frac{\omega_A}{2} \mathbb{1}_S \otimes \hat{\sigma}_z. \quad (4.2)$$

The difference in polarization bias between the register and the ancillas is therefore due to distinct energy gaps:

$$\omega_i = T \log \left( \frac{1 + \epsilon_i}{1 - \epsilon_i} \right). \quad (4.3)$$

Their Von Neumann entropy, Eq.1.23, at this initial stage reads

$$S(\hat{\rho}_0^{(i)}) = \frac{1}{2} \log \left( \frac{4}{1 - \epsilon_i^2} \right) - \epsilon_i \operatorname{arctanh} \epsilon_i. \quad (4.4)$$

As previously anticipated, in order to achieve cooling of the register, two conditions have to be met: (i)  $\epsilon_A \geq \epsilon_S$ , meaning that the ancillas must be more polarized than the register's spins, and therefore  $S(\hat{\rho}_0^{(S)}) \geq S(\hat{\rho}_0^{(A)})$ , (ii) the relaxation time of the ancillas must be shorter than that of the register,  $\tau_A \ll \tau_S$ .

## 4.1.2 (Pre-)measurement

In this stage we apply a joint unitary on the register and the ancillas in order to correlate them and hence encode some information about the local state of the former into the latter. We choose our measurement unitary  $\hat{U}_m$  to be

$$\hat{U}_m = \exp \left\{ -i \frac{\pi}{4} \hat{\sigma}_{\vec{m}} \otimes \hat{\sigma}_y \right\}, \quad (4.5)$$

with  $\hat{\sigma}_{\vec{m}} = \vec{m} \cdot \hat{\sigma}$ ,  $\hat{\sigma} = \{\hat{\sigma}_x, \hat{\sigma}_y, \hat{\sigma}_z\}$ , and  $|\vec{m}| = 1$ . This returns a state with marginals

$$\hat{\rho}_m^{(S)} = \sum_{\mu=\pm} c_{\mu\mu} |\mu_{\vec{m}}\rangle \langle \mu_{\vec{m}}|, \quad \text{and} \quad \hat{\rho}_m^{(A)} = \frac{1}{2} \mathbb{1}_A + \frac{1}{2} \epsilon_A \tilde{\epsilon}_S \hat{\sigma}_x, \quad (4.6)$$

where  $|+\vec{m}\rangle$  and  $|-\vec{m}\rangle$  are the eigenstates of  $\hat{\sigma}_{\vec{m}}$  with eigenvalues  $+1$  and  $-1$ , respectively,  $c_{\mu\mu} = \langle \mu_{\vec{m}} | \hat{\rho}_m | \mu_{\vec{m}} \rangle$ , and  $\tilde{\epsilon}_S$  is the polarization bias of the system in the basis  $\{|\pm\vec{m}\rangle\}$ , i.e.  $\tilde{\epsilon}_S \equiv \langle -\vec{m} | \hat{\rho}_0^{(S)} | -\vec{m} \rangle - \langle +\vec{m} | \hat{\rho}_0^{(S)} | +\vec{m} \rangle$ . This means that the register is decohered in the eigenbasis of  $\hat{\sigma}_{\vec{m}}$ , while its polarization bias in the same basis is recorded in the coherences of  $\hat{\rho}_m^{(A)}$ , with ‘‘efficiency’’  $\epsilon_A$ . Hence, we can say that this unitary realizes an inefficient measurement of  $\hat{\sigma}_{\vec{m}}$  on  $\hat{\rho}_0^{(S)}$ . Note also that given the initial cylindrical symmetry of the problem, we can restrict  $\vec{m}$  to the  $x$ - $z$  plane, i.e.  $\vec{m} = \{\sin \varphi, 0, \cos \varphi\}$ , with  $0 \leq \varphi \leq \frac{\pi}{2}$ .

## 4.1.3 Feedback

From the discussion in the previous paragraph, the most informative measurement on the ancillas about the register, is a  $\hat{\sigma}_x$  measurement described by the projectors  $\{|+_x\rangle \langle +_x|, |-_x\rangle \langle -_x|\}$ . In order to achieve the largest possible entropy reduction of the register, we will therefore condition the action of the controller on the register on these measurement results. In particular, as proposed in [79], we choose the feedback unitary  $\hat{U}_f$  which allows to achieve the largest entropy reduction of the target system:

$$\hat{U}_f = \exp \left\{ i \frac{\pi}{4} \hat{\sigma}_y \right\} \otimes |+_x\rangle \langle +_x| + \exp \left\{ -i \frac{\pi}{4} \hat{\sigma}_y \right\} \otimes |-_x\rangle \langle -_x|. \quad (4.7)$$

After applying this unitary, the purity of the register spins becomes the initial purity of the ancillas,  $\text{Tr}(\hat{\rho}_0^{(A)2}) = \frac{1}{2}(1 + \epsilon_A^2) = \text{Tr}(\hat{\rho}_f^{(S)2})$ , regardless of the direction  $\vec{m}$ . The entropy of the register is reduced by

$$\begin{aligned} \Delta S_{0,f}^{(S)} &\equiv S(\hat{\rho}_0^{(S)}) - S(\hat{\rho}_f^{(S)}) = \\ &= \epsilon_A \arctanh \epsilon_A - \epsilon_S \arctanh \epsilon_S + \frac{1}{2} \log \left( \frac{1 - \epsilon_A^2}{1 - \epsilon_S^2} \right) \geq 0. \end{aligned} \quad (4.8)$$

By choosing  $\vec{m} = \vec{x}$ , i.e.  $\varphi = \frac{\pi}{2}$ , the overall unitary  $\hat{U}_f \hat{U}_m$  corresponds to a swap operation:  $\hat{\rho}_f^{(S)} = \hat{\rho}_0^{(A)}$  and  $\hat{\rho}_f^{(A)} = \hat{\rho}_0^{(S)}$ .

#### 4.1.4 Reset of the ancillas

At this point, the system is allowed to relax. After a few relaxation times  $\tau_A$ , all the correlations between the register and the controller vanish due to the irreversible interactions with the surroundings:  $\hat{\rho} \mapsto \hat{\rho}_f^{(S)} \otimes \hat{\rho}_0^{(A)}$ . The system will be then ready for additional rounds of feedback cooling if necessary, i.e. if the polarization bias of the ancillas can still be increased. Since, as we have just seen, this is not the case for our specific protocol, in the following we will consider only a single iteration of the protocol.

## 4.2 THERMODYNAMICAL ANALYSIS

### 4.2.1 Energy book-keeping

Having split the overall unitary in two steps allows us to consider the energetics of the measurement and the feedback separately. During the first step, the controller has to perform net work (evaluated as the difference in average energy):

$$\begin{aligned} \Delta E_{0,m} &\equiv \text{Tr}(\hat{H}(\hat{\rho}_0 - \hat{\rho}_m)) = \\ &= -T \left( \epsilon_S \sin^2 \varphi \arctanh \epsilon_S + \epsilon_A \arctanh \epsilon_A \right) < 0. \end{aligned} \quad (4.9)$$

On the other hand, interestingly enough, the controller can recover a fraction of the work invested in the previous step. Indeed, for choices of  $\vec{m}$  with  $\varphi$  above a certain threshold value  $\varphi_{\text{crit}}$  the feedback unitary, Eq.4.7,

always succeeds at extracting work from  $\hat{Q}_m$ , besides minimizing the entropy of the register: by defining  $y \equiv \epsilon_A \operatorname{arctanh} \epsilon_S + \epsilon_S \operatorname{arctanh} \epsilon_A$  we get

$$\begin{aligned} \Delta E_{m,f} &\equiv \operatorname{Tr}(\hat{H}(\hat{Q}_m - \hat{Q}_f)) = \\ &= -T \left( y \sin \varphi - \epsilon_S \cos^2 \varphi \operatorname{arctanh} \epsilon_S \right) \geq 0, \end{aligned} \quad (4.10)$$

if and only if

$$\varphi \geq \varphi_{\text{crit}} = \arcsin \left( \frac{-y + \sqrt{y^2 + 4\epsilon_S^2 \operatorname{arctanh}^2 \epsilon_S}}{2\epsilon_S \operatorname{arctanh} \epsilon_S} \right). \quad (4.11)$$

The difference in average energy during the feedback step, Eq.4.10, is a monotonic function of  $\varphi$  for  $0 \leq \varphi \leq \frac{\pi}{2}$ , hence the maximum work recovery  $\Delta E_{m,f}$  is attained for a measurement along the  $x$  direction, although for  $\epsilon_S < \epsilon_A < 1$  not all extractable work (or “ergotropy” [52]) can be retrieved<sup>1</sup>.

During the reset operation, we assumed that the register remains unchanged, while the ancillas thermalize and the residual correlations are completely lost. The difference in average energy of the ancillary spins can be regarded as heat irreversibly dumped into the environmental bath:

$$\begin{aligned} Q &\equiv \operatorname{Tr}(\hat{H}_A(\hat{\rho}_f^{(A)} - \hat{\rho}_0^{(A)})) = \\ &= T(\epsilon_A - \epsilon_S \sin \varphi) \operatorname{arctanh} \epsilon_A > 0. \end{aligned} \quad (4.12)$$

It is worth noticing that, in the framework developed in [83], the feedback controller plays the role of a Maxwell’s demon (even though, on the contrary to our case, in [83] the authors consider a *measurement-based* feedback protocol in which the auxiliary is let decohere in the measurement basis before applying the feedback). One can easily show that the heat dumped into the environment, Eq.4.12, can be lower bounded as [79]

$$Q \geq T \Delta S_{0,f}^{(S)} + \mathcal{I}(\hat{Q}_m), \quad (4.13)$$

where  $\mathcal{I}(\hat{Q}_m)$  is the mutual information, Eq.1.26, between the system and the auxiliary after the (pre-)measurement step. The right hand side of Eq.4.13

<sup>1</sup> In the case of a measurement in the  $x$  direction, one finds that it is possible to extract an important fraction of the ergotropy: for example, for  $\epsilon_S = 0.4$  one can retrieve more than 50% of it. It is worth noticing that the fraction of ergotropy one can retrieve during the feedback stage is a decreasing function of the entropy reduction of the system.

can be considered as the minimal heat that needs to be released into the environment to reset the memory of the demon.

Notice also that while the ancillary spins perform a cycle, the registers changed their average energy by

$$\Delta E_{0,f}^{(S)} = -T(\epsilon_S - \epsilon_A \sin \varphi) \operatorname{arctanh} \epsilon_S, \quad (4.14)$$

which does not have a definite sign. This is due to the residual coherence in  $\hat{\rho}_f^{(S)}$ . Indeed, the increase in the system's purity achieved in the protocol corresponds to an increase in the polarization bias of the spins in *some basis*, which is not necessarily the energy eigenbasis.  $\Delta E_{0,f}^{(S)} < 0$  is only guaranteed to hold, regardless of the polarization bias of the ancillas,  $\epsilon_A > \epsilon_S$ , for a measurement along the  $x$  axis, in which case  $\Delta E_{0,f}^{(S)} < 0$ . In other words, even though the algorithm always reduces the entropy of the register spins, *real cooling* only happens within the 'cooling window'  $\frac{\epsilon_S}{\sin \varphi} < \epsilon_A \leq 1$ . It is therefore clear that the polarization bias in the energy eigenbasis cannot be increased if  $\sin \varphi < \epsilon_S$ , regardless of  $\epsilon_A$ .

#### 4.2.2 Performance of algorithmic cooling

We want now to characterize and optimize the performance of such an algorithm. Performance optimization is essential to determine the most energy-efficient usage of the used resources, conditioned on the maximization of the "useful effect". Depending on the particular task, one may be willing to spend more resources in order to achieve, e.g. faster cooling, or to minimize undesired side-effects, such as residual heat dumped into the surroundings. For this reason, it is convenient to introduce suitably-defined figures of merit.

In particular, since our protocol aims at maximize the entropy reduction of the register, we will define the useful effect as

$$P \equiv T \Delta S_{0,f}^{(S)}. \quad (4.15)$$

The cost the controller has to pay to achieve it, could be captured by the work they had to perform on the system

$$W = -\Delta E_{0,f}^{(S)} + Q > 0. \quad (4.16)$$

We define the *coefficient of performance* (COP) of the protocol as the quotient

$$\varepsilon \equiv \frac{P}{W}. \quad (4.17)$$

Like the ratio of the cooling rate to the input power in a conventional refrigeration cycle [84], the COP is positive and unbounded.

For fixed  $\varepsilon_S$ , by varying  $\varepsilon_A$ , we can plot the COP  $\varepsilon$  as a function of  $P$ . For every value of  $\varphi$  we find a *characteristic curve* of our feedback cooling protocol, see panel (a) of Fig.4.2. Given a measurement direction, i.e. chosen a particular value of  $\varphi$ , the COP is maximized at an intermediate polarization bias  $\varepsilon_S < \varepsilon_A^* < 1$ , corresponding to some optimally efficient entropy reduction rate  $P^*$ , the *cooling load*. It is worth noticing that the value of  $P^*$  decreases monotonically as  $\varphi$  varies from 0 to  $\frac{\pi}{2}$ . On the other hand, the COP grows monotonically with  $\varphi$  for any fixed  $\varepsilon_A$ . In the limiting case of an  $x$  measurement,  $\varphi = \frac{\pi}{2}$ , the COP attains its maximum value for  $\varepsilon_A \rightarrow \varepsilon_S$ , which means for vanishing  $P^*$ . Notice that in this case one also has  $Q \rightarrow 0$  (and  $\Delta E_{0,f}^{(S)} \rightarrow 0$ , i.e.  $W \rightarrow 0$ ), which means that the maximization of the COP occurs when the overall protocol is reversible, as should be expected.

In [79], the efficiency-like figure of merit

$$\eta \equiv \frac{P}{Q}, \quad (4.18)$$

had been proposed. Optimizing  $\eta$  corresponds to determine the most advantageous trade-off between the largest entropy reduction achievable at the minimal heat release into the thermal bath. It is easy to verify, from Eqs.4.8-4.12, that since  $Q \geq P$ , the figure of merit  $\eta$  is positive and upper-bounded by one. Its qualitative behaviour, however, is similar to that of the COP.

From the above discussion, we notice that the figures of merit  $\varepsilon$  and  $\eta$  have a downside: they are indeed optimized for an (inefficient) measurement of the polarization bias of the register in the eigenbasis of  $\hat{\sigma}_x$ . We already pointed out that for this case the overall unitary manipulation simply swaps the states of  $S$  and  $A$ . However, both  $\varepsilon$  and  $\eta$  are maximized for  $\varepsilon_A \rightarrow \varepsilon_S$ , resulting in a vanishing useful effect. In other words, the protocol is maximally efficient but not effective, as is often the case in thermal

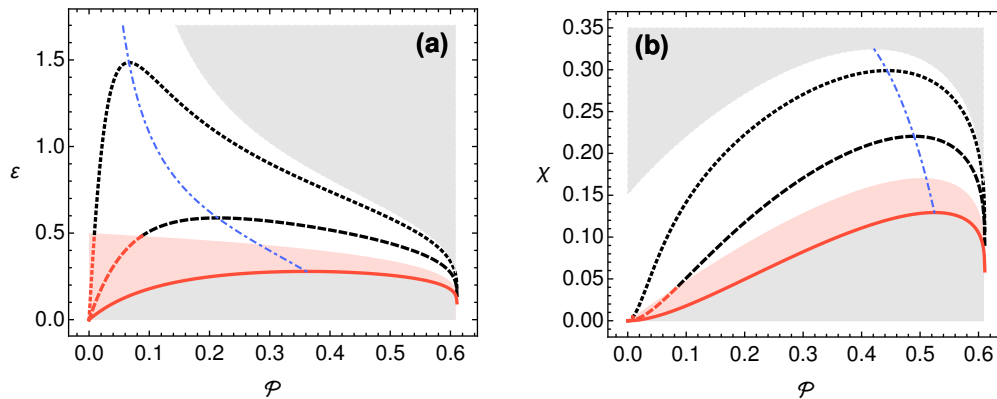


Figure 4.2.: **(a)** Coefficient of performance, Eq.4.17, and **(b)** figure of merit  $\chi$ , Eq.4.19, versus the entropy reduction on the registers  $P$ , Eq.4.15 for fixed initial polarization bias  $\epsilon_S = 0.4$  and different measurement directions:  $\varphi = 0$  (solid),  $\varphi = \pi/4$  (dashed), and  $\varphi = 2\pi/5$  (dotted). In both plots, the bias of the ancillas  $\epsilon_A$  ranges from  $\epsilon_S$  to 1 and the temperature is  $T = 1$ . The part of the curves falling inside the cooling window  $\frac{\epsilon_S}{\sin \varphi} < \epsilon_A < 1$  is depicted in black, whereas configurations for which  $\Delta E_{0,f}^{(S)} < 0$  (i.e. no real cooling occurs) lie within the shaded red areas. The gray regions correspond to inaccessible configurations, and the optimal working points  $\{P^*, \epsilon^*\}$  and  $\{P^*, \chi^*\}$  are indicated with dot-dashed blue lines.

engineering. In order to have a meaningful figure of merit which attains its maximum at a non-vanishing  $P^*$ , we introduce the function

$$\chi \equiv \epsilon P = \frac{P^2}{W}, \quad (4.19)$$

which is well suited for applications which require both effectiveness and (energy) efficiency. As one can see from Fig.4.2, panel (b),  $\chi$  is qualitatively different from  $\epsilon$  (and hence  $\eta$ ). In particular, its global maximum, still attained for  $\varphi = \frac{\pi}{2}$ , corresponds to a strictly positive (and comparatively large) entropy reduction, corresponding to the preparation of the ancillary spins at a large polarization bias.

### 4.3 INFORMATION-THEORETICAL ANALYSIS

The split of the unitary into two distinct unitaries becomes particularly useful when one wants to make an ‘information balance’ of the protocol. Indeed, recall that the measurement unitary is designed to allow the controller to acquire information about the system. This informational acquisition is

achieved by building up correlations between the register and the ancillary spins. The subsequent actions of the controller and the success of the cooling protocol are conditioned on that information, i.e. on those correlations. It seems than interesting to investigate further the amount of these correlations and, in particular, their nature, discerning their quantum share from the classical one.

We have just seen, in the previous section, that the energy efficiency is maximized when  $\hat{\sigma}_x$  is measured on the register (and the outcome is recorded inefficiently in the ancillas). We notice that in the eigenbasis of this observable, the register is initially maximally coherent. This  $x$ -measurement can therefore be regarded as the most ‘quantum’ instance of the cooling protocol. In contrast, the most inefficient and ineffective measurement (it does not even succeed in reducing the polarization bias of the register) corresponds to a  $z$ -measurement, i.e. a measurement in the energy eigenbasis, which is the only completely classical situation. These considerations seem to suggest that some ‘quantumness’ plays a crucial role for the realization of an efficient and effective cooling protocol, as suggested in [79].

For the particular case considered, the mutual information, Eq.1.46, and the entanglement of formation, Eq.1.26, have cumbersome expressions which we do not report here since they do not add anything to the discussion. Ollivier and Zurek’s quantum discord, Eq.1.33, is, in general, not easy to compute due to the maximization over all possible measurements on  $A$ . However, the bipartite state  $\hat{\rho}_m$  can be transformed by means of local unitaries (which preserve the discord) into an  $X$ -state, i.e. a state  $\hat{\sigma} \in \mathcal{B}(\mathcal{H})$  whose only non-vanishing elements are the diagonal ones,  $\hat{\sigma}_{ii}$ , and the “anti-diagonal” ones  $\hat{\sigma}_{i,5-i}$ , for  $i = 1, \dots, 4$ . For this class of states there exists an analytical formula [85] for the quantum discord [15]. The quantum discord of the state  $\hat{\rho}_m$  is symmetric under the exchange of the parties,  $\delta(\hat{\rho}_m; A : S) = \delta(\hat{\rho}_m; S : A) \equiv \delta(\hat{\rho}_m)$ , and it reads:

$$\begin{aligned} \delta(\hat{\rho}_m) = & \epsilon_s \operatorname{arctanh} \epsilon_s + \frac{1}{2} \log \left( \frac{1 - \epsilon_s^2}{1 - \epsilon_s^2 \cos^2 \varphi} \right) + \\ & + \frac{1}{2} \epsilon_s \cos \varphi \log \left( \frac{1 - \epsilon_s \cos \varphi}{1 + \epsilon_s \cos \varphi} \right). \end{aligned} \quad (4.20)$$

In Fig.4.3 we plot the entanglement of formation, the mutual information, and the quantum discord of the state  $\hat{\rho}_m$  for all working points  $\{\chi, P\}$ .

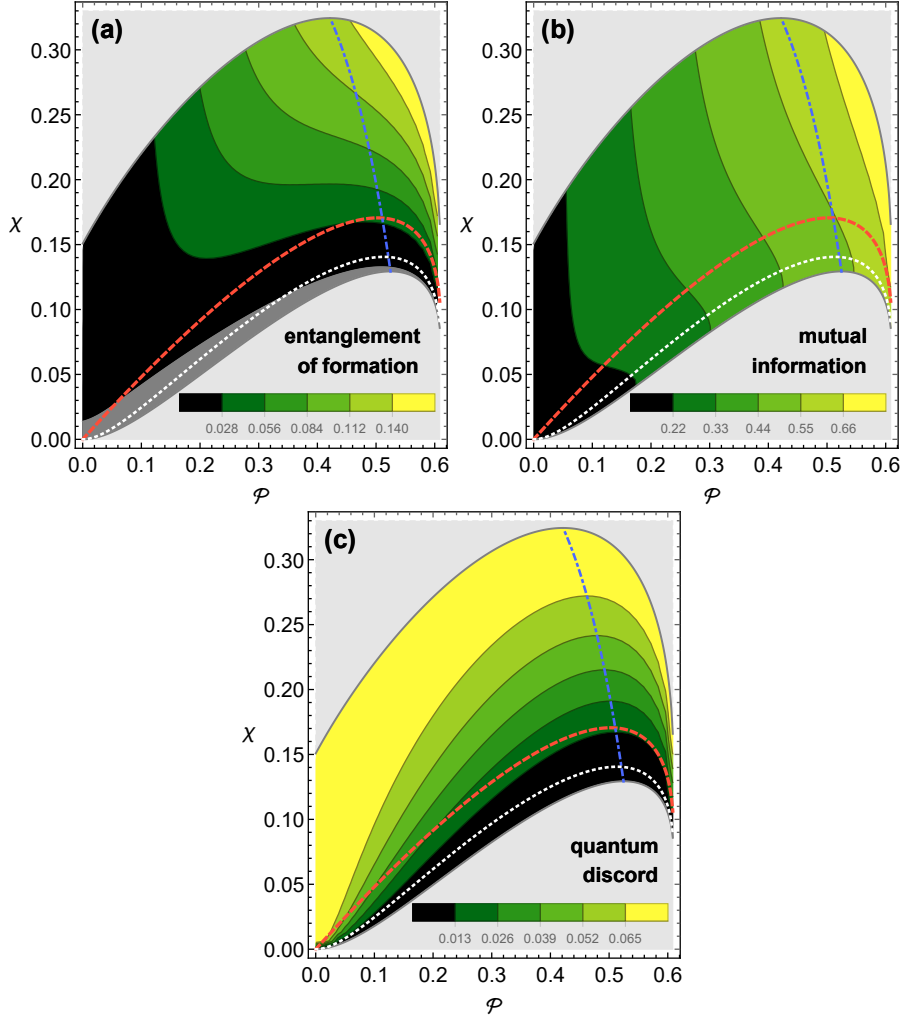


Figure 4.3.: **(a)** Entanglement of formation  $\mathcal{E}(\hat{\rho}_m)$ , **(b)** mutual information  $I(\hat{\rho}_m)$ , and **(c)** quantum discord  $\delta_A(\hat{\rho}_m)$  evaluated after the measurement step, versus the entropy reduction rate, Eq.4.15, and the figure of merit  $\chi$ . Shaded gray areas, dashed red curve, and dot-dashed blue curve as in Fig.4.2. The dotted white line marks configurations for which  $\varphi = \varphi_{\text{crit}}$ ; above this curve,  $\varphi > \varphi_{\text{crit}}$ , the feedback unitary  $\hat{U}_f$  becomes capable of extracting work from  $\hat{\rho}_m$ , see Eq.4.10. Finally, the dark shaded gray area of **(a)**, corresponds to working points with zero entanglement between  $S$  and  $A$ . We have set  $\epsilon_S = 0.4$  and  $T = 1$ .

From panel (a) we notice that setups with low enough  $\varphi$  produce separable post-measurement states  $\hat{\rho}_m$  (dark-shaded area), although entanglement is almost ubiquitous in this protocol. Moreover, it is clear that there is no apparent direct link between entanglement and the ability of the protocol in increasing the polarization bias of the register after the feedback step: once the initial polarization bias of the ancillas, and hence  $P$ , is fixed, we see that

both separable and entangled states may succeed or fail in the task. The same can be said about the potential connection between the entanglement of formation and the possibility of extracting work during the feedback step,  $\Delta E_{m,f} > 0$ : entanglement between the register and the ancillas is definitely not a resource for work extraction [86]. Furthermore, the entanglement is maximized for a perfectly efficient  $x$ -measurement, i.e.  $\varphi = \frac{\pi}{2}$  and  $\epsilon_A = 1$ , which is far from being the optimal working point of the protocol.

Analogous considerations can be done for the mutual information, panel (b). Also in this case, as for the entanglement, the mutual information is maximized for a perfectly efficient  $x$ -measurement and not for the optimal working point.

The situation becomes more intriguing when one considers the quantum discord, panel (c). Indeed, as one can notice from the explicit expression, Eq.4.20, the quantum discord does not depend on the initial polarization bias of the ancillas  $\epsilon_A$ , but only on  $\epsilon_S$ . Crucially, this implies that the performance characteristic curves previously introduced, and depicted in Fig.4.2, are curves of constant discord. In particular, the maximization of the discord  $\delta(\hat{Q}_m)$ , at fixed cooling load  $P$ , occurs for  $\varphi = \frac{\pi}{2}$ , which is compatible with the optimization of the figure of merit  $\chi$ , as well as that of  $\epsilon$  and  $\eta$ . This observation is suggestive of a deep connection between quantum discord and the thermodynamic performance of spin algorithmic cooling.

The cooling window,  $\varphi = \arcsin \frac{\epsilon_S}{\epsilon_A}$ , and the work extraction threshold,  $\varphi = \varphi_{\text{crit}}$ , are also plotted in Fig.4.3 as red-dashed and white-dotted lines, respectively. From their analytical expressions, since they explicitly depend on  $\epsilon_A$ , it is clear that they are not iso-discordant lines, therefore one cannot unambiguously claim that the build-up of a certain amount of any particular kind of correlations enable to enter these important regimes of operation. At most one can quantify the minimum amount of quantum correlations  $\delta_{\text{min}}$  required to work in an effective cooling regime, indeed  $\delta_{\text{min}}$  is easily found by setting  $\sin \varphi = \frac{\epsilon_S}{\epsilon_A}$  into Eq.4.20: applying a measurement unitary such that  $\delta(\hat{Q}_m) > \delta_{\text{min}}$  ensures an increase in the polarization bias of the register spins.

## 4.4 REMARKS

In this Chapter we characterized the performance of a simple entropy reduction algorithm. Our investigation was based on two complementary approaches. We first quantified the relevant thermodynamical quantities, such as the work performed by the controller  $W$ , the heat  $Q$  dumped into the environment during the reset operation and the entropy reduction  $\propto P$ . With these tools we introduced some suitable figures of merit which allowed us to scrutinize the performance of the protocol, specifically, the coefficient of performance  $\varepsilon$ , to assess the energy efficiency, and an alternative figure of merit  $\chi$  which seemed more suitable to balance the efficiency and, at the same time, the effectiveness of the protocol.

In the second part, we studied the correlations, built-up during the first step of the algorithm, between the system of interest and the ancillary system, part of the controller. Our main motivation was to shed light on whether some type of correlations are a resource for the protocol, i.e. we wanted to find a connection between correlations and the performance optimization. Interestingly we found that, for every choice of the measurement with which one acquires information about the system of interest, the quantum share of the correlations, as measured by the quantum discord, is constant with the entropy reduction  $P$ . This is because the quantum discord does not depend on the initial polarization bias of the ancillary spins. Moreover we found that the maximization of the discord occurs naturally when the performance is optimal, regardless of the figure of merit used. In contrast, neither the total correlations, nor the entanglement, quantified as the mutual information and the entanglement of formation respectively, relate in a clear way to the figures of merit, nor they are found to be maximal at the optimal working points.

# 5

---

## ENERGY-EFFICIENT QUANTUM FREQUENCY ESTIMATION

---

In this Chapter we want to apply a similar efficiency-oriented framework, as for the previous Chapter, to the study of a metrological protocol in which we want to estimate the frequency of some thermal qubits affected by noise. In Chapter 3, we have briefly reviewed the basics of quantum parameter estimation. Summarizing, when one wants to estimate a single parameter  $\mu$  employing quantum resources, the statistical uncertainty of the estimate  $\Delta\mu$  is tightly lower bounded by a term which is proportional to the square root of the inverse of the quantum Fisher information (QFI) of the probe in which the parameter is encoded, see Eq.3.11. While using uncorrelated probes, the mean square error on the parameter can asymptotically scale at most as  $n^{-\frac{1}{2}}$  (standard quantum limit, SQL), where  $n$  is the number of probes (with respect to the notation of Chapter 3 we consider  $\nu = 1$ , i.e.  $n = N$ ), by using entangled probes one can hope to achieve a better asymptotic scaling,  $n^{-1}$ , namely the Heisenberg limit. This happens when the parameter-encoding transformation acting on the probes is noiseless; in general, unavoidable effects of environmental noise frustrate any quantum advantage [41]. However, as we saw in Paragraph 3.2.1, under time-inhomogeneous phase-covariant noise one can asymptotically achieve the so-called Zeno scaling [42,43], i.e.  $\Delta\mu \sim n^{-\frac{3}{4}}$ . In that same Paragraph, we discussed frequency estimation in presence of noise when the total running time  $\mathcal{T}$ , and hence the length  $M$  of the data set used to build the estimate, is limited. One can, however, think that the scarce resource, instead of time, is some other quantity  $\mathcal{R}$  which is used up gradually in subsequent rounds of the protocol; calling  $r$  the amount of resource used per each run of the

protocol, the number of times the protocol can be performed is  $M = \mathcal{R}/r$ . Therefore, the quantum Crámer-Rao bound can be rewritten as

$$\Delta\mu \geq \frac{1}{\sqrt{\mathcal{R}\eta_{\mathcal{R}}}}, \quad (5.1)$$

where we defined the estimation efficiency

$$\eta_{\mathcal{R}} \equiv \frac{\mathcal{F}(\mu)}{r}. \quad (5.2)$$

A scaling such as  $\eta_{\mathcal{R}} \sim n^c$ , with  $c > 1$ , would indicate a quantum-enhanced performance of the estimation.

In this Chapter, we will consider  $\mathcal{R}$  as the total energy  $\mathcal{E}$  consumed in order to prepare the probes for the sensing and for the measurement. We will show how the notion of optimality that follows from the maximization of the energy efficiency  $\eta_{\mathcal{E}}$  differs considerably when compared with a time efficient estimation. Indeed, we show that, on the contrary to the latter case, also in presence of time-inhomogeneous noise, the creation of large multipartite correlated probes is discouraged when the energy available for the estimation is limited: the high costs associated with the creation and manipulation of such states do not pay off from the metrological viewpoint.

This Chapter is structured as follows: in the first Section we will describe the noise model which affects the parameter encoding transformation. Then, in the second Section we will introduce the estimation protocol and, for each step, we will quantify the energetic cost of the manipulation of the probe. In the third Section, we will calculate and compare the (classical) Fisher information (relative to the measurement considered) of the probe after the parameter encoding transformation with its QFI. Finally, in the Section 5.4, we will study the energy efficiency of the protocol and compare it with the time-efficiency.

## 5.1 PHASE COVARIANT NOISE: A PHENOMENOLOGICAL MODEL

### 5.1.1 Phenomenological master equation

The environmental noise is assumed to be modelled by a time-nonlocal master equation with phenomenological exponentially-decaying memory kernel [87]. With this assumption, the resulting dissipative dynamics is

phase-covariant and it is able to capture paradigmatic phenomena such as decoherence and thermalisation. This will eventually allow us to compare our results to already known results present in the literature [42, 43]. Moreover, this model can be solved exactly, simplifying our analysis.

Let us consider a two-level system with Hamiltonian  $\hat{H}_S = \frac{\omega}{2}\hat{\sigma}_z$  (here and in the following, we set  $\hbar = k_B = 1$ ) interacting with a bath at temperature  $T$ , with Hamiltonian  $\hat{H}_B$ , through the interaction  $\hat{H}_I$ . Setting  $\hat{H}_0 = \hat{H}_S + \hat{H}_B$  as the free Hamiltonian, in the interaction picture the density matrix of the system evolves according to the following phenomenological equation (see Eq.1.87), which has the advantage of explicitly introducing memory effects into the dynamics<sup>1</sup>

$$\frac{d\hat{\rho}^{(I)}}{dt} = \int_0^t f(t-s)\mathcal{L}\hat{\rho}^{(I)}(s), \quad (5.3)$$

with  $f(t) \equiv \lambda e^{-\lambda|t|}$  and where  $\mathcal{L}$  denotes the Lindbladian, acting on the density matrix as

$$\begin{aligned} \mathcal{L}\hat{\rho}_I \equiv & \Gamma_\omega \left( \hat{\sigma}_- \hat{\rho}_I \hat{\sigma}_+ - \frac{1}{2} \{ \hat{\sigma}_+ \hat{\sigma}_-, \hat{\rho}_I \}_+ \right) + \\ & + \Gamma_{-\omega} \left( \hat{\sigma}_+ \hat{\rho}_I \hat{\sigma}_- - \frac{1}{2} \{ \hat{\sigma}_- \hat{\sigma}_+, \hat{\rho}_I \}_+ \right), \end{aligned} \quad (5.4)$$

where  $\hat{\sigma}_+ = \hat{\sigma}_x + i\hat{\sigma}_y$ ,  $\hat{\sigma}_- = \hat{\sigma}_x - i\hat{\sigma}_y$ ,  $\Gamma_\omega \equiv \gamma_0[1 + (e^{\omega/T} - 1)^{-1}]$  and  $\Gamma_{-\omega} = e^{-\omega/T}\Gamma_\omega$ . The thermal state

$$\hat{\rho} = \frac{e^{-\frac{\hat{H}_S}{T}}}{\text{Tr} \left( e^{-\frac{\hat{H}_S}{T}} \right)} = \frac{1}{2} \begin{pmatrix} 1 - \epsilon & 0 \\ 0 & 1 + \epsilon \end{pmatrix}, \quad (5.5)$$

where  $\epsilon = \tanh \left( \frac{\omega}{2T} \right)$  is the polarization bias, is the stationary point of Eq.5.3. Moreover, it is important to notice that the map generated by  $\mathcal{L}$ , as defined in Eq.5.3, breaks positivity if and only if  $\frac{\gamma_0}{\lambda\epsilon} \geq \frac{1}{4}$  [89].

### 5.1.2 Dissipative dynamics as phase-covariant channel

As we have seen in Paragraph 1.2.3, an equation such as Eq.5.3 can be recast into convolutionless form, Eq.1.89, for which, in the Schrödinger picture,

<sup>1</sup> See [87] for a comparison between the master equation Eq.5.3 and the phenomenological post-Markovian master equation introduced in [88] which allows to interpolate between the exact Nakajima-Zwanzig equation and the Markovian Lindblad equation.

a Lindblad-like master equation with time-dependent coefficients can be written (see Paragraph 1.2.3):

$$\begin{aligned} \frac{d\hat{\rho}}{dt} = & -i[\hat{H}_S, \hat{\rho}] + \gamma_+(t) \left( \hat{\sigma}_+ \hat{\rho} \hat{\sigma}_- - \frac{1}{2} \{ \hat{\sigma}_- \hat{\sigma}_+, \hat{\rho} \}_+ \right) + \\ & + \gamma_-(t) \left( \hat{\sigma}_- \hat{\rho} \hat{\sigma}_+ - \frac{1}{2} \{ \hat{\sigma}_+ \hat{\sigma}_-, \hat{\rho} \}_+ \right) + \gamma_z(t) (\hat{\sigma}_z \hat{\rho} \hat{\sigma}_z - \hat{\rho}), \end{aligned} \quad (5.6)$$

where [90]

$$\gamma_{\pm}(t) = -\frac{1}{2}(1 \mp \epsilon) \frac{d}{dt} \log \xi_R(t), \quad (5.7)$$

$$\gamma_z(t) = \frac{1}{4} \frac{d}{dt} \log \frac{\xi_R(t)}{\xi_{R/2}^2(t)}, \quad (5.8)$$

with  $\xi_R(t) \equiv e^{-\lambda t/2} \left[ \frac{\sinh(\frac{\lambda t}{2} \sqrt{1-4R})}{\sqrt{1-4R}} + \cosh\left(\frac{\lambda t}{2} \sqrt{1-4R}\right) \right]$  and  $R = \frac{\gamma_0}{\lambda \epsilon}$ .

In particular, as argued in [43], the dissipative dynamics described by Eq.5.6 describes a phase-covariant channel  $\hat{\rho}(t) = \Lambda(t)\hat{\rho}(0)$ , i.e. a map such that  $\Lambda \circ \mathcal{U}_t = \mathcal{U}_t \circ \Lambda$ , where  $\mathcal{U}_t[\hat{\rho}] \equiv e^{-i\hat{H}_S t} \hat{\rho} e^{i\hat{H}_S t}$ . Such a map can be parametrised as

$$\Lambda(t) = \begin{pmatrix} 1 & 0 & 0 & 0 \\ 0 & \eta_{\perp}(t) \cos \omega t & -\eta_{\perp}(t) \sin \omega t & 0 \\ 0 & \eta_{\perp}(t) \sin \omega t & \eta_{\perp}(t) \cos \omega t & 0 \\ \kappa(t) & 0 & 0 & \eta_{\parallel}(t) \end{pmatrix}, \quad (5.9)$$

where the matrix  $\Lambda(t)$  acts on  $\mathbf{v}(0) = (1, \text{Tr}[\hat{\sigma}_x \hat{\rho}(0)], \text{Tr}[\hat{\sigma}_y \hat{\rho}(0)], \text{Tr}[\hat{\sigma}_z \hat{\rho}(0)])$  to yield  $\mathbf{v}(t) = \Lambda(t)\mathbf{v}(0)$ , so that  $\hat{\rho}(t) = \frac{1}{2}(\mathbf{v}_1(t)\mathbb{1} + \mathbf{v}_2(t)\hat{\sigma}_x + \mathbf{v}_3(t)\hat{\sigma}_y + \mathbf{v}_4(t)\hat{\sigma}_z)$ .

The complete positivity of this map, is ensured by the conditions  $\eta_{\parallel}(t) \pm \kappa(t) \leq 1$  and  $1 + \eta_{\parallel}(t) \geq \sqrt{4\eta_{\perp}^2(t) + \kappa^2(t)}$ . Moreover, since the map describes the action of a thermal bath, we require that it asymptotically brings the two-level system into the thermal state Eq.5.5, i.e. we impose  $\kappa(\infty) = -\epsilon[1 - \eta_z(\infty)]$ .

Following [43] one readily finds that Eq.5.3 corresponds to

$$\begin{aligned} \eta_{\alpha}(t) &= \frac{e^{-t\lambda(1+A_{\alpha})/2}}{2A_{\alpha}} \left[ e^{t\lambda A_{\alpha}}(1 + A_{\alpha}) + A_{\alpha} - 1 \right], \\ \kappa(t) &= -\epsilon[1 - \eta_{\parallel}(t)], \end{aligned} \quad (5.10)$$

where  $\alpha \in \{\parallel, \perp\}$ ,  $A_{\parallel} = \sqrt{1-4R}$ , and  $A_{\perp} = \sqrt{1-2R}$ .

In the Appendix B we will discuss the connection between the model described above and the damped Jaynes-Cummings model.

## 5.2 THE PROTOCOL

We consider an ensemble of  $n$  initially thermal qubits. A sequence of gates is applied to these qubits in order to transform them into a sensitive GHZ-diagonal state. The probe is then left to evolve freely under the action of phase-covariant noise. In order to prepare the probe for the readout, after the free evolution, another sequence of gates is applied. The measurement consists of an energy measurement. See Fig.5.1 for an illustration of the protocol.

## 5.2.1 Probe initialisation

The system of interest is an ensemble of  $n$  non-interacting two-level atoms thermalised at temperature  $T$ . We are interested in the estimation of the frequency  $\omega$  of these atoms. The single atom Hamiltonian is  $\hat{H}_S$  (see previous Section). At the beginning of the protocol, the state of each atom is described by the thermal state  $\hat{\rho}$ , Eq.5.5. The global Hamiltonian is  $\hat{H} = \frac{\omega}{2} \hat{J}_z$ , where  $\hat{J}_z = \hat{\sigma}_z \otimes \mathbb{1}^{\otimes n-1} + \mathbb{1} \otimes \hat{\sigma}_z \otimes \mathbb{1}^{\otimes n-1} + \dots + \mathbb{1}^{\otimes n-1} \otimes \hat{\sigma}_z$  is the total angular momentum, and the global initial state simply reads (for brevity, we introduce the notation  $\hat{A}_x = \hat{\sigma}_x \hat{A} \hat{\sigma}_x$ , and  $\hat{A}^{\otimes} \equiv \hat{A}^{\otimes n-1}$ )

$$\hat{\rho}_0 = \hat{\rho}^{\otimes n} \equiv \hat{\rho}_c \otimes \hat{\rho}_r^{\otimes} = \frac{1}{2} \begin{pmatrix} (1 - \epsilon)\hat{\rho}^{\otimes} & 0 \\ 0 & (1 + \epsilon)\hat{\rho}^{\otimes} \end{pmatrix}, \quad (5.11)$$

where we have labelled with  $c$  the ‘control qubit’, while the rest are tagged  $r$  for ‘register’ (see Fig.5.1).

By means of a CNOT =  $|0\rangle\langle 0|_c \otimes \mathbb{1}^{\otimes} + |1\rangle\langle 1|_c \otimes \hat{\sigma}_x^{\otimes}$  transformation, followed by a Hadamard gate  $H = \frac{1}{\sqrt{2}}(\hat{\sigma}_x + \hat{\sigma}_z)$  and a further CNOT, we prepare the  $n$ -qubit probe into a GHZ-diagonal state. The application of the first sequence of CNOT gates yields

$$\hat{\rho}_1 = \frac{1}{2} \begin{pmatrix} (1 - \epsilon)\hat{\rho}^{\otimes} & 0 \\ 0 & (1 + \epsilon)\hat{\rho}_x^{\otimes} \end{pmatrix}. \quad (5.12)$$

The Hadamard gate acts solely on the control qubit:

$$\hat{\rho}_2 = \frac{1 - \epsilon}{4} \begin{pmatrix} \hat{\rho}^{\otimes} & \hat{\rho}^{\otimes} \\ \hat{\rho}^{\otimes} & \hat{\rho}^{\otimes} \end{pmatrix} + \frac{1 + \epsilon}{4} \begin{pmatrix} \hat{\rho}_x^{\otimes} & -\hat{\rho}_x^{\otimes} \\ -\hat{\rho}_x^{\otimes} & \hat{\rho}_x^{\otimes} \end{pmatrix}, \quad (5.13)$$

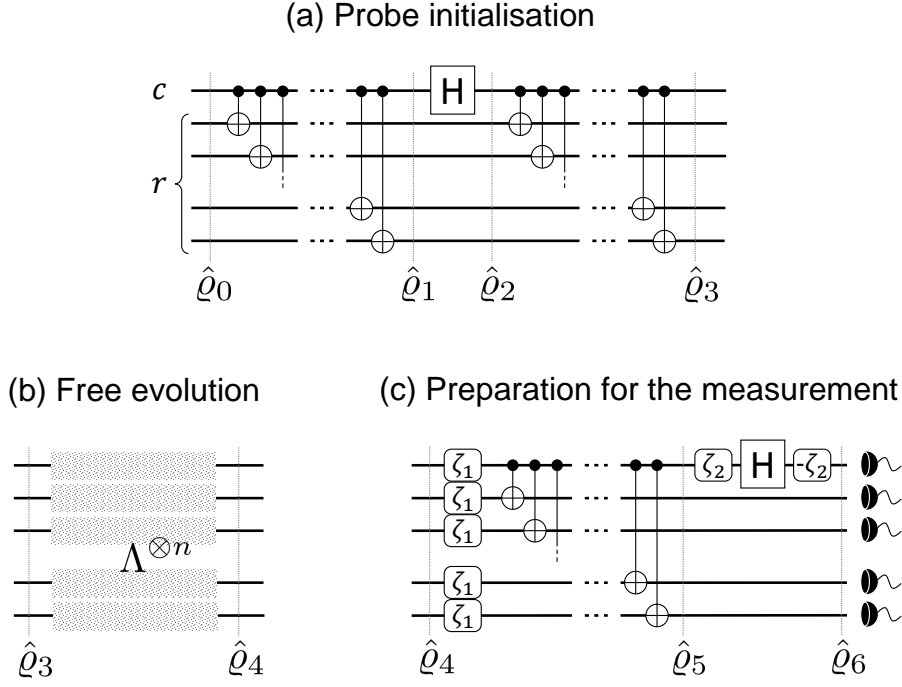


Figure 5.1.: Circuit representation of the (a) probe initialisation, (b) free evolution, and (c) preparation for the measurement stages of our estimation protocol, as discussed in the main text. (a) A probe system composed of one control ( $c$ ) qubit and  $n - 1$  register ( $r$ ) qubits, initially in a thermal state  $\hat{Q}_0$ , is prepared into a GHZ-diagonal state  $\hat{Q}_3$  by a sequence of CNOT, Hadamard [H], and CNOT gates. (b) The system is left to evolve freely for a time  $t$  under a noisy environment according to a master equation with a memory kernel; this amounts to the action of the phase-covariant channel  $\Lambda$ , which imprints a phase  $\phi = \omega t$  on the qubits while inducing dissipation effects, overall transforming the state of the system into  $\hat{Q}_4$ . (c) A pre-measurement sequence of qubit rotations, CNOT gates, and a rotated Hadamard on the control qubit is applied, leading to the state  $\hat{Q}_6$ ; each rounded rectangle ( $\zeta$ ) indicates a single-qubit rotation by an angle  $\zeta$ , described by the unitary  $e^{-i\zeta\sigma_z/2}$ . The system is finally measured in the energy basis to estimate the frequency  $\omega$  with optimal efficiency.

and eventually the second CNOT transformation leads to

$$\hat{Q}_3 = \frac{1 - \epsilon}{4} \begin{pmatrix} \hat{\rho}^\otimes & (\hat{\rho}\hat{\sigma}_x)^\otimes \\ \text{h.c.} & \hat{\rho}_x^\otimes \end{pmatrix} + \frac{1 + \epsilon}{4} \begin{pmatrix} \hat{\rho}_x^\otimes & -(\hat{\sigma}_x\hat{\rho})^\otimes \\ \text{h.c.} & \hat{\rho}^\otimes \end{pmatrix}, \quad (5.14)$$

where h.c. stands for Hermitian conjugate of the opposite corner of the matrix. This state will subsequently undergo the free evolution before being prepared for the readout.

As already mentioned, the frequency mean square error in the presence of non-Markovian phase covariant noise can be tightly lower-bounded below the SQL when considering the total running time of the estimation as the valuable resource  $\mathcal{R} \equiv \mathcal{T}$  [43]. Indeed, in this scenario, the time efficiency  $\eta_{\mathcal{T}} \equiv \mathcal{F}(\omega)/t_{*T}$ , Eq.5.2, where  $t_{*T}$  is the optimal sampling time, is shown to scale super-extensively, specifically recovering the Zeno scaling ( $\eta_{\mathcal{T}} \sim n^{\frac{3}{2}}$  and therefore  $\Delta\omega \sim n^{-\frac{3}{4}}$ ), when using as probe a maximally entangled (pure) GHZ state. On the other hand, (mixed) GHZ-diagonal states, such as  $\hat{\rho}_3$ , perform well (and are conjectured to be optimal) with non-pure probes [91] when the evolution is unitary (i.e. noiseless). In the next Section we will show that the Zeno scaling of time-efficient frequency estimation can be attained with such mixed GHZ-diagonal states.

To conclude this paragraph, we find that the energetic cost (quantified by the mean energy difference) of this initialisation stage is linear in the probe size:

$$\mathcal{E}_{\text{init}} = \text{Tr} [\hat{H}(\hat{\rho}_3 - \hat{\rho}_0)] = \frac{1}{2}\omega n \epsilon. \quad (5.15)$$

Before the initialisation, one may want to cool down the probes to the ground state, e.g. by coherent feedback cooling, so as to work with pure rather than mixed state. The energetic cost of such an operation would scale linearly with the number of atoms  $n$  in the ensemble and one should add it to the total energetic bookkeeping. Such cooling stage is anyway not essential for our purposes and we will not consider it in what follows.

### 5.2.2 Parameter encoding transformation: free evolution

After the initialisation of the probe, this is let evolve freely. The free evolution of each of the qubits is described by the phase covariant channel discussed in the previous Section. The time-evolved state reads  $\hat{\rho}_4 = \Lambda^{\otimes n}[\hat{\rho}_3]$ . The application of the channel to a generic qubit density matrix yields

$$\Lambda \left[ \begin{pmatrix} a & c \\ c^* & b \end{pmatrix} \right] = \begin{pmatrix} a\alpha_1 + b\alpha_{-1} & ce^{-i\varphi}\eta_{\perp} \\ c^*e^{i\varphi}\eta_{\perp} & a\beta_1 + b\beta_{-1} \end{pmatrix}, \quad (5.16)$$

with  $\alpha_s \equiv \frac{1}{2}(1 + s\eta_{\parallel} + \kappa)$ ,  $\beta_s \equiv \frac{1}{2}(1 - s\eta_{\parallel} - \kappa)$ , and  $\varphi \equiv \omega t$ , where we have dropped the explicit time dependence of the parameters for sake of a

lighter notation. Therefore, the state of the probe after the evolution can be rewritten as

$$\begin{aligned} \hat{\varrho}_4 = & \frac{1-\epsilon}{4} \begin{pmatrix} \alpha_1 \Lambda[\hat{\rho}]^{\otimes} + \alpha_{-1} \Lambda[\hat{\rho}_x]^{\otimes} & e^{-i\varphi} \eta_{\perp} \Lambda[\hat{\rho} \hat{\sigma}_x]^{\otimes} \\ \text{h.c.} & \beta_1 \Lambda[\hat{\rho}]^{\otimes} + \beta_{-1} \Lambda[\hat{\rho}_x]^{\otimes} \end{pmatrix} + \\ & + \frac{1+\epsilon}{4} \begin{pmatrix} \alpha_{-1} \Lambda[\hat{\rho}]^{\otimes} + \alpha_1 \Lambda[\hat{\rho}_x]^{\otimes} & -e^{-i\varphi} \eta_{\perp} \Lambda[\hat{\sigma}_x \hat{\rho}]^{\otimes} \\ \text{h.c.} & \beta_{-1} \Lambda[\hat{\rho}]^{\otimes} + \beta_1 \Lambda[\hat{\rho}_x]^{\otimes} \end{pmatrix}. \end{aligned} \quad (5.17)$$

Since this stage of the protocol corresponds to a free dissipative evolution, we do not attach any energetic cost to it.

It will be more convenient to rewrite  $\hat{\varrho}_4$  in the alternative form

$$\begin{aligned} \hat{\varrho}_4 = & \sum_{x=0}^{2^{n-1}-1} \begin{pmatrix} a_x & 0 \\ 0 & b_{\bar{x}} \end{pmatrix} \otimes |x\rangle\langle x| + \\ & + \sum_{x=0}^{2^{n-1}-1} \begin{pmatrix} 0 & e^{-if(x)\varphi} c_x \\ e^{if(x)\varphi} c_x & 0 \end{pmatrix} \otimes |x\rangle\langle \bar{x}|, \end{aligned} \quad (5.18)$$

with the definitions

$$\begin{aligned} a_x & \equiv \frac{1}{2} \left( \alpha_{-\epsilon}^{h(\bar{x})+1} \beta_{-\epsilon}^{h(x)} + \alpha_{\epsilon}^{h(\bar{x})+1} \beta_{\epsilon}^{h(x)} \right), \\ b_x & \equiv \frac{1}{2} \left( \alpha_{-\epsilon}^{h(x)} \beta_{-\epsilon}^{h(\bar{x})+1} + \alpha_{\epsilon}^{h(x)} \beta_{\epsilon}^{h(\bar{x})+1} \right), \\ c_x & \equiv \frac{\eta_{\perp}^n}{2^{n+1}} \left[ (1-\epsilon)^{h(\bar{x})+1} (1+\epsilon)^{h(x)} - (1-\epsilon)^{h(x)} (1+\epsilon)^{h(\bar{x})+1} \right], \\ f(x) & \equiv h(\bar{x}) - h(x) + 1. \end{aligned} \quad (5.19)$$

### 5.2.3 Preparation for the measurement

As one can see in Fig.5.1(c), the preparation of the probe for the measurement, consists in the sequence of three unitary transformations: (i) each atom undergoes a rotation along the  $z$  axis by an angle  $\zeta_1$ , i.e.  $\hat{U}_{\zeta_1} = e^{-i\zeta_1 \hat{\sigma}_z}$ , (ii) a CNOT gate is applied to each qubit in the register, (iii) finally, the generalised Hadamard gate

$$\hat{U}_H(\zeta_2) = e^{-i\frac{\zeta_2}{2} \hat{\sigma}_z} \text{He}^{i\frac{\zeta_2}{2} \hat{\sigma}_z} = \frac{1}{\sqrt{2}} \begin{pmatrix} 1 & e^{-i\zeta_2} \\ e^{i\zeta_2} & -1 \end{pmatrix}, \quad (5.20)$$

acts on the control qubit.

The state after the application of (i) and (ii) reads

$$\hat{\rho}_5 = \sum_{x=0}^{2^{n-1}-1} \begin{pmatrix} a_x & e^{-i\phi f(x)} c_x \\ e^{i\phi f(x)} c_x & b_x \end{pmatrix} \otimes |x\rangle\langle x|. \quad (5.21)$$

where  $\phi \equiv \omega t + \zeta_1$ . Similarly, the final state of the protocol,  $\hat{\rho}_6 = \hat{U}_H(\zeta_2) \otimes \mathbb{1}^{\otimes} \hat{\rho}_5 \hat{U}_H^\dagger(\zeta_2) \otimes \mathbb{1}^{\otimes}$  is

$$\hat{\rho}_6 = \sum_{x=0}^{2^{n-1}-1} \begin{pmatrix} \tilde{a}_x & e^{-i\zeta_2} \tilde{c}_x \\ e^{i\zeta_2} \tilde{c}_x^* & \tilde{b}_x \end{pmatrix} \otimes |x\rangle\langle x|, \quad (5.22)$$

where

$$\begin{aligned} \tilde{a}_x &\equiv \frac{1}{2} [a_x + b_x + 2c_x \cos(\zeta_2 - f(x)\phi)], \\ \tilde{b}_x &\equiv \frac{1}{2} [a_x + b_x - 2c_x \cos(\zeta_2 - f(x)\phi)], \\ \tilde{c}_x &\equiv \frac{1}{2} [a_x - b_x - 2ic_x \sin(\zeta_2 - f(x)\phi)]. \end{aligned} \quad (5.23)$$

Let us now compute the energetic cost of this sequence of transformation:  $\mathcal{E}_{\text{meas}} = \mathcal{E}(\hat{\rho}_6) - \mathcal{E}(\hat{\rho}_4)$ . We can rewrite the Hamiltonian in the same notation as 5.18, that is

$$\begin{aligned} \hat{H} = -\frac{\omega}{2} \sum_{x=0}^{2^{n-1}-1} & [(h(x) - h(\bar{x}) - 1)|0, x\rangle\langle 0, x| + \\ & + (h(x) - h(\bar{x}) + 1)|1, x\rangle\langle 1, x|]. \end{aligned} \quad (5.24)$$

Hence  $\mathcal{E}(\hat{\rho}_4) = \text{Tr}(\hat{H}\hat{\rho}_4)$  can be written as

$$\begin{aligned} \mathcal{E}(\hat{\rho}_4) &= -\frac{\omega}{2} \sum_{x=0}^{2^{n-1}-1} [(h(x) - h(\bar{x}) - 1)a_x + (h(x) - h(\bar{x}) + 1)b_x] = \\ &= \frac{\omega n}{2} (\alpha_{-\epsilon} - \beta_{-\epsilon} + \alpha_{\epsilon} - \beta_{\epsilon}) = \frac{\omega}{2} n\kappa, \end{aligned} \quad (5.25)$$

and  $\mathcal{E}(\hat{\rho}_6) = \text{Tr}(\hat{H}\hat{\rho}_6)$  reads

$$\begin{aligned} \mathcal{E}(\hat{\rho}_6) &= \sum_{x=0}^{2^{n-1}-1} [(h(x) - h(\bar{x}) - 1)\tilde{a}_x + (h(x) - h(\bar{x}) + 1)\tilde{b}_x] = \\ &= \frac{\omega}{2} (n-1)(\epsilon^2 \eta_{\parallel}^2 + \kappa^2) + \\ &\quad + \omega \sum_{m=0}^{n-1} \binom{n-1}{m} c_m \cos[\zeta_2 - f_m(\omega t + \zeta_1)]. \end{aligned} \quad (5.26)$$

After this sequence, the probe is ready to be interrogated: an energy measurement is performed on the system in order to build the frequency estimate. As we will show in the next Section, the angles  $(\zeta_1, \zeta_2)$  may be chosen so that, in the limit  $R\lambda = \frac{\gamma_0}{\epsilon} \ll 1$  the QFI of the state is (nearly) maximal. For the optimal prescription of  $(\zeta_1, \zeta_2)$  the energetic cost of the preparation for the measurement is always positive  $\mathcal{E}_{\text{meas}} > 0$ .

Notice that we are not considering in our energetic bookkeeping the projective part of the measurement. In other cases it may be necessary to add to  $\mathcal{E}_{\text{meas}}$  an additional ‘projection cost’  $\mathcal{E}_{\text{proj}}$ . While very general models of projective measurement schemes, and thermodynamic analyses thereof, may be found in the literature (see e.g. references [72,92–97]), it is not our intention to make generic statements about the energy efficiency of frequency estimation, rather we want to show how looking at the energetic aspect of parameter estimation in a specific example can change the usual notions of metrological optimality.

### 5.3 ‘ERROR BARS’ OF THE ESTIMATE

#### 5.3.1 (Classical) Fisher information

From Chapter 3, we know that the mean square error of a frequency estimate  $\omega = \tilde{\omega} \pm \Delta\omega$  for a sufficiently large number  $M$  of measurements of an observable  $\hat{O}$ , can be tightly lower-bounded by the Cràmer-Rao inequality, Eq.3.4, which in the single parameter case considered here reads

$$\Delta\omega \geq \frac{1}{\sqrt{M \mathcal{F}_\omega(\hat{O})}}. \quad (5.27)$$

In our case, the observable we chose to measure is the Hamiltonian,  $\hat{O} = \hat{H}$ . In order to calculate the Fisher Information  $\mathcal{F}_\omega(\hat{H})$ , Eq.3.3, we first compute the probability distribution of an energy measurement on  $\hat{\rho}_6$ . The Hamiltonian eigenbasis is  $\{|0\rangle \otimes |x\rangle, |1\rangle \otimes |x\rangle\}$  and the associated probabilities are

$$\begin{aligned} p_{0,h(x)} &= \langle 0, x | \hat{\rho}_6 | 0, x \rangle = \frac{1}{2} (a_x + b_x + 2c_x \cos [\zeta_2 - f(x)(\omega t + \zeta_1)]) \\ p_{1,h(x)} &= \langle 1, x | \hat{\rho}_6 | 1, x \rangle = \frac{1}{2} (a_x + b_x - 2c_x \cos [\zeta_2 - f(x)(\omega t + \zeta_1)]), \end{aligned} \quad (5.28)$$

where all eigenvectors with the same number of 1s [i.e.  $h(x)$ ] on the register yield the same probability. The Fisher information hence is

$$\begin{aligned}\mathcal{F}_\omega(\hat{H}) &= \sum_{x=0}^{2^{n-1}-1} \left[ \frac{(\partial_\omega p_{0,h(x)})^2}{p_{0,h(x)}} + \frac{(\partial_\omega p_{1,h(x)})^2}{p_{1,h(x)}} \right] = \\ &= \sum_{m=0}^{n-1} \binom{n-1}{m} \left[ \frac{(\partial_\omega p_{0,m})^2}{p_{0,m}} + \frac{(\partial_\omega p_{1,m})^2}{p_{1,m}} \right].\end{aligned}\quad (5.29)$$

When evaluating the derivatives appearing in the sum above, one must bear in mind that  $R = \frac{\gamma_0}{\lambda\epsilon}$  does depend on  $\omega$ , as  $\epsilon = \tanh\left(\frac{\omega}{2T}\right)$ . However, in our model  $\mathcal{F}_\omega(\hat{H})$  may be well approximated by considering  $R$  and  $\epsilon$  as constant in  $\omega$ . There is numerical evidence that this is justified in the limit  $R\lambda \ll 1$  (see Fig.5.2(a)). That is,

$$\begin{aligned}\mathcal{F}_\omega(\hat{H}) &\simeq \sum_{m=0}^{n-1} \binom{n-1}{m} \cdot \\ &\quad \cdot \frac{4(a_m + b_m)c_m^2(n-2m)^2t^2 \sin^2[\zeta_2 + (2m-n)(\zeta_1 + t\omega)]}{(a_m + b_m)^2 - 4c_m^2 \cos^2[\zeta_2 + (2m-n)(\zeta_1 + t\omega)]}.\end{aligned}\quad (5.30)$$

For even  $n$ , the measurement setting  $(\zeta_1, \zeta_2) = (\frac{\pi}{2} - \tilde{\omega}t, \frac{\pi}{2})$  maximises Eq.5.30, while for odd  $n$ , one needs to choose  $(\zeta_1, \zeta_2) = (\frac{\pi}{2} - \tilde{\omega}t, 0)$ . Note that  $\tilde{\omega}$  is not a variable, but rather the best available estimate of the atomic frequency at any given stage. As the knowledge about  $\omega$  is refined, the value of  $\tilde{\omega}$  should be updated, and the measurement setting, adaptively modified. *Undoing* the precession  $\hat{U}_{\zeta_1=\tilde{\omega}t}^{\otimes n}$  on all atoms after the free evolution, improves the sensitivity to small fluctuations of  $\omega$  around its average  $\tilde{\omega}$  and thus, helps to reduce the mean square error.

### 5.3.2 Quantum Fisher Information

We will now calculate the QFI which allows one to determine the ultimate bound on the precision of the frequency estimation. By comparing the QFI with the Fisher information calculated in the previous section we will be able to tell whether the measurement of another observable  $\hat{O} \neq \hat{H}$  may give a better frequency estimate. The QFI, Eq.3.15, can be computed from the state  $\hat{\rho}_4$ , right after the free evolution, or, equivalently, from  $\hat{\rho}_5$  as the QFI is

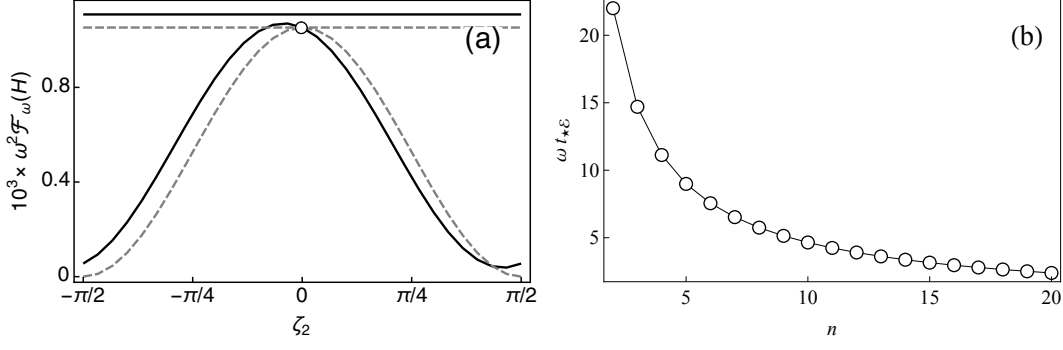


Figure 5.2.: (a) Approximate  $\mathcal{F}_\omega(\hat{H})$  for small  $R\lambda$ , as in Eq.5.30, (dashed grey curve) and exact Fisher information (solid black curve), as compared with the approximate QFI of Eq.5.32 (dashed grey line) and the exact QFI (solid black line). The angle  $\zeta_1$  is set to  $\zeta_1 = \frac{\pi}{2} - \tilde{\omega}t$ . Note the intersection of the curves at the nearly optimal measurement setting  $\zeta_2 = 0$ . (b) Optimal interrogation time  $t_{*\mathcal{E}} \sim n^{-1}$  as a function of the size of the probe  $n$ . In both plots  $\omega = \tilde{\omega} = 1$ ,  $T = 200$ ,  $\gamma_0 = 10^{-4}$ ,  $\lambda = 5$  ( $R\lambda = 0.04$ ), and  $t = 1$ . In (a),  $n = 9$ .

invariant under unitary transformations. The eigenvalues and eigenvectors of  $\hat{Q}_5$  are

$$\begin{aligned} v_x^\pm &= \frac{1}{2}(a_x + b_x \pm \Delta_x) \\ |\Xi_x^\pm\rangle &= \frac{(a_x - b_x \pm \Delta_x)|0\rangle + 2c_x e^{i\omega t f(x)}|1\rangle}{\sqrt{4c_x^2 + (a_x - b_x \pm \Delta_x)^2}} \otimes |x\rangle, \end{aligned} \quad (5.31)$$

respectively, where  $\Delta_x \equiv \sqrt{(a_x - b_x)^2 + 4c_x^2}$ . As done in the previous section, we consider the limit of small  $R\lambda$ , and find that  $\langle \Xi_x^\pm | \partial_\omega \hat{Q}_5 | \Xi_x^\mp \rangle \simeq 0$ , and thus

$$\mathcal{F}_\omega \simeq \sum_m^{n-1} \binom{n-1}{m} \frac{4(n-2m)^2 t^2 c_m^2}{a_m + b_m}, \quad (5.32)$$

which can be saturated by Eq.5.30 for the optimal choice of  $\zeta_1$  and  $\zeta_2$ . Therefore, our proposed measurement setting is optimal for  $R\lambda \ll 1$ . For arbitrary values of  $R\lambda$ , however,  $\mathcal{F}_\omega$  and  $\mathcal{F}_\omega(\hat{H})$  may differ significantly, for any choice of  $(\zeta_1, \zeta_2)$ . On the other hand, the exact  $\mathcal{F}_\omega(\hat{H})$  always coincides with Eq.5.32 for  $\zeta_1 = \frac{\pi}{2} - \tilde{\omega}t$  and  $\zeta_2 = \{\frac{\pi}{2}, 0\}$ , even when this measurement setting is sub-optimal, see Fig.5.2(a).

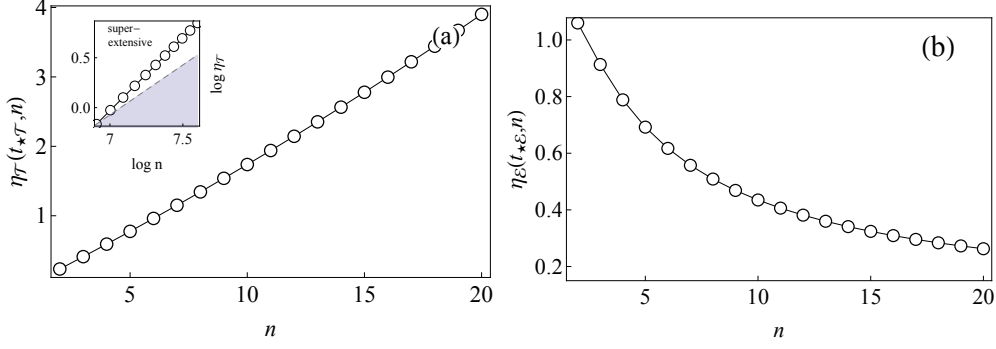


Figure 5.3.: (a) Efficiency  $\eta_{\mathcal{T}}(t_{*\mathcal{T}}, n) = F_{\omega}/t_{*\mathcal{T}}$  at the optimal interrogation time  $t_{*\mathcal{T}}$  as a function of the probe size  $n$ , in the standard frequency-estimation scenario of limited time  $\mathcal{T}$ . Note from the inset that, in spite of the fact that the probe is prepared in a *mixed* GHZ-diagonal state, the efficiency grows super-extensively, as  $\tilde{\eta}(t_{*\mathcal{E}}, n) \sim n^{3/2}$ , which corresponds to Zeno scaling. (b) Energy-efficiency  $\eta_{\mathcal{E}}(t_{*\mathcal{E}}, n) = F_{\omega}/(\mathcal{E}_{init} + \mathcal{E}_{meas})$  at the optimal interrogation time  $t_{*\mathcal{E}}$  as a function of the probe size  $n$  for the same parameters as (a). In this case, one roughly has  $\eta_{\mathcal{E}}(t_{*\mathcal{E}}, n) \sim n^{-1/3}$ , i.e. from an energetic perspective, using large entangled probes yields no metrological advantage. All parameters are the same as in figure 5.2.

#### 5.4 METROLOGICAL EFFICIENCIES OF THE PROTOCOL

Let us now discuss two different metrological efficiencies of the considered protocol. As already pointed out, the usual figure of merit in frequency estimation is the time-efficiency (see Eq.5.2):

$$\eta_{\mathcal{T}}(t_{*\mathcal{T}}, n) \equiv \frac{\mathcal{F}_{\omega}}{t_{*\mathcal{T}}}, \quad (5.33)$$

where  $t_{*\mathcal{T}}$  corresponds to the optimal sampling time and it is related to the total number of measurement  $M$  as  $t_{*\mathcal{T}} = \mathcal{T}/M$  where  $\mathcal{T}$ , the total time available for the estimation, is the scarce resource to economise on.

Placing ourself in the limit  $R\lambda \ll 1$ , as we can see from Fig.5.3, under the time-inhomogeneous dissipative dynamics considered,  $\eta_{\mathcal{T}}(t_{*\mathcal{T}}, n)$  scales super-extensively even using mixed thermal probes. Specifically, we recover the Zeno scaling  $\Delta\omega^2 \sim 1/n^{3/2}$ . This tells us that, fixed the available running time  $\mathcal{T}$ , when having a large number of qubits, it is more efficient to batch them together in a GHZ-diagonal state and run the protocol  $\mathcal{T}/t_{*\mathcal{T}} = M$  times.

On the other hand, in case our limited resource is the total energy available, in order to assess the performance of the protocol, we can define the energy-efficiency

$$\eta_{\mathcal{E}}(t, n) \equiv \frac{\mathcal{F}_{\omega}}{\mathcal{E}_{\text{init}} + \mathcal{E}_{\text{meas}}}, \quad (5.34)$$

In order to maximise  $\eta_{\mathcal{E}}(t, n)$  we will first find numerically the optimal interrogation time  $t_{*\mathcal{E}}$  for given  $n$ : as shown in Fig.5.2(b)  $t_{*\mathcal{E}}$  has a power-law-like dependence on the probe size  $\omega t_{*\mathcal{E}} \propto n^{-c}$ , where  $c \lesssim 1$  (for  $R\lambda \ll 1$ ). Then, we look at the scaling of  $\eta_{\mathcal{E}}(t_{*\mathcal{E}}, n)$  with the probe size. From Fig.5.3(b), we see that when adopting GHZ-diagonal probes, the energy-efficiency  $\eta_{\mathcal{E}}(t_{*\mathcal{E}}, n)$  decreases rapidly with the probe size. This is so because the energetic cost of the protocol is linear in  $n$ , while the QFI exhibits a slower power-law-like growth. From this we can conclude that, given a cap on the total available energy  $\mathcal{E}$ , the best performance of the frequency estimate is obtained by manipulating uncorrelated atoms locally: it is more efficient to invest the available energy to increase the number of runs of the protocol rather than in building an expensive GHZ diagonal state. Our numerics show that one observes the same qualitative behaviour even when moving away from the regime of  $R\lambda \ll 1$  and searching for the measurement setting  $(\zeta_1, \zeta_2)$  and interrogation time  $t_{*\mathcal{E}}$  which jointly maximise  $\eta_{\mathcal{E}}(t, \zeta_1, \zeta_2, n) = \mathcal{F}_{\omega}(\hat{H}) / [\mathcal{E}_{\text{init}} + \mathcal{E}_{\text{meas}}(\zeta_1, \zeta_2)]$ .

## 5.5 REMARKS

We have investigated the efficiency of a frequency estimation protocol in the presence of time-inhomogeneous phase-covariant noise. In each round of the protocol, an ensemble of  $n$  initially thermal two-level atoms is brought into a GHZ-diagonal state. The system is then let evolve freely. Eventually, the probe is prepared for an energy measurement through a sequence of qubit gates. We showed that, in a suitable range of parameters and by opportunely tuning the qubit operations in the preparation for the measurement, it is possible to globally minimise the statistical uncertainty of the final frequency estimate.

It is a known result that the time-efficiency  $\eta_{\mathcal{T}} = \mathcal{F} / t_{*\mathcal{T}}$ , where  $t_{*\mathcal{T}}$  is the optimal duration of each estimation round, scales super-extensively when

the probe used is a maximally entangled GHZ state. We showed that this regime can be asymptotically achieved even when using mixed GHZ-diagonal probes. This suggests that using large correlated probes is more convenient when there is a cap on the total time available for the estimation. On the other hand, such figure of merit, fails to capture how ‘difficult’ or ‘costly’ it may be to prepare those states in practice. We therefore introduced the notion of energy-efficiency  $\eta_{\mathcal{E}} = \mathcal{F}/(\mathcal{E}_{\text{init}} + \mathcal{E}_{\text{meas}})$  of the estimation as a means to assess the overall performance of the estimation when the available energy for the estimation is limited. We further found the optimal free-evolution time  $t_{*\mathcal{E}}$  maximising  $\eta_{\mathcal{E}}$  and studied its scaling with the probe size. Contrary to a time-efficient estimation, in this case we found that preparing larger probes in correlated GHZ-diagonal states is always detrimental for the energy efficiency of frequency estimation.

It is important to remark that our energy bookkeeping may be a too crude approach to capture the actual limitations one has to deal with in a real metrological setup. Moreover, in many situations, the total time  $\mathcal{T}$  might indeed place the most stringent limitation on the achievable precision. However, the purpose of this work was to highlight how different assessment of resources might lead to different notions of optimality. Moreover, we wanted to stress the importance of formulating quantifiers of the metrological efficiency capable to capture all the relevant limitations at work in each experimental setup.



---

 GAUSSIAN QUANTUM METROLOGY
 

---

While in Chapter 5 we considered a single parameter estimation task, here we tackle the multiparameter estimation problem. In particular, we consider the task of estimating unknown parameters (described by the vector  $\boldsymbol{\mu} = \{\mu_1, \dots, \mu_n\}$ ) encoded on a probe field initialized in a continuous variable Gaussian state  $\hat{\rho}_\mu$ , see Chapter 2. We focus on the case in which the transformation imprinting the parameters on the Gaussian probe preserves its Gaussianity. This setting is referred to as *Gaussian quantum metrology*. Many works analyzing instances of Gaussian quantum metrology can be found in the literature, including the estimation of single or multiple parameters using single-mode or multimode probes [7, 44, 98–123]. Goal of this Chapter, is to investigate the ultimate precision achievable in multimode multiparameter Gaussian quantum metrology: we will indeed derive general analytical expressions for the QFI matrix, Eq.3.23, and for the quantity in Eq.3.24, which assesses the existence of a common optimal measurement that allows to estimate jointly a pair of parameters with minimum error (see Paragraph 3.2.2), a condition known as measurement compatibility [44].

This Chapter is structured as follows: in the first Section we will introduce the SLD for continuous variable Gaussian systems. We will then enunciate a theorem which provides compact analytical formulae for the QFI matrix,  $\mathcal{F}_{\eta\zeta}$ , and the ‘measurement compatibility matrix’,  $\mathcal{J}_{\eta\zeta}$ , in the realm of Gaussian quantum metrology. In the last Section, we will apply our results to the joint estimation of a phase shift and two noise parameters specifying a generic phase covariant channel, using two-mode Gaussian probes in an interferometric setup.

## 6.1 GAUSSIAN SYMMETRIC LOGARITHMIC DERIVATIVE

Given an  $n$ -mode Gaussian state  $\hat{\rho}_\mu$ , we can write an ansatz for the SLD at most quadratic in the component of the quadrature vector  $\hat{\mathbf{R}}$  (sum over repeated indexes is assumed) [29]

$$\hat{\mathcal{L}}_\eta = L_\eta^{(0)} + L_{\eta,l}^{(1)} \hat{R}_l + L_{\eta,jk}^{(2)} \hat{R}_j \hat{R}_k, \quad (6.1)$$

with  $L_\eta^{(0)} \in \mathbb{R}$ ,  $L_\eta^{(1)} \in \mathbb{R}^{2n}$  and  $L_\eta^{(2)}$  is a  $2n \times 2n$  symmetric matrix. Rewriting the implicit definition of the SLD, Eq.3.6, by expanding the operators on both sides of the equation in terms of the displacement operator we get an equation for the characteristic functions:

$$\frac{\partial \chi_{\hat{\rho}_\mu}}{\partial \mu_\eta} = L_\eta^{(0)} \chi_{\hat{\rho}_\mu} + L_{\eta,l}^{(1)} \chi_{\hat{R}_l \hat{\rho}_\mu + \hat{\rho}_\mu \hat{R}_l} + L_{\eta,jk}^{(2)} \chi_{\hat{R}_j \hat{R}_k \hat{\rho}_\mu + \hat{\rho}_\mu \hat{R}_k \hat{R}_j}. \quad (6.2)$$

The second term on the right hand side of the above is given by Eq.2.26. To find the last term we can sum Eq.2.24, with  $\hat{O} = \hat{\rho}_\mu \hat{R}_k$ , and Eq.2.25, with  $\hat{O} = \hat{R}_k \hat{\rho}_\mu$ , obtaining

$$\begin{aligned} \chi_{\hat{R}_j \hat{R}_k \hat{\rho}_\mu + \hat{\rho}_\mu \hat{R}_k \hat{R}_j} &= -i \partial_{\tilde{r}_j} \chi_{\hat{R}_l \hat{\rho}_\mu + \hat{\rho}_\mu \hat{R}_l} + \frac{1}{2} \Omega_{jj'} \tilde{r}_{j'} \chi_{\hat{R}_l \hat{\rho}_\mu - \hat{\rho}_\mu \hat{R}_l} = \\ &= \left( -2 \partial_{\tilde{r}_j} \partial_{\tilde{r}_k} + \frac{1}{2} \Omega_{jj'} \tilde{r}_{j'} \Omega_{kk'} \tilde{r}_{k'} \right) \chi_{\hat{\rho}_\mu}, \end{aligned} \quad (6.3)$$

where in the last passage we used Eqs.2.26, 2.27. Recalling the definition of the characteristic function of a Gaussian state, Eq.2.31, and the expression of its derivative with respect to  $\tilde{r}_l$ , Eq.2.39, Eq.6.2 becomes

$$\begin{aligned} 2i \tilde{r}_p \frac{\partial d_p}{\partial \mu_\eta} - \frac{1}{2} \frac{\partial V_{lm}}{\partial \mu_\eta} \tilde{r}_l \tilde{r}_m &= 2L_\eta^{(0)} + 2L_{\eta,p}^{(1)} d_p + L_{\eta,jk}^{(2)} (V_{jk} + 2d_j d_k) + \\ &+ i \left( L_{\eta,p}^{(1)} V_{pq} + L_{\eta,jk}^{(2)} d_j V_{kq} + L_{\eta,jk}^{(2)} d_k V_{jq} \right) \tilde{r}_q + \\ &- \frac{1}{2} \tilde{r}_q \left( \Omega_{qk} L_{\eta,kj}^{(2)} \Omega_{js} + V_{qk} L_{kj}^{(2)} V_{js} \right) \tilde{r}_s. \end{aligned} \quad (6.4)$$

Since this has to hold for all values of  $\tilde{r}$ , we can equate the different orders independently. In vectorial form we get

$$\partial_\eta V = V L_\eta^{(2)} V + \mathbf{\Omega} L_\eta^{(2)} \mathbf{\Omega}, \quad (6.5)$$

$$L_\eta^{(1)} = 2V^{-1} \partial_\eta \mathbf{d} - 2L_\eta^{(2)} \mathbf{d}, \quad (6.6)$$

$$L_\eta^{(0)} = -\frac{1}{2} \text{Tr}(V L_\eta^{(2)}) - L_\eta^{(1)\top} \mathbf{d} - \mathbf{d}^\top L_\eta^{(2)} \mathbf{d}, \quad (6.7)$$

where  $\partial_\eta = \frac{\partial}{\partial \mu_\eta}$ . Hence,  $L_\eta^{(1)}$  and  $L_\eta^{(0)}$  are given once  $L_\eta^{(2)}$  is determined. This is done by finding the inverse of the superoperator  $\mathcal{M}_V$  acting on a real matrix  $A$  as  $\mathcal{M}_V(A) = VAV + \mathbf{\Omega}A\mathbf{\Omega}$ . Indeed, one would have  $L_\eta^{(2)} = \mathcal{M}_V^{-1}(\partial_\eta V)$ . In order to find the inverse one has to construct the symplectic transformation  $S$  such that  $\nu = S^{-1}VS^{-\top}$ . The eigenmatrices and eigenvalues of the superoperator  $\mathcal{M}_\nu$  are then readily found. The set of eigenmatrices  $M_l^{jk}$  have all zero entries except for the  $2 \times 2$  block in position  $jk$ , with  $j, k = 1, \dots, n$ , which is given by

$$\{M_l^{jk}\}_{l \in \{0 \dots 3\}} = \frac{1}{\sqrt{2}}\{\mathbf{\Omega}, \sigma_z, \mathbb{1}, \sigma_x\}. \quad (6.8)$$

These matrices have been chosen such that they are orthonormal with respect to the Hilbert-Schmidt inner product,  $\langle A, B \rangle = \text{Tr}(AB)$ . The eigenvalues associated to each eigenmatrix are  $(\nu_j \nu_k - (-1)^l)$ , where  $\nu_i$  are the symplectic eigenvalues of  $V$ , i.e. the diagonal entries of  $\nu$ .

The matrix  $L^{(2)}$  is then given by

$$L^{(2)} = S^{-\top} \mathcal{M}_\nu^{-1}(S^{-1} \partial_\eta V S^{-\top}) S^{-1} = a_l^{(jk)} \frac{S^{-\top} M_l^{(jk)} S^{-1}}{\nu_j \nu_k - (-1)^l}, \quad (6.9)$$

where the coefficients  $a_l^{(jk)}$  are such that  $S^{-1} \partial_\eta V S^{-\top} = a_l^{(jk)} M_l^{(jk)}$ , and hence given by

$$a_l^{(jk)} = \text{Tr} \left( S^{-1} \partial_\eta V S^{-\top} M_l^{(jk)} \right). \quad (6.10)$$

Notice that the superoperator  $\mathcal{M}_\nu$  is invertible if and only if  $\nu_j \neq 1 \ \forall j$ , i.e. if all normal modes of the state with covariance matrix  $V$  are mixed. If this is not the case, the inversion of  $\mathcal{M}_\nu$  is generally not possible unless  $S^{-1} \partial_\eta V S^{-\top}$  is orthogonal to the eigematrices associated to the singular eigenvalues. One can however perturb the unit symplectic eigenvalues by a quantity  $\varepsilon$ ,  $\nu_j \rightarrow 1 + \varepsilon$ , and send  $\varepsilon$  to zero at the end of the evaluation of the QFI: singularities in  $\mathcal{M}_\nu$  will emerge as divergences in the QFI. For a more detailed discussion on the invertibility of the superoperator, we refer the reader to [29].

## 6.2 QFI AND ‘COMPATIBILITY’ MATRICES FOR GAUSSIAN STATES

We will report in this Section our main result:

**Theorem 6.1.** *Given a Gaussian state of an arbitrary number of modes  $n$ , which depends on the set of parameters  $\boldsymbol{\mu}$ , described by its first and second statistical moments  $\mathbf{d}$  and  $V$ , respectively, we have that*

$$\mathcal{F}_{\eta\zeta} = \frac{1}{2}\text{Tr}(\partial_{\zeta}VL_{\eta}^{(2)}) + 2\partial_{\eta}\mathbf{d}^{\top}V^{-1}\partial_{\zeta}\mathbf{d} \quad (6.11)$$

$$\mathcal{J}_{\eta\zeta} = 2\text{Tr}\left(\boldsymbol{\Omega}L_{\zeta}^{(2)}VL_{\eta}^{(2)}\right) + 2\partial_{\eta}\mathbf{d}^{\top}V^{-1}\boldsymbol{\Omega}V^{-1}\partial_{\zeta}\mathbf{d} \quad (6.12)$$

with  $L_{\zeta}^{(2)}$  defined by Eq.6.9.

The proof of this Theorem is reported in Appendix C.

Eq.6.11 provides a compact expression for the QFI matrix in Gaussian quantum metrology, directly generalizing the formula for the single-parameter case which can be found e.g. in [29, 123]. Eq.6.12, on the other hand, provides a general formula for the quantity defined in Eq.3.24, which determines the measurement compatibility condition (i) (see Paragraph 3.2.2) between pairs of parameters [44]. Note that, while a formula equivalent to Eq.6.11 may be alternatively derived from the expression for the quantum fidelity between two Gaussian states as recently reported in [114], the formula in Eq.6.12 is entirely original in the context of Gaussian quantum metrology and, to the best of our knowledge, no similar expression can be found in previous literature; in particular, Eq.6.12 cannot be derived using the information geometry methods of [114].

Let us also remark that both formulae appearing in Theorem 6.1 can be evaluated efficiently for an arbitrary Gaussian state  $\hat{\rho}_{\boldsymbol{\mu}}$ , although one needs to determine explicitly the symplectic transformation  $S^{-1}$  that diagonalizes the covariance matrix  $V_{\boldsymbol{\mu}}$ . The latter transformation can be constructed analytically for one and two modes, see e.g. [124–126], and in general can be obtained numerically for a higher number of modes.

### 6.3 NOISY OPTICAL INTERFEROMETRY

In this Section we will show an application of our results: we will apply the general formalism of Theorem 6.1 to the task of quantum phase estimation using an optical interferometric setup in the presence of noise [7, 41, 98, 127, 128].

The scheme under investigation is depicted in Fig.6.1: an initial two-mode displaced squeezed state (TMDSS)  $\hat{\rho}_0$  undergoes a phase transformation

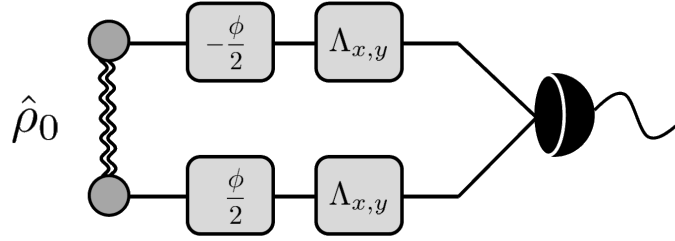


Figure 6.1.: An instance of multiparameter Gaussian quantum metrology. The initial state  $\hat{\rho}_0$  is a two-mode displaced squeezed state which passes through an interferometric set-up before a joint measurement is made. One mode undergoes a phase transformation of  $\phi/2$  and the other of  $-\phi/2$ , while both modes are affected by a phase covariant Gaussian channel  $\Lambda_{x,y}$  with noise parameters  $x$  and  $y$ . We determine optimal strategies for the estimation of the three parameters  $\{\phi, x, y\}$ .

and transmission noise in an interferometric setup, before the two modes are jointly measured. The TMDSS has displacement vector and covariance matrix

$$d_0 = \sqrt{2} \{ \text{Re}(\alpha), \text{Im}(\alpha), \text{Re}(\beta), \text{Im}(\beta) \}^\top, \quad (6.13)$$

$$V_0 = \begin{pmatrix} \cosh(2r) & 0 & -\sinh(2r) & 0 \\ 0 & \cosh(2r) & 0 & \sinh(2r) \\ -\sinh(2r) & 0 & \cosh(2r) & 0 \\ 0 & \sinh(2r) & 0 & \cosh(2r) \end{pmatrix},$$

respectively, where  $\alpha, \beta \in \mathbb{C}$  are the displacements of each mode, and  $r$  is the squeezing parameter. The phase difference between the two arms of the interferometer is  $\phi$ , and it is imprinted by each mode undergoing a unitary shift of  $\mp\phi/2$ . We will consider the noise in the form of a generic phase-covariant Gaussian channel  $\Lambda_{x,y}$  (see Paragraph 2.3.2), which includes the combined effects of loss ( $0 \leq x \leq 1$ ), amplification ( $x > 1$ ), and added thermal noise ( $y \geq |1 - x|$ ), modelling realistic transmission of the probes in free space or over telecommunication fibres [26, 29, 129–134]. Our goal is to estimate all three parameters,  $\phi$ ,  $x$  and  $y$ , as precisely and efficiently as possible by using affordable TMDSS probes.

We therefore check under which circumstances the measurement compatibility condition  $\mathcal{J}_{\eta\zeta} = 0$  is satisfied, that corresponds to the existence of a single optimal measurement for extracting all of the parameters such that the quantum Cramér-Rao bound can be saturated in the limit of infinite re-

petitions of the experiment. Using Eq.6.12 one finds that only one term of the ‘measurement compatibility matrix’ is in general not identically zero:

$$\mathcal{J}_{x\phi} = -\mathcal{J}_{\phi x} = \frac{|\beta|^2 - |\alpha|^2}{x^2 + y^2 + 2xy \cosh(2r)}, \quad (6.14)$$

i.e. the compatibility condition is satisfied if and only if  $|\alpha|^2 = |\beta|^2$ .

From Eq.6.11 one can easily calculate the QFI matrix and show that the states which give the best estimate, such that  $|\alpha|^2 = |\beta|^2$ , are given by  $\text{Re}(\alpha) = \text{Re}(\beta)$  and  $\text{Im}(\alpha) = \text{Im}(\beta) = 0$ . Indeed one easily finds that  $[\mathcal{F}]_{\text{Im}(\alpha)=\text{Im}(\beta)=0} \geq \mathcal{F}$ .

Let us now fix the mean excitation number, Eq.2.41, of the optimal input TMDSS to be  $\bar{n} = \sinh^2 r + |\alpha|^2$ , and we define  $p \equiv |\alpha|^2 / \bar{n}$  to be the portion of energy invested in displacement rather than in squeezing. It is evident that when  $p = 0$  it is not possible to estimate the phase, that is because the covariance matrix does not depend on it and the displacement vector is the null vector. Therefore we will not investigate further this case.

For  $0 < p < 1$ , in the high energy limit  $\bar{n} \gg 1$  the QFI matrix becomes

$$\mathcal{F} = \begin{pmatrix} \frac{2p\bar{n}}{xy} + c_x + o(\bar{n}^{-\frac{1}{2}}) & o(\bar{n}^{-1}) & 0 \\ o(\bar{n}^{-1}) & \frac{1}{y^2} + o(\bar{n}^{-1}) & 0 \\ 0 & 0 & \frac{2px\bar{n}}{y} + c_\phi + o(\bar{n}) \end{pmatrix}, \quad (6.15)$$

where  $c_x$  and  $c_\phi$  are some terms constant in  $n$ . We see that the off-diagonal terms scale as  $(\mathcal{F})_{xy} \sim n^{-1}$ , hence, in this limit, we can consider the compatibility condition (iii) satisfied, meaning that the parameters are statistically independent. We also notice that while terms  $\mathcal{F}_{xx}$  and  $\mathcal{F}_{\phi\phi}$  are linear in  $\bar{n}$ ,  $\mathcal{F}_{yy}$  is constant. Therefore, while the mean square error on  $x$  and  $\phi$  vanishes displaying a SQL scaling (as expected since one cannot have sub-shot noise enhancement in the presence of noise [127, 128, 135]), the mean square error on  $y$  (also called added noise) corresponds to the value of the noise parameter itself:  $\Delta y = y$ .

When all the energy is invested in displacement,  $p = 1$ , the compatibility condition (iii) is not satisfied for any value of the energy, meaning that the Cramér-Rao bound cannot be saturated using TMDSS. Indeed, the off-diagonal elements of the QFI matrix read

$$\mathcal{F}_{xy} = \frac{2}{(x+1)^2 - 1}. \quad (6.16)$$

Also in this case, one finds that  $\mathcal{F}_{xx}, \mathcal{F}_{\phi\phi} \sim \bar{n}$ , whereas  $\mathcal{F}_{yy} = \mathcal{F}_{xy}$  is constant in  $\bar{n}$ .

#### 6.4 REMARKS

In this Chapter we derived general formulae to assess the ultimate precision achievable in Gaussian quantum metrology, that is, in the estimation of multiple parameters encoded in multimode Gaussian states. Indeed we derived a compact analytical expression for the quantum Fisher information matrix, in terms of first and second statistical moments of the probe state. We also obtained an analytical formula for the ‘measurement compatibility matrix’ which allows to assess whether the quantum Cramèr-Rao bound can be asymptotically saturated, i.e. whether a common measurement able to extract information optimally on all the parameters exists.

As an illustrative example, we applied our general formalism to study the practical estimation of three relevant physical parameters in noisy optical interferometry: an unknown phase difference between the two arms of an interferometer, and two unknown noise terms which specify a generic phase-covariant Gaussian channel. We showed that TMDSS probes with optimally tuned displacement satisfy the measurement compatibility condition. We also saw that if all the available energy is invested in displacement, the compatibility condition (iii), ensuring the statistical independence of the parameters, is never satisfied. Putting a fraction of this energy into squeezing is necessary in order to satisfy this condition at least in the limit of high energy.

Our techniques can be promptly applied to a broad range of problems in fundamental science and technology [7,36,136], wherever the precise estimation of parameters encoded in quadratic Hamiltonians or noisy evolutions preserving Gaussianity is demanded. While this Chapter focused mainly on compatibility conditions (i) and (iii), namely measurement compatibility and statistical independence [44], our framework can be combined with efficient numerical algorithms to find optimal input probe states [116,137,138], in order to fulfil condition (ii) and minimize the overall error on estimating multiple parameters.



---

## GAUSSIAN NON-MARKOVIANITY

---

In Paragraph 6.3, we modelled the noise as a phase-covariant Gaussian channel, characterized by two parameters. In general, see Paragraph 2.3.1, a Gaussian quantum channel can be described by two matrices. When the Gaussian quantum channel describes an open Gaussian dynamics, these two matrices are time dependent. In this Chapter we investigate these time-continuous Gaussian channels, with a particular focus on those which violate CP-divisibility and can therefore be considered non-Markovian, see Paragraph 1.2.3.

Non-Markovian evolutions of open quantum systems have been extensively studied in recent years [139–141]. These evolutions, in contrast with Markovian evolutions, are characterized by memory effects which can appear in many forms. Efforts are made to detect, classify and characterize them by witnesses and measures that stress different manifestations [142–150]. These studies are motivated by the search for better control of quantum states. In quantum computation memory effects make an impact, for instance, on error correction schemes or reduction of decoherence rates [151–156]. Not less important is the impact on cryptography [157], where we usually assume that an eavesdropper has access to the environment and is free to manipulate it interfering in privacy and security. It appears that Markovian evolutions are not able to describe certain biological processes, that due to memory effects are driven more efficiently [158–160]. Finally the experimental techniques are now appropriate to investigate the effects beyond the Markovian regime [161–163].

We saw, in Paragraph 1.2.2, that if a quantum evolution is described by a family of maps with a semigroup structure, then it is described by the Lindblad master equation. This can be derived by microscopical models by im-

posing Born-Markov and secular approximations. By making these approximations one assumes that the system of interest and its environment are uncorrelated at every instant and that the environment does not preserve any self-correlations on the relevant timescale of the system evolution. The lack of correlations at each instant denotes the lack of memory, hence the Markovianity. Lindblad-like evolutions however, do not describe the most general Markovian dynamics. Indeed, we recognise a non-Markovian process when the proper description of an evolution cannot be found among CP-divisible maps [25], see Paragraph 1.2.3. In this case, correlations between the system and the environment and the environmental self-correlations are essential at some stage [164–166].

The association of Markovian processes with CP-divisible maps results in important restrictions. Let us mention that given a bipartite state entanglement and mutual information cannot increase if a CP map is applied locally to one of the subsystems. Similarly, certain measures of distinguishability between quantum states, like fidelity or trace distance, cannot increase if a CP map is applied to both the states. In consequence, the violation of any of the rules mentioned above at some time  $t > 0$  during a quantum evolution is an evidence that some intermediate map is not CP, hence the evolution is non-Markovian. Violation of the CP-divisibility can then be witnessed by temporary increase of the above-mentioned quantities or similar quantities subjects to the same no-go properties [142–144, 146, 151]. Proper measures of non-Markovianity are based on direct examination of complete-positivity of all intermediate maps in a process [143, 145, 147]. A unified picture of several measures of non-Markovianity has been presented recently in [145] where the authors introduced a hierarchy of the degrees of non-Markovianity based on the smallest degree of positivity of intermediate maps.

In this Chapter we are going to consider non-Markovian Gaussianity-preserving evolutions of Gaussian quantum states, or, in other words, non-Markovian Gaussian channels. In particular, in the first Section, we are going to define a non-Markovianity witness for Gaussian channels using an operational figure of merit introduced in the context of quantum metrology, namely the Gaussian interferometric power [167, 168]. This quantity assesses the guaranteed precision of phase estimation in a black-box interferometric setting, where the generator of the phase shift to be estimated

is *a priori* unknown, when using bipartite Gaussian probes. In the second Section we will define the notion of Gaussian  $k$ -mode positivity and provide necessary and sufficient criteria for it. Applying this notion to intermediate Gaussian evolutions will allow us to distinguish three classes of processes: Markovian, weakly and strongly non-Markovian. We will hence be able to classify, using an intuitive pictorial diagram divided in three regions, one per each class of the hierarchy, all one-mode Gaussian channels.

### 7.1 A NEW WITNESS FOR GAUSSIAN NON-MARKOVIANITY

Many quantum information quantities exhibit monotonic behaviour under the application of local quantum operations (CP maps). Such a property allows one to define non-Markovianity witnesses. Indeed, given a family of CP maps  $\Phi_t$ , let us consider some quantity  $\mathcal{X} : \mathcal{B}(\mathcal{H} \otimes \mathcal{H}) \rightarrow \mathbb{R}$  such that,  $\forall \hat{\rho} \in \mathcal{B}(\mathcal{H} \otimes \mathcal{H})$ , the following holds

$$\mathcal{X}(\hat{\rho}) \geq \mathcal{X}(\Phi_t \otimes \mathbb{1}(\hat{\rho})) \equiv \mathcal{X}(\hat{\rho}(t)) , \quad \forall t > 0 \quad (7.1)$$

and let us also suppose that for every time  $t$ , there exists the inverse map  $\Phi_t^{-1}$ , so that the intermediate evolution  $\Phi_{t,s}$ , Eq.1.93, is well defined. Then, if the quantum evolution describes a Markovian process, i.e. the intermediate map  $\Phi_{t,s}$  is CP, one has that

$$\mathcal{X}(\hat{\rho}(s)) \geq \mathcal{X}(\Phi_{t,s} \otimes \mathbb{1}(\hat{\rho}(s))) , \quad \forall t > s > 0 , \quad (7.2)$$

holds  $\forall \hat{\rho} \in \mathcal{B}(\mathcal{H} \otimes \mathcal{H})$ . A violation of the above is a signature of non-Markovianity. It is worth remarking that even if Eq.7.2 holds for some quantum evolution  $\Phi_t$ , the possibility that it describes a non-Markovian evolution is not ruled out. Mutual information, entanglement, quantum discord (when the map is applied on the subsystem which is not being measured), are all quantities which satisfy Eq.7.1 and are therefore good candidates to construct non-Markovianity witnesses.

As already mentioned in the introduction to this Chapter, other quantities, like for example the Bures distance, Eq.1.18, can be used in an analogous way. By using some distance  $\mathcal{D}$  which satisfies a condition like Eq.1.19, one can be sure that the evolution is non-Markovian if

$$\mathcal{D}(\hat{\rho}_1(s), \hat{\rho}_2(s)) < \mathcal{D}(\Phi_{t,s}(\hat{\rho}_1(s)), \Phi_{t,s}(\hat{\rho}_2(s))) = \mathcal{D}(\hat{\rho}_1(t), \hat{\rho}_2(t)) , \quad (7.3)$$

for some  $t > s > 0$ .

Following the line drew in the seminal work [142], given a quantity  $\Xi(t)$  monotonic under CP maps<sup>1</sup>, one can define the non-Markovianity witness as

$$\mathcal{N}_\Xi = \int_{\sigma>0} dt \sigma_t, \quad \text{with} \quad \sigma_t = \frac{d}{dt} \Xi(t), \quad (7.4)$$

where the integral is performed over all time intervals where  $\sigma > 0$ . “Re-vivals” of a quantity  $\Xi(t)$ , i.e. a temporary increase of  $\Xi(t)$ , are usually considered the fingerprint of some memory effect and described as the signature of a backflow of information from the environment into the system [142–144].

We will now introduce the Gaussian interferometric power and then exploit its non-monotonic behaviour under non-divisible CP Gaussian evolutions to define a non-Markovianity witness for CV Gaussian systems.

### 7.1.1 Gaussian interferometric power

Let us consider a two-mode Gaussian state  $\hat{\rho}_{AB}$  prepared by two parties, Alice and Bob, as a probe for an interferometer. One of the two modes,  $B$ , undergoes a Gaussian unitary transformation  $\hat{U}_B^\phi = e^{-i\phi\hat{H}_B}$ , where the parameter  $\phi$  is unknown and of the generator  $\hat{H}_B$  is only known its (harmonic) spectrum. Because of the lack of a detailed knowledge about the generator, this setup is called *black-box interferometry*. The unitary can be rewritten as  $\hat{U}_B^\phi = \hat{V}_B^\dagger \hat{W}_B^\phi \hat{V}_B$ , where  $\hat{W}_B^\phi$  is the usual phase-shift unitary as defined in Eq.2.58, and  $\hat{V}_B$  is an arbitrary Gaussian unitary transformation. The transformed two-mode state reads

$$\hat{\rho}_{AB}^{\phi, \hat{V}_B} = \left( \mathbb{1}_A \otimes \hat{U}_B^\phi \right) \hat{\rho}_{AB} \left( \mathbb{1}_A \otimes \hat{U}_B^{\phi\dagger} \right). \quad (7.5)$$

At this point, Alice and Bob are given the information about the the generator, i.e.  $\hat{V}_B$ , so that they can perform an optimal measurement on the output, Eq.7.5, in order to estimate the unknown phase  $\phi$ . We have already seen that

<sup>1</sup>  $\Xi(t)$  could be a correlation-like quantity  $\mathcal{X}$ , which is monotonic under application of the channel on a part of its single argument, or some distance-like quantity  $\mathcal{D}$ , which is contractive under CP maps. With the notation  $\Xi(t)$  we consider both cases:  $\Xi_{\mathcal{X}}(t) \equiv \max_{\hat{\rho}} \mathcal{X}(\Phi_t \otimes \mathbb{1}(\hat{\rho}))$  or  $\Xi_{\mathcal{D}}(t) \equiv \max_{\hat{\rho}_1, \hat{\rho}_2} \mathcal{D}(\hat{\rho}_1(t), \hat{\rho}_2(t))$ .

the mean-square error in the estimation of this phase is lower-bounded by the inverse of the Fisher information  $\mathcal{F}(\hat{\varrho}_{AB}^{\phi, \hat{V}_B})$  (see Eq.3.11).

The figure of merit adopted to quantify the guaranteed precision of the estimation given the probe state  $\hat{\varrho}_{AB}$  in this black-box interferometry setup is the Gaussian interferometric power (GIP)  $\mathcal{P}_B(\hat{\rho}_{AB})$  defined as the Fisher information of the state  $\hat{\varrho}_{AB}^{\phi, \hat{V}_B}$  in the worst case scenario:

$$\mathcal{P}_B(\hat{\rho}_{AB}) = \frac{1}{4} \inf_{\hat{V}_B} \mathcal{F}(\hat{\varrho}_{AB}^{\phi, \hat{V}_B}). \quad (7.6)$$

It has been shown that the GIP is a measure of discord-like correlations for general mixed states [167–169]: (i) it vanishes if and only if  $\hat{\varrho}_{AB}$  is a product state (since the only Gaussian states with no quantum correlations are product states [168, 170]), (ii) it is invariant under local Gaussian unitaries and (iii) it is monotonically nonincreasing under local quantum operations applied by Alice.

The minimization in Eq.7.6 can be done exactly for two-mode Gaussian states and a compact formula in terms of the covariance matrix

$$V_{AB} = \begin{pmatrix} A & C \\ C^\top & B \end{pmatrix}, \quad (7.7)$$

where  $A$ ,  $B$  and  $C$  are  $2 \times 2$  real matrices such that  $A = A^\top$  and  $B = B^\top$ , is given by

$$\mathcal{P}_B(V_{AB}) = \frac{f_x + \sqrt{f_x^2 + f_y f_z}}{2f_y}, \quad (7.8)$$

where

$$\begin{aligned} f_x &= (I_2 + I_3)(1 + I_1 + I_3 - I_4) - I_4^2, \\ f_y &= (I_4 - 1)(1 + I_1 + I_2 + 2I_3 + I_4), \\ f_z &= (I_2 + I_4)(I_1 I_2 - I_4) + I_3(1 + I_1)(2I_2 + I_3), \end{aligned} \quad (7.9)$$

where  $I_1 = \det A$ ,  $I_2 = \det B$ ,  $I_3 = \det C$  and  $I_4 = \det V_{AB}$ . If the covariance matrix  $V_{AB}$  is in standard form, Eq.2.75, with  $c_+ = |c_-| = c$ , i.e.

$$A = a\mathbb{1}, \quad B = b\mathbb{1}, \quad C = -c\sigma_z, \quad a, b, c \in \mathbb{R}_+, \quad (7.10)$$

then the GIP reduces to the much simpler form [168, 169]

$$\mathcal{P}_B(V_{AB}) = \frac{c^2}{2(ab - c^2 + 1)}. \quad (7.11)$$

## 7.1.2 GIP as Gaussian non-Markovianity witness

Thanks to the GIP, because of property (iii), we can construct a non-Markovianity witness  $\mathcal{N}_{\mathcal{P}}$ , Eq.7.4, for a Gaussian channel  $\Phi_t$ , using two-mode Gaussian probes. To witness the non-Markovianity of a Gaussian channel  $\Phi_t$  one prepares a two-mode Gaussian state with covariance matrix  $V_{AB}$ , mode  $A$  undergoes the quantum evolution  $\Phi_t$  while mode  $B$  is left untouched. One can therefore study the time evolution of the GIP  $\mathcal{P}_B(V_{AB})$  and define

$$\sigma_{\mathcal{P}}(t) = \frac{d}{dt} \mathcal{P}_B(V_{AB}) \quad (7.12)$$

such that any positive value of  $\sigma_{\mathcal{P}}(t)$  signify that the map  $\Phi_t$  is non CP-divisible, therefore describes a non-Markovian process. The optimized non-Markovianity witness is readily defined

$$\mathcal{N}_{\mathcal{P}}(\Phi_t) = \max_{V_{AB}} \int_{\sigma_{\mathcal{P}}(t) > 0} dt \sigma_{\mathcal{P}}(t) , \quad (7.13)$$

where the integral is over all the times such that  $\sigma_{\mathcal{P}}(t) > 0$ , i.e. when the GIP shows revivals.

A remarkable aspect of characterizing non-Markovianity using GIP is that, because of GIP's property (i), it is possible to witness the non-Markovian dynamics of a local Gaussian channel by studying the unoptimized witness

$$\mathcal{N}_{\mathcal{P}}^{V_{AB}}(\Phi_t) = \int_{\sigma_{\mathcal{P}}(t) > 0} dt \sigma_{\mathcal{P}}(t) , \quad (7.14)$$

built for a probe Gaussian state  $\hat{\rho}_{AB}$  with covariance matrix  $V_{AB}$  which exhibits quantum correlations beyond entanglement. This becomes particularly relevant when one wishes to detect non-Markovian behaviour in an experimental setting since unentangled mixed states can be easily engineered with the current toolbox of quantum optics.

## 7.2 NON-MARKOVIANITY HIERARCHY OF GAUSSIAN EVOLUTIONS

In this section we will consider the evolution of  $n$ -mode Gaussian quantum states under continuous-time Gaussianity preserving processes, i.e. Gaussian maps  $\Phi_t$  described by matrices  $(X_t, Y_t)$  such that  $Y_t = Y_t^\top$  and, see Eq.2.81,

$$Y_t - i\Omega_n + iX_t\Omega_n X_t^\top \geq 0 , \quad \forall t \geq 0 , \quad (7.15)$$

with  $\Omega_n$  being the  $n$ -mode symplectic form, Eq.2.1, and  $X_0 = \mathbb{1}$  and  $Y_0 = \mathbb{O}$ , where  $\mathbb{O}$  is the null matrix.  $X_t$  and  $Y_t$  act on the first and second statistical moments of a Gaussian state as

$$\begin{aligned} \mathbf{d} &\rightarrow \mathbf{d}_t = X_t \mathbf{d} , \\ V &\rightarrow V_t = X_t V X_t^\top + Y_t . \end{aligned} \tag{7.16}$$

Taking inspiration from the analysis for finite-dimensional processes carried in [145], and building on the methods of [147], where non-Markovian Gaussian maps have been characterized in terms of CP-divisibility, we will identify a simple hierarchy of continuous-time Gaussian evolutions based on their divisibility degree. Before doing this we have to introduce the notion of  $k$ -mode positivity of Gaussian maps  $(X, Y)$ .

### 7.2.1 $k$ -mode positivity of Gaussian maps

Inspired by the hierarchy of  $k$ -positivity for finite dimensional channels, see Paragraph 1.1.2, we define a Gaussian map  $(X, Y)$  acting on  $n$ -mode Gaussian inputs as  $k$ -mode positive ( $kP$ ) if its trivial extension on  $k$  additional modes is positive, i.e. if for all  $(n+k)$ -mode Gaussian states with covariance matrix  $V_{n+k} \geq i\Omega_{n+k}$ , the following holds:

$$(X \oplus \mathbb{1}_k) V_{n+k} (X \oplus \mathbb{1}_k)^\top + Y \oplus \mathbb{O}_k \geq i\Omega_{n+k} . \tag{7.17}$$

Interestingly, this hierarchy ‘‘collapses’’ as a consequence of this theorem (see Appendix D for the proof):

**Theorem 7.1.** *For any  $n$ , the CP condition, Eq.2.81, is equivalent to the  $kP$  condition, Eq.7.17, with  $k = 1$ .*

This theorem tells us that in the Gaussian scenario, unlike the finite dimensional case, the  $k$ -mode positivity hierarchy collapses in only three classes: completely positive (CP,  $k = 1$ ), positive (P,  $k = 0$ ) and non-positive (NP) Gaussian maps. We can derive a simple condition to distinguish between the last two classes in terms of the pair  $(X, Y)$ . Notice that, because of Eq.D.15, for Eq.7.17 to hold, it is sufficient to check its validity on pure Gaussian states, whose covariance matrix can always be written as  $V_{\text{pure}} = SS^\top$ , with  $S \in Sp(2n, \mathbb{R})$ . We can therefore state that a Gaussian map with Gaussian inputs is positive (Eq.7.17 holds for  $k = 0$ ) if and only if

$$XSS^\top X^\top + Y - i\Omega_n \geq 0 , \quad \text{with } S \in Sp(2n, \mathbb{R}) . \tag{7.18}$$

The above, together with the CP condition, Eq.2.81, allow to fully classify the positivity properties of any  $(n \rightarrow n)$ -mode Gaussian map described by the pair of matrices  $(X, Y)$  acting on Gaussian inputs.

### 7.2.2 Hierarchy of Gaussian non-Markovianity

We are now provided with the right tools to construct a non-Markovianity hierarchy for continuous-time Gaussian processes described by the matrices  $(X_t, Y_t)$  which satisfy Eq.7.15, acting on the displacement vector and covariance matrix of a Gaussian state as in Eq.7.16. We are interested in the divisibility property of these maps, therefore, following the approach of [147] we can study the positivity of the intermediate map  $(X_\tau(t), Y_\tau(t))$  acting on the evolving system between times  $t$  and  $t + \tau$  as  $V_t \rightarrow V_{t+\tau} = X_\tau(t)V_t X_\tau^\top(t) + Y_\tau(t)$ . Given two Gaussian channels  $(X_2, Y_2)$  and  $(X_1, Y_1)$ , their composition is

$$(X_2, Y_2)(X_1, Y_1) = (X_2 X_1, X_2 Y_1 X_2^\top + Y_2) . \quad (7.19)$$

Inverting the above through matrix vectorization, one finds the expression for the intermediate map  $(X_\tau(t), Y_\tau(t))$  [147]:

$$X_\tau(t) = X_{t+\tau} X_t^{-1} , \quad Y_\tau(t) = Y_{t+\tau} - X_\tau(t) Y_t X_\tau^\top(t) . \quad (7.20)$$

Imposing the CP condition on the intermediate map for all times  $t, \tau > 0$ , leads us to the condition for a Markovian evolution [147]

$$iX_\tau(t)\Omega X_\tau^\top(t) + Y_\tau - i\Omega \geq 0 . \quad (7.21)$$

Any continuous-time Gaussian map violating Eq.7.21 for some intermediate times is non-Markovian. We can, however, add an extra distinction for these kind of maps, namely, if a Gaussian CP map is not CP-divisible but is P-divisible, i.e. the positivity condition

$$X_\tau(t) S S^\top X_\tau^\top(t) + Y_\tau(t) - i\Omega \geq 0 , \quad \forall S \in Sp(2n, \mathbb{R}) , \quad (7.22)$$

holds, then the evolution is dubbed *weakly* non-Markovian. On the other hand, if there is at least one intermediate map violating Eq.7.22, then the process is *strongly* non-Markovian.

## 7.2.3 Complete classification of one-mode Gaussian maps

In what follows, we will focus on single-mode continuous-time Gaussian maps. Thanks to Eq.7.20, from the global map  $(X_t, Y_t)$ , it is possible to construct the intermediate maps described by the  $2 \times 2$  matrices  $(X_\tau(t), Y_\tau(t))$ . Since, in order to check CP(P)-divisibility of the map  $(X_t, Y_t)$ , it is sufficient to verify that inequality Eq.7.21 (Eq.7.22) holds in the limit of small  $\tau$ <sup>2</sup>, and in this limit we have that  $X_\tau(t)$  and  $Y_\tau(t)$  are close to the identity and to the null matrix respectively, we can expand these matrices up to first order in  $\tau$

$$\begin{aligned} X_\tau(t) &= \left(1 + \tau \frac{\epsilon_t}{2}\right) \mathbb{1} + \tau \mathcal{X}(t) + o(\tau^2), \\ Y_\tau(t) &= \tau \mathcal{Y}(t) + o(\tau^2), \end{aligned} \quad (7.23)$$

where  $\mathcal{X}(t)$  is some arbitrary linear combination of  $\sigma_x$ ,  $\sigma_z$ ,  $\Omega$  and  $\mathcal{Y}(t)$  is some arbitrary symmetric matrix. We will now give two theorems that completely characterize the degree of Gaussian non-Markovianity of any single-mode Gaussian map  $(X_t, Y_t)$ , in terms of three real parameters:

$$\epsilon_t \equiv \frac{d}{dt} \ln |\det X_t|, \quad (7.24)$$

$$\delta_t \equiv (\det X_t)^2 \det \left( \frac{d}{dt} \left( X_t^{-1} Y_t (X_t^\top)^{-1} \right) \right), \quad (7.25)$$

$$\kappa_t \equiv \frac{d}{dt} \text{tr} Y_t - 2 \text{tr} \left( \frac{dX_t}{dt} X_t^{-1} Y_t \right). \quad (7.26)$$

**Theorem 7.2.** *A single-mode continuous-time Gaussian process  $\Phi_t$  described by the pair of matrices  $(X_t, Y_t)$  is CP-divisible if the following condition holds:*

$$\mu_t \geq |\epsilon_t|, \quad \forall t > 0 \quad (7.27)$$

with

$$\mu_t \equiv \begin{cases} \text{sgn}(\kappa_t) \sqrt{\delta_t}, & \text{for } \delta_t \geq 0 \\ -\sqrt{|\delta_t|}, & \text{for } \delta_t < 0 \end{cases}. \quad (7.28)$$

*Proof.* Let us start with simplifying the CP condition Eq.7.21: since  $X_\tau(t)$  is a  $2 \times 2$  matrix, we have that  $X_\tau(t) \Omega X_\tau^\top(t) = \Omega \det X_\tau(t)$ . This allows us to reduce the CP-divisibility condition Eq.7.21 to the following form

$$Y_\tau(t) + i(\det X_\tau(t) - 1)\Omega \geq 0, \quad (7.29)$$

<sup>2</sup> The composition of an arbitrary number of intermediate CP(P) maps is CP(P).

Moreover, noticing that

$$X_\tau(t) = \begin{pmatrix} (1 + \tau \frac{\epsilon_t}{2}) + \tau \gamma_t & \tau \beta_t \\ \tau \alpha_t & (1 + \tau \frac{\epsilon_t}{2}) - \tau \gamma_t \end{pmatrix} + o(\tau^2), \quad (7.30)$$

we have

$$\begin{aligned} \det X_\tau(t) &= \left(1 + \tau \frac{\epsilon_t}{2}\right)^2 - \tau^2(\gamma_t^2 + \alpha_t \beta_t) + o(\tau^4) = \\ &= 1 + \tau \epsilon_t + o(\tau^2), \end{aligned} \quad (7.31)$$

and making use of Eqs.7.20, we find the expression for  $\epsilon_t$ , Eq.7.24:

$$\begin{aligned} \epsilon_t &= \lim_{\tau \rightarrow 0} \frac{\det X_\tau(t) - 1}{\tau} = \lim_{\tau \rightarrow 0} \frac{\det X_{t+\tau} X_t^{-1} - \det X_t X_t^{-1}}{\tau} = \\ &= \lim_{\tau \rightarrow 0} \left( \frac{\det X_{t+\tau} - \det X_t}{\tau} \right) \det X_t^{-1} = \frac{d \det X_t}{dt} \frac{1}{\det X_t} = \\ &= \frac{d}{dt} \ln |\det X_t|. \end{aligned}$$

Now, since  $Y_\tau$  is a  $2 \times 2$  real symmetric matrix, it can be diagonalized by orthogonal transformations. Moreover, through a symplectic transformation of the form  $Z_z \equiv \text{diag}\{z, 1/z\}$  it can be brought to a diagonal form proportional to the identity or to the Pauli matrix  $\sigma_z$ . The proportionality factor is  $\mu_t$  such that

$$\mu_t^2 = |\delta_t|, \quad (7.32)$$

where  $\delta_t \equiv \det \mathcal{Y}(t)$ . Making use of Eqs.7.20 one finds the expression for  $\delta_t$  Eq.7.25:

$$\begin{aligned} \det \mathcal{Y}(t) &= \lim_{\tau \rightarrow 0} \det \left( \frac{Y_\tau(t)}{\tau} \right) = \lim_{\tau \rightarrow 0} \det \left( \frac{Y_{t+\tau} - X_\tau(t) Y_t X_\tau^\top(t)}{\tau} \right) = \\ &= (\det X_t)^2 \det \left( \frac{d}{dt} \left( X_t^{-1} Y_t X_t^{-\top} \right) \right), \end{aligned}$$

where  $X_t^{-\top} = \left( X_t^{-1} \right)^\top$ .

Let us consider the case  $\delta_t > 0$ , i.e.  $\mathcal{Y}(t)$  is positive or negative definite, and let  $\mu_t^>$  be the symplectic eigenvalue with the sign of  $\mathcal{Y}(t)$ , i.e.  $\mu_t^> = \text{sgn}(\kappa_t) \sqrt{\delta_t}$ , where

$$\begin{aligned} \kappa_t = \text{tr } \mathcal{Y}(t) &= \lim_{\tau \rightarrow 0} \frac{\text{tr } Y_\tau(t)}{\tau} = \lim_{\tau \rightarrow 0} \frac{\text{tr} (Y_{t+\tau} - X_\tau(t) Y_t X_\tau^\top(t))}{\tau} = \\ &= \frac{d}{dt} \text{tr } Y_t - 2 \text{tr} \left( \frac{dX_t}{dt} X_t^{-1} Y_t \right). \end{aligned}$$

Since  $Y_\tau(t)$  can be brought into its diagonal form by a symplectic transformation which leaves  $\Omega$  invariant and doesn't change the sign of the inequality, we can rewrite the CP condition as

$$\mu_t^> \mathbb{1} + i \epsilon_t \Omega + o(\tau) \geq 0. \quad (7.33)$$

The CP (infinitesimal) divisibility condition can then be easily expressed in terms of  $\mu_t$  and  $\epsilon_t$ :

$$\mu_t^> \geq |\epsilon_t| \quad \forall t \geq 0. \quad (7.34)$$

In the case  $\delta_t < 0$ , through a symplectic transformation we can bring Eq.7.29 into the form

$$\pm \mu_t^< \sigma_z + i \epsilon_t \Omega + o(\tau) \geq 0, \quad (7.35)$$

with  $\mu_t^< = \sqrt{|\delta_t|}$ . This inequality is never satisfied because the eigenvalues of the lhs are one the opposite of the other. Hence, by defining  $\mu_t$  as in Eq.7.28, one can write the CP condition Eq.7.27.  $\square$

**Theorem 7.3.** *A single-mode continuous-time Gaussian process  $\Phi_t$  described by the pair of matrices  $(X_t, Y_t)$  is P-divisible if the following condition holds:*

$$\mu_t \geq \frac{|\epsilon_t| - \epsilon_t}{2}, \quad \forall t > 0, \quad (7.36)$$

with  $\mu_t$  as defined in Eq.7.28.

*Proof.* Exploiting again the property that any 2x2 matrix divided by the square root of its determinant is a symplectic matrix, the P-divisibility condition Eq.7.22 can be rewritten as

$$\forall S \in \text{Sp}(2, \mathbb{R}), \quad \det X_\tau(t) S S^\top + Y_\tau(t) - i\Omega \geq 0. \quad (7.37)$$

We first consider the case  $\delta_t \geq 0$ . The above inequality can be recast as

$$\forall S \in \text{Sp}(2, \mathbb{R}), \quad \det X_\tau(t) S S^\top + \mu_t \tau \mathbb{1} - i\Omega \geq 0. \quad (7.38)$$

Using the Euler decomposition of symplectic transformations  $S = O_1 Z_z O_2$  [28], where  $Z_z \equiv \text{diag}\{z, 1/z\}$  with  $z \in (0, 1]$  and  $O_i$  is an orthogonal matrix, we can further simplify the P-divisibility condition as follows

$$\forall z \in (0, 1], \quad \det X_\tau(t) Z_z^2 + \mu_t \tau \mathbb{1} - i\Omega \geq 0. \quad (7.39)$$

At first order in  $\tau$ , the eigenvalues of the lhs of Eq.7.39 are

$$\lambda_1 = \left( \frac{2 \epsilon_t z^2}{z^4 + 1} + \mu_t \right) \tau, \quad (7.40)$$

$$\lambda_2 = \frac{z^4 + 1}{2z^2} + \left( \frac{(z^8 + 1) \epsilon_t}{z^6 + z^2} + \mu_t \right) \tau. \quad (7.41)$$

We notice that  $\lambda_2$  is always positive for small  $\tau$ , hence the positivity of the intermediate map depends only on  $\lambda_1$ ; in particular we have that the intermediate map is positive if

$$\frac{2\epsilon_t z^2}{z^4 + 1} + \mu_t \geq 0 \quad \forall z \in (0, 1], \quad (7.42)$$

which is equivalent to Eq.7.43

$$\mu_t \geq \frac{|\epsilon_t| - \epsilon_t}{2}. \quad (7.43)$$

In the case for which  $\delta_t < 0$  the  $P$ -divisibility condition becomes

$$\forall z \in (0, 1], \quad \det X_\tau(t) Z_z^2 \pm \mu_t \tau \sigma_z - i\Omega \geq 0, \quad (7.44)$$

which is never satisfied.  $\square$

Summarizing, the single-mode continuous-time Gaussian processes for which Theorem 7.2 is satisfied are Markovian. Those for which Theorem 7.3 is satisfied while Theorem 7.2 is not, are weakly non-Markovian. Those for which Theorem 7.3 is not satisfied are strongly non-Markovian.

Thanks to Theorems 7.2, 7.3, we can therefore distinguish three regions in the space of parameters  $\epsilon$  and  $\mu$  which correspond to the intermediate map being respectively  $CP$ ,  $P$ , and  $NP$  divisible:

$$\begin{aligned} Y_{CP} &\equiv \{(\epsilon, \mu) \mid \mu \geq |\epsilon|\}, \\ Y_P &\equiv \{(\epsilon, \mu) \mid 2\mu \geq |\epsilon| - \epsilon\}, \\ Y_{NP} &\equiv \mathbb{R}^2 \setminus Y_P, \end{aligned} \quad (7.45)$$

A pictorial representation of these regions can be found in Fig.7.1. One can define a similar diagram to characterise the legitimate quantum channels, i.e. the single-mode Gaussian channels which satisfy Eq.2.84, therefore regions analogous to  $Y_{P/CP}$  and  $Y_{NP}$  are denoted as non-physical [132, 134, 171]. However, since the diagram considered here is for the intermediate maps of a globally physical process (CP), which can violate the CP condition for some intermediate times, these regions are permitted.

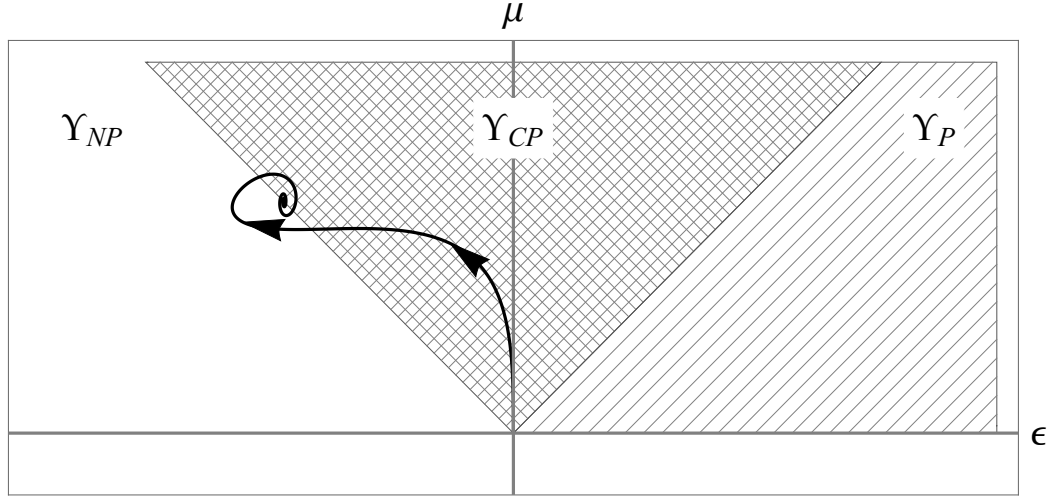


Figure 7.1.: Pictorial diagram of parameters  $(\epsilon, \mu)$  characterizing one-mode Gaussian intermediate maps. The diagonal striped pattern corresponds to the P- but not CP-divisible region  $Y_{P/CP}$ . The crosshatch pattern identifies the CP-divisible region  $Y_{CP}$ . The white region corresponds to  $Y_{NP}$ . A path,  $\Gamma_t = (\epsilon_t, \mu_t)$ , on the diagram denotes a process with parameters changed continuously in time. The solid black path represents a quantum Brownian motion process as described in the text, with  $\omega_0/\omega_c = 2$ .

Let us first establish a relation between the Gaussian non-Markovianity degree and the intermediate maps represented by points of the diagram. Processes that are continuous in time, described by time-dependent parameters  $(\epsilon_t, \mu_t)$ , define paths  $\Gamma_t \equiv \{(\epsilon_s, \mu_s) \mid s \in [0, t]\}$  on the diagram. We can then characterize the non-Markovianity of the evolution studying the paths  $\Gamma_t$  on the  $(\epsilon, \mu)$  plane. If an evolution is Markovian the trajectory will be confined for all times in the  $Y_{CP}$  region:

$$\Gamma_t \in Y_{CP} \quad \forall t > 0. \quad (7.46)$$

If for some times the trajectory trespasses in the  $Y_{P/CP}$  region but never trespasses in the  $Y_{NP}$  one, i.e.

$$\Gamma_t \in Y_P \quad \forall t > 0, \quad \text{and} \quad \exists s \leq t \text{ s.t. } (\epsilon_s, \mu_s) \notin Y_{CP} \quad (7.47)$$

then the evolution is *weakly* non-Markovian. If for some times a curve crosses into the  $Y_{NP}$  region then the evolution is said to be *strongly* non-Markovian.

## 7.2.4 Phase-insensitive maps: allowed trajectories

We intend to analyse the constraints that are given by the condition that a process is formed by a family of Gaussian CP maps represented by the pair of matrices  $(X_\tau(t), Y_\tau(t))$ , each of which transforms a state at time  $t$  to a later moment of time  $t + \tau$ . This family of maps establishes a path on the diagram introduced in the previous paragraph. Further on we consider only phase-insensitive channels for which the intermediate maps read

$$X_\tau(t) = \left(1 + \frac{\epsilon_t}{2}\tau\right) \mathbb{1}, \quad (7.48)$$

$$Y_\tau(t) = \mu_t \tau \mathbb{1}. \quad (7.49)$$

Applying the composition law for Gaussian maps Eq.7.19, we reconstruct the map from time  $t = 0$  to some time  $t = N\tau$ :

$$(X_N(t), Y_N(t)) = (X_\tau(N\tau), Y_\tau(N\tau)) \circ \cdots \circ (X_\tau(\tau), Y_\tau(\tau)). \quad (7.50)$$

It is easy to show that

$$X(N\tau) = \prod_{n=0}^N \left(1 + \tau \frac{\epsilon(n\tau)}{2}\right) \mathbb{1}, \quad (7.51)$$

$$Y(N\tau) = \prod_{n=0}^N \left(1 + \tau \frac{\epsilon(n\tau)}{2}\right)^2 \sum_{m=1}^N \frac{\mu(m\tau) \tau}{\prod_{k=0}^m \left(1 + \tau \frac{\epsilon(k\tau)}{2}\right)^2} \mathbb{1}, \quad (7.52)$$

which for  $\lim_{N \rightarrow \infty} \lim_{\tau \rightarrow 0} N\tau = t > 0$  become

$$X_t = e^{\frac{1}{2} \int_0^t \epsilon(s) ds} \mathbb{1}, \quad (7.53)$$

$$Y_t = \left( e^{\int_0^t \epsilon(s) ds} \int_0^t \mu(r) e^{-\int_0^r \epsilon(s) ds} dr \right) \mathbb{1}. \quad (7.54)$$

A paradigmatic example, widely studied in the literature [2, 172] (and references therein), is the Quantum Brownian Motion model. This model consists of a particle, subject to a harmonic potential, constrained to move in one spatial dimension and interacting linearly with a bath of harmonic oscillators in thermal equilibrium at temperature  $T$ . With a secular and weak-coupling approximation, the master equation is given by

$$\begin{aligned} \frac{d\hat{\rho}(t)}{dt} = & \frac{\Delta(t) + \gamma(t)}{2} [2\hat{a}\hat{\rho}\hat{a}^\dagger - \{\hat{a}^\dagger\hat{a}, \hat{\rho}\}] + \\ & + \frac{\Delta(t) - \gamma(t)}{2} [2\hat{a}^\dagger\hat{\rho}\hat{a} - \{\hat{a}\hat{a}^\dagger, \hat{\rho}\}]. \end{aligned} \quad (7.55)$$

$\Delta(t)$  and  $\gamma(t)$  are the diffusion and damping coefficients, respectively, given by

$$\Delta(t) = \int_0^t ds \int_0^\infty d\omega J(\omega) \left( N(\omega) + \frac{1}{2} \right) \cos(\omega_0 s) \cos(\omega s), \quad (7.56)$$

$$\gamma(t) = \int_0^t ds \int_0^\infty d\omega J(\omega) \sin(\omega_0 s) \sin(\omega s), \quad (7.57)$$

where  $N(\omega) = (\exp[\hbar\omega/k_B T] - 1)^{-1}$  is the mean number of thermal photons with frequency  $\omega$ ,  $J(\omega)$  is the spectral density of the reservoir and  $\omega_0$  is the characteristic frequency of the system.

The pair of matrices  $(X_t, Y_t)$  describing the dynamics are

$$X_t = e^{-\frac{1}{2} \int_0^t \gamma(s) ds} \mathbb{1}, \quad (7.58)$$

$$Y_t = e^{-\int_0^t \gamma(s) ds} \int_0^t e^{\int_0^s \gamma(r) dr} \Delta(s) ds \mathbb{1}, \quad (7.59)$$

which corresponds to the map given by Eqs.7.53, 7.54 with the substitutions  $\epsilon_t \rightarrow -\gamma(t)$  and  $\mu_t \rightarrow \Delta(t)$ . A trajectory on the  $\epsilon - \mu$  plane, for a Ohmic spectral density with an exponential cut-off frequency  $\omega_c$ ,  $J(\omega) = \omega e^{-\omega/\omega_c}$ , at zero temperature, is reported in Fig.7.1.

More generally, in order to have a physical evolution from a composition of infinitesimal phase-insensitive maps we have to impose the complete positivity condition Eq.7.15 on the composition given by Eqs.7.53, 7.54. The eigenvalues of the lhs of Eq.7.15 are

$$\begin{aligned} \Lambda_1 &= 1 + e^{\int_0^t \epsilon(s) ds} \left( -1 + \int_0^t e^{-\int_0^r \epsilon(s) ds} \mu(r) dr \right), \\ \Lambda_2 &= -1 + e^{\int_0^t \epsilon(s) ds} \left( 1 + \int_0^t e^{-\int_0^r \epsilon(s) ds} \mu(r) dr \right). \end{aligned}$$

The condition  $\Lambda_1 \geq 0$  can be rewritten as

$$\int_0^t e^{-\int_0^r \epsilon(r) dr} (\mu(r) - \epsilon(r)) dr \geq 0 \quad \forall t > 0. \quad (7.60)$$

Analogously, the condition  $\Lambda_2 \geq 0$  can be recast as

$$\int_0^t e^{-\int_0^r \epsilon(r) dr} (\mu(r) + \epsilon(r)) dr \geq 0 \quad \forall t > 0. \quad (7.61)$$

As one could expect, these conditions are weaker than the condition for CP-divisibility, if the latter is satisfied, then Eqs.7.60,7.61, are also satisfied. Therefore, the trajectories in the diagram Fig.7.1 can go beyond the

region  $Y_{CP}$ . It is possible, however, to derive the following constraint on the physical paths. By expanding at first order in  $t$  the lhs of the inequalities Eqs.7.60,7.61 we get

$$\mu_0 \geq |\epsilon_0|, \quad (7.62)$$

i.e. the trajectory must begin in the CP region  $Y_{CP}$ . Moreover, if the trajectory starts on the boundaries of region  $Y_{CP}$ , i.e.  $\mu_0 = |\epsilon_0|$ , then

$$\dot{\mu}_0 \geq |\dot{\epsilon}_0|. \quad (7.63)$$

This tells us that not only an allowed path described by the curve  $\Gamma_t$  must start in the CP-divisibility region, but it also has to have an initial tangent vector  $(\dot{\epsilon}_0, \dot{\mu}_0)$  entirely contained in  $Y_{CP}$  such that for the immediate subsequent time  $\Gamma_t$  remains inside  $Y_{CP}$ . A path which starts in the origin, then moves along the boundary of the crosshatched region up to time  $t_i$  and then trespasses in either  $Y_{NP}$  or  $Y_{P/CP}$  region, is not allowed. The physical significance of the last no-go rules is related to fundamental physical properties discussed in the following section.

### 7.2.5 Operational significance of Gaussian non-Markovianity degree

Let us suppose that at time  $t = 0$  a Gaussian state is described by covariance matrix  $V = \text{diag}\{\nu, \nu\}$ , with  $\nu \geq 1$ . Under the action of the map Eqs.7.53,7.54 at time  $\tilde{t} > 0$ , the product of the covariances is

$$4\langle \hat{q}^2 \rangle \langle \hat{p}^2 \rangle = e^{2 \int_0^{\tilde{t}} \epsilon(s) ds} \left( \nu + \int_0^{\tilde{t}} \mu(r) e^{-\int_0^r \epsilon(s) ds} dr \right)^2. \quad (7.64)$$

If Eq.7.61, i.e.  $\Lambda_2 < 0$ , is violated we obtain

$$\begin{aligned} \langle \hat{q}^2 \rangle \langle \hat{p}^2 \rangle &< \frac{1}{4} e^{2 \int_0^{\tilde{t}} \epsilon(s) ds} \left( \nu - \int_0^{\tilde{t}} \epsilon(r) e^{-\int_0^r \epsilon(s) ds} dr \right)^2 = \\ &= e^{\int_0^{\tilde{t}} \epsilon(s) ds} \left( \frac{\nu}{2} e^{\frac{1}{2} \int_0^{\tilde{t}} \epsilon(s) ds} - \sinh \left( \frac{1}{2} \int_0^{\tilde{t}} \epsilon(s) ds \right) \right)^2, \end{aligned}$$

and if the initial state was pure,  $\nu = 1$ , then the above inequality becomes

$$\langle \hat{q}^2 \rangle \langle \hat{p}^2 \rangle < \frac{1}{4}, \quad (7.65)$$

i.e. the uncertainty principle is violated. Indeed, a path  $\Gamma_t$  lying along the border between  $Y_{CP}$  and  $Y_{NP}$  preserves the purity of any pure state. To better understand this, let us consider the limiting case of having a map such that  $-\epsilon_t = \mu_t > 0$  for  $0 < t < t_i$  and that  $-\epsilon_t > \mu_t$  for  $t_i < t < \tilde{t}$ . Up to  $t_i$  the action of  $X_t$  decreases both variances of the pure state, on the other hand, the added noise,  $Y_t$ , compensates this loss and the state remains pure. For  $t > t_i$ , the noise introduced by  $Y_t$  is not enough and we have a violation of the Heisenberg uncertainty relation.

However, we stress that crossing the border during at time  $t_i$  is still possible if during the preceding dynamics, i.e. for all times  $t < t_i$ , the state domain of the intermediate map was shrank enough, such that its subsequent action, corresponding to a temporary dilation of this domain, does not violate the uncertainty relation. The dilation in the volume of the physical states accessible by the system during the evolution, can then be seen as a backflow of information from the environment back into the system [144], typical of non-Markovian dynamics.

Let us now briefly comment on the border of the CP region between  $Y_{CP}$  and  $Y_{P \setminus CP}$ . A trajectory along this border is such that  $\epsilon_t = \mu_t > 0$ , which is responsible for the multiplication of the displacement vector by a factor greater than 1, i.e. amplification, and for an increase of the variances. Such path indeed describes a quantum limited amplifier  $(\sqrt{x}\mathbb{1}, (1-x)\mathbb{1})$ , i.e. the added noise is the minimum allowed for quantum linear amplifiers (see Paragraph 2.3.2). The crossing of this border at some time  $t_i > 0$  is allowed only if the noise added up to this time is sufficient to permit a subsequent amplification beyond the quantum limit. We can hence conclude that a Gaussian phase-insensitive process with added noise is weakly non-Markovian if at any moment during the evolution one observes that although the covariances increase a Gaussian state is momentarily amplified beating the quantum limit. This provides an operational interpretation for the elusive concept of weak non-Markovianity in the context of quantum amplification.

## 7.3 REMARKS

In this Chapter we introduced the notion of non-Markovianity witness, i.e. a quantity which allows to detect the violation of the CP divisibility of a quantum map. We focused in particular on Gaussian quantum processes, and introduced a non-Markovianity witness based on the breakdown of monotonicity of the Gaussian Interferometric Power (GIP), an operational figure of merit in quantum metrology. Being the GIP a measure of quantum discord, our witness can detect non-Markovianity by using, in principle, any bipartite Gaussian state, since all bipartite Gaussian states, with the only exception of product states, have quantum correlations beyond entanglement.

We then investigated more in depth the divisibility of Gaussian maps. We introduced the concept of  $k$ -mode positivity of Gaussian maps. Applying this concept to intermediate time-continuous Gaussian maps, we could define a simple hierarchy of time-continuous Gaussian processes: non-divisible, P-divisible or CP-divisible, corresponding to strongly and weakly non-Markovian, and Markovian processes, respectively.

For the single-mode case, we gave analytical conditions to identify to which class a Gaussian map belongs, based on some parameters that can be easily computed from the pair of matrices  $X_t$  and  $Y_t$  describing the process. In particular, one can simply characterise any single-mode Gaussian map, by studying the path defined by these parameters, i.e.  $(\epsilon_t, \mu_t)$ , in a two-dimensional diagram. Moreover, by focusing on phase-insensitive channels, we have been able to give a physical interpretation to weakly and strongly non-Markovian processes: an instantaneous amplification or attenuation beyond the quantum limited performance is a signature of memory effects, such as non-negligible correlations or backflow of information from the environment.

---

## GAUSSIAN QUANTUM TELEPORTATION WITH LIMITED RESOURCES

---

Noisy phase-covariant Gaussian channels have also been the focus of this last Chapter: we will indeed consider here those single-mode Gaussian channels which can be simulated via continuous variable teleportation protocols in a scenario of scarcity of resources.

In the first section we will revise the quantum teleportation protocol, focusing on the teleportation of Gaussian states [173]. We will explain what is meant by *certified* and *certified secure* quantum teleportation and what are the relevant resources Alice and Bob have to exploit to achieve these. In sections Sec.8.2 and Sec.8.3, we will focus on devising the best strategies to achieve optimal certified and certified secure quantum teleportation, respectively, assuming that the above mentioned resources are limited. In order to do that we will make use of the correspondence between single-mode Gaussian channels and teleportation protocols [135, 174, 175]. In particular, we will determine a class of realistic Gaussian teleportation protocols that allow to simulate phase-covariant Gaussian channels, employing the minimum amount of resources and finite mean energy.

### 8.1 QUANTUM TELEPORTATION

Originally developed by Bennett *et al.* [5], a quantum teleportation protocol consists in the disembodied transfer of a quantum state from a sender, Alice, to a receiver, Bob, located at an arbitrary spatial distance from the former. Alice, in general, does not know the state she wants to transfer: we can assume that a third party, Charlie, provides her the state without sharing any prior knowledge about it but the set of states she drew it from

and their probability distribution. To accomplish this task, Alice and Bob share an entangled state and are able to classically communicate, i.e. the transfer happens through an *entanglement-assisted* channel. Once she receives from Charlie the quantum state (*input*), Alice performs a Bell measurement (a projection on a set of maximally entangled states) on the bipartite system composed by the input and her part of the shared entangled state. This measurement, however, tells Alice nothing about the state Charlie gave her. Moreover, by the act of measuring, given the intrinsic invasive nature of such operation, she “destroys” the input, meaning that the state she is left with after the measurement does not contain any information about it. At this point, she communicates the outcome of the measurement to Bob through the classical communication channel. Therefore, Bob performs on his part of the shared entangled state a suitable operation conditioned on the classical information received from Alice.

In the seminal paper [5], the teleportation of a discrete variable system was studied and it was showed that in order to achieve perfect teleportation, i.e. Bob’s state at the end of the protocol is an exact copy of Charlie’s state, Alice and Bob need to share a perfectly entangled state. Unfortunately, this is an unrealistic requirement to be achieved in any experimental implementation, in particular for continuous variable systems [26, 176, 177] where maximally entangled states are two-mode squeezed states with infinite squeezing, corresponding to infinite energy states. However, Braunstein and Kimble proposed a continuous variable system teleportation protocol [173] (BK), later implemented in several experiments [178–180], which employs two-mode squeezed states with finite squeezing parameter. The price to pay for not using a maximally entangled state is that the teleported state is not a perfect copy of the input.

As we will see shortly, the BK protocol realizes a Gaussian additive noise channel [181] between Alice’s input and Bob’s output. However, a variation of this protocol which introduces a non-unit classical gain [178, 182–184] allows to realize more general Gaussian channels. We will explain in detail this protocol in the next section.

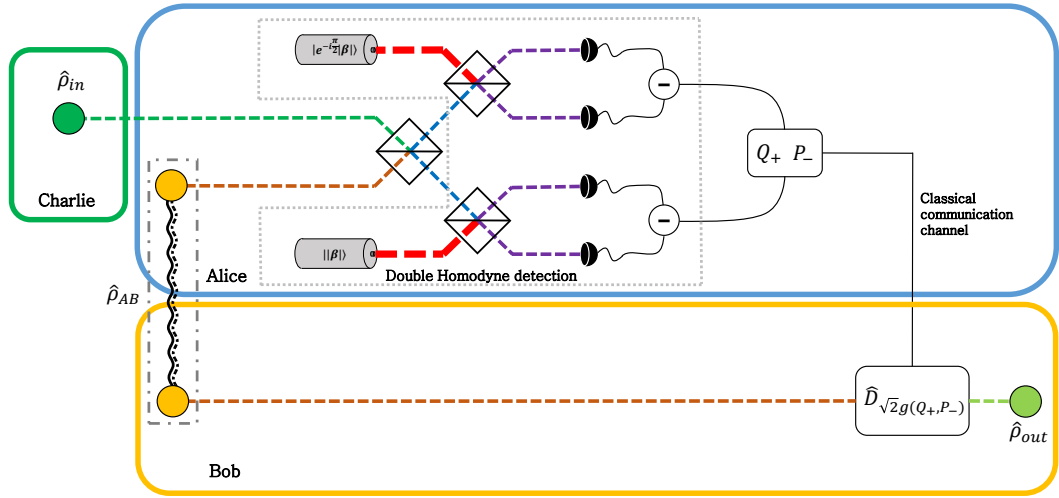


Figure 8.1.: Schematic depiction of the continuous variable teleportation protocol. The measurement scheme for the two commuting quadratures  $\hat{Q}_+$  and  $\hat{P}_-$ , i.e. the double homodyne detection scheme, has been depicted explicitly.

### 8.1.1 Gaussian teleportation protocol

The resource state  $\hat{\rho}_{AB}$  Alice and Bob share is a two-mode Gaussian state with first moment vector  $\mathbf{d}_{AB} = \mathbf{d}_A \oplus \mathbf{d}_B = \mathbf{0}$  and covariance matrix (as in Eq.8.1)

$$V_{AB} = \begin{pmatrix} A & C \\ C^\top & B \end{pmatrix}, \quad (8.1)$$

where  $A$ ,  $B$  and  $C$  are  $2 \times 2$  real matrices such that  $A = A^\top$  and  $B = B^\top$ . Charlie's input state provided to Alice is a Gaussian state with covariance matrix  $V_{in}$  and displacement  $\mathbf{d}_{in}$ .

As already anticipated, Alice needs to perform a Bell measurement in a suitable basis on the joint state of the input and her part of the shared resource. This can be accomplished as follows: Alice mixes the two modes in a balanced beam splitter and then measures the output quadratures  $\hat{Q}_+ = (\hat{q}_{in} + \hat{q}_A)/\sqrt{2}$  and  $\hat{P}_- = (\hat{p}_{in} - \hat{p}_A)/\sqrt{2}$  (notice that  $[\hat{Q}_+, \hat{P}_-] = 0$ ). This measurement is carried out by double homodyne detection, i.e. the homodyne detection of the quadrature  $\hat{Q}_+$  on one output mode and the homodyne detection of  $\hat{P}_-$  on the other. As one can see in Fig.8.1, homo-

dyne detection consists in mixing at a balanced beam splitter the mode one wishes to measure the quadrature of, with a high energy coherent state  $|e^{i\theta}|\beta|\rangle$ , i.e.  $|\beta| \rightarrow \infty$ , at the same frequency. One can show that measuring the difference between the detected intensities, as measured by (ideal) photodetectors, at the two outputs of the beam splitter, is equivalent to measuring the quadrature  $\hat{x}_\theta = \cos\theta\hat{q} - \sin\theta\hat{p}$ . This operation corresponds to a Bell measurement since the unnormalized maximally entangled vector  $|\xi\rangle = \sum_n |nn\rangle$  is a common eigenvector of  $\hat{Q}_+$  and  $\hat{P}_-$  relative to the zero eigenvalue, and therefore the also maximally entangled unnormalized vector  $\hat{D}_r \otimes \mathbb{1}|\xi\rangle$ , with  $r = (q, p)^\top$ , is a common eigenstate of the two quadratures relative to the eigenvalues  $q$  and  $p$ , respectively.

Alice then communicates the output of the measurement to Bob who conditionally displaces his part of the shared resource state by  $\delta = \sqrt{2}g(Q_+, P_-)$ , where  $g > 0$  is the *gain* parameter.

Bob's state, when the above protocol is completed, is a Gaussian state with first moment vector and covariance matrix [130, 176, 177, 185]

$$d_{\text{out}} = g d_{\text{in}} , \quad (8.2)$$

$$V_{\text{out}} = g^2 V_{\text{in}} + g^2 \sigma_z A \sigma_z + g(\sigma_z C + C^\top \sigma_z) + B , \quad (8.3)$$

respectively. The good-willing reader can find a re-derivation of the above in the Appendix E.

As anticipated, Eqs.8.2-8.3 show that a BK protocol with non-unit gain realizes a single-mode Gaussian channel  $(X, Y)$  with  $X = g\mathbb{1}$  and  $Y = g^2\sigma_z A \sigma_z + g(\sigma_z C + C^\top \sigma_z) + B$ . By choosing the resource state with covariance matrix in standard form to be

$$A = a\mathbb{1}, \quad B = b\mathbb{1}, \quad C = -c\sigma_z, \quad a, b, c \in \mathbb{R}_+, \quad (8.4)$$

we get a phase-covariant Gaussian channel,  $X = \sqrt{x} \mathbb{1}$ ,  $Y = y \mathbb{1}$ , with

$$x = g^2, \quad y = g^2 a - 2gc + b. \quad (8.5)$$

In the original BK protocol, the state shared by Alice and Bob is a TMSV, i.e.  $a = b = \cosh 2r$  and  $c = \sinh 2r$ , and the gain is set to be  $g = 1$ . One immediately sees that in the limit  $r \rightarrow \infty$  the noise matrix  $Y$  vanishes and  $V_{\text{out}} = V_{\text{in}}$ ,  $d_{\text{out}} = d_{\text{in}}$ , i.e. Bob is in possession of an exact copy of Charlie's original state.

It is natural then to ask ourselves: how can we quantify how successful the teleportation protocol above is? Is there a way for Alice and Bob to “cheat”, i.e. to create a state  $\hat{\rho}_{\text{out}}^{\Phi_{\text{cl}}}$ , through a preparation strategy  $\Phi_{\text{cl}}$  which does not make use of quantum resources? Is there a way for Charlie to say with certainty whether they cheated or not? And eventually, if Charlie wants to be sure that only Bob gets her state, how can she be sure that Alice has not kept for herself a better copy than Bob’s? The first three questions have been addressed in [186,187], the last one in [188,189], and we are going to summarize the answers in the next paragraph.

### 8.1.2 Figure of merit for certified teleportation

In what follows, we assume that Charlie’s state is a pure state  $|\psi_{\text{in}}\rangle$ . The figure of merit used to assess how good a copy of Charlie’s state is Bob’s  $\hat{\rho}_{\text{out}}$ , is the fidelity (see Par.1.1.2):

$$F(|\psi_{\text{in}}\rangle, \hat{\rho}_{\text{out}}) = \langle \psi_{\text{in}} | \hat{\rho}_{\text{out}} | \psi_{\text{in}} \rangle . \quad (8.6)$$

To answer the second question, Braunstein *et al.* [186] noticed that Alice and Bob can achieve a non-zero fidelity even without exploiting an entangled resource if they have some prior knowledge about the state Charlie prepares: if, for example, they know that Charlie will draw her state from a set of orthogonal states  $\mathcal{S} = \{|\psi_i\rangle \text{ s.t. } \langle \psi_i | \psi_j \rangle = \delta_{ij}\}$ , then they can achieve unit fidelity. Indeed, Alice can measure a non-degenerate observable diagonal in the basis  $\mathcal{S}$  and send the outcome to Bob who will prepare the appropriate state on his side.

In order to take into account this prior knowledge, we will consider that Alice and Bob know the set  $\mathcal{S}$  and the probability with which Charlie draws the state from it, i.e.  $p(|\psi_{\text{in}}\rangle)$ , and agree to prepare the output state through a strategy  $\Phi$ . It is therefore sensible to define the figure of merit to be

$$\bar{F}_{\Phi} = \int_{\mathcal{S}} p(|\psi_{\text{in}}\rangle) F(|\psi_{\text{in}}\rangle, \hat{\rho}_{\text{out}}^{\Phi}) d|\psi_{\text{in}}\rangle . \quad (8.7)$$

The maximization of the above over all classical strategies  $\Phi_{\text{cl}}$ , i.e. those strategies that make no use of entanglement, defines the so-called classical benchmark  $\bar{F}_{\text{cl}}$ . The third question is then answered: if Alice and Bob pre-

pare the output state by using the strategy  $\tilde{\Phi}$ , Charlie can certify that they made use of quantum resources if

$$\bar{F}_{\tilde{\Phi}} \geq \max_{\Phi_{\text{cl}}} \bar{F}_{\Phi_{\text{cl}}} = \bar{F}_{\text{cl}}, \quad (8.8)$$

in which case we talk of *certified* quantum teleportation.

The last question addresses the problem of *certified secure* quantum teleportation. The answer to this is based on the no-cloning theorem and also in this case one can define a benchmark average fidelity  $\bar{F}_{\text{sec}}$  such that Charlie can be sure that Alice does not keep an input's better copy than Bob's if

$$\bar{F}_{\tilde{\Phi}} \geq \bar{F}_{\text{sec}}. \quad (8.9)$$

For the case considered in this chapter, we will assume the set from which Charlie draws the input states to be the set of single mode coherent states  $\mathcal{S} = \{|\alpha\rangle = \hat{D}_\alpha|0\rangle, \alpha \in \mathbb{C}\}$ ; the probability distribution, known by Alice and Bob, she draws the input states from is assumed to be Gaussian, with variance  $\lambda^{-1}$ , centered in the vacuum:

$$p_{\text{in}}^\lambda(\alpha) = \frac{\lambda}{\pi} e^{-\lambda|\alpha|^2}. \quad (8.10)$$

It was conjectured in [186] and then proved in [187] that the classical benchmark for this case is

$$\bar{F}_{\text{cl}}^\lambda = \frac{1 + \lambda}{2 + \lambda}, \quad (8.11)$$

and it can be achieved if Alice performs a heterodyne measurement<sup>1</sup> on the input state, sends the outcome  $\alpha$  to Bob who then displaces a vacuum state by  $\frac{\alpha}{1+\lambda}$ .

The secure teleportation benchmark for an input coherent state distribution, as in Eq.8.10, in the assumption of Gaussian cloners, was shown to be [189]

$$\bar{F}_{\text{sec}}^\lambda = \begin{cases} \frac{2(1 + \lambda)}{3 + \lambda}, & \lambda < \sqrt{2} - 1, \\ \frac{2\lambda}{3 - 2\sqrt{2} + 2\lambda}, & \text{otherwise.} \end{cases} \quad (8.12)$$

<sup>1</sup> An heterodyne measurement can be realised through a scheme analogous to the homodyne scheme where the input state is mixed at a balanced beam splitter with a strong coherent state at a different frequency. The measurement outcomes correspond to the input quadratures. It can be shown that heterodyne detection is equivalent to a double homodyne detection where the input state is mixed with a vacuum at the first balanced beam splitter.

Alice can amplify the input and then send it into a balanced beam splitter. The two output modes correspond to two “clones” of Charlie’s state with fidelity given by Eq.8.12. Hence, if a “malicious” Alice plans to clone the input state (using only Gaussian operations) and only after to teleport, even perfectly (hence using a perfectly entangled resource), one of the two copies to Bob, the fidelity of the teleported state at the end of the protocol cannot exceed the benchmark Eq.8.12.

In a recent work [190], the secure continuous variable teleportation of an input alphabet of coherent states of light with uniform distribution ( $\lambda = 0$  in Eq.8.10) has been investigated, and for such a case, Einstein-Podolsky-Rosen (EPR) Gaussian steering (see Paragraph 1.1.3), i.e. steerability of a Gaussian state by Gaussian measurement,

$$\mathcal{S}_{B \rightarrow A}(V_{AB}) = \max \left\{ 0, \frac{1}{2} \log \left( \frac{\det B}{\det V_{AB}} \right) \right\}, \quad (8.13)$$

$$\mathcal{S}_{A \rightarrow B}(V_{AB}) = \max \left\{ 0, \frac{1}{2} \log \left( \frac{\det A}{\det V_{AB}} \right) \right\}. \quad (8.14)$$

has been identified as the necessary resource to attain secure teleportation, which amounts to reaching  $\bar{F} > \bar{F}_{\text{sec}}^0 = 2/3$  [188]<sup>2</sup>.

In the following we will establish the optimal average fidelity for teleporting an ensemble of coherent states sampled from the distribution Eq.8.10 once the appropriate resource (entanglement, as quantified by the logarithmic negativity, for only certified quantum teleportation, and steering for secure certified quantum teleportation) of the state shared by Alice and Bob is fixed. We will tackle this problem by exploiting the connection between teleportation protocols and phase-covariant single-mode Gaussian channels established above, Eq.8.5. Indeed, given a single-mode phase-covariant Gaussian channel  $\Phi_{x,y} \sim (\sqrt{x}\mathbb{1}, y\mathbb{1})$  one has that the input-output fidelity reads

$$\begin{aligned} \bar{F}^\lambda(x, y) &= \int_{\mathcal{C}} p_{\text{in}}^\lambda(\alpha) \langle \alpha | \Phi_{x,y} (|\alpha\rangle\langle\alpha|) |\alpha\rangle d^2\alpha = \\ &= \frac{2\lambda}{2(1 - \sqrt{x})^2 + \lambda(1 + y + x)}. \end{aligned} \quad (8.15)$$

We will therefore determine what phase-covariant Gaussian channels can be implemented through a teleportation protocol when the state shared by

<sup>2</sup> Non-Gaussian cloners can lead to a slightly higher single-clone fidelity for  $\lambda = 0$ , given by  $\approx 0.6826$  [191].

Alice and Bob is finitely resourceful (i.e. has finite entanglement or finite steerability), and then optimize the above over these sets of channels.

## 8.2 OPTIMAL CERTIFIED QUANTUM TELEPORTATION

### 8.2.1 Phase-insensitive channels implementable with finite entanglement

The problem of determining the set of implementable phase-covariant channels through a teleportation protocol exploiting a resource with finite entanglement can be reformulated as follows: given an arbitrary phase-covariant single-mode Gaussian channel  $\Phi_{x,y}$ , what two-mode Gaussian states, with the minimum amount of entanglement (quantified by the logarithmic negativity  $\mathcal{N}$ ) necessary, can be used as a resource to simulate the corresponding channel? A similar problem, but using a different entanglement measure, has been addressed in [180, 192], but, as we are about to see, the solution proposed therein is unrealistic in an experimental setting.

A constraint on the implementable channels which can be simulated is given by the fact that the entanglement  $\mathcal{N} = 2r$  of the resource state of the teleportation protocol is the maximum entanglement which can be distilled by means of Gaussian Local Operations and Classical Communication (GLOCC) [174]. Therefore, if Alice wants to pass part of a maximally entangled state to Bob through a teleportation protocol which simulates the channel  $\Phi_{x,y}$ , the entanglement of the output state  $\mathcal{N}_{\text{out}} = \max\{0, -\log \frac{y}{1+x}\} = \mathcal{N}^{(\text{Choi})}$ , where  $\mathcal{N}^{(\text{Choi})}$  is the entanglement of the Choi state associated with the channel Eq.1.14, cannot be greater than the entanglement initially shared by Alice and Bob:  $\mathcal{N}^{(\text{Choi})} \leq 2r$ . Hence, they can simulate  $\Phi_{x,y}$  only if

$$y \geq e^{-2r}(1+x) \quad \text{with} \quad y \geq |1-x|. \quad (8.16)$$

This identifies the region of Gaussian channels implementable with  $2r$  units of entanglement; or equivalently, the channels that, when applied locally to one mode of a two-mode system, always lead to an output with  $\mathcal{N}_{\text{out}} \leq 2r$ . This generalises the entanglement-breaking condition [193]

$$y \geq (1+x) \quad \text{with} \quad y \geq |1-x|. \quad (8.17)$$

Any channel satisfying Eq.8.17 applied on a single mode of a two-mode bipartite entangled state, will output a separable state.

In [174, 180] it has been shown that any channel  $\Phi_*$  saturating Eq.8.16 could be simulated through a teleportation protocol, with gain  $g = \sqrt{x}$ , which uses the Choi-state of the channel itself as a resource. Yet, continuous variable Choi states have infinite energy, and they are thus unrealistic for any practical purpose.

Here we find that there exists a class of resource states with finite energy such that, setting the gain of the protocol  $g = \sqrt{x}$ , allow to implement any channel  $\Phi_* \sim (\sqrt{x}\mathbb{1}, e^{-2r}(1+x)\mathbb{1})$  with the exclusion of only two points, i.e. the quantum limited attenuator and amplifier. These states in standard form Eq.8.4 have been determined by fixing  $c$  such that  $\mathcal{N} = 2r$ , and  $a$  such that  $y$  as in Eq.8.5 is equal to the right-hand-side of Eq.8.16:

$$a = \frac{b + e^{-2r}(x-1)}{x}, \quad c = \frac{b - e^{-2r}}{\sqrt{x}}, \quad b \geq \frac{xe^{2r} + e^{-2r} - |x-1|}{x+1 - e^{2r}|x-1|}, \quad (8.18)$$

where the condition on  $b$  is necessary to ensure that  $V_{AB} > i\Omega_2$ . All these states, for  $x > \tanh r$ , have finite energy, and between them we choose those with minimal mean energy per mode  $\bar{n}_{AB}$  which is, recalling from Eq.2.41,

$$\bar{n}_{AB} = \frac{\langle \sum_{k=1,2} \hat{a}_k^\dagger \hat{a}_k \rangle}{2} = \frac{a + b - 2}{4}, \quad (8.19)$$

given by the value of  $b$  which saturates the inequality in Eq.8.18. These are asymmetric squeezed thermal states with a unit symplectic eigenvalue and maximal  $\mathcal{N}$  among all two-mode Gaussian states with the same marginals  $a, b$  [194, 195]. As already mentioned, when the channel is the quantum limited attenuator ( $x = \tanh r, y = 1 - \tanh r$ ) or the quantum limited amplifier ( $x = \coth r, y = \coth r - 1$ ), the lower bound on  $b$  (and hence  $a$ ) of Eq.8.18 diverges, meaning that we cannot implement such channels with a teleportation protocol exploiting a resource with  $\mathcal{N} = 2r$  and finite energy.

### 8.2.2 Optimal teleportation fidelity

We know now that to find the optimal achievable average teleportation fidelity we just need to maximize Eq.8.15 over  $x$  and  $y$  such that Eq.8.16 is satisfied. One immediately sees from Fig.8.2 that this happens for one of

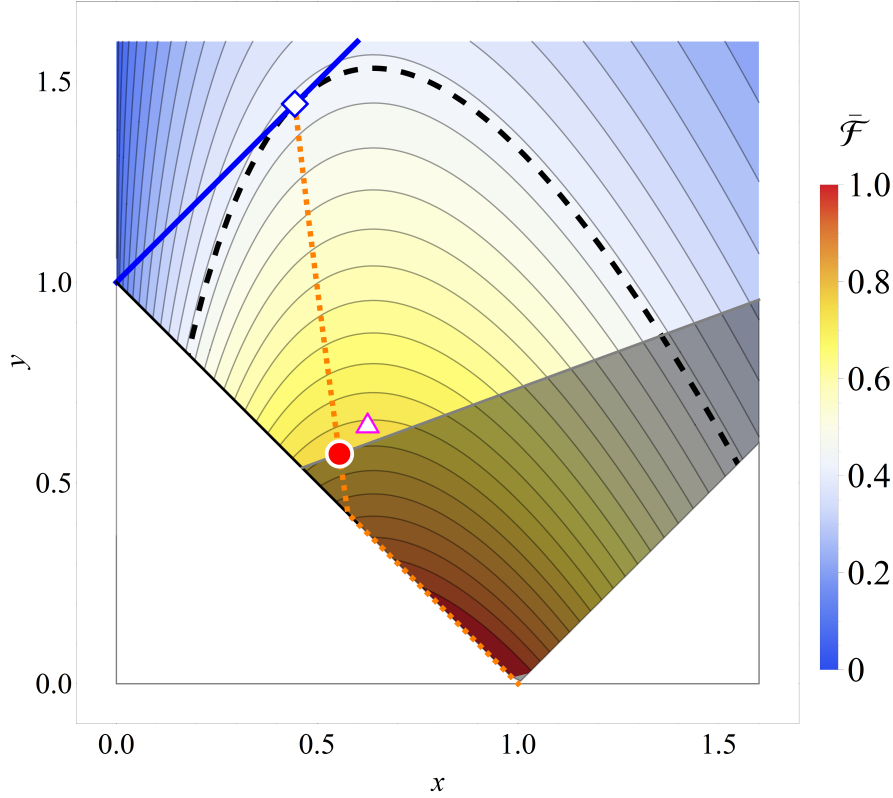


Figure 8.2.: Diagram of single-mode phase-covariant Gaussian channels in the  $(x, y)$  plane. The white area corresponds to the unphysical channels region  $y < |1 - x|$ . The contour plot corresponds to the average input-output fidelity, Eq.8.15, of an ensemble of coherent states Eq.8.10 subject to phase insensitive channel  $\Phi_{x,y}$ . The black dashed line represents the certified quantum teleportation threshold, defined by  $\bar{F}^\lambda(x, y) = \bar{F}_{\text{cl}}^\lambda$ . The shaded gray area represents the region of channels which cannot be implemented by teleportation protocols exploiting resource with finite entanglement  $\mathcal{N} = 2r$ , i.e. the complementary region of Eq.8.16. Channels above the blue line are entanglement-breaking, Eq.8.17. The big red circle corresponds to the optimal teleportation scheme. The diamond represents the best classical strategy. The triangle corresponds to the teleportation scheme which uses a TMSV state with entanglement  $\mathcal{N}$ . The orange dotted line represents the channels achievable through the optimal teleportation scheme by varying the entanglement parameter  $r \in [0, \infty)$ . The parameters used for this plot are  $r = \lambda = 1/2$ . All the plotted quantities are dimensionless.

the channels on the boundary of the region Eq.8.16. Setting  $y = e^{-2r}(1 + x)$ , inserting this into Eq.8.15 and maximizing over  $x$  one finds

$$x_{\text{opt}} = \max \left\{ \tanh r, \frac{e^{2r}}{(e^r + \lambda \cosh r)^2} \right\}. \quad (8.20)$$

The corresponding optimal average fidelity finally reads:

$$\bar{F}_{\text{opt}}^\lambda(r) = \begin{cases} \frac{\lambda}{\lambda + (1 - \sqrt{\tanh r})^2}, & \tanh r \geq \frac{e^{2r}}{(e^r + \lambda \cosh r)^2} \\ \frac{e^r(1 + \lambda + \tanh r)}{2e^r + \lambda \cosh r}, & \text{otherwise} \end{cases} \quad (8.21)$$

This fidelity can be achieved by using the resource state of Eq.8.18 with  $x = x_{\text{opt}}$  and  $y = e^{-2r}(1 + x_{\text{opt}})$ . However, for  $\tanh r \geq \frac{e^{2r}}{(e^r + \lambda \cosh r)^2}$ , i.e. the first case in Eq.8.21, the optimal channel is the quantum limited attenuator for which the needed energy diverges as previously noticed. In any other case, the optimal fidelity can be achieved with finite mean energy resources.

We will consider now some particular cases, showing that, thanks to our protocol, we can recover some known results.

The first case we consider is the one with  $r = 0$ , i.e. Alice and Bob share no entanglement, for which one gets (diamond marker in Fig.8.2)

$$\begin{aligned} x_{\text{opt}}^\lambda &= \frac{1}{(1 + \lambda)^2}, \quad y_{\text{opt}}^\lambda = 1 + x_{\text{opt}}^\lambda, \\ \bar{F}_{\text{opt}}^\lambda(0) &= \frac{1 + \lambda}{2 + \lambda} = \bar{F}_{\text{cl}}^\lambda. \end{aligned} \quad (8.22)$$

The gain is set to be  $g_{\text{opt}} = \frac{1}{1 + \lambda}$  and the resource state reduces to the two-mode vacuum. Hence, the optimal strategy in this case is equivalent to a heterodyne detection at Alice's site followed by the appropriate displacement at Bob's site. This is exactly the optimal classical strategy mentioned above.

The second interesting known case is when  $\lambda \rightarrow 0$ , which is the teleportation of an alphabet of coherent states uniformly distributed, for which one obtains

$$\begin{aligned} x_{\text{opt}}^0 &= 1, \quad y_{\text{opt}}^0 = 2e^{-2r}, \\ \bar{F}_{\text{opt}}^0(r) &= \frac{1}{1 + e^{-2r}}, \end{aligned} \quad (8.23)$$

consistent with the results obtained in Refs. [196, 197]. The resource state reduces to a TMSV state used in the original BK protocol.

In general, for arbitrary values of  $\lambda$  and  $r$ , one may compare the fidelity of the optimal teleportation strategy derived above, Eq.8.21, with the fidelity of the usual BK protocol (which uses TMSV states) with optimized gain

$g$  [178, 182–184]. Plugging Eqs.8.5 for a TMSV, i.e.  $a = b = \cosh 2r$  and  $c = \sinh 2r$ , into Eq.8.15 and optimizing over  $x = g^2$  one obtains (triangle in Fig.8.2)

$$\bar{\mathcal{F}}_{\text{TMSV}}^\lambda(r) = \frac{\text{sech}^2 r + \lambda}{2 + \lambda - 2 \tanh r}, \quad (8.24)$$

for  $g_{\text{opt}} = (2 + \lambda \sinh 2r) / (2 + \lambda + \lambda \cosh 2r)$ . One sees that a teleportation protocol exploiting a TMSV never achieves the performances of the optimal strategy, despite always beating the classical benchmark. Indeed, one has  $\bar{\mathcal{F}}_{\text{opt}}^\lambda(r) \geq \bar{\mathcal{F}}_{\text{TMSV}}^\lambda(r) \geq \bar{\mathcal{F}}_{\text{cl}}^\lambda$ , where the first inequality is saturated for  $\lambda \rightarrow 0$ . The whole chain of inequalities is saturated for  $r = 0$ . Therefore, keeping fixed the entanglement as the limited resource to implement a teleportation protocol of a nonuniform Gaussian distribution of pure coherent states, pure TMSV states are suboptimal. However, let us remark that TMSV states may still represent an experimentally practical solution when  $\tanh r \geq e^{2r} / (e^r + \lambda \cosh r)^2$  (see Eq.8.21) since their energy is finite, on the contrary to the optimal state Eq.8.18 whose energy diverges.

Regarding this final observation, it is natural to ask how much entanglement  $\mathcal{N}' = 2r'$  is necessary to simulate a quantum limited attenuator,  $x = \tanh r$  and  $y = e^{-2r}(1 - \tanh r)$  for which our optimal state with  $\mathcal{N} = 2r$  has infinite energy, using a TMSV state instead,  $a = b = \cosh 2r'$  and  $c = \sinh 2r'$ . From Eq.8.5, setting  $g = \sqrt{\tanh r}$  and  $y = e^{-2r}(1 + \tanh r)$ , one gets

$$\mathcal{N}' = \mathcal{N} + \log \left( 1 + \sqrt{1 - e^{-4r}} \right) \geq \mathcal{N}, \quad (8.25)$$

which means that it is still possible to simulate the quantum limited attenuator with finite energy provided that we have more entanglement. In the limiting case  $r = 0$  one finds  $\mathcal{N}' = \mathcal{N}$ .

### 8.3 OPTIMAL CERTIFIED SECURE QUANTUM TELEPORTATION

Following the same line of what done in the previous section we will here consider the following problem: given a finite amount of EPR Gaussian steering available as a resource between Alice and Bob, what is the best possible protocol they can implement to achieve optimal secure teleportation of an ensemble, Eq.8.10, of coherent states?

In order to answer this question we will first determine which single-mode phase-covariant Gaussian channels can be simulated with finite steerability, then we will exploit these results to derive the optimal average fidelity for secure teleportation as a function of the available steering.

### 8.3.1 Phase-insensitive channels implementable with finite steerability

Given an arbitrary single-mode phase-covariant Gaussian channel  $\Phi_{x,y} \sim (x\mathbb{1}, y\mathbb{1})$ , with  $x$  and  $y$  constrained by Eq.2.89, we want to find the two-mode Gaussian resource state with a minimum amount of steerability, and possibly finite mean energy, described by a covariance matrix  $V_{AB}$ , Eq.8.1, which can be used in a continuous variable teleportation protocol to simulate the corresponding channel. As for the finite entanglement case, not all phase-covariant channels can be implemented through a teleportation protocol for fixed Gaussian steerability (in either direction) Eqs.8.13-8.14. Again, a constraint on the implementable channels is given by the fact that, as entanglement, also steerability is monotonically nonincreasing under GLOCC [198], and cannot be distilled by means of such operations. The reasoning, analogous to the one done in Paragraph 8.2.1, makes us conclude that given a resource state specified by a covariance matrix  $V_{AB}$  with steerability degrees  $\mathcal{S}_{B \rightarrow A}(V_{AB}) = s_{ba}$  and  $\mathcal{S}_{A \rightarrow B}(V_{AB}) = s_{ab}$ , the single-mode phase-covariant Gaussian channels  $\Phi_{x,y}$  which could be implemented through a continuous variable teleportation protocol are those satisfying [199]

$$\Phi_{x,y} \quad \text{s.t.} \quad \begin{cases} y \geq e^{-s_{ba}} x \\ y \geq e^{-s_{ab}} \end{cases} \quad \text{with} \quad y \geq |1 - x|. \quad (8.26)$$

The above are a generalization of the regions of  $A \rightarrow B$ , and  $B \rightarrow A$ , steerability-breaking channels, i.e. those channels which acting on a single mode of a bipartite state  $\sigma_{AB}^{(\text{in})}$  give a non-steerable (by Gaussian measurements) from  $B \rightarrow A$ , and  $A \rightarrow B$ , output respectively. The inequalities in Eq.8.26 determine indeed those channels such that  $\mathcal{S}_{B \rightarrow A}(\mathbb{1} \otimes \Phi_{x,y}[\sigma_{AB}^{(\text{in})}]) \leq s_{ba}$  and  $\mathcal{S}_{A \rightarrow B}(\mathbb{1} \otimes \Phi_{x,y}[\sigma_{AB}^{(\text{in})}]) \leq s_{ab}$ , respectively. The steerability-breaking region is found by setting  $s_{ba} = s_{ab} = 0$  in Eq.8.26.

Again, we have that any Gaussian channel may be implemented through a teleportation protocol which uses as a shared resource the infinite-energy

Choi state of the channel itself. However, we can construct realistic classes of Gaussian resource states with minimum one-way steerability degree ( $A \rightarrow B$  or viceversa) equal to the one-way steerability of the Choi state and finite mean energy, which allows to simulate all phase insensitive channels saturating one of the boundaries of Eq.8.26, with the only exceptions of the quantum limited attenuator and amplifier.

*Optimal resources with fixed  $B \rightarrow A$  steerability*

The two-mode resource states for teleportation simulation with fixed  $s_{ba}$ , in standard form Eq.8.4, that allow to implement a phase-covariant channel  $\Phi_*$  with  $y = e^{-s_{ba}}x$  are determined by fixing  $b$  such that  $\mathcal{S}_{B \rightarrow A}(V_{AB}) = s_{ba}$  and then  $c$  such that  $y = g^2a - 2gc + b = e^{-s_{ba}}x$ , with  $g^2 = x$ :

$$b = x(a - e^{-s_{ba}}), \quad c = (a - e^{-s_{ba}})\sqrt{x}, \quad a \geq \max\{a_+, a_-\}, \quad (8.27)$$

with

$$a_{\pm} = \frac{e^{s_{ba}} + x(e^{-s_{ba}} \pm 1)}{e^{s_{ba}}(\pm x \mp 1) + x}, \quad (8.28)$$

where the condition on  $a$  is necessary to ensure  $V_{AB} \geq i\Omega_2$ . This lower bound on  $a$  diverges only at the points  $(x = \frac{1}{1+e^{-s_{ba}}}, y = \frac{1}{1+e^{s_{ba}}})$  corresponding to the quantum limited attenuator, and  $(x = \frac{1}{1-e^{-s_{ba}}}, y = \frac{1}{e^{s_{ba}}-1})$ , corresponding to the quantum limited amplifier. Within this class of states we choose those with the minimal mean energy per mode, given by the value of  $a$  which saturates the inequality in Eq.8.27. Also these states, as the class of states Eq.8.18, are two-mode asymmetric squeezed-thermal states with a unit symplectic eigenvalue.

The steerability from  $A$  to  $B$  of these states is

$$s_{ab} = -\log \left( \frac{e^{-2s_{ba}}(a e^{s_{ba}} - 1)x}{a} \right), \quad (8.29)$$

which is a decreasing function of the parameter  $a$ . This means that within the family of states of Eq.8.27, for a fixed  $B \rightarrow A$  steerability  $s_{ba}$ , the least energetic state is the one with the maximum  $A \rightarrow B$  steerability. Conversely, the state with the minimum steerability from  $A$  to  $B$ ,  $s_{ab} = s_{ba} - \log x$ , within the same family, has infinite mean energy. In this latter case, the simulated channel lies at the intersection of the boundary lines  $y = e^{-s_{ab}}$

and  $y = e^{-s_{ba}}x$ , delimiting the region of implementable channels according to Eq.8.26.

#### *Optimal resources with fixed $A \rightarrow B$ steerability*

If we consider now the case of fixed steerability from  $A$  to  $B$ ,  $\mathcal{S}_{A \rightarrow B}(V_{AB}) = s_{ab}$ , the class of states we are looking for is

$$b = ax + e^{-s_{ab}}, \quad c = a\sqrt{x}, \quad a \geq \max\{a_+, a_-\}, \quad (8.30)$$

with

$$a_{\pm} = \left[ x \left( \frac{1}{e^{s_{ab}} \pm 1} \mp 1 \right) \pm 1 \right]^{-1}. \quad (8.31)$$

Also in this case, the state with the minimal mean energy per mode is the one given by the value of  $a$  which saturates the inequality in Eq.8.30, and the lower bound for the coefficient  $a$  diverges only at the points, corresponding to a quantum limited attenuator,  $(x = 1 - e^{-s_{ab}}, y = e^{-s_{ab}})$ , and  $(x = 1 + e^{-s_{ab}}, y = e^{-s_{ab}})$ , corresponding to the quantum limited amplifier.

The steerability from  $B$  to  $A$  of these states

$$s_{ba} = -\log \left( \frac{a}{a e^{s_{ab}} x + 1} \right), \quad (8.32)$$

is a decreasing function of  $a$ . Analogously to the previous case, choosing the least energetic state in the family Eq.8.30 is equivalent to choosing the state with maximal steerability from  $B$  to  $A$ . On the other hand, for  $a \rightarrow \infty$  we have that the  $B \rightarrow A$  steerability takes its minimum value  $s_{ba} = s_{ab} + \log x$ .

#### 8.3.2 *Optimal fidelity*

To find the optimal teleportation fidelity for a teleportation protocol which exploit a state with finite one-way steerability, we can maximize Eq.8.15 over the channels Eq.8.26. One immediately sees, from Fig.8.3, that the wanted channels lie on the boundary  $\max\{e^{-s_{ab}}, e^{-s_{ba}}x\}$ . Before proceeding with this optimization, we take a moment to make a few considerations about the secure teleportation threshold.

As shown in Fig.8.3, were we contour plot the fidelity Eq.8.15 in the  $(x, y)$  plane, we see that the contour line  $\tau_{\text{th}}^{\lambda}(x) = \{(x, y) \text{ s.t. } F^{\lambda}(x, y) = F_{\lambda}^{(s)}\}$ ,

defining the secure teleportation threshold, is tangent to the line  $y = x$  (recall that  $y = x$  is the  $B \rightarrow A$  steerability-breaking line) for  $\lambda < \sqrt{2} - 1$ , and intersects with it in  $(x = 1/2, y = 1/2)$  for  $\lambda \geq \sqrt{2} - 1$ . The tangent point  $(x = (1 + \lambda)^{-2}, y = (1 + \lambda)^{-2})$  for  $\lambda < \sqrt{2} - 1$ , and the point  $(x = 1/2, y = 1/2)$  for  $\lambda \geq \sqrt{2} - 1$ , correspond then to the best channels Alice and Bob can simulate through a teleportation protocol when sharing a resource with vanishing  $s_{ba}$ . This shows that the  $B \rightarrow A$  steerability of the resource state shared by Alice and Bob, Eq.8.13, is a meaningful, necessary resource for optimal secure teleportation of coherent states of light.

Interestingly, we notice that the benchmark Eq.8.12 is defined as a piecewise function with the first branch holding for  $\lambda < \sqrt{2} - 1$ : this is the case for which the best implementable channel with vanishing  $B \rightarrow A$  steerability lies on the line  $y = x$  with  $x > 1/2$ . The second branch of Eq.8.12, corresponds to the case of the quantum limited attenuator  $(x = 1/2, y = 1/2)$  being the best implementable cloning channel.

On the other hand, the secure teleportation threshold curve is not tangent to  $y = 1$ , delimiting the region of  $A \rightarrow B$  steerability-braking channels, meaning that  $s_{ab}$  must have a finite value in order to achieve secure teleportation. Indeed we find that one must have at least

$$s_{ab}^{\min} = \begin{cases} \log\left(\frac{1}{2}(1 + \lambda)(2 + \lambda)\right), & 0 \leq \lambda < \sqrt{2} - 1; \\ \log\left(\frac{\lambda}{\lambda + 2} + \frac{3 - 2\sqrt{2}}{\lambda}\right)^{-1}, & \sqrt{2} - 1 \leq \lambda < 2(\sqrt{2} - 1); \\ \log(2), & \lambda \geq 2(\sqrt{2} - 1), \end{cases} \quad (8.33)$$

$A \rightarrow B$  steerability to beat the benchmark. This confirms the observation, originally made in [190] for the case  $\lambda \rightarrow 0$ , that secure teleportation of coherent states requires EPR steering in both directions. The first branch in Eq.8.33 corresponds to the first branch of the benchmark Eq.8.12. The second branch in Eq.8.33 correspond to the second branch in Eq.8.12 up to  $\lambda = 2(\sqrt{2} - 1)$  where the threshold curve  $\tau_{\text{th}}^{\lambda}(x)$  has the last stationary point  $x_0$ ,  $\partial\tau_{\text{th}}^{\lambda}(x)/\partial x|_{x_0} = 0$ , into the CP region  $y > |1 - x|$ ; hence, for  $\lambda \geq 2(\sqrt{2} - 1)$ , the  $B \rightarrow A$  steerability-breaking line,  $y = e^{-s_{ab}^{\min}} = 1/2$  and  $\tau_{\text{th}}^{\lambda}(x)$ , both intersect at the quantum limited attenuator point  $(1/2, 1/2)$  (see Fig.8.4).

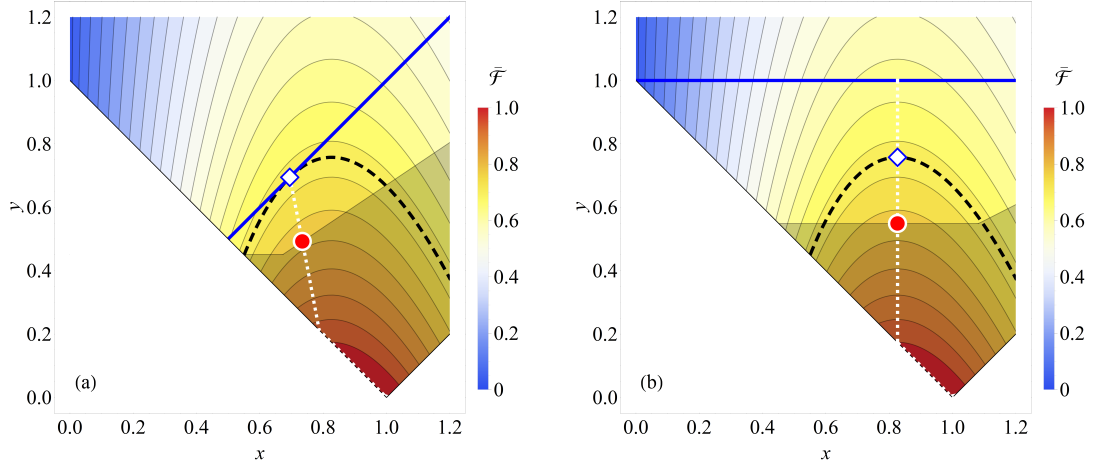


Figure 8.3.: Diagram of single-mode phase-covariant Gaussian channels in the  $(x, y)$  plane. White area and contour plot as in Fig.8.2. The black dashed line represents the certified secure quantum teleportation threshold  $\tau_{\text{th}}^\lambda(x)$  as defined in the text. The shaded gray areas represent the region of channels, complementary to the region Eq.8.26, which cannot be implemented by teleportation protocols exploiting resource with (left panel) finite  $B \rightarrow A$  steerability, (right panel) finite  $A \rightarrow B$  steerability. The channels above the blue lines correspond to the (left panel)  $B \rightarrow A$  steerability-breaking and (right panel)  $A \rightarrow B$  steerability-breaking channels. The diamonds correspond to the best implementable teleportation scheme at the boundary of the secure teleportation region, i.e. with (left panel) vanishing  $B \rightarrow A$  steerability, (right panel)  $s_{ab} = s_{ab}^{\min}$   $A \rightarrow B$  steerability. The red circles represent the optimal teleportation schemes for (left panel) finite  $B \rightarrow A$  steerability and (right panel) finite  $A \rightarrow B$  steerability. The white dotted line represents the channels achievable through the optimal teleportation scheme by varying the considered resource  $s_{ab(ba)} \in [0, \infty)$ . The parameters used for the plots are  $\lambda = 0.2$ , (left panel)  $s_{ba} = 0.4$ , (right panel)  $s_{ab} = 0.6$ . All the plotted quantities are dimensionless.

Now, let us suppose that we fix the  $B \rightarrow A$  steerability to be  $s_{ba}$ . Thanks to the results in the previous section, we look for the optimal resource state within the class Eq.8.27, which would allow Alice and Bob to maximise the average fidelity and beat the no-cloning threshold. This maximisation is done by determining the channel  $\Phi_{x,y}$  with  $x$  and  $y$  such that the line  $y = e^{-s_{ba}}x$  is tangent to the contour line of the average fidelity Eq.8.15, and preparing the corresponding resource state, given by Eq.8.27. With some simple geometry one finds:

$$x_{\text{opt}}^\lambda(s_{ba}) = \max \left\{ \frac{4e^{2s_{ba}}}{[\lambda + e^{s_{ba}}(2 + \lambda)]^2}, \frac{1}{1 + e^{-s_{ba}}} \right\}, \quad (8.34)$$

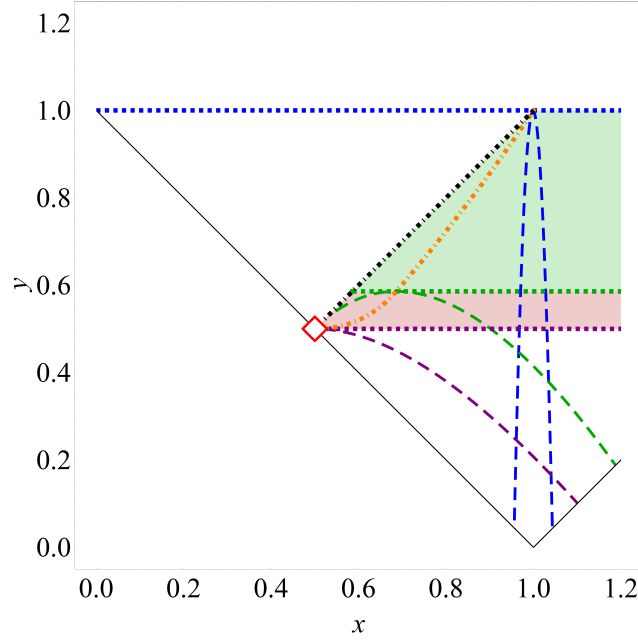


Figure 8.4.: Phase-insensitive Gaussian channels  $(x, y)$  plane. The thin black line delimits the physical region Eq.2.89. Blue dotted and black dot-dashed lines delimits the  $A \rightarrow B$  and  $B \rightarrow A$  steerability-breaking regions, respectively. The black dot-dashed line also represents the best cloning strategies for vanishing  $s_{ba}$  and  $\lambda \in [0, \sqrt{2} - 1)$ . The orange dot-dashed line represents the best cloning strategies for  $s_{ba} = s_{ba}^{\min}$  and  $\lambda \in [0, 2(\sqrt{2} - 1))$ . The green-shaded and the pink-shaded region correspond to the regions spanned by the line  $e^{-s_{ab}^{\min}}$  for  $s_{ab}^{\min}$  as defined in the first and second branches of Eq.8.33, respectively. The green and purple dotted lines corresponds to  $e^{-s_{ab}^{\min}}$  for  $\lambda = \sqrt{2} - 1$  and  $\lambda = 2(\sqrt{2} - 1)$ , respectively. The blue, green and purple dashed lines represent the secure teleportation benchmarks  $\tau_{\text{th}}^{10^{-3}}$ ,  $\tau_{\text{th}}^{\sqrt{2}-1}$ ,  $\tau_{\text{th}}^{2(\sqrt{2}-1)}$ , respectively. The diamond corresponds to the best cloning strategy for vanishing  $s_{ba}$  and  $\lambda > \sqrt{2} - 1$  and the best Gaussian cloning strategy for  $s_{ba} = s_{ba}^{\min}$  for  $\lambda \geq 2(\sqrt{2} - 1)$ . All the plotted quantities are dimensionless.

which yields the optimal average fidelity at fixed  $s_{ba}$ :

$$\bar{\mathcal{F}}_{\text{opt}}^{\lambda}(s_{ba}) = \begin{cases} \frac{2[\lambda + e^{s_{ba}}(2 + \lambda)]}{2 + \lambda + e^{s_{ba}}(4 + \lambda)}, & \lambda \leq \tilde{\lambda}; \\ \frac{\lambda(e^{s_{ba}} + 1)}{1 + \lambda + e^{s_{ba}}(2 + \lambda - 2\sqrt{e^{-s_{ba}} + 1})}, & \text{otherwise,} \end{cases} \quad (8.35)$$

$$\text{with } \tilde{\lambda} = \frac{2(\sqrt{1 + e^{-s_{ba}}} - 1)}{1 + e^{-s_{ba}}}.$$

If, on the other hand, we fix the  $A \rightarrow B$  steerability to be  $s_{ab} > s_{ab}^{\min}$ , with an analogous geometric reasoning to the above, one finds

$$x_{\text{opt}}^\lambda(s_{ab}) = \max \left\{ \frac{4}{(2 + \lambda)^2}, 1 - e^{-s_{ab}} \right\}, \quad (8.36)$$

yielding

$$\bar{F}_\lambda^{\text{opt}}(s_{ab}) = \begin{cases} \frac{2e^{s_{ab}}(2 + \lambda)}{2 + \lambda + e^{s_{ab}}(4 + \lambda)}, & \lambda \leq 2 \left( \sqrt{\frac{e^{s_{ab}}}{e^{s_{ab}} - 1}} - 1 \right); \\ \frac{\lambda}{\lambda + \left( \sqrt{1 - e^{-s_{ab}}} - 1 \right)^2}, & \text{otherwise.} \end{cases} \quad (8.37)$$

For any  $\lambda$ , the optimal average fidelity  $\bar{F}_\lambda^{\text{opt}}(s_{ab})$  Eq.8.37 is a monotonically increasing function of  $s_{ab}$  and is larger than the secure teleportation benchmark  $F_\lambda^{(s)}$  as soon as  $s_{ab} > s_{ab}^{\min}$ , reducing to the latter threshold exactly when  $s_{ab} = s_{ab}^{\min}$ . Moreover, notice that the resource states of Eq.8.30 always have  $s_{ba} > 0$  when  $s_{ab} > s_{ab}^{\min}$ . More generally,  $\mathcal{S}_{A \rightarrow B}(V_{AB}) > \log(2)$  implies  $\mathcal{S}_{B \rightarrow A}(V_{AB}) > 0$  for any two-mode Gaussian state with covariance matrix  $V_{AB}$  [200], confirming once again that two-way steerability is required for a certified secure teleportation of coherent states of light.

#### 8.4 REMARKS

We solved the long-standing problem of determining the optimal Gaussian protocols for certified and certified secure quantum teleportation of coherent states sampled from a Gaussian distribution with finite variance, exploiting resources with finite entanglement and finite one-way Gaussian steerability. In order to perform this optimization, we devised a way to construct classes of states which allow to implement teleportation protocols for simulating single-mode phase-covariant Gaussian channels employing the minimum amount of entanglement or one-way steerability. With the only exceptions of the quantum limited attenuator and amplifier, these classes of states have finite energy and are thus quite suitable for practical applications in quantum communication.



---

## CONCLUSIONS

---

We finally reached the end of this thesis. We explored different scenarios, involving both discrete and continuous variables quantum systems, and tried to answer questions about the performance of several quantum protocols in non-ideal, noisy and/or resource-limited situations.

In the first original Chapter, Chapter 4, we studied a simple coherent feedback cooling protocol aimed at reducing entropy and average energy of an ensemble of thermal qubits by exploiting an ancillary ensemble of purer qubits, part of the so-called controller. We defined some figures of merit which allowed us to quantify the efficiency of the protocol. Interestingly, from our information-theoretical analysis we noticed that there is a strong connection between the optimal working point, obtained by optimizing the efficiency, and the quantum correlations, quantified by the quantum discord, shared by target and controller: indeed, we noticed that maximizing the efficiency of the protocol at a fixed cooling load, i.e. the entropy reduction of the target, is equivalent to the maximization of the quantum discord of the system-ancilla state. It is worth noticing that this happens also in the case in which, because of the initial mixedness of the target system and the ancilla, it is not possible to create entanglement between target and controller.

In Chapter 5 we showed how, by considering different limiting resources in a frequency estimation protocol, one obtains different notions of optimality. In particular, by putting a cap on the total amount of time available for the estimation, the efficiency in presence of time-inhomogeneous noise can give a super-extensive scaling with the size of the probe, namely the Zeno scaling, even when starting from an ensemble of thermal probes, implying that the most efficient strategy consists in correlating a huge number of qubits in a GHZ-diagonal state. On the contrary, if one considers energy, instead of time, as the scarce resource, preparing the probe in large correlated GHZ-diagonal states results very inefficient.

We then tackled the problem of estimating multiple parameters using Gaussian states, Chapter 6. In particular, we derived general formulae to assess the ultimate achievable precision when trying to estimate simultaneously multiple parameters encoded in a multimode Gaussian state. The main original result of this Chapter is the compact analytical formula for the so-called ‘measurement-compatibility matrix’ whose evaluation is necessary to determine whether the Cramèr-Rao bound can be asymptotically saturated. We applied our general results to the practical estimation of three parameters in noisy optical interferometry (a phase difference between the two arms of the interferometer and two parameters characterizing a generic phase-covariant Gaussian channel) using two-mode displaced squeezed Gaussian states. We found that by displacing by the same magnitude the two momentum quadratures of the probe state, the measurement compatibility condition is always satisfied.

In the following Chapter, Chapter 7 we focused predominantly on a novel classification of time-continuous Gaussian channels according to their divisibility properties. We identified three degrees of Gaussian non-Markovianity: Markovian, strong and weak non-Markovian. A strongly non-Markovian dynamics corresponds to a violation of the divisibility of the Gaussian map describing it, i.e. at some point during the evolution, the infinitesimal intermediate map is non-positive. On the other hand, a weakly non-Markovian Gaussian process is characterized by a positive but not completely positive infinitesimal intermediate map at some time during the evolution. We then gave an operational interpretation of this non-Markovianity degree for single-mode Gaussian channels. In particular, we showed that non-Markovian dynamics is related to instantaneous attenuation or amplification of a Gaussian state beyond the quantum limited performance, a signature of memory effects affecting the dynamics.

Finally, in Chapter 8, we studied a protocol to teleport coherent states of light sampled from a Gaussian distribution with finite variance. We found the states that can be used to implement any phase-covariant Gaussian channels with the minimum amount of entanglement or steerability necessary. Thanks to this result, we solved the so-far open problem of determining the optimal Gaussian protocols for certified and certified secure teleportation when the resource states available have finite entanglement or one-way

steerability. Quite interestingly, the optimal states we found are asymmetric squeezed thermal states and, most importantly, have finite energy.

To conclude, it is becoming more and more important to characterize the performance of quantum technologies, and this thesis tried to provide a few instances. It is out of question that this is just a drop in the ocean and much more has to be done. Many are the questions still open, even if we just consider the simple cases studied and presented here: are quantum correlations beyond entanglement a true resource for cooling protocols or, more generally, for quantum feedback control tasks? Is it possible to develop a more general framework for efficient frequency estimation protocols which can be adapted to the most stringent limitations in realistic experimental setups? Could other multipartite quantum states, alternative to GHZ-diagonal, give a more energetically favourable scaling of the mean square error on the frequency estimate with the number of probes? How would the figures of merit assessing the efficiency of a given quantum protocol change when taking into account the thermodynamic-informational cost of measurements? Can we devise new algorithms, or tailoring existing ones, to find optimal Gaussian states which would give the best performance when estimating simultaneously multiple parameters? Can purely weakly non-Markovian Gaussian processes be engineered so that one can fruitfully exploit the instantaneous amplification of Gaussian states? Is it possible to identify finite-energy resource states, to be used in a Gaussian teleportation protocol, to simulate phase-sensitive and possibly multimode Gaussian channels? How would the form of these optimal states change when considering alternative entanglement and Gaussian steerability measures?

The road ahead for a total quantum technological revolution may be long, but the journey is going to be exciting.



Part III.  
Appendices



# A

---

## GAUSSIAN CHANNELS

---

In this Appendix we are going to provide the proofs of Propositions 2.2 and 2.3 enunciated in Chapter 2.

### A.1 PROOF OF PROPOSITION 2.2

*Proof.* The joint Gaussian unitary evolution of an  $m$ -mode Gaussian state, described by covariance matrix  $V$  and first moment vector  $\mathbf{d}$ , with a  $k$ -mode environment with covariance matrix  $V_E$  and displacement vector that, without loss of generality, we can choose to be the null vector  $\mathbf{d}_E = \mathbf{0}_k$ , initially uncorrelated, can be described by a symplectic matrix acting on the system-environment covariance matrix:

$$V \oplus V_E \rightarrow \mathbf{S}(V \oplus V_E)\mathbf{S}^\top, \quad \mathbf{d} \oplus \mathbf{0}_k \rightarrow \mathbf{S}(\mathbf{d} \oplus \mathbf{0}_k) \quad (\text{A.1})$$

We can now rewrite  $\mathbf{S}$  in block form

$$\mathbf{S} = \begin{pmatrix} A & B \\ C & D \end{pmatrix}, \quad (\text{A.2})$$

where  $A$ ,  $B$ ,  $C$ ,  $D$  are  $2n \times 2m$ ,  $2m \times 2k$ ,  $2k \times 2m$  and  $2k \times 2k$  matrices respectively, and, since  $\mathbf{S}$  is symplectic,  $\mathbf{S}\mathbf{\Omega}\mathbf{S}^\top = \mathbf{\Omega}$ , they have to satisfy the following relations:

$$A\mathbf{\Omega}_m A^\top + B\mathbf{\Omega}_k B^\top = \mathbf{\Omega}_m, \quad (\text{A.3})$$

$$A\mathbf{\Omega}_m C^\top + B\mathbf{\Omega}_k D^\top = 0, \quad (\text{A.4})$$

$$C\mathbf{\Omega}_m C^\top + D\mathbf{\Omega}_k D^\top = \mathbf{\Omega}_k. \quad (\text{A.5})$$

The evolved displacement vector for the system is simply  $A\mathbf{d}$ , while the evolved system covariance matrix reads

$$V \rightarrow AVA^\top + BV_E B^\top, \quad (\text{A.6})$$

where it is straightforward to identify  $X = A$  and  $Y = BV_E B^\top$  which is clearly symmetric.

Now, since  $V_E$  describes a physical state, it satisfies the Robertson-Schrödinger relation, which remains true under a congruence transformation

$$BV_E B^\top + iB\Omega_k B^\top = BV_E B^\top + i\Omega_m - iA\Omega_m A^\top \geq 0, \quad (\text{A.7})$$

where we used Eq.A.3, which corresponds to the condition Eq.2.81. Notice that, since  $i\Omega_m - iA\Omega_m A^\top$  is antisymmetric, given any real vector  $v \in \mathbb{R}^{2m}$  one has from eq.A.7

$$v^\top \left( BV_E B^\top + i\Omega_m - iA\Omega_m A^\top \right) v = v^\top BV_E B^\top v \geq 0, \quad (\text{A.8})$$

i.e.  $BV_E B^\top = Y \geq 0$ . □

## A.2 PROOF OF PROPOSITION 2.3

Before proving Proposition 2.3 we will enunciate and prove the following

**Lemma 1.** *Given a real antisymmetric  $2m \times 2m$  matrix  $M = -M^\top$ , there exist an orthogonal transformation  $R \in O(2m)$  such that*

$$RMR^\top = \bigoplus_{i=1}^m d_i \Omega \quad \text{with } d_i \geq 0. \quad (\text{A.9})$$

*Proof. (Lemma)* The matrix  $M^2$  is a symmetric matrix. It exists then an orthogonal matrix  $R \in O(2m)$  that diagonalize it. Let  $x_j$  be a normalized eigenvector of  $M^2$  with eigenvalue  $\lambda_j$ :  $M^2 x_j = \lambda_j x_j$ . Then  $u_j = Mx_j$  is also an eigenvector of  $M^2$  relative to the same eigenvalue  $\lambda_j$  and, given that  $M$  is antisymmetric, it is perpendicular to  $x_j$ :

$$\begin{aligned} M^2 u_j &= M M^2 x_j = \lambda_j M x_j = \lambda_j u_j, \\ x_j^\top u_j &= x_j^\top M x_j = -x_j^\top M x_j = 0. \end{aligned}$$

Therefore  $M^2$  has  $m$  double degenerate eigenvalues and the bi-dimensional eigenspace corresponding to the eigenvalue  $\lambda_j$  is spanned by two vectors  $\{x_j, Mx_j\} = \{x, u\}$ . It is also possible to show that all the eigenvalues are negative:

$$0 \leq u_j^\top u_j = x_j^\top M^\top M x_j = -x_j^\top M^2 x_j = -\lambda_j x_j^\top x_j = -\lambda_j. \quad (\text{A.10})$$

Hence we define  $\lambda_j = -d_j^2$ , with  $0 \leq d_j \in \mathbb{R}$ .

We can then define the orthonormal basis  $\{\mathbf{u}_1/d_1, \mathbf{x}_1, \dots, \mathbf{u}_m/d_m, \mathbf{x}_m\} = \{\tilde{\mathbf{x}}_1, \mathbf{x}_1, \dots, \tilde{\mathbf{x}}_m, \mathbf{x}_m\}$ . The matrix element of  $M$  in such a basis are easily found:

$$\tilde{\mathbf{x}}_i^\top M \mathbf{x}_j = \frac{1}{d_i} \mathbf{x}_i^\top M^\top M \mathbf{x}_j = -\frac{1}{d_i} \mathbf{x}_i^\top M^2 \mathbf{x}_j = \frac{d_j^2}{d_i} \mathbf{x}_i^\top \mathbf{x}_j = d_i \delta_{ij}, \quad (\text{A.11})$$

on the other hand one has  $\mathbf{x}_i^\top M \mathbf{x}_j \equiv 0$  and analogously  $\tilde{\mathbf{x}}_i^\top M \tilde{\mathbf{x}}_j \equiv 0$ , and since  $\tilde{\mathbf{x}}_i^\top M \mathbf{x}_j = -\mathbf{x}_j^\top M \tilde{\mathbf{x}}_i$ , we have shown that

$$\tilde{\mathbf{x}}_i^\top M \mathbf{x}_j = \left( \bigoplus_{k=1}^m d_k \Omega \right)_{ij} \quad \text{with } d_k > 0. \quad (\text{A.12})$$

The orthogonal transformation  $R$  is therefore the matrix whose columns are the normalised eigenvector of  $M^2$ :  $R = (\tilde{\mathbf{x}}_1 \ \mathbf{x}_1 \ \dots \ \tilde{\mathbf{x}}_m \ \mathbf{x}_m)$ .  $\square$

**Proposition A.1.** *Given any pair of  $2m \times 2m$  matrices  $(X, Y)$  such that they satisfy Eq.2.81 and such that  $\text{rank}[Y] = \text{rank}[\Omega - X\Omega X^\top] = 2m$ , one can find a symplectic matrix which describes a joint Gaussian unitary evolution of an  $m$ -mode system with a product of  $m$  thermal states, whose reduced dynamics is given by Eq.2.80.*

*Proof.* From the proof of Prop.2.2 one immediately notice that in order to construct a symplectic matrix as in Eq.A.2 able to describe a reduced dynamics of the first  $m$  modes as in Eq.2.80, one has to impose  $A = X$ . On the other hand, as we are going to show, one has a certain freedom in the choice of  $B$ . Indeed, we have to impose that the matrices  $A$  and  $B$  satisfy Eq.A.3 (since we have fixed the environmental number of modes to  $m$ , we will drop the index from the symplectic form:  $\Omega_m \equiv \Omega$ ) which can be rewritten as

$$B\Omega B^\top = \Omega - A\Omega A^\top. \quad (\text{A.13})$$

We notice that the matrix on the left hand side of the above equation is antisymmetric, hence, because of Lemma 1 we have that there exists  $R \in O(2m)$  such that

$$RB\Omega B^\top R^\top = R(\Omega - A\Omega A^\top)R^\top = \bigoplus_{i=1}^m d_i \Omega, \quad (\text{A.14})$$

with  $d_i > 0$ . We can then choose  $B$  to be

$$B = R^\top \Sigma S, \quad (\text{A.15})$$

with  $\Sigma = \bigoplus_{i=1}^m \sqrt{d_i} \mathbb{1}$  and  $S$  symplectic.

We can then determine the covariance matrix of the environment thanks to the relation  $Y = BV_E B^\top$ :

$$V_E = S^{-1} \Sigma^{-1} R Y R^\top \Sigma^{-1} S^{-\top}. \quad (\text{A.16})$$

It is easy to verify that this covariance matrix satisfies the *bona fide* condition:

$$\begin{aligned} V_E + i\Omega \geq 0 &\Leftrightarrow S^{-1} \Sigma^{-1} R Y R^\top \Sigma^{-1} S^{-\top} + i\Omega \geq 0 \Leftrightarrow \\ &\Leftrightarrow \Sigma^{-1} R Y R^\top \Sigma^{-1} + i\Omega \geq 0 \Leftrightarrow \\ &\Leftrightarrow R Y R^\top + i\Sigma \Omega \Sigma \geq 0 \Leftrightarrow \\ &\Leftrightarrow R(Y + i\Omega - iA\Omega A^\top) R^\top \geq 0 \Leftrightarrow \\ &\Leftrightarrow Y + i\Omega - iX\Omega X^\top \geq 0, \end{aligned}$$

which is true by hypothesis (in the second to last passage we used the fact that from Eqs.A.14,A.15 one has  $\Sigma\Omega\Sigma = R(\Omega - A\Omega A^\top)R^\top$ ).

As previously noticed,  $\Sigma$  and  $R$  are fully determined by the matrix  $X$ , however, the symplectic matrix  $S$  appearing in  $B$ , and hence in  $V_E$ , allows for some freedom. Without loss of generality one can then choose  $S^{-1}$  to be the symplectic transformation which puts  $\Sigma^{-1} R Y R^\top \Sigma^{-1}$  in its Williamson's diagonal form, i.e. one can always choose the environmental state to be a product of  $m$  thermal modes.

So far, we have proven that for all  $X$  and  $Y$  satisfying Eq.2.81 one can construct the matrices  $A$ ,  $B$  and  $V_E$  such that  $X = A$ ,  $Y = BV_E B^\top$ , with  $V_E$  being the covariance matrix of a collection of  $m$  thermal modes, and  $A\Omega A^\top + B\Omega B^\top = \Omega$ . Now, let us consider the  $2m \times 4m$  real matrix

$$(A \ B) = \begin{pmatrix} \mathbf{a}_1^\top & \mathbf{b}_1^\top \\ \vdots & \vdots \\ \mathbf{a}_{2m}^\top & \mathbf{b}_{2m}^\top \end{pmatrix} = \begin{pmatrix} \mathbf{v}_1^\top \\ \vdots \\ \mathbf{v}_{2m}^\top \end{pmatrix}, \quad (\text{A.17})$$

where  $\mathbf{a}_j$  and  $\mathbf{b}_j$  are the vectors forming the rows of the matrices  $A$  and  $B$  respectively. The  $4m$ -dimensional vectors  $\mathbf{v}_j = (\mathbf{a}_j \ \mathbf{b}_j)$ , forming the rows of  $(A \ B)$  are a  $2m$ -set of vectors which verify

$$\mathbf{v}_j^\top \Omega_{2m} \mathbf{v}_k = (\Omega_m)_{jk} = (\Omega_{2m})_{jk}, \quad (\text{A.18})$$

as one can see by rewriting Eq.A.3 as  $(A \ B)\Omega_{2m}(A \ B)^\top$ . From Eq.A.18 it is also clear that the vectors  $\{\mathbf{v}_i\}_{i=1,\dots,2m}$  are linearly independent, indeed,

let us suppose there exists  $\mathbf{v}_k$  such that  $\mathbf{v}_k = \sum_{i \neq k} c_i \mathbf{v}_i$ , then  $\mathbf{v}_j^\top \Omega_{2m} \mathbf{v}_k = \sum_{i \neq k} c_i \mathbf{v}_j^\top \Omega_{2m} \mathbf{v}_i = \sum_{i \neq k} c_i (\Omega_{2m})_{ij} \neq \Omega_{jk}$ , i.e.  $\mathbf{v}_k$  cannot be a linear combination of the other vectors in the set. Eq.A.18 is hence telling us that the set  $\{\mathbf{v}_i\}_{i=1, \dots, 2m}$  is an incomplete symplectic basis of  $\mathbb{R}^{4m}$ . It is always possible to complete this basis with the  $4m$ -dimensional vectors  $\{\mathbf{v}_i\}_{i=2m+1, \dots, 4m}$  constructed as follows: given a  $4m$ -dimensional vector  $\mathbf{y} \in \text{Span}\{\mathbf{v}_i\}_{i=1, \dots, 2m}^\perp$ , one can construct

$$\tilde{\mathbf{v}}_{2m+1} = \mathbf{y} + \sum_{k,l=1}^{2m} (\Omega_{2m})_{kl} \mathbf{v}_l^\top \Omega_{2m} \mathbf{y} \mathbf{v}_k, \quad (\text{A.19})$$

$$\tilde{\mathbf{v}}_{2m+2} = -\Omega_{2m} \tilde{\mathbf{v}}_{2m+1} + \sum_{k,l=1}^{2m} (\Omega_{2m})_{kl} (\mathbf{v}_l^\top \tilde{\mathbf{v}}_{2m+1}) \mathbf{v}_k. \quad (\text{A.20})$$

It is easy to verify that

$$\begin{aligned} \mathbf{v}_j^\top \Omega_{2m} \tilde{\mathbf{v}}_{2m+1} &= \mathbf{v}_j^\top \Omega_{2m} \mathbf{y} + \sum_{k,l=1}^{2m} (\Omega_{2m})_{kl} (\Omega_{2m})_{jk} \mathbf{v}_l^\top \Omega_{2m} \mathbf{y} = \\ &= \mathbf{v}_j^\top \Omega_{2m} \mathbf{y} - \sum_{l=1}^{2m} \delta_{lj} \mathbf{v}_l^\top \Omega_{2m} \mathbf{y} = 0 = (\Omega_{2m})_{j, 2m+1}, \\ \mathbf{v}_j^\top \Omega_{2m} \tilde{\mathbf{v}}_{2m+2} &= \mathbf{v}_j^\top \tilde{\mathbf{v}}_{2m+1} + \sum_{k,l=1}^{2m} (\Omega_{2m})_{kl} (\Omega_{2m})_{jk} (\mathbf{v}_l^\top \tilde{\mathbf{v}}_{2m+1}) = \\ &= \mathbf{v}_j^\top \tilde{\mathbf{v}}_{2m+1} - \sum_{l=1}^{2m} \delta_{lj} (\mathbf{v}_l^\top \tilde{\mathbf{v}}_{2m+1}) = 0 = (\Omega_{2m})_{j, 2m+2}, \\ \tilde{\mathbf{v}}_{2m+1}^\top \Omega_{2m} \tilde{\mathbf{v}}_{2m+2} &= -\tilde{\mathbf{v}}_{2m+1}^\top \Omega_{2m} \Omega_{2m} \tilde{\mathbf{v}}_{2m+1} + \\ &\quad + \sum_{k,l=1}^{2m} (\Omega_{2m})_{kl} (\mathbf{v}_l^\top \tilde{\mathbf{v}}_{2m+1}) \tilde{\mathbf{v}}_{2m+1}^\top \Omega_{2m} \mathbf{v}_k = |\tilde{\mathbf{v}}_{2m+1}|^2. \end{aligned}$$

One can then rescale  $\tilde{\mathbf{v}}_{2m+1}$  and  $\tilde{\mathbf{v}}_{2m+2}$  as

$$\mathbf{v}_{2m+1} = c \frac{\tilde{\mathbf{v}}_{2m+1}}{|\tilde{\mathbf{v}}_{2m+1}|}, \quad \mathbf{v}_{2m+2} = \frac{1}{c} \frac{\tilde{\mathbf{v}}_{2m+2}}{|\tilde{\mathbf{v}}_{2m+1}|}, \quad (\text{A.21})$$

where  $c \in \mathbb{R}$  is an arbitrary constant, add them to the incomplete symplectic basis and iterate this procedure up to  $\mathbf{v}_{4m-1}$  and  $\mathbf{v}_{4m}$ . The wanted open Gaussian dynamics then reads

$$\mathbf{S} = \begin{pmatrix} \mathbf{v}_1^\top \\ \vdots \\ \mathbf{v}_{4m}^\top \end{pmatrix}. \quad (\text{A.22})$$

This completes the proof.  $\square$



# B

---

## DAMPED JAYNES-CUMMINGS MODEL

---

We will see in this Appendix how, although the choice of memory kernel Eq.5.3 may seem arbitrary, it can be justified by considering the Jaynes-Cummings model on resonance. The system considered is that of a two-level atom in an empty and leaky cavity, effectively described by the Hamiltonian

$$\hat{H}_{\text{JC}} = \frac{\omega_0}{2} \hat{\sigma}_z + \left( \hat{\sigma}_+ \hat{B} + \hat{\sigma}_- \hat{B}^\dagger \right) + \sum_{\mu} \omega_{\mu} \hat{b}_{\mu}^{\dagger} \hat{b}_{\mu} , \quad (\text{B.1})$$

where  $\hat{b}_{\mu}$  and  $\hat{b}_{\mu}^{\dagger}$  are the creation and annihilation operators of the bath bosonic field,  $\hat{B} \equiv \sum_{\mu} g_{\mu} (\hat{b}_{\mu} + \hat{b}_{\mu}^{\dagger})$  and  $g_{\mu}$  represent the system-bath coupling constants and they are such that they make up the Lorentzian spectral density  $J(\omega) = \sum_{\mu} g_{\mu}^2 \delta(\omega - \omega_{\mu}) = \frac{1}{2\pi} \frac{\gamma_0 \lambda^2}{(\omega_0 - \omega)^2 + \lambda^2}$  [9].

Assuming weak coupling, it is possible to write the second-order Nakajima-Zwanzig master, Eq.1.88, for the density matrix of the two-level atom in the interaction picture:

$$\frac{d\hat{\rho}_I}{dt} = - \int_0^t ds \text{Tr}_B [\hat{H}_{\text{JC}}(t), [\hat{H}_{\text{JC}}(s), \hat{\rho}_I(s) \otimes \hat{\rho}_B]] , \quad (\text{B.2})$$

where  $\hat{\rho}_B$  is the state of the bath and the interaction picture Hamiltonian is  $\hat{H}_{\text{JC}}(t) = \hat{\sigma}_+(t) \hat{B}(t) + \hat{\sigma}_-(t) \hat{B}^\dagger(t)$ , with  $\hat{\sigma}_{\pm}(t) = \hat{\sigma}_{\pm} e^{\pm i\omega_0 t}$  and  $\hat{B}(t) = \sum_{\mu} g_{\mu} (\hat{b}_{\mu} e^{-i\omega_{\mu} t} + \hat{b}_{\mu}^{\dagger} e^{i\omega_{\mu} t})$ .

Combining Eq.B.1 and Eq.B.2 one obtains a master equation equivalent to Eq.5.3 at zero temperature [9], with the memory kernel  $f(t-s)$  given by the bath self-correlation function:  $\langle \hat{B}(t) \hat{B}(s)^{\dagger} \rangle = \int d\omega' J(\omega') e^{i(\omega_0 - \omega')(t-s)} = \frac{\gamma_0 \lambda}{2} e^{-\lambda(t-s)}$ .

In spite of this remark, we want to emphasise that, since the decay rates  $\Gamma_{\omega}$  are evaluated at arbitrary temperature  $T$ , Eq.5.3 remains a purely phenomenological equation.



---

## MEASUREMENT COMPATIBILITY MATRIX

---

In this Appendix we are going to give a proof of Theorem 6.1

*Proof.* To prove Theorem 6.1 we will calculate explicitly, term by term, the following expression

$$\begin{aligned} \text{Tr}(\hat{\rho}\hat{\mathcal{L}}_\eta\hat{\mathcal{L}}_\zeta) = & \text{Tr}\left(\hat{\rho}\left(L_\eta^{(0)} + L_{\eta l}^{(1)}\hat{R}_l + L_{\eta jk}^{(2)}\hat{R}_j\hat{R}_k\right) \cdot \right. \\ & \left. \cdot \left(L_\zeta^{(0)} + L_{\zeta m}^{(1)}\hat{R}_m + L_{\zeta pq}^{(2)}\hat{R}_p\hat{R}_q\right)\right). \end{aligned} \quad (\text{C.1})$$

The linear term is just the displacement vector,  $\text{Tr}(\hat{\rho}\hat{R}_l) = d_l$ . The quadratic term is straightforwardly found from Eq.2.40 to be

$$\text{Tr}(\hat{\rho}\hat{R}_p\hat{R}_q) = \chi_{\hat{\rho}\hat{R}_p\hat{R}_q}(\tilde{\mathbf{r}} = 0) = d_p d_q + \frac{1}{2}(V_{pq} + i\Omega_{pq}), \quad (\text{C.2})$$

(notice that in Eq.2.40 we were actually calculating  $\text{Tr}(\sum_i \hat{R}_i \hat{R}_i \hat{\rho})$ ). We have left to find the explicit expressions for the cubic,  $\text{Tr}(\hat{\rho}\hat{R}_l\hat{R}_p\hat{R}_q)$ , and quartic,  $\text{Tr}(\hat{\rho}\hat{R}_j\hat{R}_k\hat{R}_p\hat{R}_q)$ , terms.

As for Eq.2.40, we will make use of the properties Eq.2.39 and Eq.2.24. In the rest of the proof, for the sake of a lighter notation, we will write  $\partial_j$  (roman indexes) for  $\frac{\partial}{\partial \tilde{r}_j}$ , while  $\partial_\eta$  (greek indexes) for the derivative with respect to the parameters  $\mu_\eta$ ,  $\partial_\mu \equiv \frac{\partial}{\partial \mu_\eta}$ . Moreover we will indicate with  $\mathfrak{D}_q$  the operator

$$\mathfrak{D}_q \equiv -i\partial_q - \frac{1}{2}\Omega_{qq'}\tilde{r}_{q'}, \quad (\text{C.3})$$

acting on the characteristic function.

### Cubic term

Applying property Eq.2.24

$$\begin{aligned}
 \text{Tr}(\hat{\rho}\hat{R}_l\hat{R}_p\hat{R}_q) &= \mathfrak{D}_q\mathfrak{D}_p\mathfrak{D}_l\chi|_{\tilde{r}=0} = \\
 &= \left[ (-i)^3\partial_q\partial_p\partial_l\chi - \frac{(-i)^2}{2}\Omega_{ll'}\partial_q\partial_p(\tilde{r}_{l'}\chi) - \right. \\
 &\quad \frac{i}{4}\Omega_{pp'}\Omega_{ll'}\partial_q(\tilde{r}_{p'}\tilde{r}_{l'}\chi) - \frac{(-i)^2}{2}\Omega_{pp'}\partial_q(\tilde{r}_{p'}\partial_l\chi) - \\
 &\quad - \frac{(-i)^2}{2}\Omega_{qq'}\tilde{r}_{q'}\partial_p\partial_q\chi - \frac{i}{4}\Omega_{qq'}\Omega_{ll'}\tilde{r}_{q'}\partial_p(\tilde{r}_{l'}\chi) - \\
 &\quad \left. - \frac{i}{4}\Omega_{qq'}\Omega_{pp'}\tilde{r}_{q'}\tilde{r}_{p'}\partial_l\chi - \frac{1}{8}\Omega_{qq'}\Omega_{pp'}\Omega_{ll'}\tilde{r}_{q'}\tilde{r}_{p'}\tilde{r}_{l'}\chi \right]_{\tilde{r}=0} = \\
 &= \left[ i\partial_q\partial_p\partial_l\chi + \frac{1}{2}\Omega_{ll'}\partial_q\partial_p(\tilde{r}_{l'}\chi) + \frac{1}{2}\Omega_{pp'}\partial_q(\tilde{r}_{p'}\partial_l\chi) \right]_{\tilde{r}=0} .
 \end{aligned} \tag{C.4}$$

Making use of Eq.2.39, the three terms in the above, when evaluated in  $\tilde{r} = 0$ , are readily found to be

$$\partial_q\partial_p(\tilde{r}_{l'}\chi)|_{\tilde{r}=0} = id_q\delta_{pl'} + id_p\delta_{ql'} , \tag{C.5}$$

$$\partial_q(\tilde{r}_{p'}\partial_l\chi)|_{\tilde{r}=0} = id_l\delta_{qp'} , \tag{C.6}$$

$$\partial_q\partial_p\partial_l\chi|_{\tilde{r}=0} = -id_p d_l d_q - \frac{i}{2}(V_{pl}d_q + V_{pq}d_l + V_{lq}d_p) . \tag{C.7}$$

Hence we get (notice that  $V_{jk} = V_{kj}$  as the covariance matrix is symmetric)

$$\begin{aligned}
 \text{Tr}(\hat{\rho}\hat{R}_l\hat{R}_p\hat{R}_q) &= \frac{1}{2} [(V_{lp} + i\Omega_{lp})d_q + (V_{pq} + i\Omega_{pq})d_l + (V_{lq} + i\Omega_{lq})d_p] + \\
 &\quad + d_p d_l d_q .
 \end{aligned} \tag{C.8}$$

### Quartic term

Considering that the linear term in  $\tilde{r}_q$  gives no contribution when evaluated in  $\tilde{r} = 0$  we have

$$\begin{aligned}
 \text{Tr}(\hat{\rho}\hat{R}_j\hat{R}_k\hat{R}_p\hat{R}_q) &= -i\partial_q\mathfrak{D}_p\mathfrak{D}_k\mathfrak{D}_j\chi|_{\tilde{r}=0} = \\
 &= -i\partial_q \left[ (-i)^3\partial_p\partial_k\partial_j\chi - \frac{(-i)^2}{2}\Omega_{jj'}\partial_p\partial_k(\tilde{r}_{j'}\chi) - \right. \\
 &\quad - \frac{i}{4}\Omega_{kk'}\Omega_{jj'}\partial_p(\tilde{r}_{k'}\tilde{r}_{j'}\chi) - \frac{(-i)^2}{2}\Omega_{kk'}\partial_p(\tilde{r}_{k'}\partial_j\chi) - \\
 &\quad - \frac{(-i)^2}{2}\Omega_{pp'}\tilde{r}_{p'}\partial_k\partial_j\chi - \frac{i}{4}\Omega_{pp'}\Omega_{jj'}\tilde{r}_{p'}\partial_k(\tilde{r}_{j'}\chi) - \\
 &\quad \left. - \frac{i}{4}\Omega_{pp'}\Omega_{kk'}\tilde{r}_{p'}\tilde{r}_{k'}\partial_j\chi - \frac{1}{8}\Omega_{pp'}\Omega_{kk'}\Omega_{jj'}\tilde{r}_{p'}\tilde{r}_{k'}\tilde{r}_{j'}\chi \right]_{\tilde{r}=0} .
 \end{aligned}$$

Notice that the last two terms do not contribute when evaluated in  $\tilde{r} = 0$  since they are second and third order in  $\tilde{r}$ , and, when derived wrt  $\tilde{r}_q$ , they give a linear and a quadratic term, respectively.

$$\begin{aligned} \text{Tr}(\hat{\rho}\hat{R}_j\hat{R}_k\hat{R}_p\hat{R}_q) = & \left[ (-i)^4 \partial_q \partial_p \partial_k \partial_j \chi - \frac{(-i)^3}{2} \Omega_{jj'} \partial_q \partial_p \partial_k (\tilde{r}_{j'} \chi) + \right. \\ & + \frac{(-i)^2}{4} \Omega_{kk'} \Omega_{jj'} \partial_q \partial_p (\tilde{r}_{k'} \tilde{r}_{j'} \chi) - \\ & - \frac{(-i)^3}{2} \Omega_{kk'} \partial_q \partial_p (\tilde{r}_{k'} \partial_j \chi) \\ & - \frac{(-i)^3}{2} \Omega_{pp'} \partial_q (\tilde{r}_{p'} \partial_k \partial_j \chi) + \\ & \left. + \frac{(-i)^2}{4} \Omega_{pp'} \Omega_{jj'} \partial_q (\tilde{r}_{p'} \partial_k (\tilde{r}_{j'} \chi)) \right]_{\tilde{r}=0}. \end{aligned} \quad (\text{C.9})$$

The six terms in the above when evaluated in  $\tilde{r} = 0$  give

$$\partial_q \partial_p \partial_k (\tilde{r}_{j'} \chi)|_{\tilde{r}=0} = \delta_{kj'} \partial_q \partial_p \chi|_0 + \delta_{pj'} \partial_q \partial_k \chi|_0 + \delta_{qj'} \partial_p \partial_k \chi|_0, \quad (\text{C.10})$$

$$\partial_q \partial_p (\tilde{r}_{k'} \tilde{r}_{j'} \chi)|_{\tilde{r}=0} = \delta_{pk'} \delta_{qj'} + \delta_{pj'} \delta_{qk'}, \quad (\text{C.11})$$

$$\partial_q \partial_p (\tilde{r}_{k'} \partial_j \chi)|_{\tilde{r}=0} = \delta_{pk'} \partial_q \partial_j \chi|_0 + \delta_{qk'} \partial_p \partial_j \chi|_0, \quad (\text{C.12})$$

$$\partial_q (\tilde{r}_{p'} \partial_k \partial_j \chi)|_{\tilde{r}=0} = \delta_{qp'} \partial_k \partial_j \chi|_0, \quad (\text{C.13})$$

$$\partial_q (\tilde{r}_{p'} \partial_k (\tilde{r}_{j'} \chi))|_{\tilde{r}=0} = \delta_{qp'} \delta_{kj'}, \quad (\text{C.14})$$

$$\begin{aligned} \partial_q \partial_p \partial_k \partial_j \chi|_{\tilde{r}=0} = & d_k d_j d_q d_p + \frac{1}{4} (V_{kp} V_{jq} + V_{jp} V_{kq} + V_{kj} V_{qp}) + \\ & + \frac{1}{2} (V_{qp} d_k d_j + V_{kj} d_p d_q + V_{kq} d_j d_p + \\ & + V_{jq} d_k d_p + V_{kp} d_j d_q + V_{jp} d_k d_q). \end{aligned} \quad (\text{C.15})$$

Plugging these expressions into Eq.C.9 we get

$$\begin{aligned} \text{Tr}(\hat{\rho}\hat{R}_j\hat{R}_k\hat{R}_p\hat{R}_q) = & d_j d_k d_p d_q + \frac{1}{2} d_p d_q V_{jk} + \frac{1}{2} d_k d_q V_{jp} + \frac{1}{2} d_j d_q V_{kp} + \\ & + \frac{1}{2} d_k d_p V_{jq} + \frac{1}{2} d_j d_p V_{kq} + \frac{1}{2} d_j d_k V_{pq} + \\ & + \frac{i}{2} \left\{ \Omega_{jk} \left( d_p d_q + \frac{V_{pq}}{2} \right) + \Omega_{jp} \left( d_k d_q + \frac{V_{kq}}{2} \right) + \right. \\ & + \Omega_{kp} \left( d_j d_q + \frac{V_{jq}}{2} \right) + \Omega_{jq} \left( d_k d_p + \frac{V_{kp}}{2} \right) + \\ & \left. + \Omega_{kq} \left( d_j d_p + \frac{V_{jp}}{2} \right) + \Omega_{pq} \left( d_j d_k + \frac{V_{jk}}{2} \right) \right\} - \\ & - \frac{1}{4} (\Omega_{jq} \Omega_{kp} + \Omega_{jp} \Omega_{kq} + \Omega_{jk} \Omega_{pq}) + \\ & + \frac{1}{4} (V_{jq} V_{kp} + V_{jp} V_{kq} + V_{jk} V_{pq}). \end{aligned} \quad (\text{C.16})$$

Before moving to the last section we recall that the expectation value of the SLD operator is zero. This is easy to check:

$$\begin{aligned} \langle \hat{\mathcal{L}}_\zeta \rangle &= \text{Tr}(\hat{\rho} \hat{\mathcal{L}}_\zeta) = L_\zeta^{(0)} \text{Tr}(\hat{\rho}) + L_{\zeta m}^{(1)} \text{Tr}(\hat{\rho} \hat{R}_m) + L_{\zeta jk}^{(2)} \text{Tr}(\hat{\rho} \hat{R}_j \hat{R}_k) = \\ &= L_\zeta^{(0)} + L_{\zeta m}^{(1)} d_m + L_{\zeta jk}^{(2)} \left( d_j d_k + \frac{1}{2} (V_{jk} + i\Omega_{jk}) \right), \end{aligned} \quad (\text{C.17})$$

which in vectorial form reads

$$\langle \hat{\mathcal{L}}_\zeta \rangle = L_\zeta^{(0)} + \mathbf{L}_\zeta^{(1)\top} \mathbf{d} + \mathbf{d}^\top \mathbf{L}_\zeta^{(2)} \mathbf{d} + \frac{1}{2} \text{Tr}(\mathbf{L}_\zeta^{(2)} V) + \frac{i}{2} \text{Tr}(\mathbf{L}_\zeta^{(2)} \Omega). \quad (\text{C.18})$$

When substituting the expression for  $L^{(0)}$ , Eq.6.7, we are left with a term proportional to  $\text{Tr}(\mathbf{L}_\zeta^{(2)} \Omega)$  which vanishes because  $\mathbf{L}^{(2)}$  is symmetric, while  $\Omega$  is skew-symmetric.

**Expressions for  $\text{Tr}(\hat{\rho} \hat{\mathcal{L}}_\eta \hat{\mathcal{L}}_\zeta)$ ,  $\mathcal{F}_{\eta\zeta}$ ,  $\mathcal{J}_{\eta\zeta}$**

We have that

$$\begin{aligned} \text{Tr}(\hat{\rho} \hat{\mathcal{L}}_\eta \hat{\mathcal{L}}_\zeta) &= L_\eta^{(0)} L_\zeta^{(0)} + L_\eta^{(0)} L_{\zeta m}^{(1)} \text{Tr}(\hat{\rho} \hat{R}_m) + L_\eta^{(0)} L_{\zeta pq}^{(2)} \text{Tr}(\hat{\rho} \hat{R}_p \hat{R}_q) + \\ &+ L_{\eta l}^{(1)} L_\zeta^{(0)} \text{Tr}(\hat{\rho} \hat{R}_l) + L_{\eta l}^{(1)} L_{\zeta m}^{(1)} \text{Tr}(\hat{\rho} \hat{R}_l \hat{R}_m) + \\ &+ L_{\eta l}^{(1)} L_{\zeta pq}^{(2)} \text{Tr}(\hat{\rho} \hat{R}_l \hat{R}_p \hat{R}_q) + L_{\eta jk}^{(2)} L_\zeta^{(0)} \text{Tr}(\hat{\rho} \hat{R}_j \hat{R}_k) + \\ &+ L_{\eta jk}^{(2)} L_{\zeta m}^{(1)} \text{Tr}(\hat{\rho} \hat{R}_j \hat{R}_k \hat{R}_m) + L_{\eta jk}^{(2)} L_{\zeta pq}^{(2)} \text{Tr}(\hat{\rho} \hat{R}_j \hat{R}_k \hat{R}_p \hat{R}_q), \end{aligned}$$

and substituting the results of the previous parts of the proof we get

$$\begin{aligned}
 \text{Tr}(\hat{\rho}\hat{\mathcal{L}}_\eta\hat{\mathcal{L}}_\zeta) = & L_\eta^{(0)}L_\zeta^{(0)} + L_\eta^{(0)}L_\zeta^{(1)}d_m + L_\eta^{(1)}L_\zeta^{(0)}d_l + \\
 & + L_\eta^{(0)}L_\zeta^{(2)}\left(d_p d_q + \frac{1}{2}(V_{pq} + i\Omega_{pq})\right) + \\
 & + L_\eta^{(1)}L_\zeta^{(1)}\left(d_l d_m + \frac{1}{2}(V_{lm} + i\Omega_{lm})\right) + \\
 & + L_\eta^{(2)}L_\zeta^{(0)}\left(d_j d_k + \frac{1}{2}(V_{jk} + i\Omega_{jk})\right) + \\
 & + L_\eta^{(1)}L_\zeta^{(2)}\left(d_p d_l d_q + (V_{lp} + i\Omega_{lp})\frac{d_q}{2} + \right. \\
 & \quad \left. + (V_{pq} + i\Omega_{pq})\frac{d_l}{2} + (V_{lq} + i\Omega_{lq})\frac{d_p}{2}\right) + \\
 & + L_\eta^{(2)}L_\zeta^{(1)}\left(d_j d_k d_m + (V_{jk} + i\Omega_{jk})\frac{d_m}{2} + \right. \\
 & \quad \left. + (V_{km} + i\Omega_{km})\frac{d_j}{2} + (V_j + i\Omega_{jm})\frac{d_k}{2}\right) + \\
 & + L_\eta^{(2)}L_\zeta^{(2)}\left\{d_j d_k d_p d_q + \frac{1}{2}d_p d_q V_{jk} + \frac{1}{2}d_k d_q V_{jp} + \right. \\
 & \quad + \frac{1}{2}d_j d_q V_{kp} + \frac{1}{2}d_k d_p V_{jq} + \frac{1}{2}d_j d_p V_{kq} + \\
 & \quad + \frac{1}{2}d_j d_k V_{pq} + \frac{1}{4}V_{jq} V_{kp} + \frac{1}{4}V_{jp} V_{kq} + \frac{1}{4}V_{jk} V_{pq} + \\
 & \quad + \frac{i}{2}\left[\Omega_{jk}\left(d_p d_q + \frac{V_{pq}}{2}\right) + \Omega_{jp}\left(d_k d_q + \frac{V_{kq}}{2}\right) + \right. \\
 & \quad + \Omega_{kp}\left(d_j d_q + \frac{V_{jq}}{2}\right) + \Omega_{jq}\left(d_k d_p + \frac{V_{kp}}{2}\right) + \\
 & \quad \left. + \Omega_{kq}\left(d_j d_p + \frac{V_{jp}}{2}\right) + \Omega_{pq}\left(d_j d_k + \frac{V_{jk}}{2}\right)\right] - \\
 & \quad \left. - \frac{1}{4}(\Omega_{jq}\Omega_{kp} + \Omega_{jp}\Omega_{kq} + \Omega_{jk}\Omega_{pq})\right\}.
 \end{aligned} \tag{C.19}$$

To this expression we subtract

$$\begin{aligned}
 0 \equiv \langle \hat{\mathcal{L}}_\zeta \rangle \langle \hat{\mathcal{L}}_\eta \rangle = & L_\zeta^{(0)}L_\eta^{(0)} + L_\zeta^{(0)}L_\eta^{(1)}d_p + L_\zeta^{(1)}L_\eta^{(0)}d_m + L_\zeta^{(1)}L_\eta^{(1)}d_m d_p + \\
 & + L_\zeta^{(0)}L_\eta^{(2)}\left(d_p d_q + \frac{V_{pq} + i\Omega_{pq}}{2}\right) + L_\zeta^{(1)}L_\eta^{(2)}d_m\left(d_p d_q + \frac{V_{pq} + i\Omega_{pq}}{2}\right) + \\
 & + L_\zeta^{(2)}L_\eta^{(0)}\left(d_j d_k + \frac{V_{jk} + i\Omega_{jk}}{2}\right) + L_\zeta^{(2)}L_\eta^{(1)}d_p\left(d_j d_k + \frac{V_{jk} + i\Omega_{jk}}{2}\right) + \\
 & + L_\zeta^{(2)}L_\eta^{(2)}\left(d_j d_k + \frac{V_{jk} + i\Omega_{jk}}{2}\right)\left(d_p d_q + \frac{V_{pq} + i\Omega_{pq}}{2}\right),
 \end{aligned}$$

and we get

$$\begin{aligned}
 \text{Tr} (\hat{\rho} \hat{\mathcal{L}}_\eta \hat{\mathcal{L}}_\zeta) &= \frac{1}{2} d_k V_{jm} L_{\eta jk}^{(2)} L_{\zeta m}^{(1)} + \frac{1}{2} d_j L_{\eta jk}^{(2)} V_{km} L_{\zeta m}^{(1)} + \\
 &+ \frac{1}{2} i d_k \Omega_{jm} L_{\eta jk}^{(2)} L_{\zeta m}^{(1)} + \frac{1}{2} i d_j L_{\eta jk}^{(2)} \Omega_{km} L_{\zeta m}^{(1)} + \\
 &+ \frac{1}{2} d_k d_q V_{jp} L_{\eta jk}^{(2)} L_{\zeta pq}^{(2)} + \frac{1}{2} d_j d_q L_{\eta jk}^{(2)} V_{kp} L_{\zeta pq}^{(2)} + \\
 &+ \frac{1}{2} d_k d_p V_{jq} L_{\eta jk}^{(2)} L_{\zeta pq}^{(2)} + \frac{1}{2} d_j d_p L_{\eta jk}^{(2)} V_{kq} L_{\zeta pq}^{(2)} + \\
 &+ \frac{1}{2} i d_k d_q \Omega_{jp} L_{\eta jk}^{(2)} L_{\zeta pq}^{(2)} + \frac{1}{2} i d_k d_p \Omega_{jq} L_{\eta jk}^{(2)} L_{\zeta pq}^{(2)} + \\
 &+ \frac{1}{2} i d_j d_q L_{\eta jk}^{(2)} \Omega_{kp} L_{\zeta pq}^{(2)} + \frac{1}{2} i d_j d_p L_{\eta jk}^{(2)} \Omega_{kq} L_{\zeta pq}^{(2)} + \\
 &+ \frac{1}{2} d_q L_{\eta l}^{(1)} V_{lp} L_{\zeta pq}^{(2)} + \frac{1}{2} d_p L_{\eta l}^{(1)} V_{lq} L_{\zeta pq}^{(2)} + \\
 &+ \frac{1}{2} i d_q L_{\eta l}^{(1)} \Omega_{lp} L_{\zeta pq}^{(2)} + \frac{1}{2} i d_p L_{\eta l}^{(1)} \Omega_{lq} L_{\zeta pq}^{(2)} + \\
 &+ \frac{1}{4} i \Omega_{jp} L_{\eta jk}^{(2)} V_{kq} L_{\zeta pq}^{(2)} + \frac{1}{4} i \Omega_{jq} L_{\eta jk}^{(2)} V_{kp} L_{\zeta pq}^{(2)} + \\
 &+ \frac{1}{4} i V_{jq} L_{\eta jk}^{(2)} \Omega_{kp} L_{\zeta pq}^{(2)} + \frac{1}{4} i V_{jp} L_{\eta jk}^{(2)} \Omega_{kq} L_{\zeta pq}^{(2)} + \\
 &+ \frac{1}{4} V_{jq} L_{\eta jk}^{(2)} V_{kp} L_{\zeta pq}^{(2)} + \frac{1}{4} V_{jp} L_{\eta jk}^{(2)} V_{kq} L_{\zeta pq}^{(2)} - \\
 &- \frac{1}{4} \Omega_{jq} L_{\eta jk}^{(2)} \Omega_{kp} L_{\zeta pq}^{(2)} - \frac{1}{4} \Omega_{jp} L_{\eta jk}^{(2)} \Omega_{kq} L_{\zeta pq}^{(2)} + \\
 &+ \frac{1}{2} L_{\eta l}^{(1)} V_{lm} L_{\zeta m}^{(1)} + \frac{1}{2} i L_{\eta l}^{(1)} \Omega_{lm} L_{\zeta m}^{(1)}, \tag{C.20}
 \end{aligned}$$

which in vectorial form becomes

$$\begin{aligned}
 \text{Tr} (\hat{\rho} \hat{\mathcal{L}}_\eta \hat{\mathcal{L}}_\zeta) &= \mathbf{d}^\top L_\eta^{(2)} V L_\zeta^{(1)} + i \mathbf{d}^\top L_\eta^{(2)} \Omega L_\zeta^{(1)} + 2 \mathbf{d}^\top L_\eta^{(2)} V L_\zeta^{(2)} \mathbf{d} + \\
 &+ 2 i \mathbf{d}^\top L_\eta^{(2)} \Omega L_\zeta^{(2)} \mathbf{d} + \mathbf{d}^\top L_\zeta^{(2)} V L_\eta^{(1)} + i L_\eta^{(1)\top} \Omega L_\zeta^{(2)} \mathbf{d} + \\
 &+ 2 i \text{Tr} \left( \Omega L_\zeta^{(2)} V L_\eta^{(2)} \right) + \frac{1}{2} \text{Tr} \left( V L_\zeta^{(2)} V L_\eta^{(2)} \right) + \\
 &+ \frac{1}{2} \text{Tr} \left( \Omega L_\zeta^{(2)} \Omega L_\eta^{(2)} \right) + \frac{1}{2} L_\eta^{(1)\top} V L_\zeta^{(1)} + \frac{i}{2} L_\eta^{(1)\top} \Omega L_\zeta^{(1)}. \tag{C.21}
 \end{aligned}$$

Now, since for any two hermitian operators  $\hat{A}$  and  $\hat{B}$  it holds that that  $2\text{Tr} (\hat{\rho} \hat{A} \hat{B}) = \text{Tr} (\hat{\rho} \{\hat{A}, \hat{B}\}_+) + \text{Tr} (\hat{\rho} [\hat{A}, \hat{B}])$ , we find

$$\text{Re} \{ \text{Tr} (\hat{\rho} \hat{\mathcal{L}}_\eta \hat{\mathcal{L}}_\zeta) \} = \frac{1}{2} \text{Tr} (\hat{\rho} \{ \hat{\mathcal{L}}_\eta, \hat{\mathcal{L}}_\zeta \}_+) = \mathcal{F}_{\eta\zeta} = \mathcal{F}_{\zeta\eta}, \tag{C.22}$$

$$\text{Im} \{ \text{Tr} (\hat{\rho} \hat{\mathcal{L}}_\eta \hat{\mathcal{L}}_\zeta) \} = \frac{1}{2i} \text{Tr} (\hat{\rho} [\hat{\mathcal{L}}_\eta, \hat{\mathcal{L}}_\zeta]) = \mathcal{J}_{\eta\zeta} = -\mathcal{J}_{\zeta\eta}. \tag{C.23}$$

Using the cyclic property of the trace and the identity Eq.6.5 we have that

$$\begin{aligned} \frac{1}{2}\text{Tr}\left(VL_{\zeta}^{(2)}VL_{\eta}^{(2)}\right) + \frac{1}{2}\text{Tr}\left(\Omega L_{\zeta}^{(2)}\Omega L_{\eta}^{(2)}\right) &= \frac{1}{2}\text{Tr}\left(\partial_{\zeta}VL_{\eta}^{(2)}\right) \\ &= \frac{1}{2}\text{Tr}\left(\partial_{\eta}VL_{\zeta}^{(2)}\right), \end{aligned} \quad (\text{C.24})$$

therefore, for Eq.C.22, we have:

$$\begin{aligned} \text{Re}\left\{\text{Tr}\left(\hat{\rho}\hat{\mathcal{L}}_{\eta}\hat{\mathcal{L}}_{\zeta}\right)\right\} &= \mathbf{d}^{\top}L_{\eta}^{(2)}VL_{\zeta}^{(1)} + 2\mathbf{d}^{\top}L_{\eta}^{(2)}VL_{\zeta}^{(2)}\mathbf{d} + \mathbf{d}^{\top}L_{\zeta}^{(2)}VL_{\eta}^{(1)} + \\ &+ \frac{1}{2}\text{Tr}\left(\partial_{\zeta}VL_{\eta}^{(2)}\right) + \frac{1}{2}L_{\eta}^{(1)}VL_{\zeta}^{(1)}. \end{aligned} \quad (\text{C.25})$$

Finally, substituting in the expression for  $L^{(1)}$ , Eq.6.6, and adopting in what follows the shorthand notation  $\mathbf{d}_{\eta} \equiv \partial_{\eta}\mathbf{d}$ , we get

$$\text{Re}\left\{\text{Tr}\left(\hat{\rho}\hat{\mathcal{L}}_{\eta}\hat{\mathcal{L}}_{\zeta}\right)\right\} = \frac{1}{2}\text{Tr}\left(\partial_{\zeta}VL_{\eta}^{(2)}\right) + 2\mathbf{d}_{\eta}^{\top}V^{-1}\mathbf{d}_{\zeta} = \mathcal{F}_{\eta\zeta}. \quad (\text{C.26})$$

Similarly, for Eq.C.23 we have

$$\begin{aligned} \text{Im}\left\{\text{Tr}\left(\hat{\rho}\hat{\mathcal{L}}_{\eta}\hat{\mathcal{L}}_{\zeta}\right)\right\} &= \mathbf{d}^{\top}L_{\eta}^{(2)}\Omega L_{\zeta}^{(1)} + 2\mathbf{d}^{\top}L_{\eta}^{(2)}\Omega L_{\zeta}^{(2)}\mathbf{d} + L_{\eta}^{(1)\top}\Omega L_{\zeta}^{(2)}\mathbf{d} + \\ &+ 2\text{Tr}\left(\Omega L_{\zeta}^{(2)}VL_{\eta}^{(2)}\right) + \frac{1}{2}L_{\eta}^{(1)\top}\Omega L_{\zeta}^{(1)} = \\ &= 2\text{Tr}\left(\Omega L_{\zeta}^{(2)}VL_{\eta}^{(2)}\right) + 2\mathbf{d}_{\eta}^{\top}V^{-1}\Omega V^{-1}\mathbf{d}_{\zeta} = \mathcal{J}_{\eta\zeta}. \end{aligned} \quad (\text{C.27})$$

In conclusion, to summarize:

$$\text{Tr}\left(\hat{\rho}\hat{\mathcal{L}}_{\eta}\hat{\mathcal{L}}_{\zeta}\right) = \mathcal{F}_{\eta\zeta} + i\mathcal{J}_{\eta\zeta}, \quad (\text{C.28})$$

with

$$\mathcal{F}_{\eta\zeta} = \frac{1}{2}\text{Tr}\left(\partial_{\zeta}VL_{\eta}^{(2)}\right) + 2\mathbf{d}_{\eta}^{\top}V^{-1}\mathbf{d}_{\zeta}, \quad (\text{C.29})$$

$$\mathcal{J}_{\eta\zeta} = 2\text{Tr}\left(\Omega L_{\zeta}^{(2)}VL_{\eta}^{(2)}\right) + 2\mathbf{d}_{\eta}^{\top}V^{-1}\Omega V^{-1}\mathbf{d}_{\zeta}. \quad (\text{C.30})$$

This completes the proof.  $\square$



# D

---

## $k$ -MODE POSITIVITY OF GAUSSIAN MAPS

---

In this Appendix we are going to prove Theorem 7.1. In order to prove it we will enunciate and prove the following first:

**Lemma 2.** *For any  $2n \times 2n$  Hermitian matrix  $R$  we have*

$$\min \{ \text{eig} (i\Omega_n + R) \} = \min \left\{ \text{eig} \left( i\Omega_{n-k} \oplus \mathbb{1}_k + QRQ^\top \right) \right\} , \quad (\text{D.1})$$

for some orthogonal symplectic matrix  $Q$  and for any  $k < n$ .

*Proof.* Let us denote  $\lambda = \min \{ \text{eig}(R + i\Omega_n) \}$  which corresponds to an eigenvector

$$v_\lambda = \begin{pmatrix} \alpha + i\beta \\ \mathbf{a}_{n-1} + i\mathbf{b}_{n-1} \\ \mathbf{a}_n + i\mathbf{b}_n \end{pmatrix} , \quad (\text{D.2})$$

where  $\alpha$  and  $\beta$  are  $2n - 4$  dimensional real vectors and  $\mathbf{a}_{n-1}$ ,  $\mathbf{a}_n$ ,  $\mathbf{b}_{n-1}$  and  $\mathbf{b}_n$  are two-dimensional real vectors. A transformation  $Q \in \text{Sp}(2n, \mathbb{R}) \cap \text{SO}(2n)$  preserves the eigenvalues changing the corresponding eigenvector into  $v'_\lambda = Qv_\lambda$ . In order to prove the Lemma we start showing that there exists  $Q_1 \in \text{Sp}(2n, \mathbb{R}) \cap \text{SO}(2n)$  such that  $v_\lambda^{(1)} = Q_1 v_\lambda$  is an eigenvector for both  $i\Omega_n + Q_1 R Q_1^\top$  and  $i\Omega_{n-1} \oplus \mathbb{1} + Q_1 R Q_1^\top$  for the same eigenvalue  $\lambda$ . Denote

$$v_\lambda^{(1)} = \begin{pmatrix} \alpha^{(1)} + i\beta^{(1)} \\ \mathbf{a}_{n-1}^{(1)} + i\mathbf{b}_{n-1}^{(1)} \\ \mathbf{a}_n^{(1)} + i\mathbf{b}_n^{(1)} \end{pmatrix} . \quad (\text{D.3})$$

Observe the action of  $i\Omega_{n-1} \oplus \mathbb{1} + Q_1 R Q_1^\top$  on  $v_\lambda^{(1)}$

$$\begin{aligned} (Q_1 R Q_1^\top + i\Omega_n + \mathbf{O}_{n-1} \oplus (\mathbb{1} - i\Omega)) \begin{pmatrix} \boldsymbol{\alpha}^{(1)} + i\boldsymbol{\beta}^{(1)} \\ \mathbf{a}_{n-1}^{(1)} + i\mathbf{b}_{n-1}^{(1)} \\ \mathbf{a}_n^{(1)} + i\mathbf{b}_n^{(1)} \end{pmatrix} = \\ = \lambda v_\lambda^{(1)} + \begin{pmatrix} \mathbf{0}_{2n-4} \\ \mathbf{0} \\ \mathbf{a}_n^{(1)} + \Omega \mathbf{b}_n^{(1)} - i\Omega(\mathbf{a}_n^{(1)} + \Omega \mathbf{b}_n^{(1)}) \end{pmatrix}. \end{aligned} \quad (\text{D.4})$$

Consider the following symplectic orthogonal transformation

$$Q_1 = \mathbb{1}_{n-2} \oplus \begin{pmatrix} \cos \phi_1 \mathbb{1} & -\sin \phi_1 O_1 \\ \sin \phi_1 O_1 & \cos \phi_1 \mathbb{1} \end{pmatrix}, \quad (\text{D.5})$$

where  $O_1$  is a  $2 \times 2$  orthogonal matrix. Using this transformation we have

$$\begin{aligned} v_\lambda^{(1)} = \begin{pmatrix} \boldsymbol{\alpha} \\ \cos \phi_1 \mathbf{a}_{n-1} - \sin \phi_1 O_1 \mathbf{a}_n \\ \cos \phi_1 \mathbf{a}_n + \sin \phi_1 O_1 \mathbf{a}_{n-1} \end{pmatrix} + \\ + i \begin{pmatrix} \boldsymbol{\beta} \\ \cos \phi_1 \mathbf{b}_{n-1} - \sin \phi_1 O_1 \mathbf{b}_n \\ \cos \phi_1 \mathbf{b}_n + \sin \phi_1 O_1 \mathbf{b}_{n-1} \end{pmatrix}. \end{aligned} \quad (\text{D.6})$$

The two-dimensional vector  $\mathbf{a}_n^{(1)} + \Omega \mathbf{b}_n^{(1)}$  in the last term of Eq.D.4 can now be written as

$$\mathbf{a}_n^{(1)} + \Omega \mathbf{b}_n^{(1)} = \cos \phi_1 (\mathbf{a}_n + \Omega \mathbf{b}_n) + \sin \phi_1 O_1 (\mathbf{a}_{n-1} + \Omega \mathbf{b}_{n-1}). \quad (\text{D.7})$$

Notice that given any two real two-dimensional vectors  $\mathbf{r}_1$  and  $\mathbf{r}_2$  one can always find a rotation  $O_1$  and an angle  $\phi_1$  such that  $\cos \phi_1 \mathbf{r}_1 + \sin \phi_1 O_1 \mathbf{r}_2 = \mathbf{0}$ . Indeed, the rotation  $O_1$  directs the second vector to be parallel to the first and  $\sin \phi_1$  and  $\cos \phi_1$  adjust the lengths. Therefore, we showed that it is possible to find a symplectic orthogonal transformation  $Q_1$ , i.e.  $O_1$  and  $\phi_1$ , such that the last term of Eq.D.4 vanishes, hence that  $v_\lambda^{(1)}$  is an eigenvector of  $i\Omega_{n-1} \oplus \mathbb{1} + Q_1 R Q_1^\top$  corresponding to the eigenvalue  $\lambda$ .

Using an analogous argument we can show that  $\lambda$  is also an eigenvalue of  $i\Omega_{n-2} \oplus \mathbb{1}_2 + Q_2 \tilde{R} Q_2^\top$ , where  $\tilde{R} = Q_1 R Q_1^\top$ , corresponding to the eigenvector  $v_\lambda^{(2)} = Q_2 v_\lambda^{(1)}$ , with

$$Q_2 = \mathbb{1}_{n-3} \oplus \begin{pmatrix} \cos \phi_2 \mathbb{1} & -\sin \phi_2 O_2 \\ \sin \phi_2 O_2 & \cos \phi_2 \mathbb{1} \end{pmatrix} \oplus \mathbb{1}, \quad (\text{D.8})$$

with  $O_2$ ,  $2 \times 2$  orthogonal matrix, and  $\phi_2$  satisfying

$$\cos \phi_2(\mathbf{a}_{n-1}^{(1)} + \Omega \mathbf{b}_{n-1}^{(1)}) + \sin \phi_2 O_2(\mathbf{a}_{n-2}^{(1)} + \Omega \mathbf{b}_{n-2}^{(1)}) = 0. \quad (\text{D.9})$$

Iterating this procedure we find that  $Q = Q_k \cdot Q_{k-1} \cdots Q_2 \cdot Q_1$ . This completes the proof.  $\square$

We can now prove Th.7.1:

*Proof.* We want now to deliver a condition on a map  $(X, Y)$  acting on an  $n$ -mode quantum system guaranteeing that the inequality Eq.7.17 is satisfied for every  $V_{n+k}$  where  $1 \leq k$ . We consider a generic bipartite  $(n+k)$ -mode covariance matrix

$$V_{n+k} = \begin{pmatrix} A & C \\ C^\top & B \end{pmatrix}, \quad (\text{D.10})$$

where  $A$  is a  $2n \times 2n$  symmetric matrix,  $B$  is a  $2k \times 2k$  symmetric matrix and  $C$  is a  $2n \times 2k$  matrix. Inequality Eq.7.17 reads

$$\begin{aligned} & \begin{pmatrix} XAX^\top + Y - i\Omega_n & XC \\ C^\top X^\top & B - i\Omega_k \end{pmatrix} \geq 0 \Leftrightarrow \\ & \Leftrightarrow \begin{pmatrix} A + X^{-1}(Y - i\Omega_n)(X^\top)^{-1} & C \\ C^\top & B - i\Omega_k \end{pmatrix} \geq 0, \end{aligned} \quad (\text{D.11})$$

where we assume that  $X$  is invertible. As  $V_{n+k} \geq i\Omega_{n+k}$ , we also have that  $B - i\Omega_k \geq 0$ . Assuming invertibility of  $B - i\Omega_k$ , the Schur's complement Lemma ensures that condition Eq.D.11 is equivalent to positivity of the Schur's complement of the block  $B - i\Omega_k$ , i.e.

$$A + X^{-1}(Y - i\Omega_n)(X^\top)^{-1} - C(B - i\Omega_k)^{-1}C^\top \geq 0. \quad (\text{D.12})$$

Moreover, applying the Schur's complement Lemma to  $V_{n+k} - i\Omega_{n+k}$  we get

$$A - i\Omega_n - C(B - i\Omega_k)^{-1}C^\top \geq 0. \quad (\text{D.13})$$

Hence, the left hand side of Eq.D.12 can be decomposed in a positive state-dependent term and in a map-dependent one:

$$\begin{aligned} & \underbrace{A - i\Omega_n - C(B - i\Omega_k)^{-1}C^\top}_{\text{state-dependent}} + \\ & \quad + \underbrace{X^{-1}(Y - i\Omega_n)(X^\top)^{-1} + i\Omega_n}_{\text{map-dependent}} \geq 0. \end{aligned} \quad (\text{D.14})$$

This condition has to be satisfied for any  $n + k$ -modes state. Due to the Williamson's theorem we can derive that for any mixed state  $V_{\text{mixed}}$  there exists a pure state  $V_{\text{pure}}^S$  such that

$$V_{\text{mixed}} = S \boldsymbol{\nu} S^\top \geq S \mathbb{1}_{n+k} S^\top = V_{\text{pure}}^S, \quad (\text{D.15})$$

with  $\boldsymbol{\nu} = \text{diag}\{\nu_1, \nu_1, \dots, \nu_{n+k}, \nu_{n+k}\}$ . It is then sufficient to check that inequality Eq.D.14 holds for pure states to guarantee that it is satisfied for all states. By using again the Williamson's Theorem we find that local symplectic transformations  $S_n$  and  $S_k$  can bring the covariance matrix of any pure  $n + k$ -mode Gaussian state  $(S_n \oplus S_k) V_{\text{pure}}^S (S_n \oplus S_k)^\top$  to the normal form, i.e. the block form with non-zero entries only on the diagonal of each block, see Section 2.2.3. For  $k \leq n$  the blocks are

$$A = S_n \left( \bigoplus_{j=1}^k \cosh r_j \mathbb{1} \oplus \mathbb{1}_{n-k} \right) S_n^\top, \quad (\text{D.16})$$

$$B = S_k \left( \bigoplus_{j=1}^k \cosh r_j \mathbb{1} \right) S_k^\top, \quad (\text{D.17})$$

$$C = S_n \left( \frac{\bigoplus_{j=1}^k -\sinh r_j \sigma_z}{\diamond} \right) S_n^\top, \quad (\text{D.18})$$

where  $\diamond$  is an  $2(n - k) \times 2n$  null matrix. We have then

$$C(B - i\boldsymbol{\Omega}_k)^{-1} C^\top = S_n \left( \bigoplus_{j=1}^k (\cosh r_j \mathbb{1} - i\boldsymbol{\Omega}) \oplus \mathbf{O}_{n-k} \right) S_n^\top. \quad (\text{D.19})$$

As a consequence, Eq.D.14 is satisfied for any state if

$$S_n (i\boldsymbol{\Omega}_k \oplus \mathbb{1}_{n-k}) S_n^\top + X^{-1} (Y - i\boldsymbol{\Omega}_n) (X^\top)^{-1} \geq 0, \quad (\text{D.20})$$

holds for every  $S_n \in \text{Sp}(2n, \mathbb{R})$ . Notice that for every  $S_n$

$$\begin{aligned} S_n (i\boldsymbol{\Omega}_k \oplus \mathbb{1}_{n-k}) S_n^\top + X^{-1} (Y - i\boldsymbol{\Omega}_n) (X^\top)^{-1} &\geq \\ &\geq i\boldsymbol{\Omega}_n + X^{-1} (Y - i\boldsymbol{\Omega}) (X^\top)^{-1}. \end{aligned} \quad (\text{D.21})$$

This inequality implies that the left hand side cannot have an eigenvalue smaller than the smallest eigenvalue of the right hand side. To complete the proof of Theorem 7.1 it is sufficient to show that there exists  $S_n$  such that the left hand side and the right hand side have the same the smallest eigenvalue

for any  $1 \leq k$ . For  $1 \leq k \leq n$ , this is guaranteed by Lemma 2. Indeed, this lemma shows that there exists a symplectic orthogonal transformation  $Q$  such that

$$\begin{aligned} \min \left\{ \text{eig} \left( Q^\top (i\mathbf{\Omega}_k \oplus \mathbb{1}_{n-k}) Q + X^{-1}(Y - i\mathbf{\Omega})(X^\top)^{-1} \right) \right\} = \\ = \min \left\{ \text{eig} \left( i\mathbf{\Omega}_n + X^{-1}(Y - i\mathbf{\Omega})(X^\top)^{-1} \right) \right\}. \end{aligned} \quad (\text{D.22})$$

If  $k > n$ , then Eq.D.14 becomes equal to the right hand side of Eq.D.21. Summarizing, the positivity condition Eq.7.17 for  $k = 1$  is equivalent to the positivity condition for any  $k \geq 1$ . This completes the proof of the Theorem.  $\square$



---

## TELEPORTATION OUTPUT

---

We will derive here Eqs.8.3-8.2.

Thanks to the Fourier-Weyl relation, we can express the state of the global system, given by the input state  $(V_{\text{in}}, \mathbf{d}_{\text{in}})$  and by the state shared by Alice and Bob  $(V_{AB}, \mathbf{d}_{AB})$ , up to a normalization constant, as

$$\hat{\rho}_{\text{inAB}}^{(0)} \propto \int d\mathbf{r}_{\text{in}} d\mathbf{r}_A d\mathbf{r}_B e^{-\frac{1}{4}\mathbf{r}^\top \Omega_3^\top (V_{\text{in}} \oplus V_{AB}) \Omega_3 \mathbf{r} + i\mathbf{d}^\top \Omega_3 \mathbf{r}} \hat{D}_{\mathbf{r}_{\text{inA}}} \otimes \hat{D}_{\mathbf{r}_B}, \quad (\text{E.1})$$

where  $\hat{D}_{\mathbf{r}_{\text{inA}}}$  is the displacement operator acting on  $\mathcal{H}_{\text{in}} \otimes \mathcal{H}_A$  and  $\mathbf{r} = \mathbf{r}_{\text{inA}} \oplus \mathbf{r}_B$ , with  $\mathbf{r}_{\text{inA}} = \mathbf{r}_{\text{in}} \oplus \mathbf{r}_A$  (analogously for  $\mathbf{d}$ ). We rewrite  $\Omega_3^\top (V_{\text{in}} \oplus V_{AB}) \Omega_3$  in block form as follows

$$\Omega_3^\top (V_{\text{in}} \oplus V_{AB}) \Omega_3 = \begin{pmatrix} \tilde{V}_{\text{inA}} & \tilde{V}_{\text{inAB}} \\ \tilde{V}_{\text{inAB}}^\top & \tilde{V}_B \end{pmatrix}, \quad (\text{E.2})$$

where the upper-left  $4 \times 4$  block is  $\tilde{V}_{\text{inA}} = \Omega_2 (V_{\text{in}} \oplus A) \Omega_2$ , the off-diagonal  $4 \times 2$  block is  $\tilde{V}_{\text{inAB}} = (\diamond \Omega^\top C^\top \Omega)^\top$  and the bottom-right  $2 \times 2$  block on the diagonal  $\tilde{V}_B = \Omega^\top B \Omega$ . We can rewrite Eq.E.1 as

$$\begin{aligned} \hat{\rho}_{\text{inAB}}^{(0)} \propto \int d\mathbf{r} \exp \left\{ -\frac{1}{4}\mathbf{r}_{\text{inA}}^\top \tilde{V}_{\text{inA}} \mathbf{r}_{\text{inA}} - i \left( \Omega_2 \mathbf{d}_{\text{inA}} + \frac{i}{2} \tilde{V}_{\text{inAB}} \mathbf{r}_B \right)^\top \mathbf{r}_{\text{inA}} \right\} \\ \cdot \exp \left\{ -\frac{1}{4}\mathbf{r}_B^\top \tilde{V}_B \mathbf{r}_B - i(\Omega \mathbf{d}_B)^\top \mathbf{r}_B \right\} \hat{D}_{\mathbf{r}_{\text{inA}}} \otimes \hat{D}_{\mathbf{r}_B}. \end{aligned}$$

Alice mixes in a 50:50 beam splitter the input mode and her part of the shared state

$$\begin{aligned} \hat{\rho}_{\text{inAB}}^{(0)} \rightarrow \hat{\rho}_{\text{inAB}}^{(1)} &= \hat{\mathcal{B}}_{\text{inA}} \otimes \mathbb{1}^B \hat{\rho}_{\text{inAB}}^{(0)} \hat{\mathcal{B}}_{\text{inA}}^\dagger \otimes \mathbb{1}^B \propto \\ &\propto \int d\mathbf{r} \exp \left\{ -\frac{1}{4}\mathbf{r}_{\text{inA}}^\top \tilde{V}_{\text{inA}} \mathbf{r}_{\text{inA}} - i \left( \Omega_2 \mathbf{d}_{\text{inA}} + \frac{i}{2} \tilde{V}_{\text{inAB}} \mathbf{r}_B \right)^\top \mathbf{r}_{\text{inA}} \right\} \\ &\cdot \exp \left\{ -\frac{1}{4}\mathbf{r}_B^\top \tilde{V}_B \mathbf{r}_B - i(\Omega \mathbf{d}_B)^\top \mathbf{r}_B \right\} \hat{\mathcal{B}}_{\text{inA}} \hat{D}_{\mathbf{r}_{\text{inA}}} \hat{\mathcal{B}}_{\text{inA}}^\dagger \otimes \hat{D}_{\mathbf{r}_B}, \end{aligned}$$

where  $\hat{B}_{\text{in}A}$  is the beam splitter unitary. Let  $\mathcal{B}$  be the beam-splitter symplectic transformation on phase space defined as

$$\mathcal{B} = \frac{1}{\sqrt{2}} \begin{pmatrix} \mathbb{1} & \mathbb{1} \\ \mathbb{1} & -\mathbb{1} \end{pmatrix}. \quad (\text{E.3})$$

Since  $\hat{B}_{\text{in}A} \hat{D}_{r_{\text{in}A}} \hat{B}_{\text{in}A}^\dagger = \hat{D}_{\mathcal{B}^{-1}r_{\text{in}A}}$ , a change of variables  $\mathbf{u} = \mathcal{B}^{-1}r_{\text{in}A} = r_+ \oplus r_-$  gives

$$\begin{aligned} \hat{\rho}_{\text{in}AB}^{(1)} &\propto \int d\mathbf{u} d\mathbf{r}_B \hat{D}_{\mathbf{u}} \otimes \hat{D}_{r_B} \exp \left\{ -\frac{1}{4} \mathbf{r}_B^\top \tilde{V}_B \mathbf{r}_B - i(\Omega \mathbf{d}_B)^\top \mathbf{r}_B \right\} \\ &\cdot \exp \left\{ -\frac{1}{4} \mathbf{u}^\top \mathcal{B}^\top \tilde{V}_{\text{in}A} \mathcal{B} \mathbf{u} - i \left( \Omega_2 \mathbf{d}_{\text{in}A} + \frac{i}{2} \tilde{V}_{\text{in}AB} r_B \right)^\top \mathcal{B} \mathbf{u} \right\}. \end{aligned}$$

At this point, Alice measures, through a double homodyne detection, the commuting quadratures  $\hat{Q}_+ = \frac{\hat{q}_{\text{in}+} + \hat{q}_A}{\sqrt{2}}$  and  $\hat{P}_- = \frac{\hat{p}_{\text{in}-} - \hat{p}_A}{\sqrt{2}}$  and communicates the outcomes  $(Q_+, P_-)$  to Bob who will displace his part of the shared state accordingly, i.e. he applies the displacement  $\hat{D}_{-\delta}$ , with  $\delta = g\sqrt{2}(Q_+, P_-)$  to his mode. To describe mathematically this part of the protocol we make use of the fact that it is possible to define a set of POVMs that correspond to ideal general-dyne detections on  $m$  modes thanks to the non-orthogonal set of projectors [29]

$$\left\{ \hat{\Pi}_v^{(\hat{S})} \right\}_{v \in \mathbb{R}^{2m}} = \left\{ \frac{\hat{D}_v \hat{S} |0\rangle \langle 0| \hat{S}^\dagger \hat{D}_v^\dagger}{(2\pi)^m} \right\}_{v \in \mathbb{R}^{2m}}, \quad (\text{E.4})$$

where  $\hat{S}$  is a Gaussian unitary transformation. It is easy to verify this set of projectors resolve the identity. The homodyne detection of the quadrature  $\hat{q}$  ( $\hat{p}$ ) corresponds to choose  $\hat{S}$  to be the single-mode squeezing operation, described on phase-space by the symplectic  $S_{\hat{q}} = \text{diag}\{1/z, z\}$  ( $S_{\hat{p}} = \text{diag}\{z, 1/z\}$ ) in the limit of infinite squeezing parameter  $z \rightarrow \infty$ .

The measurement performed by Alice and Bob's conditional displacement are hence described by

$$\begin{aligned} \hat{\rho}_{\text{in}AB}^{(1)} &\rightarrow \hat{\rho}_{\text{in}AB}^{(2)} = \int d\mathbf{v}_+ d\mathbf{v}_- \Pi_{v_+} \otimes \Pi_{v_-} \otimes \hat{D}_{-\delta} \hat{\rho}_{\text{in}AB}^{(1)} \Pi_{v_+} \otimes \Pi_{v_-} \otimes \hat{D}_{-\delta}^\dagger \propto \\ &\propto \int d\mathbf{u} d\mathbf{r}_B d\mathbf{v}_+ d\mathbf{v}_- p(v_+, v_-) \Pi_{v_+} \otimes \Pi_{v_-} \otimes \hat{D}_{-\delta} \hat{D}_{r_B} \hat{D}_{-\delta}^\dagger \cdot \\ &\cdot \exp \left\{ -\frac{1}{4} \mathbf{u}^\top \mathcal{B}^\top \tilde{V}_{\text{in}A} \mathcal{B} \mathbf{u} - i \left( \Omega_2 \mathbf{d}_{\text{in}A} + \frac{i}{2} \tilde{V}_{\text{in}AB} r_B \right)^\top \mathcal{B} \mathbf{u} \right\} \cdot \\ &\cdot \exp \left\{ -\frac{1}{4} \mathbf{r}_B^\top \tilde{V}_B \mathbf{r}_B - i(\Omega \mathbf{d}_B)^\top \mathbf{r}_B \right\} \end{aligned}$$

where  $p(\nu_+, \nu_-) = p(Q_+, P_+, Q_-, P_-) = p(\nu)$  is the probability density of the measurement outcomes  $(\nu_+, \nu_-) = (Q_+, P_+, Q_-, P_-)$ :

$$p(\nu_+, \nu_-) \propto \langle 0 | \hat{S}_{\hat{Q}_+}^\dagger \hat{D}_{\nu_+}^\dagger \hat{D}_{r_+} \hat{D}_{\nu_+} \hat{S}_{\hat{Q}_+} | 0 \rangle \langle 0 | \hat{S}_{\hat{P}_-}^\dagger \hat{D}_{\nu_-}^\dagger \hat{D}_{r_-} \hat{D}_{\nu_-} \hat{S}_{\hat{P}_-} | 0 \rangle .$$

Since  $\hat{D}_x^\dagger \hat{D}_y \hat{D}_x = e^{ix^\top \Omega y} \hat{D}_y$  and calling  $S_+ = \text{diag}\{1/z, z\}$  and  $S_- = \text{diag}\{z, 1/z\}$  the symplectic matrices associated to  $\hat{S}_{\hat{Q}_+}$  and  $\hat{S}_{\hat{P}_-}$  respectively, the above becomes

$$\begin{aligned} p(\nu_+, \nu_-) &\propto \exp \left\{ i \nu^\top \Omega_2 \mathbf{u} \right\} \langle 0 | \hat{D}_{(S_+ \oplus S_-) \mathbf{u}} | 0 \rangle = \\ &= \exp \left\{ i \nu^\top \Omega_2 \mathbf{u} \right\} \exp \left\{ -\frac{1}{4} \mathbf{u}^\top \Omega_2^\top (S_+^\top S_+ \oplus S_-^\top S_-) \Omega_2 \mathbf{u} \right\} = \\ &= \exp \left\{ i \nu^\top \Omega_2 \mathbf{u} \right\} \exp \left\{ -\frac{1}{4} \mathbf{u}^\top \tilde{S}^\top \tilde{S} \mathbf{u} \right\} , \end{aligned}$$

where  $\tilde{S} = \Omega_2^\top (S_+ \oplus S_-) \Omega_2$ . We can now integrate over  $\mathbf{u}$ :

$$\int d\mathbf{u} \exp \left\{ -\frac{1}{4} \mathbf{u}^\top \Gamma \mathbf{u} + i \left( \nu^\top \Omega_2 - \mathbf{d}_{\text{in}A}^\top \Omega_2^\top \mathcal{B} - \frac{i}{2} \mathbf{r}_B^\top \tilde{V}_{\text{in}AB}^\top \mathcal{B} \right) \mathbf{u} \right\} , \quad (\text{E.5})$$

where  $\Gamma = \mathcal{B}^\top \tilde{V}_{\text{in}A} \mathcal{B} + \tilde{S}^\top \tilde{S}$ . Recalling that for a symmetric  $2n \times 2n$  matrix  $V$  and  $2n$ -dimensional vector  $\mathbf{b}$  we have the identity

$$\int_{\mathbb{R}^{2n}} d\mathbf{x} e^{-\mathbf{x}^\top V \mathbf{x} + \mathbf{b}^\top \mathbf{x}} = \frac{\pi^n}{\sqrt{\det V}} e^{\frac{1}{4} \mathbf{b}^\top V^{-1} \mathbf{b}} , \quad (\text{E.6})$$

the above integral Eq.E.5 becomes  $1/\sqrt{\det \Gamma} e^{-k}$  with

$$\begin{aligned} k &= \nu^\top \Omega_2 \Gamma^{-1} \Omega_2^\top \nu - 2 \nu^\top \Omega_2 \Gamma^{-1} \mathcal{B}^\top \Omega_2 \mathbf{d}_{\text{in}A} - \\ &\quad - i \nu^\top \Omega_2 \Gamma^{-1} \mathcal{B}^\top \tilde{V}_{\text{in}AB} \mathbf{r}_B + \mathbf{d}_{\text{in}A}^\top \Omega_2^\top \mathcal{B} \Gamma^{-1} \mathcal{B}^\top \Omega_2 \mathbf{d}_{\text{in}A} + \\ &\quad + i \mathbf{d}_{\text{in}A}^\top \Omega_2^\top \mathcal{B} \Gamma^{-1} \mathcal{B}^\top \tilde{V}_{\text{in}AB} \mathbf{r}_B - \frac{1}{4} \mathbf{r}_B^\top \tilde{V}_{\text{in}AB}^\top \mathcal{B} \Gamma^{-1} \mathcal{B}^\top \tilde{V}_{\text{in}AB} \mathbf{r}_B \end{aligned}$$

We can trace over the first two degrees of freedom to obtain Bob's state

$$\begin{aligned} \text{Tr}_{\text{in}A} \hat{\rho}_{\text{in}AB}^{(2)} &\propto \int d\mathbf{r}_B d\nu \hat{D}_{-\delta} \hat{D}_{r_B} \hat{D}_{-\delta}^\dagger \text{Tr}_{\text{in}A} [\Pi_{\nu_+} \otimes \Pi_{\nu_-}] \cdot \\ &\quad \cdot \frac{e^{-k}}{\sqrt{\det \Gamma}} \exp \left\{ -\frac{1}{4} \mathbf{r}_B^\top \tilde{V}_B \mathbf{r}_B - i (\Omega^\top \mathbf{d}_B)^\top \mathbf{r}_B \right\} , \end{aligned}$$

and since the trace of a projector is equal to 1 we get

$$\begin{aligned}
 & \propto \int \frac{d\nu dr_B}{\sqrt{\det\Gamma}} \hat{D}_{-\delta} \hat{D}_{r_B} \hat{D}_{-\delta}^\dagger \exp \left\{ -\mathbf{d}_{\text{in}A} \boldsymbol{\Omega}^\top \mathcal{B} \Gamma^{-1} \mathcal{B}^\top \boldsymbol{\Omega} \mathbf{d}_{\text{in}A} \right\} \cdot \\
 & \cdot \exp \left\{ -\nu^\top \boldsymbol{\Omega}_2 \Gamma^{-1} \boldsymbol{\Omega}_2^\top \nu + \left( 2\boldsymbol{\Omega}_2 \Gamma^{-1} \mathcal{B}^\top \boldsymbol{\Omega}_2 \mathbf{d}_{\text{in}A} + i\boldsymbol{\Omega}_2 \Gamma^{-1} \mathcal{B}^\top \tilde{V}_{\text{in}AB} \mathbf{r}_b \right)^\top \nu \right\} \cdot \\
 & \cdot \exp \left\{ -\frac{1}{4} \mathbf{r}_B^\top \left( \tilde{V}_B - \tilde{V}_{\text{in}AB}^\top \mathcal{B} \Gamma^{-1} \mathcal{B}^\top \tilde{V}_{\text{in}AB} \right) \mathbf{r}_b - \right. \\
 & \quad \left. - i \left( \boldsymbol{\Omega} \mathbf{d}_b + \tilde{V}_{\text{in}AB}^\top \mathcal{B} \Gamma^{-1} \mathcal{B}^\top \boldsymbol{\Omega}_2 \mathbf{d}_{\text{in}A} \right)^\top \mathbf{r}_B \right\} .
 \end{aligned}$$

Defining the  $4 \times 2$  gain matrix  $G$  as

$$G = g\sqrt{2} \begin{pmatrix} 0 & 1 \\ 0 & 0 \\ 0 & 0 \\ -1 & 0 \end{pmatrix} = g\sqrt{2} \begin{pmatrix} \sigma_+ \\ -\sigma_- \end{pmatrix} , \quad (\text{E.7})$$

where the  $2 \times 2$  matrices  $\sigma_\pm$  are the shift Pauli matrices, we have

$$\hat{D}_{-\delta} \hat{D}_{r_B} \hat{D}_{-\delta}^\dagger = e^{i\mathbf{r}_B^\top \boldsymbol{\Omega} \delta} \hat{D}_{r_B} = e^{i\mathbf{r}_B^\top G^\top \nu} \hat{D}_{r_B} . \quad (\text{E.8})$$

To conclude the derivation we average over the measurement outcomes, i.e. we integrate over  $\nu$ . This is again a Gaussian integral Eq.E.6 with

$$\begin{aligned}
 V &= \boldsymbol{\Omega}_2 \Gamma^{-1} \boldsymbol{\Omega}_2^\top , \\
 \mathbf{b} &= 2\boldsymbol{\Omega}_2 \Gamma^{-1} \mathcal{B}^\top \boldsymbol{\Omega}_2 \mathbf{d}_{\text{in}A} + i\boldsymbol{\Omega}_2 \Gamma^{-1} \mathcal{B}^\top \tilde{V}_{\text{in}AB} \mathbf{r}_B + iG \mathbf{r}_B .
 \end{aligned}$$

The result of this integral is

$$\begin{aligned}
 & \propto \sqrt{\det\Gamma} \exp \left\{ \mathbf{d}_{\text{in}A}^\top \boldsymbol{\Omega}_2^\top \mathcal{B} \Gamma^{-1} \mathcal{B}^\top \boldsymbol{\Omega}_2 \mathbf{d}_{\text{in}A} + i\mathbf{d}_{\text{in}A}^\top \boldsymbol{\Omega}^\top \mathcal{B} \Gamma^{-1} \mathcal{B}^\top \tilde{V}_{\text{in}AB} \mathbf{r}_B + \right. \\
 & \quad + i\mathbf{d}_{\text{in}A}^\top \boldsymbol{\Omega}_2^\top \mathcal{B} \boldsymbol{\Omega}_2^\top G \mathbf{r}_B - \frac{1}{4} \mathbf{r}_B^\top \tilde{V}_{\text{in}AB}^\top \mathcal{B} \Gamma^{-1} \mathcal{B}^\top \tilde{V}_{\text{in}AB} \mathbf{r}_B - \\
 & \quad - \frac{1}{4} \mathbf{r}_B^\top \tilde{V}_{\text{in}AB} \mathcal{B} \boldsymbol{\Omega}_2 G \mathbf{r}_B - \frac{1}{4} \mathbf{r}_B^\top G^\top \boldsymbol{\Omega}_2 \mathcal{B}^\top \tilde{V}_{\text{in}AB} \mathbf{r}_B - \\
 & \quad \left. - \frac{1}{4} \mathbf{r}_B^\top G^\top \boldsymbol{\Omega}_2 \Gamma \boldsymbol{\Omega}_2 G \mathbf{r}_B \right\} .
 \end{aligned}$$

The output state Bob is left with is

$$\begin{aligned}
 \hat{\rho}_B^{(\text{out})} & \propto \int d\mathbf{r}_B \hat{D}_{r_B} \exp \left\{ i \left( \mathbf{d}_B^\top + \mathbf{d}_{\text{in}A}^\top \boldsymbol{\Omega}_2^\top \mathcal{B} \boldsymbol{\Omega}_2^\top G \boldsymbol{\Omega}^\top \right) \boldsymbol{\Omega} \mathbf{r}_B \right\} \cdot \\
 & \exp \left\{ -\frac{1}{4} \mathbf{r}_B^\top \left( \tilde{V}_B + G^\top \boldsymbol{\Omega}_2 \Gamma \boldsymbol{\Omega}_2^\top G + \right. \right. \\
 & \quad \left. \left. + \tilde{V}_{\text{in}AB}^\top \mathcal{B} \boldsymbol{\Omega}_2^\top G + G^\top \boldsymbol{\Omega}_2 \mathcal{B}^\top \tilde{V}_{\text{in}AB} \right) \mathbf{r}_B \right\} \\
 & \quad (\text{E.9})
 \end{aligned}$$

which is a Gaussian state with first moment vector

$$\mathbf{d}_{\text{out}} = \mathbf{d}_B + \Omega G^\top \Omega_2 \mathcal{B}^\top \Omega_2 \mathbf{d}_{\text{in}A} = \mathbf{d}_B - \Omega G^\top \mathcal{B}^\top \mathbf{d}_{\text{in}A} = \mathbf{d}_B + \sqrt{2}g\delta .$$

If  $\mathbf{d}_A = \mathbf{d}_B = \mathbf{0}$ , then the above simply reduces to Eq.8.2. The covariance matrix is

$$V_{\text{out}} = B + \Omega \left( \tilde{V}_{\text{in}AB}^\top \mathcal{B} \Omega_2^\top G + G^\top \Omega_2 \mathcal{B}^\top \tilde{V}_{\text{in}AB} + G^\top \Omega_2 \Gamma \Omega_2^\top G \right) \Omega^\top .$$

Notice that

$$\begin{aligned} \Omega \tilde{V}_{\text{in}AB}^\top \mathcal{B} \Omega_2^\top G \Omega^\top &= g \left( \diamond C^\top \Omega \right) \begin{pmatrix} \mathbb{1} & \mathbb{1} \\ \mathbb{1} & -\mathbb{1} \end{pmatrix} \Omega_2^\top \begin{pmatrix} \sigma_+ \Omega^\top \\ \sigma_- \Omega^\top \end{pmatrix} = \\ &= g \left( C^\top \Omega \quad -C^\top \Omega \right) \begin{pmatrix} \Omega^\top \sigma_+ \Omega^\top \\ -\Omega^\top \sigma_- \Omega^\top \end{pmatrix} = \\ &= g C^\top (\sigma_+ \Omega^\top + \sigma_- \Omega^\top) = g C^\top \sigma_z , \end{aligned}$$

and

$$\Omega G^\top \Omega_2 \mathcal{B}^\top \tilde{V}_{\text{in}AB} \Omega^\top = (\Omega \tilde{V}_{\text{in}AB}^\top \mathcal{B} \Omega_2^\top G \Omega^\top)^\top = g \sigma_z C^\top . \quad (\text{E.10})$$

Let us focus now on the last term: we can rewrite it as

$$\Omega G^\top \Omega_2 \Gamma \Omega_2^\top G \Omega^\top = \Omega G^\top \left( \mathcal{B}^\top V_{\text{in}A} \mathcal{B} + (S_+^\top S_+ \oplus S_-^\top S_-) \right) G \Omega ,$$

recasting this in block matrices form one gets

$$\begin{aligned} &g^2 (\Omega \sigma_- \quad \Omega \sigma_+) \begin{pmatrix} \frac{V_{\text{in}+A}}{2} + S_+^\top S_+ & \frac{V_{\text{in}-A}}{2} \\ \frac{V_{\text{in}-A}}{2} & \frac{V_{\text{in}+A}}{2} + S_-^\top S_- \end{pmatrix} \begin{pmatrix} \sigma_+ \Omega^\top \\ -\sigma_- \Omega^\top \end{pmatrix} = \\ &= g^2 \left( \Omega \sigma_- \frac{V_{\text{in}+A}}{2} \sigma_+ \Omega^\top + \Omega \sigma_- S_+^\top S_+ \sigma_+ \Omega^\top - \Omega \sigma_- \frac{V_{\text{in}-A}}{2} \sigma_- \Omega^\top - \right. \\ &\quad \left. - \Omega \sigma_+ \frac{V_{\text{in}-A}}{2} \sigma_+ \Omega^\top + \Omega \sigma_+ \frac{V_{\text{in}+A}}{2} \sigma_- \Omega^\top + \Omega \sigma_+ S_-^\top S_- \sigma_- \Omega^\top \right) . \end{aligned}$$

Now, given a symmetric matrix  $M = \begin{pmatrix} a & b \\ b & c \end{pmatrix}$  it is easy to verify that

$$\begin{aligned} \Omega \sigma_- M \sigma_+ \Omega &= \begin{pmatrix} a & 0 \\ 0 & 0 \end{pmatrix} , & \Omega \sigma_- M \sigma_- \Omega &= \begin{pmatrix} 0 & -b \\ 0 & 0 \end{pmatrix} , \\ \Omega \sigma_+ M \sigma_- \Omega &= \begin{pmatrix} 0 & 0 \\ 0 & c \end{pmatrix} , & \Omega \sigma_+ M \sigma_+ \Omega &= \begin{pmatrix} 0 & 0 \\ -b & 0 \end{pmatrix} , \end{aligned}$$

from which follows

$$\Omega G^\top \Omega_2 \Gamma \Omega_2^\top G \Omega^\top = g^2 V_{\text{in}} + g^2 \sigma_z A \sigma_z + \frac{1}{z^2} \mathbb{1}. \quad (\text{E.11})$$

The last term in the above vanishes in the limit of ideal homodyne detection  $z \rightarrow \infty$  and the final form for the output covariance matrix is finally derived:

$$V_{\text{out}} = g^2 V_{\text{in}} + g^2 \sigma_z A \sigma_z + g \left( \sigma_z C^\top + C^\top \sigma_z \right) + B. \quad (\text{E.12})$$

---

## BIBLIOGRAPHY

---

- [1] W. H. Zurek, “Decoherence, einselection, and the quantum origins of the classical,” *Rev. Mod. Phys.*, vol. 75, pp. 715–775, May 2003. (cited on page 1).
- [2] M. Schlosshauer, *Decoherence and the quantum-to-classical transition*. No. 1 in The Frontiers Collection, Springer-Verlag Berlin Heidelberg, 2007. (cited on pages 1, 7, 28, and 118).
- [3] R. Horodecki, P. Horodecki, M. Horodecki, and K. Horodecki, “Quantum entanglement,” *Rev. Mod. Phys.*, vol. 81, pp. 865–942, Jun 2009. (cited on pages 1, 20).
- [4] A. Streltsov, G. Adesso, and M. B. Plenio, “Colloquium: Quantum coherence as a resource,” *Rev. Mod. Phys.*, vol. 89, p. 041003, Oct 2017. (cited on page 1).
- [5] C. H. Bennett, G. Brassard, C. Crépeau, R. Jozsa, A. Peres, and W. K. Wootters, “Teleporting an unknown quantum state via dual classical and Einstein-Podolsky-Rosen channels,” *Phys. Rev. Lett.*, vol. 70, p. 1895, 1993. (cited on pages 1, 123, and 124).
- [6] R. Schnabel, N. Mavalvala, D. E. McClelland, and P. K. Lam, “Quantum metrology for gravitational wave astronomy,” *Nature Commun.*, vol. 1, p. 121, 2010. (cited on page 1).
- [7] V. Giovannetti, S. Lloyd, and L. Maccone, “Advances in quantum metrology,” *Nature Photon.*, vol. 5, p. 222, 2011. (cited on pages 1, 62, 97, 100, and 103).
- [8] M. A. Nielsen and I. L. Chuang, *Quantum Computation and Quantum Information: 10th Anniversary Edition*. New York, NY, USA: Cambridge University Press, 10th ed., 2011. (cited on page 7).

## Bibliography

- [9] H. P. Breuer and F. Petruccione, *The theory of open quantum systems*. Great Clarendon Street: Oxford University Press, 2002. (cited on pages 7, 155).
- [10] W. K. Wootters and W. H. Zurek, "A single quantum cannot be cloned," *Nature*, vol. 299, pp. 802–, Oct. 1982. (cited on page 10).
- [11] D. Dieks, "Communication by epr devices," *Physics Letters A*, vol. 92, no. 6, pp. 271 – 272, 1982. (cited on page 10).
- [12] C. A. Fuchs and C. M. Caves, "Mathematical techniques for quantum communication theory," *Open Systems & Information Dynamics*, vol. 3, pp. 345–356, Oct 1995. (cited on page 13).
- [13] H. Barnum, C. M. Caves, C. A. Fuchs, R. Jozsa, and B. Schumacher, "Noncommuting mixed states cannot be broadcast," *Phys. Rev. Lett.*, vol. 76, pp. 2818–2821, Apr 1996. (cited on page 14).
- [14] H. Ollivier and W. H. Zurek, "Quantum discord: A measure of the quantumness of correlations," *Phys. Rev. Lett.*, vol. 88, p. 017901, Dec 2001. (cited on pages 16, 17).
- [15] L. Henderson and V. Vedral, "Classical, quantum and total correlations," *Journal of Physics A: Mathematical and General*, vol. 34, no. 35, p. 6899, 2001. (cited on pages 16, 17, and 77).
- [16] G. Adesso, T. R. Bromley, and M. Cianciaruso, "Measures and applications of quantum correlations," *Journal of Physics A: Mathematical and Theoretical*, vol. 49, no. 47, p. 473001, 2016. (cited on page 18).
- [17] M. B. Plenio, "Logarithmic negativity: A full entanglement monotone that is not convex," *Phys. Rev. Lett.*, vol. 95, p. 090503, 2005. (cited on page 19).
- [18] C. H. Bennett, D. P. DiVincenzo, J. A. Smolin, and W. K. Wootters, "Mixed-state entanglement and quantum error correction," *Phys. Rev. A*, vol. 54, pp. 3824–3851, Nov 1996. (cited on page 20).
- [19] W. K. Wootters, "Entanglement of formation of an arbitrary state of two qubits," *Phys. Rev. Lett.*, vol. 80, pp. 2245–2248, Mar 1998. (cited on page 20).

- [20] H. M. Wiseman, S. J. Jones, and A. C. Doherty, "Steering, entanglement, nonlocality, and the Einstein-Podolsky-Rosen paradox," *Phys. Rev. Lett.*, vol. 98, p. 140402, 2007. (cited on page 21).
- [21] I. Kogias, *Entanglement, Einstein-Podolsky-Rosen steering and cryptographic applications*. PhD thesis, School of Mathematical Sciences, University of Nottingham, 2016. (cited on page 21).
- [22] I. Kogias, P. Skrzypczyk, D. Cavalcanti, A. Acín, and G. Adesso, "Hierarchy of steering criteria based on moments for all bipartite quantum systems," *Phys. Rev. Lett.*, vol. 115, p. 210401, Nov 2015. (cited on page 22).
- [23] N. Brunner, D. Cavalcanti, S. Pironio, V. Scarani, and S. Wehner, "Bell nonlocality," *Rev. Mod. Phys.*, vol. 86, pp. 419–478, Apr 2014. (cited on page 23).
- [24] J. Preskill, "Lecture notes on Quantum Computation." (cited on page 23).
- [25] H.-P. Breuer, E.-M. Laine, J. Piilo, and B. Vacchini, "Colloquium : Non-markovian dynamics in open quantum systems," *Rev. Mod. Phys.*, vol. 88, p. 021002, Apr 2016. (cited on pages 31, 106).
- [26] S. L. Braunstein and P. van Loock, "Quantum information with continuous variables," *Rev. Mod. Phys.*, vol. 77, p. 513, 2005. (cited on pages 33, 101, and 124).
- [27] A. Ferraro, S. Olivares, and M. G. A. Paris, *Gaussian States in Quantum Information*. Bibliopolis, 2005. (cited on page 33).
- [28] G. Adesso, S. Ragy, and A. R. Lee, "Continuous variable quantum information: Gaussian states and beyond," *Open Syst. Inf. Dyn.*, vol. 21, p. 1440001, 2014. (cited on pages 33, 115).
- [29] A. Serafini, *Quantum Continuous Variables: A Primer of Theoretical Methods*. Taylor & Francis, Oxford, 2017. (cited on pages 33, 38, 52, 53, 98, 99, 100, 101, and 172).

## Bibliography

- [30] W.-M. Zhang, D. H. Feng, and R. Gilmore, "Coherent states: Theory and some applications," *Rev. Mod. Phys.*, vol. 62, pp. 867–927, Oct 1990. (cited on pages 35, 36).
- [31] S. Barnett and P. Radmore, *Methods in Theoretical Quantum Optics*. Oxford: Oxford University Press, 2002. (cited on page 39).
- [32] R. Simon, "Peres-horodecki separability criterion for continuous variable systems," *Phys. Rev. Lett.*, vol. 84, p. 2726, 2000. (cited on page 51).
- [33] F. Caruso, J. Eisert, V. Giovannetti, and A. S. Holevo, "Optimal unitary dilation for bosonic gaussian channels," *Phys. Rev. A*, vol. 84, p. 022306, Aug 2011. (cited on pages 52, 53).
- [34] C. W. Helstrom, "Quantum detection and estimation theory," *Journal of Statistical Physics*, vol. 1, pp. 231–252, Jun 1969. (cited on pages 57, 58).
- [35] A. S. Holevo, *Probabilistic and Statistical Aspects of Quantum Theory; 2nd ed.* Publications of the Scuola Normale Superiore Monographs, Dordrecht: Springer, 2011. (cited on pages 57, 58).
- [36] M. G. Paris, "Quantum estimation for quantum technology," *Int. J. Quantum Inf.*, vol. 7, no. supp01, pp. 125–137, 2009. (cited on pages 57, 103).
- [37] S. Ragy, *Resources in quantum imaging, detection and estimation*. PhD thesis, School of Mathematical Sciences, University of Nottingham, 2015. (cited on pages 57, 64).
- [38] S. L. Braunstein and C. M. Caves, "Statistical distance and the geometry of quantum states," *Phys. Rev. Lett.*, vol. 72, pp. 3439–3443, May 1994. (cited on page 59).
- [39] J. Liu, H.-N. Xiong, F. Song, and X. Wang, "Fidelity susceptibility and quantum fisher information for density operators with arbitrary ranks," *Physica A: Statistical Mechanics and its Applications*, vol. 410, pp. 167 – 173, 2014. (cited on page 60).

- [40] L. Maccone, “Intuitive reason for the usefulness of entanglement in quantum metrology,” *Phys. Rev. A*, vol. 88, p. 042109, Oct 2013. (cited on page 61).
- [41] S. F. Huelga, C. Macchiavello, T. Pellizzari, A. K. Ekert, M. B. Plenio, and J. I. Cirac, “Improvement of frequency standards with quantum entanglement,” *Phys. Rev. Lett.*, vol. 79, pp. 3865–3868, Nov 1997. (cited on pages 63, 81, and 100).
- [42] K. Macieszczak, “Zeno limit in frequency estimation with non-Markovian environments,” *Phys. Rev. A*, vol. 92, p. 010102, Jul 2015. (cited on pages 63, 81, and 83).
- [43] A. Smirne, J. Kołodyński, S. F. Huelga, and R. Demkowicz-Dobrzański, “Ultimate Precision Limits for Noisy Frequency Estimation,” *Phys. Rev. Lett.*, vol. 116, p. 120801, Mar 2016. (cited on pages 63, 81, 83, 84, and 87).
- [44] S. Ragy, M. Jarzyna, and R. Demkowicz-Dobrzański, “Compatibility in multiparameter quantum metrology,” *Phys. Rev. A*, vol. 94, p. 052108, Nov 2016. (cited on pages 64, 97, 100, and 103).
- [45] W. D. Phillips, “Nobel lecture: Laser cooling and trapping of neutral atoms,” *Rev. Mod. Phys.*, vol. 70, pp. 721–741, Jul 1998. (cited on page 67).
- [46] N. Masuhara, J. M. Doyle, J. C. Sandberg, D. Kleppner, T. J. Greytak, H. F. Hess, and G. P. Kochanski, “Evaporative cooling of spin-polarized atomic hydrogen,” *Phys. Rev. Lett.*, vol. 61, pp. 935–938, Aug 1988. (cited on page 67).
- [47] A. Hopkins, K. Jacobs, S. Habib, and K. Schwab, “Feedback cooling of a nanomechanical resonator,” *Phys. Rev. B*, vol. 68, p. 235328, Dec 2003. (cited on page 67).
- [48] D. Kleckner and D. Bouwmeester, “Sub-kelvin optical cooling of a micromechanical resonator,” *Nature*, vol. 444, pp. 75–, Nov. 2006. (cited on page 67).

## Bibliography

- [49] M. Poggio, C. L. Degen, H. J. Mamin, and D. Rugar, "Feedback cooling of a cantilever's fundamental mode below 5 mk," *Phys. Rev. Lett.*, vol. 99, p. 017201, Jul 2007. (cited on page 67).
- [50] C. Belthangady, N. Bar-Gill, L. M. Pham, K. Arai, D. Le Sage, P. Cappellaro, and R. L. Walsworth, "Dressed-state resonant coupling between bright and dark spins in diamond," *Phys. Rev. Lett.*, vol. 110, p. 157601, Apr 2013. (cited on page 67).
- [51] D. Gelbwaser-Klimovsky, K. Szczygielski, U. Vogl, A. Saß, R. Alicki, G. Kurizki, and M. Weitz, "Laser-induced cooling of broadband heat reservoirs," *Phys. Rev. A*, vol. 91, p. 023431, Feb 2015. (cited on page 67).
- [52] A. E. Allahverdyan, K. Hovhannisyan, and G. Mahler, "Optimal refrigerator," *Phys. Rev. E*, vol. 81, p. 051129, May 2010. (cited on pages 67, 73).
- [53] R. Kosloff and T. Feldmann, "Optimal performance of reciprocating demagnetization quantum refrigerators," *Phys. Rev. E*, vol. 82, p. 011134, Jul 2010. (cited on page 67).
- [54] Y.-X. Chen and S.-W. Li, "Quantum refrigerator driven by current noise," *EPL (Europhysics Letters)*, vol. 97, no. 4, p. 40003, 2012. (cited on page 67).
- [55] D. Venturelli, R. Fazio, and V. Giovannetti, "Minimal self-contained quantum refrigeration machine based on four quantum dots," *Phys. Rev. Lett.*, vol. 110, p. 256801, Jun 2013. (cited on page 67).
- [56] L. A. Correa, J. P. Palao, G. Adesso, and D. Alonso, "Performance bound for quantum absorption refrigerators," *Phys. Rev. E*, vol. 87, p. 042131, Apr 2013. (cited on page 67).
- [57] L. A. Correa, J. P. Palao, G. Adesso, and D. Alonso, "Optimal performance of endoreversible quantum refrigerators," *Phys. Rev. E*, vol. 90, p. 062124, Dec 2014. (cited on page 67).
- [58] L. A. Correa, J. P. Palao, and D. Alonso, "Internal dissipation and heat leaks in quantum thermodynamic cycles," *Phys. Rev. E*, vol. 92, p. 032136, Sep 2015. (cited on page 67).

- [59] J. P. Palao, R. Kosloff, and J. M. Gordon, “Quantum thermodynamic cooling cycle,” *Phys. Rev. E*, vol. 64, p. 056130, Oct 2001. (cited on page 67).
- [60] R. Kosloff, “Quantum thermodynamics: A dynamical viewpoint,” *Entropy*, vol. 15, no. 6, pp. 2100–2128, 2013. (cited on page 67).
- [61] D. Gelbwaser-Klimovsky and G. Kurizki, “Heat-machine control by quantum-state preparation: From quantum engines to refrigerators,” *Phys. Rev. E*, vol. 90, p. 022102, Aug 2014. (cited on page 67).
- [62] L. A. Correa, “Multistage quantum absorption heat pumps,” *Phys. Rev. E*, vol. 89, p. 042128, Apr 2014. (cited on page 67).
- [63] J. V. Koski, A. Kutvonen, I. M. Khaymovich, T. Ala-Nissila, and J. P. Pekola, “On-chip maxwell’s demon as an information-powered refrigerator,” *Phys. Rev. Lett.*, vol. 115, p. 260602, Dec 2015. (cited on page 67).
- [64] A. Kutvonen, J. Koski, and T. Ala-Nissila, “Thermodynamics and efficiency of an autonomous on-chip maxwell’s demon,” *Scientific Reports*, vol. 6, pp. 21126–, Feb. 2016. (cited on page 67).
- [65] Y. Rezek, P. Salamon, K. H. Hoffmann, and R. Kosloff, “The quantum refrigerator: The quest for absolute zero,” *EPL (Europhysics Letters)*, vol. 85, no. 3, p. 30008, 2009. (cited on page 67).
- [66] M. Kolář, D. Gelbwaser-Klimovsky, R. Alicki, and G. Kurizki, “Quantum bath refrigeration towards absolute zero: Challenging the unattainability principle,” *Phys. Rev. Lett.*, vol. 109, p. 090601, Aug 2012. (cited on page 67).
- [67] A. Levy, R. Alicki, and R. Kosloff, “Quantum refrigerators and the third law of thermodynamics,” *Phys. Rev. E*, vol. 85, p. 061126, Jun 2012. (cited on page 67).
- [68] M. Lostaglio, D. Jennings, and T. Rudolph, “Description of quantum coherence in thermodynamic processes requires constraints beyond free energy,” *Nature Communications*, vol. 6, pp. 6383–, Mar. 2015. (cited on page 67).

## Bibliography

- [69] M. Lostaglio, K. Korzekwa, D. Jennings, and T. Rudolph, “Quantum coherence, time-translation symmetry, and thermodynamics,” *Phys. Rev. X*, vol. 5, p. 021001, Apr 2015. (cited on page 67).
- [70] W. Niedenzu, D. Gelbwaser-Klimovsky, and G. Kurizki, “Performance limits of multilevel and multipartite quantum heat machines,” *Phys. Rev. E*, vol. 92, p. 042123, Oct 2015. (cited on page 67).
- [71] R. Uzdin, A. Levy, and R. Kosloff, “Equivalence of quantum heat machines, and quantum-thermodynamic signatures,” *Phys. Rev. X*, vol. 5, p. 031044, Sep 2015. (cited on page 67).
- [72] P. Kammerlander and J. Anders, “Coherence and measurement in quantum thermodynamics,” *Scientific Reports*, vol. 6, pp. 22174–, Feb. 2016. (cited on pages 67, 90).
- [73] K. Korzekwa, M. Lostaglio, J. Oppenheim, and D. Jennings, “The extraction of work from quantum coherence,” *New Journal of Physics*, vol. 18, no. 2, p. 023045, 2016. (cited on page 67).
- [74] G. Francica, J. Goold, F. Plastina, and M. Paternostro, “Daemonic ergotropy: enhanced work extraction from quantum correlations,” *npj Quantum Information*, vol. 3, no. 1, pp. 12–, 2017. (cited on page 67).
- [75] P. O. Boykin, T. Mor, V. Roychowdhury, F. Vatan, and R. Vrijen, “Algorithmic cooling and scalable nmr quantum computers,” *Proceedings of the National Academy of Sciences*, vol. 99, no. 6, pp. 3388–3393, 2002. (cited on page 67).
- [76] J. M. Fernandez, S. Lloyd, T. Mor, and V. Roychowdhury, “Algorithmic cooling of spins: a practicable method for increasing polarization,” *International Journal of Quantum Information*, vol. 02, no. 04, pp. 461–477, 2004. (cited on page 67).
- [77] S. Lloyd, “Coherent quantum feedback,” *Phys. Rev. A*, vol. 62, p. 022108, Jul 2000. (cited on pages 68, 69).
- [78] S. Habib, K. Jacobs, and H. Mabuchi, “Quantum feedback control,” *Los Alamos Science*, vol. 27, pp. 126–135, 2002. (cited on page 68).

- [79] J. M. Horowitz and K. Jacobs, "Quantum effects improve the energy efficiency of feedback control," *Phys. Rev. E*, vol. 89, p. 042134, Apr 2014. (cited on pages 68, 71, 73, 75, and 77).
- [80] D. Dong and I. Petersen, "Quantum control theory and applications: a survey," *IET Control Theory & Applications*, vol. 4, pp. 2651–2671(20), December 2010. (cited on page 69).
- [81] H. M. Wiseman and G. J. Milburn, *Quantum Measurement and Control*. Cambridge University Press, 2010. (cited on page 69).
- [82] J. E. Gough and S. Wildfeuer, "Enhancement of field squeezing using coherent feedback," *Phys. Rev. A*, vol. 80, p. 042107, Oct 2009. (cited on page 69).
- [83] T. Sagawa and M. Ueda, "Second law of thermodynamics with discrete quantum feedback control," *Phys. Rev. Lett.*, vol. 100, p. 080403, Feb 2008. (cited on page 73).
- [84] J. M. Gordon and K. Ng, *Cool Thermodynamics*. Cambridge International Science Publishing, 2000. (cited on page 75).
- [85] M. Ali, A. R. P. Rau, and G. Alber, "Quantum discord for two-qubit  $x$  states," *Phys. Rev. A*, vol. 81, p. 042105, Apr 2010. (cited on page 77).
- [86] K. V. Hovhannisyan, M. Perarnau-Llobet, M. Huber, and A. Acín, "Entanglement generation is not necessary for optimal work extraction," *Phys. Rev. Lett.*, vol. 111, p. 240401, Dec 2013. (cited on page 79).
- [87] S. Maniscalco and F. Petruccione, "Non-Markovian dynamics of a qubit," *Phys. Rev. A*, vol. 73, p. 012111, Jan 2006. (cited on pages 82, 83).
- [88] A. Shabani and D. A. Lidar, "Completely positive post-markovian master equation via a measurement approach," *Phys. Rev. A*, vol. 71, p. 020101, Feb 2005. (cited on page 83).
- [89] S. Maniscalco, "Complete positivity of a spin-1/2 master equation with memory," *Phys. Rev. A*, vol. 75, p. 062103, Jun 2007. (cited on page 83).

## Bibliography

- [90] L. Mazzola, E.-M. Laine, H.-P. Breuer, S. Maniscalco, and J. Piilo, "Phenomenological memory-kernel master equations and time-dependent Markovian processes," *Phys. Rev. A*, vol. 81, p. 062120, Jun 2010. (cited on page 84).
- [91] K. Modi, H. Cable, M. Williamson, and V. Vedral, "Quantum Correlations in Mixed-State Metrology," *Phys. Rev. X*, vol. 1, p. 021022, Dec 2011. (cited on page 87).
- [92] T. Sagawa and M. Ueda, "Minimal energy cost for thermodynamic information processing: measurement and information erasure," *Physical review letters*, vol. 102, no. 25, p. 250602, 2009. (cited on page 90).
- [93] N. Erez, "Thermodynamics of projective quantum measurements," *Physica Scripta*, vol. 2012, no. T151, p. 014028, 2012. (cited on page 90).
- [94] K. Jacobs, "Quantum measurement and the first law of thermodynamics: The energy cost of measurement is the work value of the acquired information," *Physical Review E*, vol. 86, no. 4, p. 040106, 2012. (cited on page 90).
- [95] K. Micadei, R. M. Serra, and L. C. Céleri, "Thermodynamic cost of acquiring information," *Physical Review E*, vol. 88, no. 6, p. 062123, 2013. (cited on page 90).
- [96] P. Faist, F. Dupuis, J. Oppenheim, and R. Renner, "The minimal work cost of information processing," *Nature communications*, vol. 6, 2015. (cited on page 90).
- [97] K. Abdelkhalek, Y. Nakata, and D. Reeb, "Fundamental energy cost for quantum measurement," *arXiv/quant-physics:1609.06981*, 2016. (cited on page 90).
- [98] C. M. Caves, "Quantum-mechanical noise in an interferometer," *Phys. Rev. D*, vol. 23, p. 1693, Apr 1981. (cited on pages 97, 100).
- [99] A. Monras, "Optimal phase measurements with pure gaussian states," *Phys. Rev. A*, vol. 73, p. 033821, Mar 2006. (cited on page 97).

- [100] A. Monras and M. G. Paris, "Optimal quantum estimation of loss in bosonic channels," *Physical Review Letters*, vol. 98, no. 16, p. 160401, 2007. (cited on page 97).
- [101] G. Adesso, F. Dell'Anno, S. De Siena, F. Illuminati, and L. A. M. Souza, "Optimal estimation of losses at the ultimate quantum limit with non-gaussian states," *Phys. Rev. A*, vol. 79, p. 040305, Apr 2009. (cited on page 97).
- [102] R. Gaiba and M. G. Paris, "Squeezed vacuum as a universal quantum probe," *Physics Letters A*, vol. 373, no. 10, pp. 934 – 939, 2009. (cited on page 97).
- [103] M. Aspachs, G. Adesso, and I. Fuentes, "Optimal quantum estimation of the unruh-hawking effect," *Phys. Rev. Lett.*, vol. 105, p. 151301, Oct 2010. (cited on page 97).
- [104] A. Monras and F. Illuminati, "Measurement of damping and temperature: Precision bounds in gaussian dissipative channels," *Phys. Rev. A*, vol. 83, p. 012315, Jan 2011. (cited on page 97).
- [105] O. Pinel, J. Fade, D. Braun, P. Jian, N. Treps, and C. Fabre, "Ultimate sensitivity of precision measurements with intense gaussian quantum light: A multimodal approach," *Phys. Rev. A*, vol. 85, p. 010101, Jan 2012. (cited on page 97).
- [106] O. Pinel, P. Jian, N. Treps, C. Fabre, and D. Braun, "Quantum parameter estimation using general single-mode gaussian states," *Phys. Rev. A*, vol. 88, p. 040102, Oct 2013. (cited on page 97).
- [107] A. Monras, "Phase space formalism for quantum estimation of Gaussian states." Mar. 2013. (cited on page 97).
- [108] Y. Gao and H. Lee, "Bounds on quantum multiple-parameter estimation with gaussian state," *The European Physical Journal D*, vol. 68, p. 347, Nov 2014. (cited on page 97).
- [109] Z. Jiang, "Quantum fisher information for states in exponential form," *Phys. Rev. A*, vol. 89, p. 032128, Mar 2014. (cited on page 97).

## Bibliography

- [110] M. Ahmadi, D. E. Bruschi, and I. Fuentes, “Quantum metrology for relativistic quantum fields,” *Phys. Rev. D*, vol. 89, p. 065028, Mar 2014. (cited on page 97).
- [111] L. A. Correa, M. Mehboudi, G. Adesso, and A. Sanpera, “Individual quantum probes for optimal thermometry,” *Phys. Rev. Lett.*, vol. 114, p. 220405, Jun 2015. (cited on page 97).
- [112] D. Šafránek, A. R. Lee, and I. Fuentes, “Quantum parameter estimation using multi-mode gaussian states,” *New Journal of Physics*, vol. 17, no. 7, p. 073016, 2015. (cited on page 97).
- [113] N. Friis, M. Skotiniotis, I. Fuentes, and W. Dür, “Heisenberg scaling in gaussian quantum metrology,” *Phys. Rev. A*, vol. 92, p. 022106, Aug 2015. (cited on page 97).
- [114] L. Banchi, S. L. Braunstein, and S. Pirandola, “Quantum fidelity for arbitrary gaussian states,” *Phys. Rev. Lett.*, vol. 115, p. 260501, Dec 2015. (cited on pages 97, 100).
- [115] L. Rigovacca, A. Farace, A. De Pasquale, and V. Giovannetti, “Gaussian discriminating strength,” *Phys. Rev. A*, vol. 92, p. 042331, Oct 2015. (cited on page 97).
- [116] D. Šafránek and I. Fuentes, “Optimal probe states for the estimation of gaussian unitary channels,” *Phys. Rev. A*, vol. 94, p. 062313, Dec 2016. (cited on pages 97, 103).
- [117] K. Duivenvoorden, B. M. Terhal, and D. Weigand, “Single-mode displacement sensor,” *Phys. Rev. A*, vol. 95, p. 012305, Jan 2017. (cited on page 97).
- [118] C. N. Gagatsos, D. Branford, and A. Datta, “Gaussian systems for quantum-enhanced multiple phase estimation,” *Phys. Rev. A*, vol. 94, p. 042342, Oct 2016. (cited on page 97).
- [119] M. Tsang, R. Nair, and X.-M. Lu, “Quantum theory of superresolution for two incoherent optical point sources,” *Phys. Rev. X*, vol. 6, p. 031033, Aug 2016. (cited on page 97).

- [120] R. Nair and M. Tsang, "Far-field superresolution of thermal electromagnetic sources at the quantum limit," *Phys. Rev. Lett.*, vol. 117, p. 190801, Nov 2016. (cited on page 97).
- [121] C. Lupo and S. Pirandola, "Ultimate precision bound of quantum and subwavelength imaging," *Phys. Rev. Lett.*, vol. 117, p. 190802, Nov 2016. (cited on page 97).
- [122] S. Pirandola and C. Lupo, "Ultimate precision of adaptive noise estimation," *Phys. Rev. Lett.*, vol. 118, p. 100502, Mar 2017. (cited on page 97).
- [123] D. Braun, G. Adesso, F. Benatti, R. Floreanini, U. Marzolino, M. W. Mitchell, and S. Pirandola, "Quantum enhanced measurements without entanglement." 2017. (cited on pages 97, 100).
- [124] A. Serafini, G. Adesso, and F. Illuminati, "Unitarily localizable entanglement of gaussian states," *Phys. Rev. A*, vol. 71, p. 032349, Mar 2005. (cited on page 100).
- [125] S. Pirandola, A. Serafini, and S. Lloyd, "Correlation matrices of two-mode bosonic systems," *Phys. Rev. A*, vol. 79, p. 052327, May 2009. (cited on page 100).
- [126] L. Mišta, Jr. and K. Baksová, "Gaussian intrinsic entanglement for states with partial minimum uncertainty," 2017. arXiv:1710.10809v1. (cited on page 100).
- [127] B. M. Escher, R. L. de Matos Filho, and L. Davidovich, "General framework for estimating the ultimate precision limit in noisy quantum-enhanced metrology," *Nature Phys.*, vol. 7, pp. 406–411, Mar. 2011. (cited on pages 100, 102).
- [128] R. Demkowicz-Dobrzański, J. Kolodyński, and M. Guta, "The elusive Heisenberg limit in quantum-enhanced metrology," *Nature Commun.*, vol. 3, p. 1063, 2012. (cited on pages 100, 102).
- [129] C. M. Caves and P. D. Drummond, "Quantum limits on bosonic communication rates," *Rev. Mod. Phys.*, vol. 66, p. 481, 1994. (cited on page 101).

## Bibliography

- [130] M. M. Wolf, D. Pérez-García, and G. Giedke, “Quantum capacities of bosonic channels,” *Phys. Rev. Lett.*, vol. 98, p. 130501, 2007. (cited on pages 101, 126).
- [131] C. Weedbrook, S. Pirandola, R. García-Patrón, N. J. Cerf, T. C. Ralph, J. H. Shapiro, and S. Lloyd, “Gaussian quantum information,” *Rev. Mod. Phys.*, vol. 84, p. 621, 2012. (cited on page 101).
- [132] J. Schäfer, E. Karpov, R. García-Patrón, O. V. Pilyavets, and N. J. Cerf, “Equivalence relations for the classical capacity of single-mode gaussian quantum channels,” *Phys. Rev. Lett.*, vol. 111, p. 030503, 2013. (cited on pages 101, 116).
- [133] A. Mari, V. Giovannetti, and A. S. Holevo, “Quantum state majorization at the output of bosonic gaussian channels,” *Nature Communications*, vol. 5, pp. 3826–, May 2014. (cited on page 101).
- [134] V. Giovannetti, R. García-Patrón, N. J. Cerf, and A. S. Holevo, “Ultimate classical communication rates of quantum optical channels,” *Nature Photon.*, vol. 8, p. 796, 2014. (cited on pages 101, 116).
- [135] S. Pirandola, R. Laurenza, C. Ottaviani, and L. Banchi, “Fundamental limits of repeaterless quantum communications,” *Nature Commun.*, vol. 8, p. 15043, 2017. (cited on pages 102, 123).
- [136] J. P. Dowling and K. P. Seshadreesan, “Quantum optical technologies for metrology, sensing, and imaging,” *J. Lightwave Technol.*, vol. 33, p. 2359, June 2015. (cited on page 103).
- [137] F. Fröwis, M. Skotiniotis, B. Kraus, and W. Dür, “Optimal quantum states for frequency estimation,” *New J. Phys.*, vol. 16, no. 8, p. 083010, 2014. (cited on page 103).
- [138] P. A. Knott, “A search algorithm for quantum state engineering and metrology,” *New J. Phys.*, vol. 18, no. 7, p. 073033, 2016. (cited on page 103).
- [139] M. M. Wolf, J. Eisert, T. S. Cubitt, and J. I. Cirac, “Assessing non-markovian quantum dynamics,” *Phys. Rev. Lett.*, vol. 101, p. 150402, Oct 2008. (cited on page 105).

- [140] S. F. Huelga, A. Rivas, and M. B. Plenio, "Non-markovianity-assisted steady state entanglement," *Phys. Rev. Lett.*, vol. 108, p. 160402, Apr 2012. (cited on page 105).
- [141] I. de Vega and D. Alonso, "Dynamics of non-markovian open quantum systems," *Rev. Mod. Phys.*, vol. 89, p. 015001, Jan 2017. (cited on page 105).
- [142] H.-P. Breuer, E.-M. Laine, and J. Piilo, "Measure for the degree of non-markovian behavior of quantum processes in open systems," *Phys. Rev. Lett.*, vol. 103, p. 210401, Nov 2009. (cited on pages 105, 106, and 108).
- [143] Á. Rivas, S. F. Huelga, and M. B. Plenio, "Entanglement and non-markovianity of quantum evolutions," *Phys. Rev. Lett.*, vol. 105, p. 050403, Jul 2010. (cited on pages 105, 106, and 108).
- [144] S. Lorenzo, F. Plastina, and M. Paternostro, "Geometrical characterization of non-markovianity," *Phys. Rev. A*, vol. 88, p. 020102, Aug 2013. (cited on pages 105, 106, 108, and 121).
- [145] D. Chruściński and S. Maniscalco, "Degree of Non-Markovianity of Quantum Evolution," *Phys. Rev. Lett.*, vol. 112, p. 120404, mar 2014. (cited on pages 105, 106, and 111).
- [146] B. Bylicka, D. Chruściński, and S. Maniscalco, "Non-markovianity and reservoir memory of quantum channels: a quantum information theory perspective," *Sci. Rep.*, vol. 4, 2014. (cited on pages 105, 106).
- [147] G. Torre, W. Roga, and F. Illuminati, "Non-markovianity of gaussian channels," *Phys. Rev. Lett.*, vol. 115, p. 070401, Aug 2015. (cited on pages 105, 106, 111, and 112).
- [148] H. S. Dhar, M. N. Bera, and G. Adesso, "Characterizing non-markovianity via quantum interferometric power," *Phys. Rev. A*, vol. 91, p. 032115, Mar 2015. (cited on page 105).
- [149] F. A. Pollock, C. Rodríguez-Rosario, T. Frauenheim, M. Paternostro, and K. Modi, "Complete framework for efficient characterisation of non-Markovian processes," *arXiv:1512.00589*, 2015. (cited on page 105).

## Bibliography

- [150] F. A. Pollock, C. Rodríguez-Rosario, T. Frauenheim, M. Paternostro, and K. Modi, “Operational markov condition for quantum processes,” *Phys. Rev. Lett.*, vol. 120, p. 040405, Jan 2018. (cited on page 105).
- [151] E.-M. Laine, J. Piilo, and H.-P. Breuer, “Measure for the non-markovianity of quantum processes,” *Phys. Rev. A*, vol. 81, p. 062115, Jun 2010. (cited on pages 105, 106).
- [152] W.-M. Zhang, P.-Y. Lo, H.-N. Xiong, M. W.-Y. Tu, and F. Nori, “General Non-Markovian Dynamics of Open Quantum Systems,” *Phys. Rev. Lett.*, vol. 109, p. 170402, Oct. 2012. (cited on page 105).
- [153] M. J. Biercuk, H. Uys, A. P. VanDevender, N. Shiga, W. M. Itano, and J. J. Bollinger, “Optimized dynamical decoupling in a model quantum memory,” *Nature*, vol. 458, pp. 996–1000, Apr. 2009. (cited on page 105).
- [154] C. J. Myatt, B. E. King, Q. A. Turchette, C. A. Sackett, D. Kielpinski, W. M. Itano, C. Monroe, and D. J. Wineland, “Decoherence of quantum superpositions through coupling to engineered reservoirs,” *Nature (London)*, vol. 403, pp. 269–273, 2000. (cited on page 105).
- [155] F. Verstraete, M. M. Wolf, and J. I. Cirac, “Quantum computation and quantum-state engineering driven by dissipation,” *Nature Phys.*, vol. 5, pp. 633–636, 2009. (cited on page 105).
- [156] S. Haseli, G. Karpat, S. Salimi, A. S. Khorashad, F. F. Fanchini, B. Çakmak, G. H. Aguilar, S. P. Walborn, and P. H. S. Ribeiro, “Non-markovianity through flow of information between a system and an environment,” *Phys. Rev. A*, vol. 90, p. 052118, Nov 2014. (cited on page 105).
- [157] R. Vasile, S. Maniscalco, M. G. A. Paris, H.-P. Breuer, and J. Piilo, “Quantifying non-markovianity of continuous-variable gaussian dynamical maps,” *Phys. Rev. A*, vol. 84, p. 052118, Nov 2011. (cited on page 105).
- [158] M. Thorwart, J. Eckel, J. Reina, P. Nalbach, and S. Weiss, “Enhanced quantum entanglement in the non-markovian dynamics of biomolecular excitons,” *Chem. Phys. Lett.*, vol. 478, no. 4–6, pp. 234 – 237, 2009. (cited on page 105).

- [159] A. W. Chin, J. Prior, R. Rosenbach, F. Caycedo-Soler, S. F. Huelga, and M. B. Plenio, "The role of non-equilibrium vibrational structures in electronic coherence and recoherence in pigment-protein complexes," *Nature Phys.*, vol. 9, p. 113, 2013. (cited on page 105).
- [160] S. Huelga and M. Plenio, "Vibrations, quanta and biology," *Contemp. Phys.*, vol. 54, no. 4, pp. 181–207, 2013. (cited on page 105).
- [161] N. K. Bernardes, A. R. R. Carvalho, C. H. Monken, and M. F. Santos, "Environmental correlations and Markovian to non-Markovian transitions in collisional models," *Phys. Rev. A*, vol. 90, p. 032111, sep 2014. (cited on page 105).
- [162] N. K. Bernardes, A. Cuevas, A. Orioux, C. H. Monken, P. Mataloni, F. Sciarrino, and M. F. Santos, "Experimental observation of weak non-Markovianity." apr 2015. (cited on page 105).
- [163] N. K. Bernardes, J. P. S. Peterson, R. S. Sarthour, A. M. Souza, C. H. Monken, I. Roditi, I. S. Oliveira, and M. F. Santos, "High resolution non-markovianity in nmr," *Sci. Rep.*, vol. 6, p. 33945, Sept. 2016. (cited on page 105).
- [164] F. Ciccarello, G. M. Palma, and V. Giovannetti, "Collision-model-based approach to non-markovian quantum dynamics," *Phys. Rev. A*, vol. 87, p. 040103, Apr 2013. (cited on page 106).
- [165] F. Ciccarello and V. Giovannetti, "A quantum non-markovian collision model: incoherent swap case," *Physica Scripta*, vol. 2013, no. T153, p. 014010, 2013. (cited on page 106).
- [166] R. McCloskey and M. Paternostro, "Non-markovianity and system-environment correlations in a microscopic collision model," *Phys. Rev. A*, vol. 89, p. 052120, May 2014. (cited on page 106).
- [167] D. Girolami, A. M. Souza, V. Giovannetti, T. Tufarelli, J. G. Filgueiras, R. S. Sarthour, D. O. Soares-Pinto, I. S. Oliveira, and G. Adesso, "Quantum discord determines the interferometric power of quantum states," *Phys. Rev. Lett.*, vol. 112, p. 210401, May 2014. (cited on pages 106, 109).

## Bibliography

- [168] G. Adesso, "Gaussian interferometric power," *Phys. Rev. A*, vol. 90, p. 022321, Aug. 2014. (cited on pages 106, 109).
- [169] M. N. Bera, "Quantum Fisher information as the measure of Gaussian quantum correlation: Role in quantum metrology." June 2014. (cited on page 109).
- [170] L. Mišta, D. McNulty, and G. Adesso, "No-activation theorem for gaussian nonclassical correlations by gaussian operations," *Phys. Rev. A*, vol. 90, p. 022328, Aug 2014. (cited on page 109).
- [171] G. De Palma, A. Mari, V. Giovannetti, and A. S. Holevo, "Normal form decomposition for gaussian-to-gaussian superoperators," *J. Math. Phys.*, vol. 56, no. 5, p. 052202, 2015. (cited on page 116).
- [172] H. P. Breuer and F. Petruccione. Oxford: Oxford University Press, 2002. (cited on page 118).
- [173] S. L. Braunstein and H. J. Kimble, "Teleportation of continuous quantum variables," *Phys. Rev. Lett.*, vol. 80, p. 869, 1998. (cited on pages 123, 124).
- [174] G. Giedke and J. I. Cirac, "Characterization of gaussian operations and distillation of gaussian states," *Phys. Rev. A*, vol. 66, p. 032316, 2002. (cited on pages 123, 130, and 131).
- [175] J. Niset, J. Fiurášek, and N. J. Cerf, "No-go theorem for gaussian quantum error correction," *Phys. Rev. Lett.*, vol. 102, p. 120501, 2009. (cited on page 123).
- [176] P. van Loock, "Quantum communication with continuous variables," *Fortsch. Phys.*, vol. 50, no. 12, p. 1177, 2002. (cited on pages 124, 126).
- [177] S. Pirandola and S. Mancini, "Quantum teleportation with continuous variables: A survey," *Laser Phys.*, vol. 16, no. 10, p. 1418, 2006. (cited on pages 124, 126).
- [178] A. Furusawa, J. L. Sørensen, S. L. Braunstein, C. A. Fuchs, H. J. Kimble, and E. S. Polzik, "Unconditional quantum teleportation," *Science*, vol. 282, no. 5389, p. 706, 1998. (cited on pages 124, 134).

- [179] W. P. Bowen, N. Treps, B. C. Buchler, R. Schnabel, T. C. Ralph, H.-A. Bachor, T. Symul, and P. K. Lam, "Experimental investigation of continuous-variable quantum teleportation," *Phys. Rev. A*, vol. 67, p. 032302, 2003. (cited on page 124).
- [180] S. Pirandola, J. Eisert, C. Weedbrook, A. Furusawa, and S. L. Braunstein, "Advances in quantum teleportation," *Nature Photon.*, vol. 9, p. 641, 2015. (cited on pages 124, 130, and 131).
- [181] M. Ban, M. Sasaki, and M. Takeoka, "Continuous variable teleportation as a generalized thermalizing quantum channel," *J. Phys. A: Math. Gen.*, vol. 35, no. 28, p. L401, 2002. (cited on page 124).
- [182] R. E. S. Polkinghorne and T. C. Ralph, "Continuous variable entanglement swapping," *Phys. Rev. Lett.*, vol. 83, p. 2095, 1999. (cited on pages 124, 134).
- [183] H. F. Hofmann, T. Ide, T. Kobayashi, and A. Furusawa, "Fidelity and information in the quantum teleportation of continuous variables," *Phys. Rev. A*, vol. 62, p. 062304, 2000. (cited on pages 124, 134).
- [184] T. Ide, H. F. Hofmann, A. Furusawa, and T. Kobayashi, "Gain tuning and fidelity in continuous-variable quantum teleportation," *Phys. Rev. A*, vol. 65, p. 062303, 2002. (cited on pages 124, 134).
- [185] J. Fiurášek, "Improving the fidelity of continuous-variable teleportation via local operations," *Phys. Rev. A*, vol. 66, p. 012304, 2002. (cited on page 126).
- [186] S. L. Braunstein, C. A. Fuchs, and H. J. Kimble, "Criteria for continuous-variable quantum teleportation," *J. Mod. Opt.*, vol. 47, no. 2-3, pp. 267–278, 2000. (cited on pages 127, 128).
- [187] K. Hammerer, M. M. Wolf, E. S. Polzik, and J. I. Cirac, "Quantum benchmark for storage and transmission of coherent states," *Phys. Rev. Lett.*, vol. 94, p. 150503, 2005. (cited on pages 127, 128).
- [188] F. Grosshans and P. Grangier, "Quantum cloning and teleportation criteria for continuous quantum variables," *Phys. Rev. A*, vol. 64, p. 010301, 2001. (cited on pages 127, 129).

## Bibliography

- [189] P. T. Cochrane, T. C. Ralph, and A. Dolińska, “Optimal cloning for finite distributions of coherent states,” *Phys. Rev. A*, vol. 69, p. 042313, 2004. (cited on pages 127, 128).
- [190] Q. He, L. Rosales-Zárate, G. Adesso, and M. D. Reid, “Secure continuous variable teleportation and Einstein-Podolsky-Rosen steering,” *Phys. Rev. Lett.*, vol. 115, p. 180502, 2015. (cited on pages 129, 138).
- [191] N. J. Cerf, O. Krüger, P. Navez, R. F. Werner, and M. M. Wolf, “Non-gaussian cloning of quantum coherent states is optimal,” *Phys. Rev. Lett.*, vol. 95, p. 070501, 2005. (cited on page 129).
- [192] M. M. Wilde, M. Tomamichel, and M. Berta, “Converse bounds for private communication over quantum channels,” *IEEE Trans. Inf. Theory*, vol. 63, no. 3, pp. 1792–1817, 2017. (cited on page 130).
- [193] A. S. Holevo, “Entanglement-breaking channels in infinite dimensions,” *Problems of Information Transmission*, vol. 44, pp. 171–184, Sep 2008. (cited on page 130).
- [194] G. Adesso and F. Illuminati, “Gaussian measures of entanglement versus negativities: Ordering of two-mode gaussian states,” *Phys. Rev. A*, vol. 72, p. 032334, 2005. (cited on page 131).
- [195] G. Adesso, A. Serafini, and F. Illuminati, “Extremal entanglement and mixedness in continuous variable systems,” *Phys. Rev. A*, vol. 70, p. 022318, 2004. (cited on page 131).
- [196] G. Adesso and F. Illuminati, “Equivalence between entanglement and the optimal fidelity of continuous variable teleportation,” *Phys. Rev. Lett.*, vol. 95, p. 150503, 2005. (cited on page 133).
- [197] A. Mari and D. Vitali, “Optimal fidelity of teleportation of coherent states and entanglement,” *Phys. Rev. A*, vol. 78, p. 062340, 2008. (cited on page 133).
- [198] L. Lami, C. Hirche, G. Adesso, and A. Winter, “Schur complement inequalities for covariance matrices and monogamy of quantum correlations,” *Phys. Rev. Lett.*, vol. 117, p. 220502, 2016. (cited on page 135).

- [199] T. Heinosaari, J. Kiukas, and J. Schultz, "Breaking gaussian incompatibility on continuous variable quantum systems," *J. Math. Phys.*, vol. 56, no. 8, p. 082202, 2015. (cited on page 135).
- [200] I. Kogias, S. Ragy, and G. Adesso, "Continuous-variable versus hybrid schemes for quantum teleportation of gaussian states," *Phys. Rev. A*, vol. 89, p. 052324, 2014. (cited on page 141).